Methods in Molecular Biology 1328

Springer Protocols

Diana P. Bratu
Gerard P. McNeil *Editors*

Drosophila Oogenesis

Methods and Protocols

Humana Press

METHODS IN MOLECULAR BIOLOGY

Series Editor
John M. Walker
School of Life and Medical Sciences
University of Hertfordshire
Hatfield, Hertfordshire, AL10 9AB, UK

For further volumes:
http://www.springer.com/series/7651

Drosophila Oogenesis

Methods and Protocols

Edited by

Diana P. Bratu

Department of Biological Sciences,
Hunter College of the City University of New York, New York, NY, USA;
Molecular, Cellular, and Developmental Biology Program,
The Graduate Center, CUNY, New York, NY, USA

Gerard P. McNeil

Department of Biology, School of Arts and Sciences, York College CUNY, Jamaica, NY, USA

Humana Press

Editors
Diana P. Bratu
Department of Biological Sciences
Hunter College of the City University
of New York
New York, NY, USA

Molecular, Cellular, and
Developmental Biology Program
The Graduate Center, CUNY
New York, NY, USA

Gerard P. McNeil
Department of Biology
School of Arts and Sciences
York College CUNY
Jamaica, NY, USA

ISSN 1064-3745 ISSN 1940-6029 (electronic)
Methods in Molecular Biology
ISBN 978-1-4939-2850-7 ISBN 978-1-4939-2851-4 (eBook)
DOI 10.1007/978-1-4939-2851-4

Library of Congress Control Number: 2015944980

Springer New York Heidelberg Dordrecht London

Printed on acid-free paper

Humana Press is a brand of Springer
Springer Science+Business Media LLC New York is part of Springer Science+Business Media (www.springer.com)

Preface

Drosophila melanogaster is one of the most powerful model organisms in genetic studies of animal development and behavior. Entire tissues, from egg to adult, have been studied and continue to be the focus of cutting-edge biological research. With the accelerating pace of *Drosophila* genetics, the fruit fly will remain on the center stage for the foreseeable future. In this book we compiled a series of methods that have been developed to specifically address the fly ovary. In particular we aimed to address the relevant needs of both the beginner and expert researcher, as modern molecular methods are combined with genetic techniques.

In the last couple of decades, *Drosophila* oogenesis has received particular attention due in part to the revolutionary advances in imaging RNAs and proteins. Here we begin with updated protocols for preparing the ovary for various imaging techniques (fixed vs. live imaging, fluorescence microscopy vs. electron microscopy, in situ hybridization vs. immunohistochemistry, cellular structures vs. single molecule detection), followed by genetic protocols for generating mutant clones, performing mosaic analysis, and assessing cell death, to name a few. We conclude with chapters addressing methods for performing genome-wide gene expression analysis and bioinformatics for studies of RNA–protein interactions.

We thank all our expert authors for their contribution to this volume and we hope that as part of the collection of this relevant series, our book will be widely received by molecular, cell, and developmental biologists, as well as educators who wish to use this powerful model system in their research or classrooms.

New York, NY, USA ***Diana P. Bratu***
Jamaica, NY, USA ***Gerard P. McNeil***

Contents

Contributors

Mona Batish • *Department of Microbiology and Molecular Genetics, Rutgers New Jersey Medical School, Newark, NJ, USA*

Livia V. Bayer • *Department of Biological Sciences, Hunter College of the City University of New York, New York, NY, USA; Molecular, Cellular, and Developmental Biology Program, The Graduate Center, CUNY, New York, NY, USA*

Diana P. Bratu • *Department of Biological Sciences, Hunter College of the City University of New York, New York, NY, USA; Molecular, Cellular, and Developmental Biology Program, The Graduate Center, CUNY, New York, NY, USA*

Danfeng Cai • *Department of Biological Chemistry, Johns Hopkins School of Medicine, Baltimore, MD, USA; Molecular, Cellular and Developmental Biology Department, University of California, Santa Barbara, CA, USA*

Kristen Dancel-Manning • *Office of Collaborative Science Microscopy Core, New York University School of Medicine, New York, NY, USA*

Wu-Min Deng • *Department of Biological Science, Florida State University, Tallahassee, FL, USA*

Daniela Drummond-Barbosa • *Division of Reproductive Biology, Department of Biochemistry and Molecular Biology, Johns Hopkins Bloomberg School of Public Health, Baltimore, MD, USA; Department of Environmental Health Sciences, Johns Hopkins Bloomberg School of Public Health, Baltimore, MD, USA*

Stephen K. Formel • *Department of Biological Sciences, Hunter College of the City University of New York, New York, NY, USA*

Joseph G. Gall • *Department of Embryology, Carnegie Institution for Science, Baltimore, MD, USA*

Christopher M. Groen • *Anatomy and Cell Biology, Carver College of Medicine, University of Iowa, Iowa City, IA, USA*

Antoine Guichet • *Institut Jacques Monod, UMR 7592 – CNRS, Université Paris Diderot, Paris, France*

Li He • *Department of Biological Chemistry, Johns Hopkins School of Medicine, Baltimore, MD, USA; Department of Genetics, Harvard Medical School, Boston, MA, USA*

Yi-Chun Huang • *Department of Biological Science, Florida State University, Tallahassee, FL, USA*

Thomas R. Hurd • *Howard Hughes Medical Institute (HHMI), New York University School of Medicine, New York, NY, USA; Kimmel Center for Biology and Medicine of the Skirball Institute, New York University School of Medicine, New York, NY, USA; Department of Cell Biology, New York University School of Medicine, New York, NY, USA*

Jean-René Huynh • *Department of Genetics and Developmental Biology, Institut Curie, Paris, France; CNRS UMR3215, Paris, France; Inserm U934, Paris, France*

Dongyu Jia • *Department of Biological Science, Florida State University, Tallahassee, FL, USA*
Tony F. Joudi • *Department of Biology, Boston University, Boston, MA, USA*
Kaitlin M. Laws • *Division of Reproductive Biology, Department of Biochemistry and Molecular Biology, Johns Hopkins Bloomberg School of Public Health, Baltimore, MD, USA*
Kevin Legent • *Institut Jacques Monod, UMR 7592 – CNRS, Université Paris Diderot, Paris, France*
Ruth Lehmann • *Howard Hughes Medical Institute (HHMI), New York University School of Medicine, New York, NY, USA; Kimmel Center for Biology and Medicine of the Skirball Institute, New York University School of Medicine, New York, NY, USA; Department of Cell Biology, New York University School of Medicine, New York, NY, USA*
Feng-Xia A. Liang • *Department of Cell Biology, New York University School of Medicine, New York, NY, USA; Office of Collaborative Science Microscopy Core, New York University School of Medicine, New York, NY, USA*
Ji-Long Liu • *MRC Functional Genomics Unit, Department of Physiology, Anatomy and Genetics, University of Oxford, Oxford, UK*
Lathiena Manning • *Department of Biological Sciences, University of Maryland Baltimore County, Baltimore, MD, USA*
Kimberly McCall • *Department of Biology, Boston University, Boston, MA, USA*
John M. McLaughlin • *Department of Biological Sciences, Hunter College of the City University of New York, New York, NY, USA; Molecular, Cellular, and Developmental Biology Program, The Graduate Center, CUNY, New York, NY, USA*
Tracy L. Meehan • *Department of Biology, Boston University, Boston, MA, USA*
Denise J. Montell • *Department of Biological Chemistry, Johns Hopkins School of Medicine, Baltimore, MD, USA; Molecular, Cellular and Developmental Biology Department, University of California, Santa Barbara, CA, USA*
Yukiko Murota • *Department of Biological Sciences, Graduate School of Science, The University of Tokyo, Tokyo, Japan*
Toshihiro Nagai • *Electron Microscope Laboratory, School of Medicine, Keio University, Tokyo, Japan*
Yoshinori Nishimoto • *Department of Physiology, School of Medicine, Keio University, Tokyo, Japan*
Zehra F. Nizami • *Department of Embryology, Carnegie Institution for Science, Baltimore, MD, USA*
Amanda Norvell • *Department of Biology, The College of New Jersey, Ewing, NJ, USA*
Hideyuki Okano • *Department of Physiology, School of Medicine, Keio University, Tokyo, Japan*
Chris Petzold • *Office of Collaborative Science Microscopy Core, New York University School of Medicine, New York, NY, USA*
Mohit Prasad • *Department of Biological Chemistry, Johns Hopkins School of Medicine, Baltimore, MD, USA; Department of Biological Sciences, IISER Kolkata, Mohanpur, West Bengal, India*
Kristen Randolph • *Department of Biology, The College of New Jersey, Ewing, NJ, USA*
Nikolay V. Rozhkov • *Cold Spring Harbor Laboratory, Cold Spring Harbor, NY, USA*
Thomas Rubin • *Department of Genetics and Developmental Biology, Institut Curie, Paris, France; CNRS UMR3215, Paris, France; Inserm U934, Paris, France*

Carlos G. Sanchez • *Howard Hughes Medical Institute (HHMI), New York University School of Medicine, New York, NY, USA; Kimmel Center for Biology and Medicine of the Skirball Institute, New York University School of Medicine, New York, NY, USA; Department of Cell Biology, New York University School of Medicine, New York, NY, USA*

Shinsuke Shibata • *Department of Physiology, School of Medicine, Keio University, Tokyo, Japan*

Ravinder Singh • *Department of Molecular, Cellular and Developmental Biology, University of Colorado at Boulder, Boulder, CO, USA*

Mikiko C. Siomi • *Department of Biological Sciences, Graduate School of Science, The University of Tokyo, Tokyo, Japan*

Michelle Starz-Gaiano • *Department of Biological Sciences, University of Maryland Baltimore County, Baltimore, MD, USA*

Ömür Y. Tastan • *MRC Functional Genomics Unit, Department of Physiology, Anatomy and Genetics, University of Oxford, Oxford, UK*

Felipe K. Teixeira • *Howard Hughes Medical Institute (HHMI), New York University School of Medicine, New York, NY, USA; Kimmel Center for Biology and Medicine of the Skirball Institute, New York University School of Medicine, New York, NY, USA; Department of Cell Biology, New York University School of Medicine, New York, NY, USA*

Letitia Thompson • *Department of Biology, The College of New Jersey, Ewing, NJ, USA; University of Pennsylvania School of Veterinary Medicine, Philadelphia, PA, USA*

Nicolas Tissot • *Institut Jacques Monod, UMR 7592 – CNRS, Université Paris Diderot, Paris, France*

Tina L. Tootle • *Anatomy and Cell Biology, Carver College of Medicine, University of Iowa, Iowa City, IA, USA*

Ju-Yu S. Wang • *Howard Hughes Medical Institute (HHMI), New York University School of Medicine, New York, NY, USA; Kimmel Center for Biology and Medicine of the Skirball Institute, New York University School of Medicine, New York, NY, USA; Department of Cell Biology, New York University School of Medicine, New York, NY, USA*

Xiaobo Wang • *Department of Biological Chemistry, Johns Hopkins School of Medicine, Baltimore, MD, USA; Université P. Sabatier Toulouse III, Toulouse, France*

Alla Yalonetskaya • *Department of Biology, Boston University, Boston, MA, USA*

Mana Yoshimura • *Department of Physiology, School of Medicine, Keio University, Tokyo, Japan*

Chapter 1

Drosophila melanogaster Oogenesis: An Overview

John M. McLaughlin and Diana P. Bratu

Abstract

The *Drosophila melanogaster* ovary has served as a popular and successful model for understanding a wide range of biological processes: stem cell function, germ cell development, meiosis, cell migration, morphogenesis, cell death, intercellular signaling, mRNA localization, and translational control. This review provides a brief introduction to *Drosophila* oogenesis, along with a survey of its diverse biological topics and the advanced genetic tools that continue to make this a popular developmental model system.

Key words Flp-FRT, Patterning, Follicle cells, Morphogenesis, Germ plasm, Mosaics, P element, RNAi, *Drosophila*, Oogenesis, Oocyte, mRNA localization, Gal4, Live, Imaging, CRISPR, Fluorescence

1 Ovary Structure in Insects and Higher Flies

The *Drosophila* genus, which includes *D. melanogaster*, is a member of the order Diptera, or the higher flies. As a holometabolous insect, *Drosophila* undergoes a complete metamorphosis, including a transition from larval to pupal form; the complete life cycle consists of four stages [1].

In the class Insecta, several ovarian morphologies have evolved, each of which utilizes a different organizational layout for oocyte development (Fig. 1). In the majority of examined cases, basal insects contain **panoistic** ovaries, in which oogonia, ensheathed by follicular cells, mature into oocytes in the absence of additional support cells [2]. In contrast, higher insects have **meroistic** ovaries in which support cells linked to the oocyte provide it with large amounts of mRNA, protein and other cellular material [3]. Meroistic ovarian morphology is further subdivided into two categories. **Telotrophic meroistic** oocytes maintain connections to support cells via a nutritive cord that extends anteriorly through the ovariole to the germarium. The support cells remain localized at the anterior end of the ovariole throughout oogenesis. In contrast, **polytrophic meroistic** oocytes are connected directly to

Diana P. Bratu and Gerard P. McNeil (eds.), *Drosophila Oogenesis: Methods and Protocols*, Methods in Molecular Biology, vol. 1328, DOI 10.1007/978-1-4939-2851-4_1,

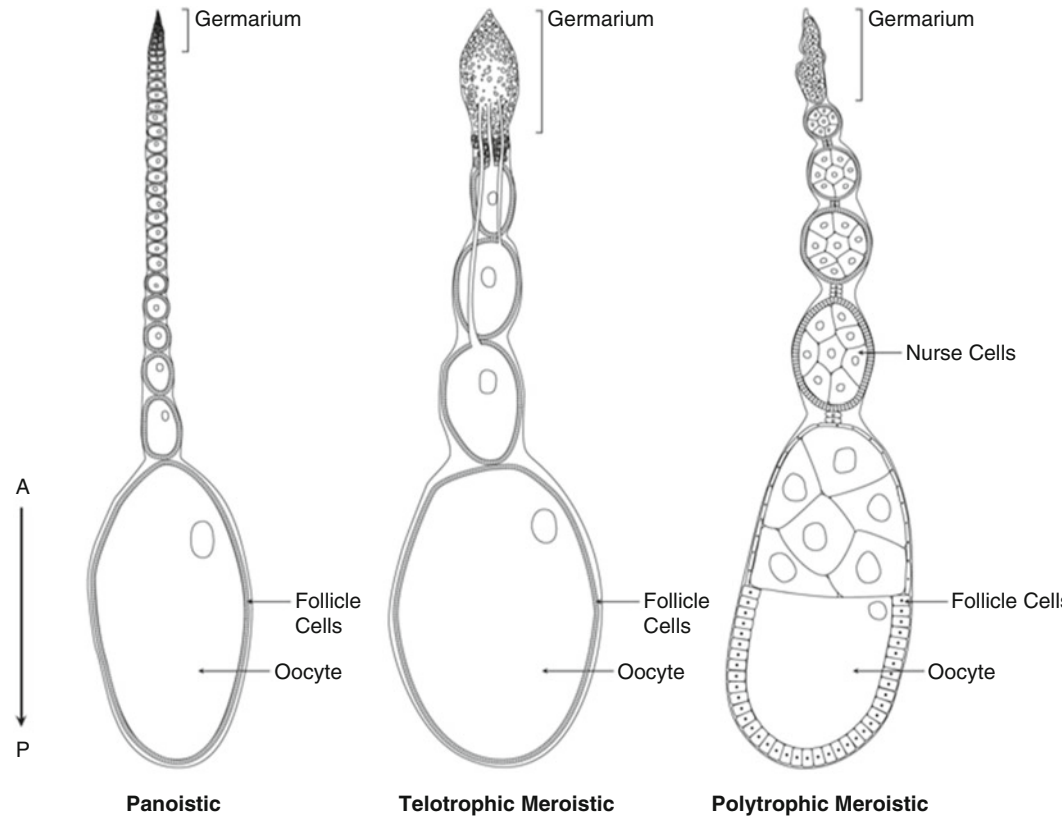

Fig. 1 Three distinct organizations of insect ovaries. Schematic representation of ovarioles derived from panoistic, telotrophic meroistic, and polytrophic meroistic ovaries (anterior—*top*; posterior—*bottom*). The germarium region, somatic follicle cells, support/nurse cells, and the developing oocyte are indicated within each ovariole chain

adjacent supporting nurse cells by cytoplasmic junctions (ring canals). In this system, the entire cyst moves as a unit through the ovariole; this is the strategy utilized by *Drosophila* species.

The basic unit of the ovary is the ovariole; there are 16–20 ovarioles per ovary, each being autonomous and containing its own stem cell populations and egg chambers at varying developmental stages. The ovariole can be divided into three principal regions (from anterior–posterior): the **terminal filament**, **germarium**, and **vitellarium** (reviewed in ref. 4). The terminal filament (TF) consists of a stack of 8–9 flattened cells which connect the germarium to the surrounding ovariole sheath and determine the orientation of ovariole development [5]. The germarium is divided into four regions (1, 2a, 2b, and 3) and is the site of **germline stem cell** (GSC) division, differentiation, and germline cyst formation. In germarium region 3, the germline cyst, containing nurse cells and oocyte, is ensheathed by a somatic cell layer (becoming an egg chamber) before being passed into the vitellarium [4]. The

remaining development of the egg chamber, including vitellogenesis and choriogenesis, is completed in the vitellarium [4]. The entire process of oogenesis is thus divided into 14 morphologically distinct stages.

2 Stem Cell Compartmentalization Within the Germarium

Stem cells are essential in many adult organs to provide a localized renewed source of differentiated cells, thereby maintaining tissue homeostasis; they reside in "niches" in specific anatomical locations which contribute to their proper maintenance and function. The *D. melanogaster* ovary contains two main stem cell populations, the germline (GSC) and **follicle stem cells** (FSC), which collectively give rise to the nurse cells, oocyte, and follicle cells of the mature egg chamber. Each stem cell population resides in a unique, specialized niche containing several types of support cells (reviewed in ref. 6).

The niche microenvironment is essential for the regulated balance between stem cell self-renewal and differentiation. In the case of ovarian stem cell niches, this is achieved by both an array of secreted signaling molecules and direct adhesive connections between stem cells and their niche components ([7, 8] and reviewed in refs. 9, 10). The germline stem cell niche resides at the anterior tip of the germarium; it contains 2–3 GSCs and their support cells, the **cap** (CC) and TF cells [9] (Fig. 2a). GSCs can be reliably identified by their direct anchorage to CCs, and by the presence of an anteriorly localized spectrosome (also known as the fusome in cystocytes). In addition to CCs, the GSCs require **escort cells** (ECs, also known as inner germarial sheath cells) for their regulated differentiation; ECs are glial-like cells which surround germline cysts with cytoplasmic processes, preventing adjacent cysts from making direct contact [11, 12]. In the anterior half of the germarium, germline cysts are surrounded by ECs before they migrate posteriorly and become ensheathed by an epithelial follicle cell layer [12]. While CCs act to prevent GSC differentiation and promote self-renewal, the ECs support their differentiation [13]. Collectively, the CCs, TFs, and ECs constitute the complete niche for GSCs (reviewed in ref. 14).

Technical advances in live tissue culture have made it possible to visualize ovarian stem cells in their in vivo niche environments [15]. This has yielded insight into the dynamic interactions among stem cells and their niche components, which would otherwise be impossible to elucidate from fixed samples. For example, it was recently demonstrated by live imaging that ECs do not migrate with their encircled cyst, but rather use their cellular extensions to "pass" developing cysts posteriorly through the germarium [15].

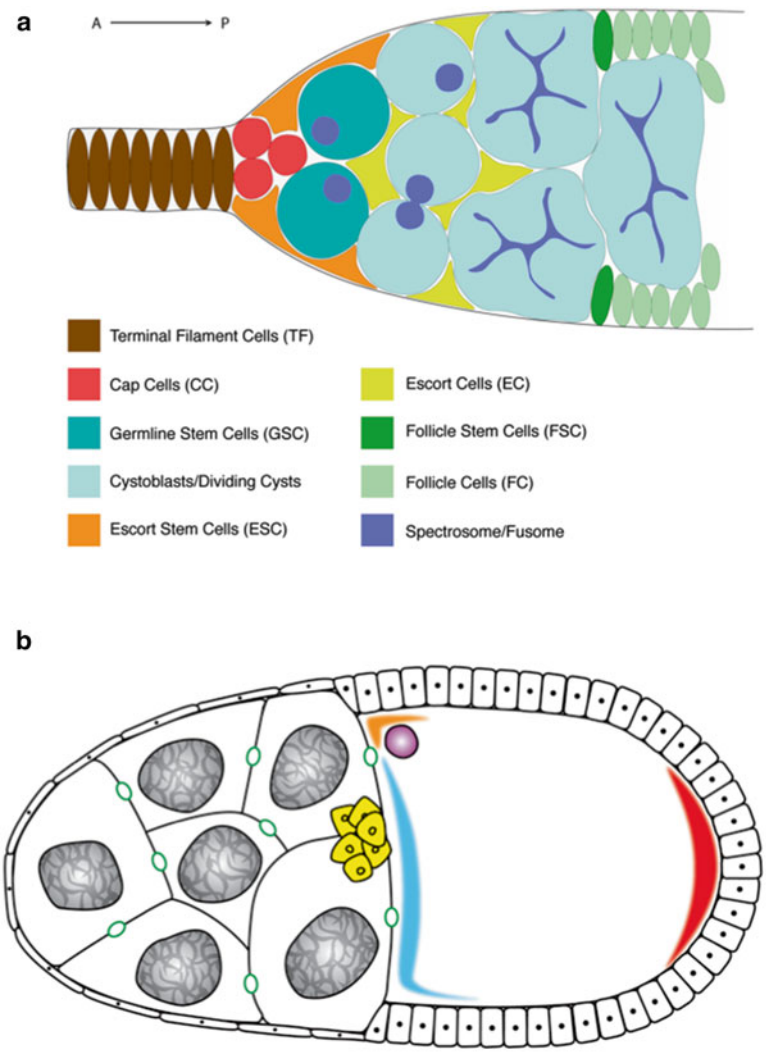

Fig. 2 The germarium and mid-stage egg chamber: Structure and cell types. (**a**) A diagram of the cells housed in the germarium. They illustrate the initial GSC division, formation of the germline cyst, and its enclosure by a layer of follicle cells. Each cell type is denoted by its corresponding color in the key. (**b**) During stage 10, the oocyte encompasses about 50 % of the egg chamber, with the follicle cells surrounding the oocyte having a columnar morphology, in contrast to the squamous follicle cells covering the nurse cells compartment. Ring canals (*green*) bridge the cytoplasm of adjacent nurse cells and the oocyte. At this stage, border cells (*yellow*) have completed their migration from the anterior of the egg chamber towards the oocyte. The oocyte nucleus (*purple*) is localized to the dorsal anterior quadrant, along with *gurken* mRNA (*orange*). *bicoid* (*blue*) and *oskar* (*red*) mRNAs are localized at the anterior and posterior cortex of the oocyte, respectively

3 Cystoblast Division, Oocyte Differentiation, and Formation of the Egg Chamber

A differentiated GSC is termed a **cystoblast** (CB); this CB will divide a total of four times to produce 16 **cystocytes**. Each mitotic division is accompanied by incomplete cytokinesis, forming intercellular cytoplasmic bridges near the mitotic spindle called ring canals [16]. The invariant pattern of cystocyte division and ring canal formation was dissected in the 1960s through light and electron microscopy of sectioned ovaries [16]. Central to this process is the **fusome**, a specialized cytoplasmic organelle composed of skeletal membranous proteins, which helps form and maintain ring canals following each mitotic division (reviewed in refs. 17, 18). The nurse cell ring canals are composed of F-actin and accessory proteins [19], including the actin-binding protein Anillin, which is required for the earliest stages of ring canal development in the egg chamber [20]. Additional proteins are localized to the actin rings and necessary for later stages of nurse cell formation [21].

The determination of the oocyte from among the 16 cells of the cyst involves a series of "symmetry breaking" events beginning at the first CB division. The germarium is divided into discrete regions, which indicate the developmental stage of the nascent germline cyst and its oocyte. Region 1 of the germarium contains the GSC niche and germline cysts of 2, 4, or 8 cells; region 2a contains 16 cell germline cysts in which two pro-oocytes are determined [22]. At the time of egg chamber entry into region 2b of the germarium, the oocyte has been specified and can be distinguished by the presence of several mRNA and protein markers [23–25]. An intact, polarized microtubule (MT) cytoskeleton is also required for differentiation of the oocyte, as well as the localization of oocyte-specific markers. In the absence of an intact MT cytoskeleton, such as following colchicine treatment, the oocyte fails to differentiate and an egg chamber containing 16 nurse cells is formed. One model for oocyte differentiation proposes that the oocyte is always formed from the cystoblast inheriting the most fusome from the first mitotic division [26]. In region 3 of the germarium, the germline cyst (egg chamber) is almost completely ensheathed by an epithelial follicle cell layer. The budding of the egg chamber from the germarium marks stage 1 of oogenesis (reviewed in ref. 27).

4 Follicle Cell Development

The somatic follicle cells of the egg chamber originate from a pair of stem cell niches, positioned laterally on each side of the germarium between regions 2a and 2b [28]. These niches contain the follicle stem cells and make direct contact with ECs that are required for

maintenance of the FC niche [29]. There is regulatory overlap between the GSC and FSC niches, as FSCs also require secreted signaling molecules from the CCs to maintain their self-renewal capacity [30–32]. Three distinct types of follicle cell are formed during egg chamber development: **polar cells**, **stalk cells**, and **epithelial follicle cells** [33]. Polar cells are located at the anterior and posterior tips of each egg chamber, while stalk cells connect and bridge adjacent egg chambers; both populations originate from the same precursor follicle cell lineage [34]. By the end of stage 5, there are two polar cells at each egg chamber terminus; these cells, along with the TGF-α homolog Gurken protein, participate in signaling events that determine the egg chamber posterior pole and induce the reorganization of the MT cytoskeleton during mid-oogenesis [35].

The epithelial follicle cells ensheath the entire egg chamber and compose the bulk of the total follicle cell population; beginning at stage 1 of oogenesis, they can be distinguished on the basis of specific protein markers [36]. These cells are further subdivided into two categories: **terminal follicular cells**, which are contained within an area of ~10 cell diameters from each egg chamber pole, and **mainbody follicular cells** which cover the lateral surface area of the germline cyst (reviewed in ref. 33). The terminal follicle cells are specified by secreted signals from polar cells [37]. Until stage 6, the follicle cells proliferate by mitosis giving rise to a maximum number of ~1000 cells surrounding the egg chamber [38].

5 Cell Migration and Egg Chamber Morphogenesis

The development of a complex structure such as the egg chamber requires cell migratory and morphogenetic events; at various developmental stages, different cell populations within the egg chamber contribute to processes that are necessary for egg chamber development. One such migratory event is the long-range movement of **border cells** during mid-to-late oogenesis. Border cells are specified from a small population of terminal follicle cells at the egg chamber anterior, via secretion by adjacent polar cells of the Unpaired (Upd) ligand [39]. This population of 6–8 cells then detaches from their neighboring FCs, migrates between nurse cells towards the egg chamber posterior, and inserts into the dorsal side of the oocyte to form the micropyle [40]. Recent developments in ex vivo culturing techniques and live imaging have made border cell migration a popular model for the study of cell movement in general, as well as the related process of cancer metastasis [41].

During the same developmental time period as border cell migration, the epithelial follicle cells also undergo migration as well as morphological change. Before stage 9, most FCs are cuboidal in shape (reviewed in ref. 42). The mainbody follicular

cells migrate posteriorly to surround the oocyte, at the same time adopting a columnar morphology [37]. These cells then secrete eggshell components onto the underlying oocyte membrane [33]. The anterior terminal FCs undergo a "flattening" that creates a squamous morphology, covering the nurse cell compartment of the egg chamber; this flattening event involves a remodeling of existing cell junctions [43]. Following these migratory and cell shape changes during stages 9–10, there is a characteristic demarcation between squamous and columnar FC morphologies at the nurse cell-oocyte junction [42].

One additional and striking example of a large-scale morphogenetic change during oogenesis is the recently characterized mechanism by which the egg chamber progressively elongates along its A-P axis. Through live imaging, it was demonstrated that the follicular epithelium rotates circumferentially around the A-P axis of the egg chamber, in the process depositing a polarized matrix of collagen and other extracellular matrix proteins. This matrix acts as a "corset" which physically constricts the egg chamber and causes its elongation in the A-P direction ([44] and reviewed in refs. 45, 46).

6 Cell Cycle Regulation and Meiosis

The several distinct cell types of the ovary differ in the regulation of their cell cycles. However, one similarity between the nurse and follicle cells is their use of endocycles (also known as endoreduplication or endoreplication): DNA synthesis (S) and gap phases without an intervening mitosis or cell division (reviewed in refs. 47, 48). The resulting polyploidy allows cells to increase their quantity of mRNA and protein production, which is essential for oocyte growth and development. Follicle cells typically undergo six to eight endocycles, while nurse cells undergo 10–12 ([49] and reviewed in ref. 50). Beginning at stage 10b, the follicle cells surrounding the oocyte cease normal endocycles and begin gene amplification cycles (this event is termed the E/A switch). Four specific genomic loci, encoding genes involved in chorion (eggshell) and vitelline membrane synthesis, are amplified from 4 to 80-fold [47, 51]. This allows for the production of high levels of chorion-related proteins.

The oocyte undergoes both developmental maturation and meiosis throughout the course of oogenesis, and these processes are intimately linked. Meiotic double-stranded breaks must be repaired in order to maintain the integrity of the MT cytoskeleton and proper translational control of localized mRNAs [52, 53]. The balance of oocyte differentiation and progression through meiosis is achieved by two major meiotic checkpoints in oogenesis. Prophase I of meiosis begins early in egg chamber development, in

region 2a of the germarium, and is indicated by the presence of the synaptonemal complex in the two pro-oocytes (reviewed in refs. 54, 55). Beginning at stage 5, the oocyte arrests in diplotene stage of prophase I; this arrest lasts until roughly stage 13, at which point meiosis progresses to metaphase I [53]. A metaphase I arrest occurs at stage 14, and is maintained until egg activation triggers the resumption and completion of meiosis [53]. Egg activation in *Drosophila* occurs independently of fertilization, and is triggered instead by mechanical pressure on the oocyte during passage into the oviduct [56].

7 mRNA Localization in the Egg Chamber

One of the well-studied processes occurring during *D. melanogaster* oogenesis is the localization and translational control of the key embryonic patterning transcripts. As a result of the pioneering work of Wieschaus and Nusslein-Volhard on the genetic control of *D. melanogaster* embryonic patterning [57], the late 1980s and early 1990s saw a flurry of publications on oocyte-localized mRNAs and their involvement in different aspects of germ plasm formation and embryonic development [58–60]. The mRNAs mainly responsible for patterning of the early embryo, *oskar*, *bicoid*, *gurken*, and *nanos*, are each localized to a distinct compartment of the oocyte before fertilization (reviewed in refs. 61–63) (Fig. 2b). The large size of the egg chamber's nurse cell and oocyte compartments demands that mRNA is transported long distances. This process requires the microtubule and actin cytoskeletons as well as various trans-acting proteins that affect their transport, localization, and stability [64]. Advances in imaging technology have also made this an ideal system for investigating live trafficking of mRNAs [40, 65].

One example of a long-distance traveling transcript is *oskar* (*osk*) mRNA, which encodes the *D. melanogaster* germline determinant. *osk* was cloned in the early 1990s and shown to be localized as mRNA to the oocyte posterior pole [58, 59]. Genetic analyses conducted over the past 20 years have identified some of the protein factors required for transport and translational control of *osk* (and other mRNAs), including the RNA-binding protein Bruno [66, 67]. Live imaging studies of *osk* mRNA have shed light on the dynamic nature of the mRNA transport process [68, 69], and helped to refine models on how the localization of mRNA is achieved in large, complex tissues [70]. The oocyte MT cytoskeleton, and its interactions with mRNA and other cellular cargoes, has also been studied using live imaging techniques [71, 72]. One such study, using fluorescently labeled RNA injected into live oocytes, demonstrated the necessity of Exuperantia protein for the anterior transport of *bicoid* mRNA in the oocyte [73].

8 Formation and Function of Germ plasm

There are two main strategies for specifying germ cells during animal development: cytoplasmic inheritance of germline determinants (also known as preformation) or zygotic induction (epigenesis) of germ cell fate. Most insects use the inductive method, in which germ cells are specified during embryogenesis by signals from adjacent somatic cells [74]. In contrast, the holometabolous insects, including *Drosophila* species, employ the preformative method of germ cell specification. In this developmental mode, germline determinants, in the form of germ plasm (also known as pole plasm), are inherited maternally and specify germ cells during early embryonic development (reviewed in ref. 75).

The germ plasm is a specialized cytoplasm, assembled at the oocyte posterior pole; it has been studied for its role in germ cell determination in insects and other animals for over 100 years ([76] and reviewed in ref. 77). Germ plasm is characterized by the presence of polar granules, non-membranous electron-dense organelles containing mRNA, protein, ribosomes, and noncoding RNA, most notably the mitochondrial large ribosomal RNA (reviewed in refs. 78, 79). Three classes of proteins are highly represented in the *Drosophila* germ plasm: Tudor-domain containing proteins (e.g., Tudor), DEAD-box RNA helicases (e.g., Vasa), and Piwi family proteins (e.g., Aubergine) (reviewed in ref. 80). In addition, interactions between Tudor domain and Piwi proteins are important for assembly of the germplasm in *Drosophila* [81].

One of the critical upstream factors required for germ plasm formation is *osk* mRNA. Upon its localization to the oocyte posterior, *osk* is translated. Genetic manipulations or mutations causing mislocalization of *osk* to the oocyte anterior result in ectopic formation of germ cells at the anterior of the embryo ([82] and reviewed in refs. 83, 84). The use of two alternative translation start sites in *osk* mRNA produces two Oskar protein isoforms: Short Osk and Long Osk. The short isoform initiates formation of the germ plasm ([85] and reviewed in refs. 27, 78, 86), while Long Osk is required for the posterior anchoring of both Short Osk and *osk* mRNA. Loss of Long Osk from egg chambers causes dispersion of Short Osk from the oocyte posterior pole and a reduced number of pole cells formed during embryogenesis [87]. Classic transplantation experiments, in which a fraction of early embryonic germ plasm is transferred to the anterior pole of a separate embryo, first demonstrated the sufficiency of germ plasm for germ cell specification [88].

The germ plasm's functional role begins ~1.5 h into embryonic development, at which point ~10 pole cells are formed from the cellularization of posteriorly localized nuclei and the surrounding germline determinants. These are the first cells formed in the

blastoderm embryo; they will be carried into the embryo during gastrulation and eventually migrate to form the primordial germ cells of the gonad (reviewed in ref. 84). The newly formed PGCs will differentiate into sperm or egg depending on the zygote's sex, and participate in the formation of the next generation.

9 Approaches for Manipulating Gene Expression in the Ovary

One of the biggest strengths of *D. melanogaster* as a model system is its variety of advanced genetic tools. Below, we review a few of the most widely used tools for studying gene function and development in the ovary.

9.1 The Use of P elements for Mutagenesis and Gene Transfer in Drosophila

Forward genetic screens often involve the use of chemical agents or transposons to induce mutations in DNA sequence, which are then analyzed for their phenotypic effects on the organism. In *D. melanogaster*, the most popular chemical mutagen has been ethyl methanesulfonate (EMS), due to its ease of use and efficient induction of random point mutations (reviewed in ref. 89). An alternative to chemical mutagenesis is the use of mobile genetic elements (transposons) to transpose to new genomic locations and in the process disrupt gene function (reviewed in ref. 90). While many transposons exist in flies, the most commonly used has been the *P* element. A wild-type *P* element consists of a pair of terminal inverted repeats flanking the *P transposase* coding sequence, both of which are necessary for transposition. DNA sequences of interest can be placed between the *P* element inverted repeats and transformed into random locations in the fly genome; removing the transposase component, and instead supplying it in *trans* on a donor plasmid, allows control of the *P* element's mobilization [90]. Since the first use of *P* elements for gene transfer in the early 1980s [91, 92], this transposon has become the main workhorse of *D. melanogaster* genetic engineering.

9.2 The Gal4-UAS System

9.2.1 General Principle of Operation

One of the more versatile and widely used genetic tools available in *D. melanogaster* is the Gal4-UAS system. This two-component system for inducible activation of gene expression originated in yeast, and was subsequently adapted to drive tissue-specific gene expression in flies [93]. The operating principle of this system is simple and consists of two parts: (1) the transcriptional activator protein Gal4, which selectively binds (2) upstream activation sequences (UAS) in DNA, thereby activating transcription of a downstream gene. The system as used in flies consists of a "driver" line, expressing a Gal4-encoding transgene under the control of tissue-specific promoter or enhancer elements, and a Gal4-responsive "UAS" line containing a gene of interest downstream of five or more tandem UAS sites (Fig. 3a). A simple genetic cross of these two lines will

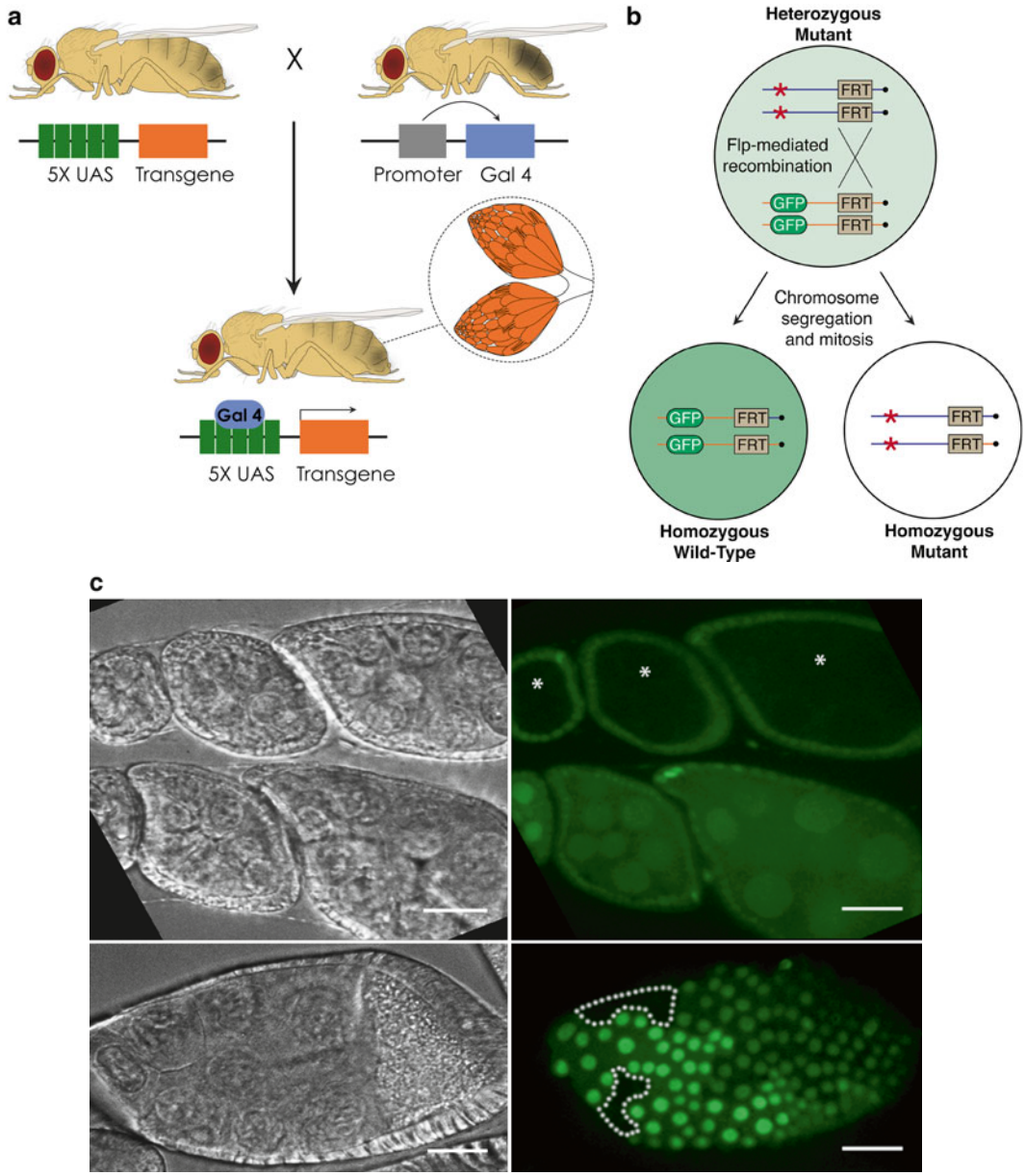

Fig. 3 The Gal4-UAS and Flp-FRT systems: Principles of operation. (**a**) A female fly bearing a transgene under UAS control is crossed to a male fly containing a Gal4 transgene under the control of a tissue-specific promoter (in this example, a maternal promoter expressing at all stages of oogenesis). The progeny of the cross displays ovary-specific expression of the transgene, indicated by the *orange signal*. (**b**) Use of the Flp-FRT recombination system for creating homozygous mutant clones in the ovary. An original heterozygous mutant cell in G2 phase is shown. The induction of Flp recombinase activates recombination between homologous FRT sites of non-sister chromatids. Following mitosis and cell division, one daughter cell is homozygous for the mutation of interest (*red asterisk*) while the other daughter cell is homozygous WT (GFP). (**c**) Examples of germline (*top*) and follicle cell (*bottom*) clones in the ovary. The presence of a homozygous mutant clone [*white asterisk* (*top*); *white broken line* (*bottom*)] is indicated by loss of the GFP signal. Scale bar is 25 μm

yield progeny with the desired tissue-specific expression pattern of the gene of interest (reviewed in ref. 94).

The modular nature of this system, with each transgene carried in a separate fly line, has many advantages. The specific requirement of Gal4 protein for UAS activation means that UAS-transgenes encoding toxic or lethal gene products can be stably maintained in a fly stock without deleterious effects. In addition, a single Gal4 driver line can be mated with thousands of different UAS lines, and vice versa, to achieve a huge variety of spatio-temporal gene expression patterns [94]. Genes that can be placed under UAS control include fluorescently tagged proteins, double-stranded RNA, or site-specific recombinases (e.g., FLPase and Cre). Currently, there are thousands of Gal4 "driver" lines that have been generated [95–98]. Their level of tissue specificity ranges from ubiquitous expression (e.g., through the use of *Ub* or *Act5C* promoters) to expression in one or a few cells (e.g., used in the central nervous system), depending on the choice of promoter or regulatory elements. Many of these lines, both Gal4 and UAS, are publically available from *Drosophila* stock centers [99–101].

9.2.2 Germline-Specific Caveats of the Gal4-UAS System

Although its general principle of operation applies across all tissues, attention should be paid to a few specific details when using Gal4-UAS in the female germ line. The ability of Gal4-UAS to function in the germ line is a more recent improvement, following the discovery that the basal promoter, terminator, and 3′ UTR sequences of the UAS construct were critical for its proper expression [102]. The UAS vector modified for female germline expression, containing the *P transposase* promoter, *K10* terminator, and 3′ UTR sequence, was named "UASp" [102]. This is in contrast to the standard "UAST" vector that is most commonly used for expression in somatic tissues. An extensive list of characterized Gal4 drivers for use in the female germ line has been recently assembled [103].

9.2.3 Gal4-Inducible RNA Interference (RNAi)

One of the more recently developed and powerful applications of Gal4-UAS is the inducible, tissue-specific activation of RNAi for knockdown of specific mRNA transcripts. This technology is especially useful for the study of genes that are highly pleiotropic or lacking in classical mutant alleles. Two popular consortiums that have designed and stock RNAi lines are the *Drosophila* Transgenic RNAi Project (TRiP) [104] and the Vienna *Drosophila* RNAi Center (VDRC) [100]. While the TRiP has exclusively used a site-specific insertion strategy, via the ΦC31 integrase system, to generate its inducible RNAi lines [105], the VDRC carries both *P* element and ΦC31-mediated insertions [106]. The TRiP has created a few "generations" of vectors containing inducible RNAi transgenes. The most notable difference between these

vectors is their level of expression in somatic versus germline tissues. Therefore, the details of each type of vector must be examined carefully before choosing a fly line for a particular experiment; descriptions of each vector and its components are listed on the TRiP's web page [104].

The large number of existing transgenic RNAi stocks has provided a platform for high-throughput loss of function screens in ovaries and other tissues [107–109]. Inducible RNAi is now a commonly used tool for studying gene function and development in *D. melanogaster* ovaries [110–112]. In principle, a specific mRNA transcript can be knocked down in any tissue(s) for which there is an appropriate Gal4 line. A myriad of additional applications of Gal4-UAS has been devised by using different combinations of recombinases and fluorescent markers ([113] and reviewed in ref. 114).

9.3 Mosaic Analysis Using the Flp-FRT System

Mosaic analysis is an extremely valuable tool for studying gene function in a developing organism; it allows the production of homozygous mutant cells in a heterozygous mutant animal [115]. Traditionally, the use of mosaic analysis in *D. melanogaster* was a laborious and inefficient process. Ionizing radiation could be used to induce mitotic recombination between non-sister chromatids [116]; however, the efficiency of this process was very low (~1 %), the recombination events occurred at random locations, and the high levels of radiation often caused tissue damage to the fly. The later incorporation of a yeast site-specific recombination system, FLPase (Flp) and its FRT target sites (FLPase recombination targets), allowed the restriction of mitotic recombination to a single, known chromosome arm and greatly increased its efficiency [117].

Performing mosaic analysis with the Flp-FRT system typically involves crossing a mutation of interest, carried on an FRT chromosome, in *trans* to a homologous FRT chromosome bearing a fluorescent or histological marker (e.g., GFP or LacZ, respectively) (Fig. 3b). On a separate chromosome, either Gal4, a heat-shock promoter, or a tissue-specific promoter can drive the expression of Flp. In the progeny of this cross, mitotic recombination will occur between the two FRT sites; clones that are homozygous for the mutation of interest will be produced, and can be identified by their lack of visual marker. In the context of a specific tissue, the homozygous mutant clones will be surrounded by cells that are either WT homozygous (also descended from mitotically recombined cells) or heterozygous (Fig. 3c).

As egg chambers are multicellular structures containing a shared cytoplasm, a distinction must be made between transient and stem cell derived clones. Transient clones are produced when a mitotic recombination event takes place within the germline cyst *after* the first cystoblast division. In this case, the population of

nurse cells within one egg chamber will contain a mixture of genotypes: homozygous WT, homozygous mutant, and heterozygous. The visual marker protein, along with other gene products, can diffuse freely through ring canals and confound one's ability to unambiguously determine the genotype of each nurse cell. Therefore only egg chambers that completely lack the visual marker in each germline cell, indicating that they are derived from a GSC recombination event, would be examined. Similarly, stem cell derived and transient clones can be generated in the FCs, which also contain ring canals that bridge small clusters of cells [118].

9.4 The Dominant Female-Sterile Method for Generating Germline Mosaics

One alternative version of germline mosaic analysis is the dominant female-sterile (DFS) technique: Instead of using visual markers to identify clonal cell populations carrying a mutation of interest, a dominant female-sterile allele is used to block the development of non-homozygous mutant egg chambers. There are several dominant female-sterile alleles available, yet the most commonly used is *ovoD1* [119, 120]. The purpose of this technique is to exclusively permit the formation of egg chambers that are homozygous for the mutation of interest (i.e., cells that have lost *ovoD1*); egg chambers carrying cells that are heterozygous or homozygous for the *ovoD1* allele degenerate early in development.

The *ovoD1* allele was originally recovered on the X chromosome, and therefore the early use of this technique was limited to studying X-linked mutations. However, by engineering this allele into *P* element vectors and creating transformants on additional chromosomes, this system was later expanded to include analysis of autosomal mutations [121]. The main benefit of the DFS method, as opposed to using the fluorescent or histological markers described above, is for obtaining a uniform population of embryos that are maternally homozygous for a mutation of interest. In this way, the putative maternal effects of a gene can be analyzed by genetic or biochemical methods.

9.5 Emerging Technologies for Genome Engineering: The CRISPR/Cas System

A recent development in genome engineering technology, which has gained popularity in *Drosophila* and other model organisms, is CRISPR, for "Clustered Regularly Interspaced Palindromic Repeats". These genomic repeats are the basis of a bacterial and archaeal RNA-based immune system through which organisms acquire the ability to recognize invading genomic material [122]. Adaptive immunity is built over time by incorporating small DNA repeats, captured from viral genomes or plasmids, into these specialized genomic clusters. CRISPR-associated (Cas) proteins, in complex with small guide RNAs transcribed from these clusters, are guided to homologous sequences to create double-stranded DNA (dsDNA) breaks. There are three known types of CRISPR systems, with the best characterized being Type II; these systems,

as well as the mechanistic details of CRISPR repeat acquisition and function, have been characterized (reviewed in refs. 122, 123).

CRISPR's great value as a genome-engineering tool is its ability to generate dsDNA breaks at specific genomic locations in a variety of model systems [124]. These breaks then serve as an entry point for different genome modification protocols (non-homologous end joining, gene targeting with a dsDNA donor template, etc.). A template encoding a chimeric RNA (chiRNA), which combines the function of both guide and *trans-activating* CRISPR RNA (tracrRNA), is designed to target a specific DNA sequence. The chiRNA and Cas-expressing vectors are co-transfected or transformed, depending on the model system; the expression of both transgenes results in targeting of the desired DNA sequence (reviewed in ref. 125). The use of sequence-specific DNA breaks greatly improves the efficiency of knockout creation in mammalian cell culture, and organisms such as mice and flies. More recent technical improvements in the efficiency and specificity of guide RNA targeting have been applied in *D. melanogaster* (reviewed in ref. 126). This system is gaining popularity as a method for creating transgenic flies, with gene knockout lines having been generated using both non-homologous end joining (NHEJ) and homology-directed repair with a dsDNA donor template [127, 128]. One additional technical advance has been the creation of transgenic lines stably expressing germline-driven Cas9, dramatically increasing the efficiency of germline CRISPR targeting [128, 129]. Some of these lines are available from the Bloomington *Drosophila* Stock Center [99]. More information on the CRISPR system is available online, including the "CRISPR design tool" (based on [130]), discussion forum, FAQ, and troubleshooting [131].

10 Conclusion

Drosophila melanogaster oogenesis continues to serve as an important model system for understanding fundamental aspects of cell biology and development; in addition to its large variety of biological topics being actively investigated, it remains at the cutting edge of technological innovation. Techniques such as live imaging of cell migration, high-resolution light and electron microscopic imaging of mRNA trafficking, and genetic/genomic manipulations with site-specific recombinases and transgenic RNAi have all been applied, increasing the depth of our biological knowledge. Moving forward, the study of the *Drosophila* ovary is poised to further advance our understanding of basic mechanisms in eukaryotic biology.

Acknowledgements

We thank Emily Hudson for assistance with the art included in the figures, and members of the Bratu laboratory for helpful comments on the manuscript. JMM and DPB were supported by an NSF CAREER Award to DPB.

References

1. Roote J, Prokop A (2013) How to design a genetic mating scheme: a basic training package for *Drosophila* genetics. G3 (Bethesda) 3:353–358
2. Telfer WH (1975) Development and physiology of the oocyte-nurse cell syncytium. Adv Insect Physiol 11:223–319
3. Tworzydlo W, Bilinski SM, Kocarek P et al (2010) Ovaries and germline cysts and their evolution in Dermaptera (Insecta). Arthropod Struct Dev 39:360–368
4. Swevers L, Raikhel AS, Sappington TW et al (2005) Vitellogenesis and post-vitellogenic maturation of the insect ovarian follicle. In: Gilbert L (ed) Comprehensive molecular insect science, vol 1. Elsevier BV, Oxford, pp 87–155
5. Godt D, Laski FA (1995) Mechanisms of cell rearrangement and cell recruitment in *Drosophila* ovary morphogenesis and the requirement of *bric à brac*. Development 121:173–187
6. Voog J, Jones DL (2010) Stem cells and the niche: a dynamic duo. Cell Stem Cell 6:103–115
7. Lopez-Onieva L, Fernandez-Minan A, Gonzalez-Reyes A (2008) Jak/Stat signalling in niche support cells regulates dpp transcription to control germline stem cell maintenance in the *Drosophila* ovary. Development 135:533–540
8. Forbes AJ, Lin H, Ingham PW et al (1996) *hedgehog* is required for the proliferation and specification of ovarian somatic cells prior to egg chamber formation in *Drosophila*. Development 122:1125–1135
9. Spradling A, Fuller MT, Braun RE et al (2011) Germline stem cells. Cold Spring Harb Perspect Biol. doi:10.1101/cshperspect.a002642
10. Losick VP, Morris LX, Fox DT et al (2011) *Drosophila* stem cell niches: a decade of discovery suggests a unified view of stem cell regulation. Dev Cell 21:159–171
11. King RC (1970) Ovarian development in *Drosophila melanogaster*. Academic, New York
12. Kirilly D, Wang S, Xie T (2011) Self-maintained escort cells form a germline stem cell differentiation niche. Development 138: 5087–5097
13. Decotto E, Spradling AC (2005) The *Drosophila* ovarian and testis stem cell niches: similar somatic stem cells and signals. Dev Cell 9:501–510
14. Xie T (2012) Control of germline stem cell self-renewal and differentiation in the *Drosophila* ovary: concerted actions of niche signals and intrinsic factors. Wiley Interdiscip Rev Dev Biol 2:261–273
15. Morris LX, Spradling AC (2011) Long-term live imaging provides new insight into stem cell regulation and germline-soma coordination in the *Drosophila* ovary. Development 138:2207–2215
16. King RC, Aggarwal SK, Aggarwal U (1968) The development of the *Drosophila* female reproductive system. J Morphol 124: 142–166
17. Roth S, Lynch JA (2009) Symmetry breaking during *Drosophila* oogenesis. Cold Spring Harb Perspect Biol. doi:10.1101/cshperspect.a001891
18. Huynh JR (2005) Fusome as a cell-cell communication channel of *Drosophila* ovarian cyst. In: Baluska F, Volkmann D, Barlow PW (eds) Cell-cell channels. Eurekah Bioscience, Georgetown, TX, pp 1–19
19. Warn RM, Gutzeit HO, Smith L et al (1985) F-actin rings are associated with the ring canals of the *Drosophila* egg chamber. Exp Cell Res 157:355–363
20. Field CM, Alberts BM (1995) Anillin, a contractile ring protein that cycles from the nucleus to the cell cortex. J Cell Biol 131: 165–178
21. Robinson DN, Cant K, Cooley L (1994) Morphogenesis of *Drosophila* ovarian ring canals. Development 120:2015–2025

22. Huynh JR, St Johnston D (2004) The origin of asymmetry: early polarisation of the *Drosophila* germline cyst and oocyte. Curr Biol 14:R438–R449
23. Keyes LN, Spradling AC (1997) The *Drosophila* gene fs*(2)cup* interacts with *otu* to define a cytoplasmic pathway required for the structure and function of germ-line chromosomes. Development 124:1419–1431
24. Lantz V, Chang JS, Horabin JI et al (1994) The *Drosophila* orb RNA-binding protein is required for the formation of the egg chamber and establishment of polarity. Genes Dev 8:598–613
25. Suter B, Romberg LM, Steward R (1989) *Bicaudal-D*, a *Drosophila* gene involved in developmental asymmetry: localized transcript accumulation in ovaries and sequence similarity to myosin heavy chain tail domains. Genes Dev 3:1957–1968
26. de Cuevas M, Spradling AC (1998) Morphogenesis of the *Drosophila* fusome and its implications for oocyte specification. Development 125:2781–2789
27. Riechmann V, Ephrussi A (2001) Axis formation during *Drosophila* oogenesis. Curr Opin Genet Dev 11:374–383
28. Nystul T, Spradling A (2007) An epithelial niche in the *Drosophila* ovary undergoes long-range stem cell replacement. Cell Stem Cell 1:277–285
29. Sahai-Hernandez P, Nystul TG (2013) A dynamic population of stromal cells contributes to the follicle stem cell niche in the *Drosophila* ovary. Development 140:4490–4498
30. Song X, Xie T (2003) *wingless* signaling regulates the maintenance of ovarian somatic stem cells in *Drosophila*. Development 130:3259–3268
31. Kirilly D, Spana EP, Perrimon N et al (2005) BMP signaling is required for controlling somatic stem cell self-renewal in the *Drosophila* ovary. Dev Cell 9:651–662
32. Bolivar J, Pearson J, Lopez-Onieva L et al (2006) Genetic dissection of a stem cell niche: the case of the *Drosophila* ovary. Dev Dyn 235:2969–2979
33. Wu X, Tanwar PS, Raftery LA (2008) *Drosophila* follicle cells: morphogenesis in an eggshell. Semin Cell Dev Biol 19:271–282
34. Tworoger M, Larkin MK, Bryant Z et al (1999) Mosaic analysis in the *Drosophila* ovary reveals a common hedgehog-inducible precursor stage for stalk and polar cells. Genetics 151:739–748
35. Roth S, Neuman-Silberberg FS, Barcelo G et al (1995) *cornichon* and the EGF receptor signaling process are necessary for both anterior-posterior and dorsal-ventral pattern formation in *Drosophila*. Cell 81:967–978
36. Bai J, Montell D (2002) Eyes absent, a key repressor of polar cell fate during *Drosophila* oogenesis. Development 129:5377–5388
37. St Johnston D, Gonzalez-Reyes A (1998) Patterning of the follicle cell epithelium along the anterior-posterior axis during *Drosophila* oogenesis. Development 125:2837–2846
38. Deng WM, Althauser C, Ruohola-Baker H (2001) Notch-Delta signaling induces a transition from mitotic cell cycle to endocycle in *Drosophila* follicle cells. Development 128: 4737–4746
39. Yoon WH, Meinhardt H, Montell DJ (2011) miRNA-mediated feedback inhibition of JAK/STAT morphogen signalling establishes a cell fate threshold. Nat Cell Biol 13: 1062–1069
40. He L, Wang X, Montell DJ (2011) Shining light on *Drosophila* oogenesis: live imaging of egg development. Curr Opin Genet Dev 21:612–619
41. Prasad M, Wang X, He L et al (2011) Border cell migration: a model system for live imaging and genetic analysis of collective cell movement. Methods Mol Biol 769:277–286
42. Dobens L, Raftery LA (2008) Integration of epithelial patterning and morphogenesis in *Drosophila* ovarian follicle cells. Dev Dyn 218:80–93
43. Grammont M (2007) Adherens junction remodeling by the Notch pathway in *Drosophila melanogaster* oogenesis. J Cell Biol 177:139–150
44. Haigo SL, Bilder D (2011) Global tissue revolutions in a morphogenetic movement controlling elongation. Science 331:1071–1074
45. Bilder D, Haigo SL (2012) Expanding the morphogenetic repertoire: perspectives from the *Drosophila* egg. Dev Cell 22:12–23
46. Gates J (2012) *Drosophila* egg chamber elongation: insights into how tissues and organs are shaped. Fly 6:213–227
47. Claycomb JM, Orr-Weaver TL (2005) Developmental gene amplification: insights into DNA replication and gene expression. Trends Genet 21:149–162
48. Royzman I, Orr-Weaver TL (1998) S phase and differential DNA replication during *Drosophila* oogenesis. Genes Cells 3:767–776
49. Dej KJ, Spradling AC (1999) The endocycle controls nurse cell polytene chromosome structure during *Drosophila* oogenesis. Development 126:293–303

50. Nordman J, Orr-Weaver TL (2012) Regulation of DNA replication during development. Development 139:455–464
51. Klusza S, Deng WM (2011) At the crossroads of differentiation and proliferation: precise control of cell-cycle changes by multiple signaling pathways in *Drosophila* follicle cells. Bioessays 33:124–134
52. Kronja I, Orr-Weaver TL (2011) Translational regulation of the cell cycle: when, where, how and why? Philos Trans R Soc Lond B Biol Sci 366:3638–3652
53. Von Stetina JR, Orr-Weaver TL (2011) Developmental control of oocyte maturation and egg activation in metazoan models. Cold Spring Harb Perspect Biol. doi:10.1101/cshperspect.a005553
54. Bosco G, Orr-Weaver TL (2002) The cell cycle during oogenesis and early embryogenesis in *Drosophila*. Adv Dev Biol Biochem. doi:10.1016/S1569-1799(02)12026-0
55. Smith PA, King RC (1968) Genetic control of synaptonemal complexes in *Drosophila melanogaster*. Genetics 60:335–351
56. Mahowald AP, Goralski TJ, Caulton JH (1983) In vitro activation of *Drosophila* eggs. Dev Biol 98:437–445
57. Nusslein-Volhard C, Wieschaus E (1980) Mutations affecting segment number and polarity in *Drosophila*. Nature 287:795–801
58. Ephrussi A, Dickinson LK, Lehmann R (1991) *oskar* organizes the germ plasm and directs localization of the posterior determinant *nanos*. Cell 66:37–50
59. Kim-Ha J, Smith JL, Macdonald PM (1991) *oskar* mRNA is localized to the posterior pole of the *Drosophila* oocyte. Cell 66:23–35
60. St Johnston D, Beuchle D, Nusslein-Volhard C (1991) *staufen*, a gene required to localize maternal RNAs in the *Drosophila* egg. Cell 66:51–63
61. Kugler JM, Lasko P (2009) Localization, anchoring and translational control of *oskar*, *gurken*, *bicoid* and *nanos* mRNA during *Drosophila* oogenesis. Fly 3:15–28
62. Lasko P (2011) Posttranscriptional regulation in *Drosophila* oocytes and early embryos. Wiley Interdiscip Rev RNA 2:408–416
63. Martin KC, Ephrussi A (2009) mRNA localization: gene expression in the spatial dimension. Cell 136:719–730
64. Cooperstock RL, Lipshitz HD (2001) RNA localization and translational regulation during axis specification in the *Drosophila* oocyte. Int Rev Cytol 203:541–566
65. Becalska AN, Gavis ER (2009) Lighting up mRNA localization in *Drosophila* oogenesis. Development 136:2493–2503
66. Chekulaeva M, Hentze MW, Ephrussi A (2006) Bruno acts as a dual repressor of *oskar* translation, promoting mRNA oligomerization and formation of silencing particles. Cell 124:521–533
67. Vardy L, Orr-Weaver TL (2007) Regulating translation of maternal messages: multiple repression mechanisms. Trends Cell Biol 17:547–554
68. Bratu DP, Cha BJ, Mhlanga MM et al (2003) Visualizing the distribution and transport of mRNAs in living cells. Proc Natl Acad Sci U S A 100:13308–13313
69. Mhlanga MM, Bratu DP, Genovesio A et al (2009) *In vivo* colocalisation of *oskar* mRNA and trans-acting proteins revealed by quantitative imaging of the *Drosophila* oocyte. PLoS One. doi:10.1371/journal.pone.0006241
70. Zimyanin VL, Belaya K, Pecreaux J et al (2008) In vivo imaging of *oskar* mRNA transport reveals the mechanism of posterior localization. Cell 134:843–853
71. Parton RM, Hamilton RS, Ball G et al (2011) A PAR-1-dependent orientation gradient of dynamic microtubules directs posterior cargo transport in the *Drosophila* oocyte. J Cell Biol 194:121–135
72. Sinsimer KS, Lee JJ, Thiberge SY et al (2013) Germ plasm anchoring is a dynamic state that requires persistent trafficking. Cell Rep 5: 1169–1177
73. Cha BJ, Koppetsch BS, Theurkauf WE (2001) In vivo analysis of *Drosophila bicoid* mRNA localization reveals a novel microtubule-dependent axis specification pathway. Cell 106:35–46
74. Ewen-Campen B, Donoughe S, Clarke DN et al (2013) Germ cell specification requires zygotic mechanisms rather than germ plasm in a basally branching insect. Curr Biol 23:835–842
75. Extavour CG, Akam M (2003) Mechanisms of germ cell specification across the metazoans: epigenesis and preformation. Development 130:5869–5884
76. Hegner RW (1908) Effects of removing the germ-cell determinants from the eggs of some chrysomelid beetles. Preliminary report. Biol Bull 16:19–26
77. Kloc M, Bilinksi S, Etkin LD (2004) The balbiani body and germ cell determinants: 150 years later. Curr Top Dev Biol 59:1–36
78. Mahowald AP (2001) Assembly of the *Drosophila* germ plasm. Int Rev Cytol 203: 187–213
79. Kobayashi S, Amikura R, Okada M (1994) Localization of mitochondrial large rRNA in germinal granules and the consequent segregation of germ line. Int J Dev Biol 38:193–199

80. Arkov AL, Ramos A (2010) Building RNA-protein granules: insight from the germline. Trends Cell Biol 20:482–490
81. Kirino Y, Vourekas A, Sayed N et al (2010) Arginine methylation of Aubergine mediates Tudor binding and germ plasm localization. RNA 16:70–78
82. Ephrussi A, Lehmann R (1992) Induction of germ cell formation by *oskar*. Nature 358: 387–392
83. Rongo C, Lehmann R (1996) Regulated synthesis, transport and assembly of the *Drosophila* germ plasm. Trends Genet 12: 102–109
84. Starz-Gaiano M, Lehmann R (2001) Moving towards the next generation. Mech Dev 105:5–18
85. Markussen FH, Michon AM, Breitwieser W et al (1995) Translational control of *oskar* generates Short OSK, the isoform that induces pole plasm assembly. Development 121:3723–3732
86. Saffman EE, Lasko P (1999) Germline development in vertebrates and invertebrates. Cell Mol Life Sci 55:1141–1163
87. Vanzo NF, Ephrussi A (2002) Oskar anchoring restricts pole plasm to the posterior of the *Drosophila* oocyte. Development 129:3705–3714
88. Illmensee K, Mahowald AP (1974) Transplantation of posterior polar plasm in *Drosophila*. Induction of germ cells at the anterior pole of the egg. Proc Natl Acad Sci U S A 71:1016–1020
89. St Johnston D (2002) The art and design of genetic screens: *Drosophila melanogaster*. Nat Rev Genet 3:176–188
90. Venken KJ, Bellen HJ (2014) Chemical mutagens, transposons, and transgenes to interrogate gene function in *Drosophila melanogaster*. Methods 68:15–28
91. Spradling AC, Rubin GM (1982) Transposition of cloned P elements into *Drosophila* germ line chromosomes. Science 218:341–347
92. Rubin GM, Spradling AC (1982) Genetic transformation of *Drosophila* with transposable element vectors. Science 218:348–353
93. Brand AH, Perrimon N (1993) Targeted gene expression as a means of altering cell fates and generating dominant phenotypes. Development 118:401–415
94. Duffy JB (2002) GAL4 system in *Drosophila*: A fly geneticist's Swiss army knife. Genesis 34:1–15
95. Jory A, Estella C, Giorgianni MW et al (2012) A survey of 6,300 genomic fragments for cis-regulatory activity in the imaginal discs of *Drosophila melanogaster*. Cell Rep 2: 1014–1024
96. Manning L, Heckscher ES, Purice MD et al (2012) A resource for manipulating gene expression and analyzing cis-regulatory modules in the *Drosophila* CNS. Cell Rep 2:1002–1013
97. Pfeiffer BD, Jenett A, Hammonds AS et al (2008) Tools for neuroanatomy and neurogenetics in *Drosophila*. Proc Natl Acad Sci U S A 105:9715–9720
98. Jenett A, Rubin GM, Ngo TT et al (2012) A GAL4-Driver line resource for *Drosophila* neurobiology. Cell Rep 2:991–1001
99. Bloomington *Drosophila* Stock Center. http://flystocks.bio.indiana.edu
100. Vienna *Drosophila* RNAi Center (VDRC). http://stockcenter.vdrc.at/control/main
101. Kyoto *Drosophila* Genetic Resource Center (DGRC). https://kyotofly.kit.jp/cgi-bin/stocks/index.cgi
102. Rørth P (1998) Gal4 in the *Drosophila* female germline. Mech Dev 78:113–118
103. Hudson AM, Cooley L (2014) Methods for studying oogenesis. Methods 68:207–217
104. *Drosophila* Transgenic RNAi Project (TRiP). http://www.flyrnai.org/TRiP-HOME.html
105. Ni JQ, Markstein M, Binari R et al (2008) Vector and parameters for targeted transgenic RNA interference in *Drosophila melanogaster*. Nat Methods 5:49–51
106. Dietzl G, Chen D, Schnorrer F et al (2007) A genome-wide transgenic RNAi library for conditional gene inactivation in *Drosophila*. Nature 448:151–156
107. Czech B, Preall JB, McGinn J et al (2013) A transcriptome-wide RNAi screen in the *Drosophila* ovary reveals factors of the germline piRNA pathway. Mol Cell 50: 749–761
108. Handler D, Meixner K, Pizka M et al (2013) The genetic makeup of the *Drosophila* piRNA pathway. Mol Cell 50:762–777
109. Preall JB, Czech B, Guzzardo PM et al (2012) *shutdown* is a component of the *Drosophila* piRNA biogenesis machinery. RNA 18: 1446–1457
110. McConnell KH, Dixon M, Calvi BR (2012) The histone acetyltransferases CBP and Chameau integrate developmental and DNA replication programs in *Drosophila* ovarian follicle cells. Development 139:3880–3890
111. Geisbrecht ER, Sawant K, Su Y et al (2013) Genetic interaction screens identify a role for Hedgehog signaling in *Drosophila* border cell migration. Dev Dyn 242:414–431

112. Gu T, Elgin SC (2013) Maternal depletion of Piwi, a component of the RNAi system, impacts heterochromatin formation in *Drosophila*. PLoS Genet. doi:10.1371/journal.pgen.1003780
113. Pfeiffer BD, Ngo TT, Hibbard KL et al (2010) Refinement of tools for targeted gene expression in *Drosophila*. Genetics 186:735–755
114. del Valle Rodriguez A, Didiano D, Desplan C (2012) Power tools for gene expression and clonal analysis in *Drosophila*. Nat Methods 9:47–55
115. Xu T, Rubin GM (2012) The effort to make mosaic analysis a household tool. Development 139:4501–4503
116. Patterson JT (1929) The production of mutations in somatic cells of *Drosophila melanogaster* by means of X-rays. J Exp Zool 53:327–372
117. Golic KG, Lindquist S (1989) The FLP recombinase of yeast catalyzes site-specific recombination in the *Drosophila* genome. Cell 59:499–509
118. McLean PF, Cooley L (2013) Protein equilibration through somatic ring canals in *Drosophila*. Science 340:1445–1447
119. Perrimon N (1984) Clonal analysis of dominant female-sterile germline-dependent mutations in *Drosophila melanogaster*. Genetics 108:927–939
120. Perrimon N, Gans M (1983) Clonal analysis of the tissue specificity of recessive female-sterile mutations of *Drosophila melanogaster* using a dominant female-sterile mutation *Fs(1)K1237*. Dev Biol 100:365–373
121. Chou TB, Perrimon N (1996) The autosomal FLP-DFS technique for generating germline mosaics in *Drosophila melanogaster*. Genetics 144:1673–1679
122. Horvath P, Barrangou R (2010) CRISPR/Cas, the immune system of bacteria and archaea. Science 327:167–170
123. Karginov FV, Hannon GJ (2010) The CRISPR system: small RNA-guided defense in bacteria and archaea. Mol Cell 37:7–19
124. Cong L, Ran FA, Cox D et al (2013) Multiplex genome engineering using CRISPR/Cas systems. Science 339:819–823
125. Ran FA, Hsu PD, Wright J et al (2013) Genome engineering using the CRISPR-Cas9 system. Nat Protoc 8:2281–2308
126. Bassett AR, Liu JL (2014) CRISPR/Cas9 and genome editing in *Drosophila*. J Genet Genomics 41:7–19
127. Gratz SJ, Cummings AM, Nguyen JN et al (2013) Genome engineering of *Drosophila* with the CRISPR RNA-guided Cas9 nuclease. Genetics 194:1029–1035
128. Gratz SJ, Ukken FP, Rubinstein CD et al (2014) Highly specific and efficient CRISPR/Cas9-catalyzed homology-directed repair in *Drosophila*. Genetics 196:961–971
129. Port F, Chen HM, Lee T et al (2014) Optimized CRISPR/Cas tools for efficient germline and somatic genome engineering in *Drosophila*. Proc Natl Acad Sci U S A 111:2967–2976
130. Hsu PD, Scott DA, Weinstein JA et al (2013) DNA targeting specificity of RNA-guided Cas9 nucleases. Nat Biotechnol 31:827–832
131. CRISPR Genome-Engineering. http://www.genome-engineering.org/crispr/

Chapter 2

Basic Techniques in *Drosophila* Ovary Preparation

Letitia Thompson, Kristen Randolph, and Amanda Norvell

Abstract

Drosophila melanogaster oogenesis has emerged as an excellent model system to study multiple aspects of eukaryotic cell biology. Ovarian tissue can easily be isolated and analyzed through microscopy or biochemical and molecular biology techniques. Here we describe the isolation of ovarian tissues, techniques to enrich for egg chambers at distinct developmental stages, preparation of protein and nucleic acid extracts, and preparation for microscopic analysis of fixed tissues.

Key words *Drosophila* oogenesis, Ovary dissection, Staging oocytes, Ovary lysate

1 Introduction

Drosophila melanogaster oogenesis has proven to provide a tractable and versatile genetic system in which to study many aspects of cell biology. Each oocyte develops within the context of a cluster of 16 germline-derived cells (oocyte and 15 nurse cells) surrounded by a somatically derived follicular epithelium [1, 2]. Because of their large size and ease of manipulation and culture, the cells of the ovary are an excellent system for microscopic analysis. Furthermore, because of the cytoplasmic connections among the germline cells, this system also provides an opportunity to study intracellular, as well as intercellular transport [3–5]. The follicular epithelial cells surrounding the germline cluster have emerged as a model to study epithelial cell polarity and behavior in the context of normal cellular processes, thus providing insight into how these processes can be deregulated [6–8]. More recently, it has also become apparent that the stem cells that reside in the germarium of the ovary are an excellent system in which to analyze stem cell behaviors and cell–cell communication within their natural niche [9].

Isolated egg chambers are highly suitable for microscopic analysis, both of fixed tissues and live-imaging experiments. The availability of reagents appropriate for fluorescent imaging of

Diana P. Bratu and Gerard P. McNeil (eds.), *Drosophila Oogenesis: Methods and Protocols*, Methods in Molecular Biology, vol. 1328, DOI 10.1007/978-1-4939-2851-4_2,

proteins and nucleic acids, has allowed high resolution analysis of the intracellular distribution and trafficking of molecules within the context of the egg chamber [10, 11]. Additionally, ovarian extracts (protein or RNA) are relatively easy to prepare for biochemical or molecular analyses. However, due to the mosaic nature of the egg chamber, such extracts contain both somatic and germline components, which can complicate these types of studies. Furthermore, oogenesis is a dynamic process and within each egg chamber alterations in chromosome morphology, cytoskeletal organization, and gene expression patterns occur as the oocyte and nurse cells mature. Although it is possible to enrich for egg chambers at particular stages of development, it can be difficult to ensure that egg chamber populations are not somewhat heterogeneous. Thus, when using ovarian extracts for biochemical or molecular experiments, it is important to be aware of the known heterogeneity of the population; somatic and germline derived tissues, as well as potential differences in the maturation or developmental stage of the egg chambers.

2 Materials

2.1 Ovary Dissection Components

1. Flies that have been fed on yeast for 24–48 h.
2. Dissecting Buffer (10× PBS): 80 g of 1.37 M NaCl, 2 g of 27 mM KCl, 14.4 g of 100 mM Na_2HPO_4 (dibasic anhydrous), 2.4 g of 18 mM KH_2PO_4, pH 7.4 (monobasic anhydrous). Combine the ingredients with 800 ml of dH_2O while on a stir plate. After dissolving, adjust the pH to 7.4 with HCl. Add H_2O to bring the solution to 1 L. Autoclave to sterilize and store at room temperature. To make 1× PBS, add 100 ml of 10× PBS into a graduated cylinder with 900 ml of dH_2O.
3. Glass depression slide.
4. Two forceps (Dumont #5).
5. Dissecting microscope.
6. Ice.
7. Kimwipes.

2.2 Late-Staged Egg Chamber Enrichment Components

1. Empty fly stock bottle.
2. Kimwipes.

2.3 Protein Lysate Components

1. Lysis Buffer: 10 mM Tris, pH 7.4, 100 mM NaCl, 2.5 mM $MgCl_2$, 0.5 % Triton™ X-100.
2. Mini-cordless pestle pellet motor.
3. Sterilized pestle pellets.
4. Centrifuge (*see* **Note 1**).

2.4 RNA Extraction Components

1. TRIzol® Reagent (*see* **Note 2**).
2. Mini-cordless pestle pellet motor.
3. Sterilized pestle pellets.
4. Chloroform.
5. Isopropyl alcohol.
6. 70 % ethanol.
7. RNase-free dH_2O.
8. Centrifuge (*see* **Note 1**).
9. DNase (*see* **Note 3**).
10. 10× DNase buffer: 100 mM Tris, 25 mM $MgCl_2$, 5 mM $CaCl_2$, pH 7.6.
11. Water bath or heat block (*see* **Note 4**).

2.5 Tissue Fixation Components

1. 4 % PFA solution: Dilute 16 % paraformaldehyde (EM Grade) in 1× PBS. 4 % PFA can be frozen in 500 µl aliquots.
2. *n*-Heptane.
3. 1× PBS + 0.3 % Triton™ X-100.
4. Nutator.

3 Methods

3.1 Dissection of Ovarian Tissues

1. Feed the flies on yeast 24–48 h before dissecting (*see* **Note 5**).
2. Using a fly pad, anesthetize the flies using CO_2.
3. Fill the depression slide with 1× PBS.
4. Using the forceps, pick up a female fly holding it by the posterior end of the thorax. Submerge it under the PBS (*see* **Note 6**) (Fig. 1a).
5. Using the second pair of forceps, gently pinch the cuticle at the posterior end of the abdomen and pull the intestines and other internal organs out (Fig. 1b).
6. While still holding the thorax of the fly, use the second pair of forceps to push out the ovaries (*see* **Note 7**) (Fig. 1c).
7. Place the ovaries into a microcentrifuge tube with 1× PBS (*see* **Note 8**).
8. Once the dissection is complete, the ovaries can be stored at −80 °C in PBS until further use.
9. For all the subsequent protocols, remove all the PBS before continuing to the next step.

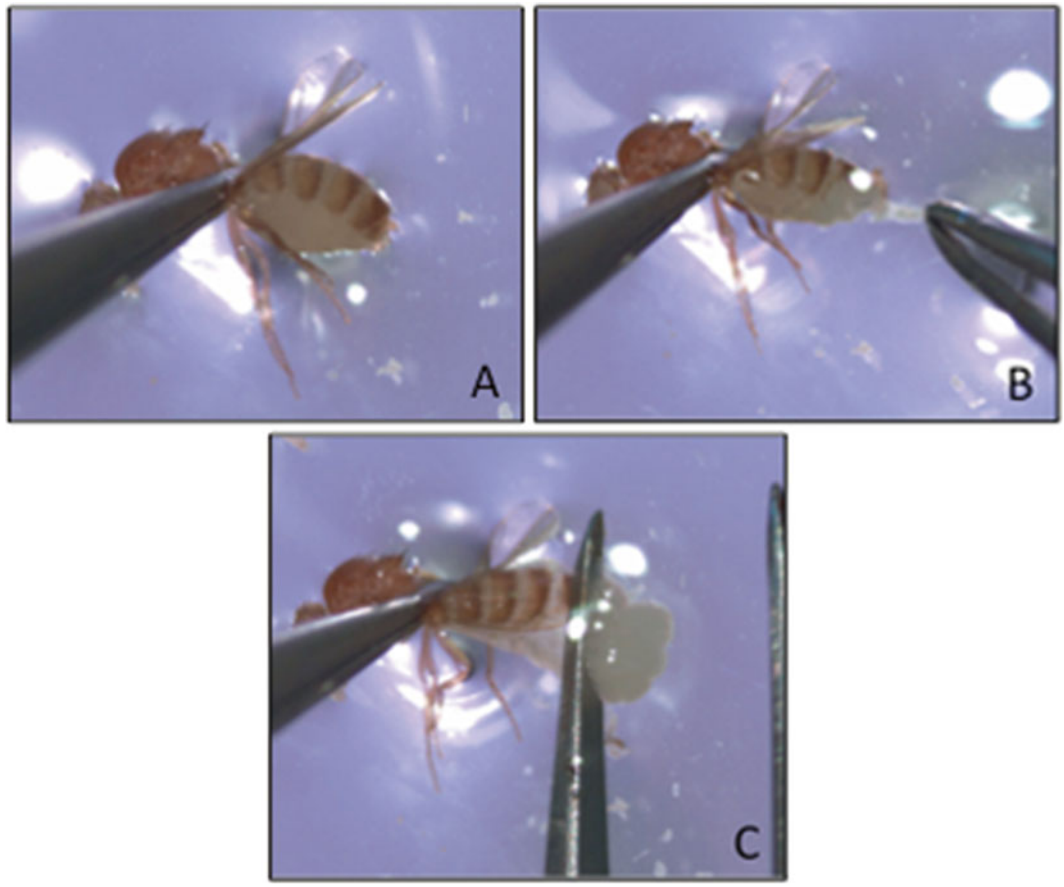

Fig. 1 Ovary dissection. (**a**) Grasp the female firmly at the posterior end of the thorax. (**b**) Using your dominant hand, use a second pair of forceps to gently pinch the posterior base of the abdomen and carefully pull to release the intestines and open the body cavity. (**c**) Carefully push the ovaries out of the body cavity, using the side of the forceps to push the abdomen down and gently force the ovaries out

3.2 Staging the Oocytes to Enrich for Late Stages [12]

1. Feed the flies on yeast paste for 72 h (*see* **Note 9**).
2. Starve the flies for 20 h and then transfer them to empty bottles containing only a wet Kimwipe (*see* **Note 10**).
3. After 20 h, immediately dissect the ovaries.
4. Following dissection, gently pipet the ovaries in a 200 μl pipette tip to separate stage 10 and 14 egg chambers (*see* **Note 11**) and transfer the late stage egg chambers to a new microcentrifuge tube.

3.3 Preparation of Protein Lysate

1. Homogenize approximately 20 pairs of ovaries in 100 μl of cold lysis buffer using the pestle pellet motor and pestle pellet.
2. Centrifuge the sample for 5 min at 12,000 rcf at 4 °C.

3. Remove the supernatant and transfer to a new microcentrifuge tube (*see* **Note 12**).
4. The protein lysate can be used for standard western blotting or immunoprecipitation.

3.4 Preparation of Ovarian RNA

1. Homogenize the ovaries, approximately 20 pairs, in 100 µl of TRIzol® Reagent using the pestle pellet motor and pestle pellet.
2. Incubate for 5 min at room temperature.
3. Add 20 µl of chloroform to the sample and shake vigorously for 15 s.
4. Incubate for 2–3 min at room temperature.
5. Centrifuge the sample for 15 min at 12,000 rcf at 4 °C (*see* **Note 13**).
6. Remove the upper aqueous phase to a new microcentrifuge tube (*see* **Notes 14** and **15**).
7. Add the designated amount of DNase buffer and DNase enzyme directly to the sample.
8. Incubate at 37 °C for 30 min to 1 h.
9. Add 50 µl of isopropyl alcohol to the sample and incubate for 10 min at room temperature.
10. Centrifuge for 15 min at 12,000 rcf at 4 °C (*see* **Note 16**).
11. Remove the supernatant and wash the pellet with cold 70 % ethanol (*see* **Note 17**).
12. Centrifuge for 5 min at 7500 rcf at 4 °C.
13. Allow the pellet to air-dry for 5–10 min at room temperature.
14. Resuspend the pellet in RNase-free dH_2O and store at –80 °C.

3.5 Fixation of Ovarian Tissue

1. Following the dissection, gently tease the ovarioles apart using fine tungsten needles (*see* **Note 18**).
2. Place in microfuge tube containing 1× PBS (*see* **Note 19**).
3. Remove the PBS and add 200 µl of 4 % paraformaldehyde and 600 µl of *n*-heptane (*see* **Note 20**).
4. Incubate for 20 min on a nutator at room temperature.
5. Remove the 4 % paraformaldehyde and n-heptane.
6. Wash the ovaries 3× with 1× PBS and 0.3 % Triton™ X-100 (*see* **Note 21**).
7. Following the washes, the ovarian tissue may be incubated with primary antibodies or stained with other reagents (*see* **Note 22**).

4 Notes

1. The centrifuge must be capable of reaching up to 12,000 rcf. Additionally, the centrifuge should be refrigerated or placed at 4 °C during RNA extraction.
2. The TRIzol® Reagent can be hazardous and therefore cautious handling of this reagent is necessary in order to avoid direct contact of the skin and eyes.
3. Depending on the subsequent analysis, DNase treatment is optional during the extraction of RNA. For RNA samples that will be reverse transcribed into DNA for analysis of gene expression, DNase treatment should be done to avoid contamination of the cDNA with genomic DNA.
4. The water bath or heat block should be set at 37 °C.
5. Add a small amount of baker's yeast to the vial of flies that will be used for dissection. The yeast will help to enlarge the ovaries. Select young females, less than a week old. To enrich for earlier stage egg chambers, supplement the females with yeast for 24 h prior to dissection and 48 h for later stage egg chambers.
6. It may be easier to pick up the fly with your dominant hand, but once positioned correctly, switch to your non-dominant hand to hold the pair of tweezers holding the thorax of the fly.
7. Using your dominant hand, place the forceps at the anterior of the abdomen and squeeze by carefully pushing the forceps against the abdomen while moving to the posterior end. Once the ovaries emerge, place the forceps in between the two ovaries and pull them out.
8. Keep the ovaries on ice until dissecting is complete. The ovaries can be kept in a microcentrifuge tube or a clean dissecting well filled with 1× PBS. Place the fly carcass on a Kimwipe to remove.
9. Using a fly bottle supplied with corn meal agar food, add baker's yeast to one side of the bottle. Then add H_2O until the yeast turns into a thick paste. Let the vial sit on its side for a few minutes until the yeast is no longer dry and there is no excess H_2O. Add the flies that will be used for dissection to the bottle with the yeast paste. Vials may also be used instead of bottles.
10. Make sure there is no remaining food or yeast made available to the flies. Wet the Kimwipe with a few drops of H_2O until it is damp.
11. Cut the tip off of a 200 μl pipette tip to widen the opening. Gently pipet the ovaries up and down in the tip in the depression slide. This will help to dislodge the later stage egg chambers from the ovaries. Pipet several times, then examine the

ovaries in the dissecting microscope. Intact ovaries containing germaria and young egg chambers can be lifted from the depression slide and saved as enriched early fractions or discarded. Use a pipette to transfer the separated late stage, predominantly stage 10–14, egg chambers to a fresh microcentrifuge tube with 1× PBS.

12. The whole cell lysate will contain a large amount of lipid, and this will be visible as a cloudy, white layer at the top of the supernatant following centrifugation. When transferring the protein lysate to a fresh tube, be sure to put the pipette tip below this lipid layer and take care not to transfer large amounts of lipid with the protein lysate.
13. Phase separation begins to occur at this step.
14. The sample will now be separated into the upper aqueous phase (clear in color), interphase (white in color), and lower phenol–chloroform phase (pink in color). Take care not to disturb the upper aqueous phase when removing the sample from the centrifuge.
15. The RNA is contained within the upper aqueous phase and care should be taken not to disturb the interphase. Pipette slowly in order to avoid transferring the interphase or phenol–chloroform phase with the upper aqueous phase.
16. Place the microcentrifuge tube with the hinge facing out. The pellet should form directly under the hinge on the bottom side of the tube.
17. Pipet carefully so that the pellet is not disturbed. The pellet may be difficult to see. If the pellet is not visible continue as though the pellet is in the general area under the hinge of the tube.
18. Use a pair of tungsten needles to open up the ovarioles. Use one needle to hold the ovaries down in the PBS, then using a second needle in your dominant hand, carefully draw the needle through the ovary, between individual ovarioles. Try to keep the ovaries intact, without completely separating the ovarioles away from one another.
19. Prior to fixation, the ovaries may be a bit sticky and will likely not settle to the bottom of the microcentrifuge tube. Once all the ovaries have been dissected and added to the tube, gently tap the side of the tube to get them to fall to the bottom.
20. Following the fixation, the ovaries will more easily and naturally settle to the bottom of the microcentrifuge tube. Be sure to let them settle completely before removing the fixation or wash solutions. Over the subsequent wash steps, take care to not pipet the ovaries out of the microcentrifuge tube when changing the solutions.

21. Alternative wash solutions may be used, depending on the conditions for the optimal visualization of specific proteins. Both the percentages of detergent (0.1 % up to 0.5 %) and the detergent itself (Triton™ X-100, NP-40, Tween 20, SDS) may be modified.
22. For any subsequent washes that involve fluorescent antibodies or reagents, or for ovarian samples isolated from females expressing fluorescent transgenic proteins, take care to cover the tubes with aluminum foil during all the fixation and wash steps.

References

1. Mahowald A, Kambysellis M (1980) Oogenesis. In: Ashburner M, Wright T (eds) The genetics and biology of *Drosophila*, vol 2. Academic, London, pp 141–224
2. Spradling AC (1993) Developmental genetics of oogenesis. In: The development of *Drosophila melanogaster*. Cold Spring Harbor Laboratory Press, Cold Spring Harbor, NY, pp 1–70
3. Robinson DN, Cooley L (1997) Genetic analysis of the actin cytoskeleton in the *Drosophila* ovary. Annu Rev Cell Dev Biol 13: 147–170
4. Lasko P (2012) mRNA localization and translational control in *Drosophila* oogenesis. Cold Spring Harb Perspect Biol 4:1–15
5. Deng W, Lin H (2001) Asymmetric germ cell division and oocyte determination during *Drosophila* oogenesis. Int Rev Cytol 203: 93–138
6. Müller HA (2000) Genetic control of epithelial cell polarity: lessons from *Drosophila*. Dev Dyn 218:52–67
7. Bilder D (2004) Epithelial polarity and proliferation control: links from the *Drosophila* neoplastic tumor suppressors. Genes Dev 18: 1909–1925
8. Jang AC, Starz-Gaiano M, Montell DJ (2007) Modeling migration and metastasis in *Drosophila*. J Mammary Gland Biol Neoplasia 12:103–114
9. Losick VP, Morris LX, Fox DT, Spradling A (2011) *Drosophila* stem cell niches: a decade of discovery suggests a unified view of stem cell regulation. Dev Cell 21:159–171
10. Becalska AN, Gavis ER (2009) Lighting up mRNA localization in *Drosophila* oogenesis. Development 136:2493–2503
11. He L, Wang X, Montell DJ (2011) Shining light on *Drosophila* oogenesis: live imaging of egg development. Curr Opin Genet Dev 21:612–619
12. Andrews S, Snowflack DR, Clark IE, Gavis ER (2011) Multiple mechanisms collaborate to repress nanos translation in the *Drosophila* ovary and embryo. RNA 17:967–977

Chapter 3

Mosaic Analysis in the *Drosophila melanogaster* Ovary

Thomas Rubin and Jean-René Huynh

Abstract

Drosophila melanogaster oogenesis is a versatile model system used to address many important questions of cell and developmental biology such as stem cell regulation, cell determination, cell polarization, cell–cell signaling, cell–cell adhesion, and cell-cycle regulation. The ovary is composed of germline and somatic cells of different origins and functions. Mosaic analysis using the powerful genetic tools available in *Drosophila melanogaster* allows deciphering the contribution of each cell type in the different processes leading to the formation of a mature egg. Germ cells and follicle cells are produced by actively dividing stem cells, which permit the use of recombinases, such as FLP, to generate genetic mosaics using mitotic recombination. This chapter summarizes the different methods used to create genetic mosaics in the germline and in somatic cells of adult ovaries. We briefly introduce the morphology and development of the adult female ovary. We then describe in practical terms how to generate mosaics with examples of cross schemes and recombining strains. We also explain how to identify the appropriate progeny and how to prepare clonal tissues for phenotypic analysis.

Key words *Drosophila*, Mitotic recombination, FLP recombinase, Clonal analysis, Germline, Oogenesis

1 Introduction

1.1 The Adult Ovary

The *Drosophila melanogaster* ovary is composed of 16–20 ovarioles, each of which contains a chain of progressively more and more mature egg chambers [1] (Fig. 1). New egg chambers are generated at the anterior of the ovariole in a region called the germarium, which can be divided into four regions according to the developmental stage of the cyst. Oogenesis begins in region 1, when a Germline Stem Cell (GSC) divides asymmetrically to produce a posterior cystoblast (CB), and a new GSC, which remains attached to neighboring somatic cells at the anterior. The cystoblast then undergoes precisely four rounds of mitosis with incomplete cytokinesis to form a cyst of 16 germline cells, which are interconnected by stable cytoplasmic bridges called ring canals. These 16 cells are thus all sister cells and share the same cytoplasm. However, only one cell will become the oocyte and complete meiosis, while the 15 other cells become nurse cells, endoreplicate

Diana P. Bratu and Gerard P. McNeil (eds.), *Drosophila Oogenesis: Methods and Protocols*, Methods in Molecular Biology, vol. 1328, DOI 10.1007/978-1-4939-2851-4_3,

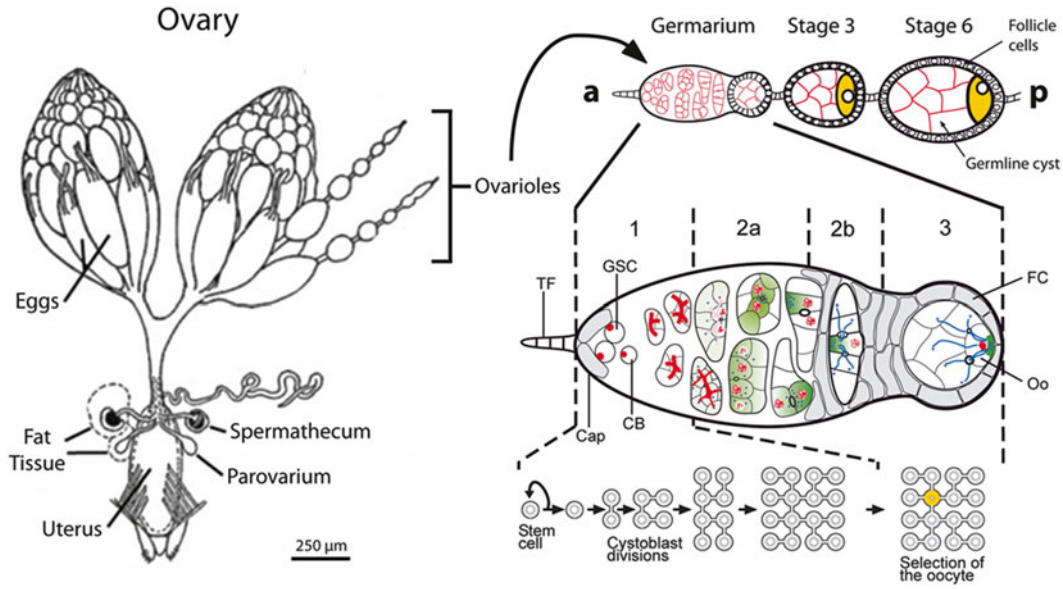

Fig. 1 ***Drosophila*** **Oogenesis**. *On the left*—depiction of the female reproductive tract redrawn after [55], Scale Bar is ~250 μm; *on the top right*—structure of an ovariole; *on the bottom right*—organization of the germline development in the germarium. Each ovariole is made of a chain of progressively more mature egg chambers toward the posterior (p). An egg chamber comprises 16 germline cells surrounded by a monolayer of follicle cells. The egg chambers are produced in a specialized structure, called the germarium, at the anterior (a) of the ovariole. The germarium is divided into four morphological regions along the anterior–posterior axis. The germline stem cells reside at the anterior tip of the germarium (*left*) and divide to produce cystoblasts, which divide four more times in region 1 to produce 16 cell germline cysts that are connected by ring canals. The stem cells and cystoblasts contain a spectrosome (*red circles*), which develops into a branched structure called the fusome, which orients each division of the cyst. In early region 2a, the synaptonemal complex (*red lines*) forms along the chromosomes of the two cells with four ring canals (pro-oocytes) as they enter meiosis. The synaptonemal complex then appears transiently in the two cells with three ring canals, before becoming restricted to the pro-oocytes in late region 2a. By region 2b, the oocyte has been selected (*yellow*), and is the only cell to remain in meiosis. In region 2a, cytoplasmic proteins, mRNAs and mitochondria (*green*), and the centrosomes (*blue circles*) progressively accumulate at the anterior of the oocyte. In region 2b, the minus-ends of the microtubules are focused in the oocyte, and the plus-ends extend through the ring canals into the nurse cells. The follicle cells (*gray*) also start to migrate and surround the germline cells. As the cyst moves down to region 3, the oocyte adheres strongly to the posterior follicle cells and repolarizes along its anterior–posterior axis, with the microtubule minus-ends and specific cytoplasmic components now localized at the posterior cortex

their DNA and provide the oocyte with organelles and nutrients. During the four divisions, a cytoplasmic structure called the fusome anchors one pole of each mitotic spindle and therefore ensures that cells follow an invariant pattern of divisions [2]. This leads to the formation of a symmetric cyst with two cells with four ring canals, two with three, four with two, and eight with one. This invariant pattern of divisions is important, as the oocyte always differentiates from one of the two cells with four ring canals, which are therefore called the pro-oocytes.

Three types of somatic cells can be distinguished in region 1. Cap Cells (CCs) are directly in contact with GSCs and send signals, which regulate GSC behavior. CCs define a niche for GSCs. More anteriorly, Terminal Filament Cells (TFCs) attach each ovariole to the surrounding muscular sheath. More posteriorly, Escort Cells (ECs) unsheathe each GSC and dividing germline cysts. Importantly, CCs, ECs, and TFCs do not divide under normal conditions in the adult ovary; it is thus impossible to perform mosaic analysis using mitotic recombination in these cell types in the adult. Once the 16-cells cyst has formed, it enters region 2a of the germarium. At this stage, all the cells of one cyst appear similar, but by the time it reaches region 2b, one cell will have differentiated as an oocyte. This differentiation can be followed with several types of markers [3]: (1) oocyte-specific proteins, such as Bicaudal-D (BicD), Orb, Barentsz (Btz), and Cup, and mRNAs, such as *oskar*, *BicD* and *orb*, which first concentrate in the two pro-oocytes, and come to lie on either side of the largest ring canal which connects them [4–9]; (2) the centrosomes of each cell of the germline cyst appear to be inactivated after the last mitotic division, and migrate along the fusome into the pro-oocytes, and then into the oocyte [10–12]; (3) the oocyte is the only cell of the cyst to remain in meiosis, and this can be followed by the formation of the synaptonemal complex as the chromosomes pair during the pachytene stage [13, 14]. By region 2b of the germarium, all these markers are restricted to only one cell of the cyst showing that the oocyte is already clearly selected. These components remain associated with the fusome remnants and therefore accumulate at the anterior of the oocyte to form a Balbiani body [15] .

Follicle Stem Cells (FSCs) are located at the border between region 2a and 2b. FSCs are somatic cells producing follicle cells, which migrate and surround each germline cyst to form an egg chamber. As the cyst moves down to region 3 (also called stage 1), it rounds up to form a sphere with the oocyte always lying at the posterior pole. Follicle cells form a monolayered epithelium encasing the 16 germline cells. Main body follicle cells surround most of the egg chamber, while terminal cells cover the anterior and posterior poles of each egg chamber. Two additional populations of somatic cells, called polar and stalk cells, have a common ancestor. Each pair of polar cells patterns the follicular epithelium at each pole, while stalk cells connect two adjacent egg chambers. FCs divide until stage 6 of oogenesis reaching around 900–1000 cells. Interestingly, FC divisions are also incomplete and groups of FCs remain linked by ring canals. Some level of synchrony can thus be detected among small groups of FCs and small molecules can diffuse from one cell to another. This can complicate the analysis of mosaic experiments in the follicular epithelium. After stage 6, FCs remain interconnected but stop dividing, endoreplicate their DNA and become polyploid. During the final stages of oogenesis, there

is a huge increase in the oocyte volume due to yolk uptake through the follicular cells and transfer of nurse cell cytoplasm into the oocyte. FCs undergo important morphogenetic movements to accommodate the volume increase and to form the micropyle and the dorsal appendages.

1.2 Mitotic Recombination

1.2.1 Mosaic Mutant Analysis: Background and Theory

To investigate the function of a specific gene, geneticists use mutations disrupting the function of this gene. However, developmental biologists want to know in which cell(s) this gene is required. In other words, in which cell(s) does the mutation cause the observed phenotype? Geneticists have designed methods allowing them to generate a single individual/tissue/organ with cells homozygous and cells heterozygous for this mutation, and cells with two wild type copies of the gene. Thus, within the same individual, all the cells do not have the same genotype and this individual/tissue/organ is thus called a genetic mosaic. This method has many advantages. When studying a mutation inducing lethality in the homozygous state, it allows the generation of homozygous mutant cells only in specific organs, while the rest of the fly is heterozygous for the mutation and thus viable. It allows the determination of whether the defects caused by a mutation are restricted to the genetically mutant cells (cell autonomous) or if the mutation affects neighboring cells (cell non-autonomous). It is equally important to mark the different genotypes to identify the homozygous, heterozygous, or wild type cells. Mosaic analysis is thus combined with dominant markers, which are genetic and heritable by the progeny. It is thus possible to perform lineage tracing, i.e., to determine the number and fate of cells that descend from one original cell by successive mitotic divisions, for the establishment of fate and specification maps.

One widespread method to generate homozygous mutant cells in an otherwise heterozygous individual is to induce mitotic recombination at the G2 stage (each chromosome is then made of two sister chromatids) in mitotically active cells (Fig. 2). After recombination between non-sister chromatids and depending on the orientation of chromosomes on the metaphase plate, there is 50 % chance that both mutant alleles will segregate into the same cell (homozygous mutant), while the two wild type copies of the gene under study will segregate into the sister cell (aka "twin spot"). In the absence of recombination, only heterozygous cells are produced. In the following divisions, the homozygous mutant cell will only generate homozygous mutant cells. This group of mutant cells derived from a single mutant cell is called a mutant "clone." Likewise, the twin-spot wild-type cell will generate a "clone" of wild type cells. The twin-spot clone is used as an internal control for the mutant clone. Heterozygous cells surround both wild type and mutant clones. The number of cells within a clone depends on the mitotic rate and the timing of clone induction.

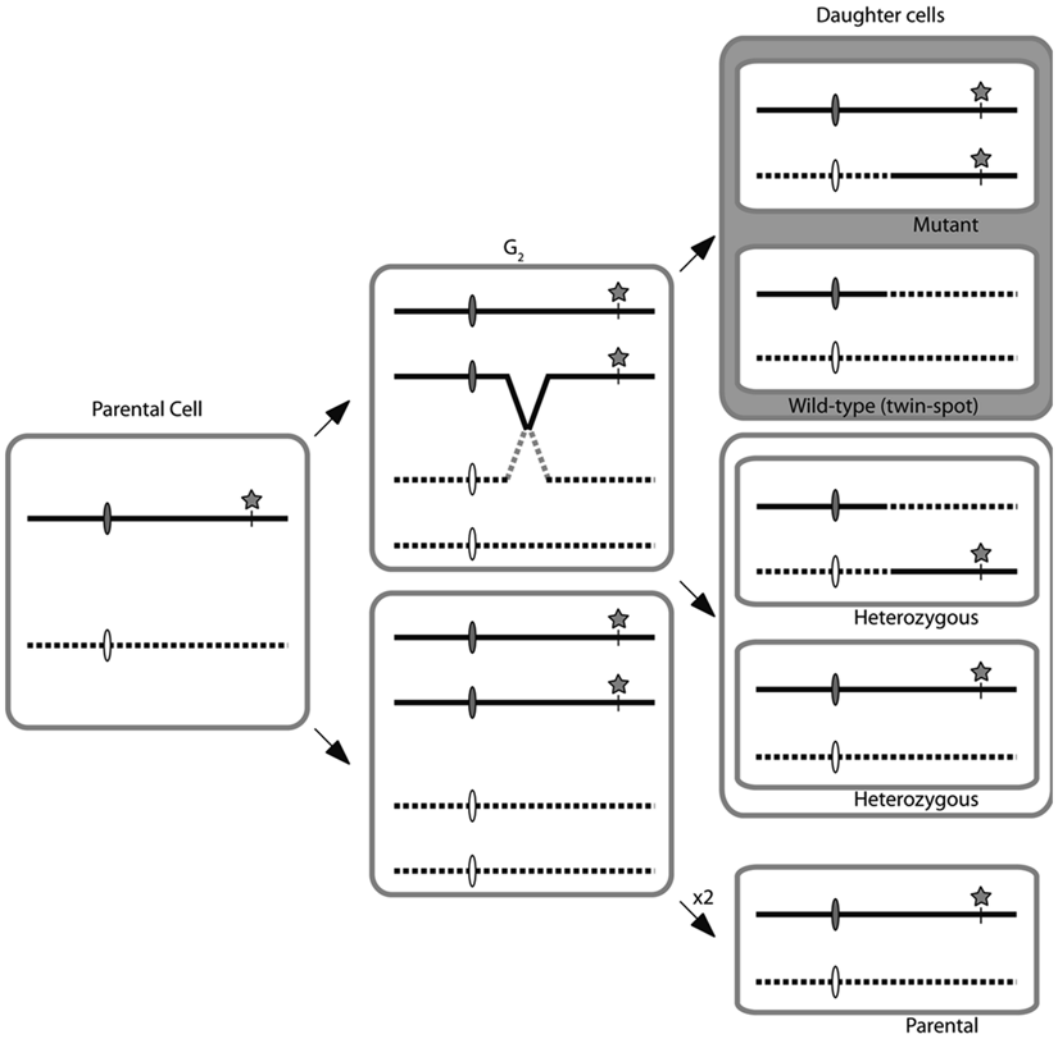

Fig. 2 Mitotic recombination. In the absence of mitotic recombination, the daughter cells are identical to the parent cell (*bottom way*). Each daughter cell has an arm of each of two homologous chromosomes: one carrying the mutation (*star*) and the other the wild-type allele. If recombination occurs, there is recombination between homologous chromosomes before mitosis. After the mitotic division, the mother cell has a 50 % chance of giving a daughter cell homozygous for the mutation and a daughter cell homozygous for the wild-type allele (*upper way*). The remaining 50 % produces two daughter cells both heterozygous for the mutation (*middle way*)

1.2.2 Recombination Methods

Ionizing radiation was the first method used to induce mitotic recombination between two chromatids. Adult flies, larvae or embryos heterozygous for a given mutation are placed in an X-ray machine, and subjected to a calibrated dose of radiation. Recombination events occur randomly along chromosomes. This method has the advantage to be simple and can be used with any genotype. However, radiation is unhealthy for the fly, and lethality is common.

X-rays can also induce genetic rearrangements. It can then be difficult to distinguish phenotypes caused by the mutation of interest or by the radiation exposure.

Genome manipulation has been transformed by the use of site-specific DNA recombinases such as Cre or FLP to perform site-specific recombination (SSR) [16–20]. Cre and FLP belong to the same family of recombinases, and recognize sequence-specific loxP or FRT sites, respectively. The more efficient Cre/loxP system is widely used in mammals, while the less efficient, but less toxic, FLP/FRT system is commonly used in *Drosophila*. FRT and loxP sites do not exist in the host genome and are uniquely recognized by the enzyme that can mediate recombination between two sites. This recombination event can induce chromatid exchange between two homologous chromosomes, but can also induce the deletion of an endogenous gene, the activation of a transgene or a reporter gene for cell-lineage analysis [16–20]. The expression of Cre or FLP can be targeted to specific groups of cells by the use of specific promoters driving the transcription of the gene encoding the enzyme.

The FLP/FRT method relies on the use of the site-specific recombination enzyme, FLP recombinase, from *Saccharomyces cerevisiae*. This enzyme specifically targets FRT sites (FLP recombination target site) and mediates site-specific recombination reactions between two identical FRT sites [21, 22]. The minimal FRT site is 34 bp and comprises 13 bp inverted repeats on either side of an asymmetric sequence or "spacer." FLP binds a FRT site, dimerizes with another FRT-bound FLP, making a synaptic complex between the two FRT sites, and catalyzes a recombination event between them [23]. The asymmetry of the spacer imposes directionality on the FRT sites, and enzyme mediated recombination only occurs between FRT sites in a specific orientation. The position and relative orientation (i.e., same or opposite direction) of the two FRT sites determine the outcome (i.e., insertion, excision, inversion, or reciprocal translocation) of the FLP recombinase-mediated recombination reaction [24]. FLP can be expressed in specific groups of cells with the use of specific promoters. However, a limited number of promoters have been well characterized over extended periods of time and in the entire organism [25]. These promoters are often expressed in several groups of cells and not in single cells, and their expression can vary in time, or in contrast they can remain constitutively active after specific time points. Promoters are available that lead to constitutive expression in certain tissues (e.g., *actin*-FLP, *tubulin*-FLP) and near complete mosaicism, whereas others are inducible (e.g., *heat-shock*-FLP). Since most of the FRT insertion stocks were equipped with the transgene encoding the *hs*-FLP, planning for a FLP/FRT experiment is especially user-friendly. With *hs*-FLP, the level of expression is dependent on the severity and duration of the heat shock [26] (*see* **Note 1**). Brief heat shocks at lower temperatures result in

lower levels of expression whereas long heat shocks at higher temperatures cause higher expression levels. The *hs*-FLP is the most widely used FLP to induce clones both in germline cells and in somatic cells.

The major advantages of the FLP/FRT mitotic recombination system are: (1) the recombination rates are much higher than achieved by X-ray irradiation; (2) the site of FLP-mediated recombination is precisely determined by the location of the FRTs; (3) the system does not cause significant cell death or developmental delay. The main disadvantages of this system include: (1) Cells must divide after the clone induction to follow the mutant progeny; (2) it requires to first recombine a mutation onto the appropriate FRT chromosome; (3) mutations on the fourth chromosome and those proximal to the FRT sites on the other chromosomes cannot be analyzed (recombining a mutation and an FRT site is not easily possible on the fourth chromosome, because no meiotic recombination occurs on this chromosome).

In the Cre/Lox system, Cre comes from bacteriophage P1 and catalyzes recombination between two loxP sites. Cre is in the same family of site-specific recombinases as FLP, therefore its function and mechanism of action is analogous [23]. Likewise, loxP sites have the same inverted repeat and spacer structure as FRT sites. However, Cre appears to be toxic to *Drosophila* cells in some cases, but these effects can be mitigated by reducing the expression levels [27]. Over the years, the Cre/Lox system has not been commonly used to induce mosaics of whole chromosome arms. LoxP sites have not been inserted close to each centromere. This system is mostly used in a "FLPout" configuration to remove transient markers or selection cassettes (*see* Subheading 1.2.7).

1.2.3 Production of Germline Clones of Maternal-Effect Genes

The first stages of embryonic development do not rely on the zygotic genome, but on mRNAs deposited by the mother in the egg cytoplasm during oogenesis. Thus, an embryo can be genetically homozygous for a given mutation, but the consequences of this mutation can be masked during the early stages of embryonic development by the presence of wild type mRNAs of the same gene deposited by the mother during oogenesis. To remove this "maternal contribution," the wild type copies of the gene need to be removed in the germline of the mother during the formation of the egg. This can be achieved by inducing mitotic recombination in the mother's germline stem cells which are the progenitors of all germ cells [28]. Mitotic recombination in germline stem cells can be induced using X-rays, but are more commonly done using the FLP/FRT system. FRT sites have been introduced close to centromeres of chromosome X, 2L, 2R, 3L, and 3R. FLP-mediated recombination between two corresponding FRT-sites will then produce an exchange of an entire chromosome arm [16, 20, 29]. If a mutation is localized distally (away from the centromere) on

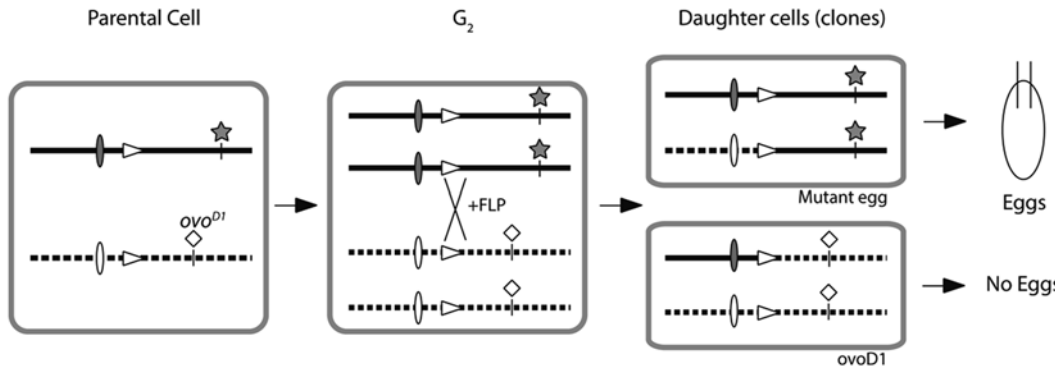

Fig. 3 Generating females with homozygous mutant germ cells. Before mitotic recombination, a parental cell has an arm of each of two homologous chromosomes: one carrying the mutation (*star*) and the other carrying the DFS *ovoD1* mutation. Activation of the FLP recombinase induces recombination between the two FRT sites present on homologous chromosomes before mitosis. After the mitotic division, the mother cell has a 50 % chance of giving a daughter cell homozygous for the mutation and lacking the DFS *ovoD1* mutation, and thus oogenesis can proceed with a homozygous mutant germline. The other daughter cell will be homozygous for the DFS o*voD1* mutation

this chromosome arm, there is a 50 % chance that the same cell will inherit both mutant copies. If this event happens in a germline stem cell, all the daughter cells produced by this stem cell will be homozygous for the mutation of interest, and the egg will be devoid of wild type mRNAs.

One important issue with this method is the ability to distinguish the homozygous cells from the heterozygous and wild-type twin spot cells. In order to identify each chromatid (mutant or wild type), a dominant marker is placed on the wild type chromatid arm. Thus, homozygous mutant cells can be recognized by the absence of the dominant marker. This method can even be improved by adding a selectable dominant marker such that only the homozygous mutant cells will develop. Indeed, in regular conditions homozygous mutant cells can be counter-selected when surrounded by wild type cells. However, this can be reversed if all heterozygous or wild type cells expressed a selectable marker slowing down their growth (Minute mutations) or arresting their development. In the case of germ cells, the *ovoD1* dominant mutation arrests oogenesis at stage 6 and females are thus sterile (Fig. 3) [30]. The only germ cells, which will develop past stage 6 are thus the ones which have recombined out any copy of *ovoD1*, meaning the germ cells homozygous for the mutation of interest [31]. The only eggs laid by these females are those produced by homozygous mutant germline stem cells. The combination of the FRT system with the *ovoD1* mutation allows a positive selection of eggs with no maternal contribution. The original *ovoD1* mutation is located on the X-chromosome, but transgenes expressing the mutation have

been inserted on each chromosome arm. This method is thus applicable to all genes on the X, 2 and 3 chromosomes [29, 31].

Importantly, when planning an experiment using the *ovoD1* mutation, one should keep in mind that the perdurance of the OvoD1 protein can last for a few cell divisions [30]. The OvoD1 protein may be stable in the cytoplasm of a germline stem cell even though this GSC has segregated away all copies of the *ovoD1* transgene. The antimorphic activity of *ovoD1* can thus be detected in a few daughter cells before being diluted out by cell division. This can create artifacts such as an abnormal number of germ cells in each egg chamber [32].

An alternative method to generate mosaic ovaries with mutant germ cells is to transplant pole cells from a donor X into a host Y. Pole cells are the future germline stem cells. They can be removed from the posterior of an embryo with a glass pipet and injected at the posterior pole of a different embryo. They will be incorporated into the future ovaries and form germline stem cells, which will produce germ cells of genotype X. Usually the donor X is homozygous mutant for a gene of interest and the host is a mutant embryo with no germ cells, such as *germ cell-less* or *grandchildless* mutants. In the resulting adult female, all germ cells will be of genotype X, while all somatic cells, including follicle cells, will be of genotype Y. However, this method is technically very challenging, and the transplantation procedure can introduce artifacts not caused by the mutation.

1.2.4 Germline Clones of Genes Required for Oogenesis

The induction of germline clones mutant for a specific gene during oogenesis follows the same principle as removing the maternal contribution using the FLP/FRT system as described above. In both cases, mitotic recombination is induced in mitotically active germline stem cells (Fig. 4). GSCs then produce homozygous mutant cysts until they differentiate. However, it is highly advised not to use the *ovoD1* transgene as a dominant marker. Firstly, *ovoD1* stops oogenesis at stage 6, and it is thus impossible to distinguish mutant from wild type clones before this stage. Secondly, the perdurance of the OvoD1 protein can induce phenotypes independently of the mutation. Instead, one can use a ubiquitous and neutral GFP or β-gal marker to label heterozygous and wild type cells [13, 33]. The homozygous mutant cells are thus identified by the absence of these markers.

1.2.5 Production of Clones in a Cyst

As cyst cells undergo four rounds of mitosis, it is possible to induce mitotic recombination during these divisions. The germline cyst can thus also be mosaic and all 16 cells will not be genetically identical. The number of cells sharing the same genotype depends on when the recombination has been induced. For example, if recombination happens during the first division, there is a 50 % chance that half of cyst cells will be identical, and 8 cells is the maximum

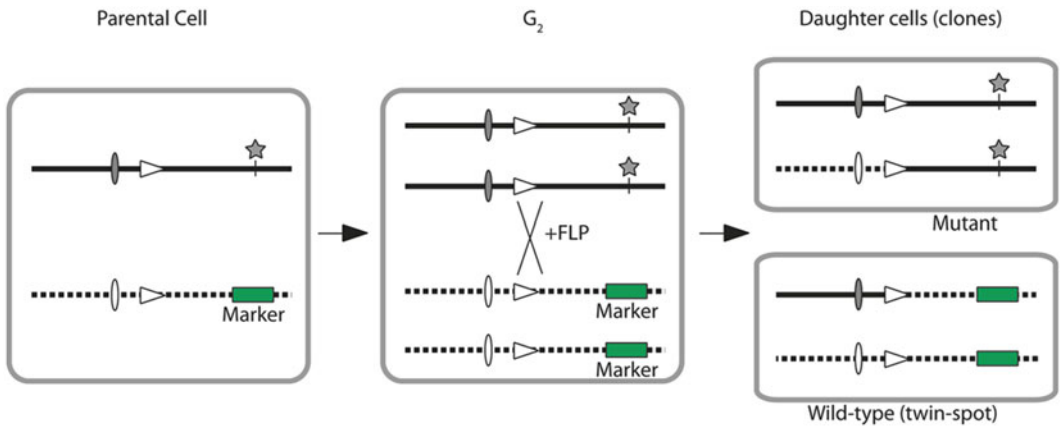

Fig. 4 Generating mutant clones using FLP-mediated mitotic recombination and a visible dominant marker. Before replication, both homologous chromosomes have one chromatid each: one carrying the mutation (*star*); and the other carrying the wild-type allele associated with a dominant marker gene such as a GFP. Activation of the FLP recombinase in G2 induces recombination between the two FRT sites present at the centromere of each homologue. After mitotic division, the mother cell has a 50 % chance of giving a daughter cell homozygous for the mutation and lacking the marker. The other daughter cell will be homozygous for the wild-type allele (giving rise to the "twin-spot") and will express two copies of the genetic marker. Cells, which have not recombined, will be heterozygous and identical to the parental cell

number of cells in intra-cyst clones. These experiments can be useful to decipher the relative contribution of the oocyte compared to nurse cells to a given process. However, these cells share the same cytoplasm through ring canals, which makes the analysis more challenging. GFP or β-gal can diffuse from one cell to another, and the genotype of each cell may not correspond to the visible marker. Secondly, mutant and wild type proteins can also pass through the ring canals, it is thus difficult to conclude on the cell autonomy or non-autonomy of a gene.

To circumvent the problem of diffusion of GFP or β-gal between germ cells, it is possible to directly label the chromatids with strictly cell-autonomous markers (Fig. 5). These germline mosaics are made with a transgene containing direct repeats of the *lac* operator (*lacO*) as a strictly cell autonomous genetic marker [34–36]. The presence of the transgene is indicated by the binding of a nuclear GFP-tagged Lac repressor protein (GFP-LacI) that binds to the *lacO* transgene and yields a discrete focus of nuclear fluorescence. In ovaries from females heterozygous for the lacO transgene, a single focus is present in the oocyte nucleus, whereas in the nurse cell nuclei, which are highly polyploid with partially dispersed chromatids multiple foci are visible. To create germline mosaics, one must construct a chromosome containing the *lacO* transgene in cis to the mutant allele, so that homozygous mutant cells would be homozygous for the transgene as well. This configuration allows the recognition of a homozygous mutant oocyte

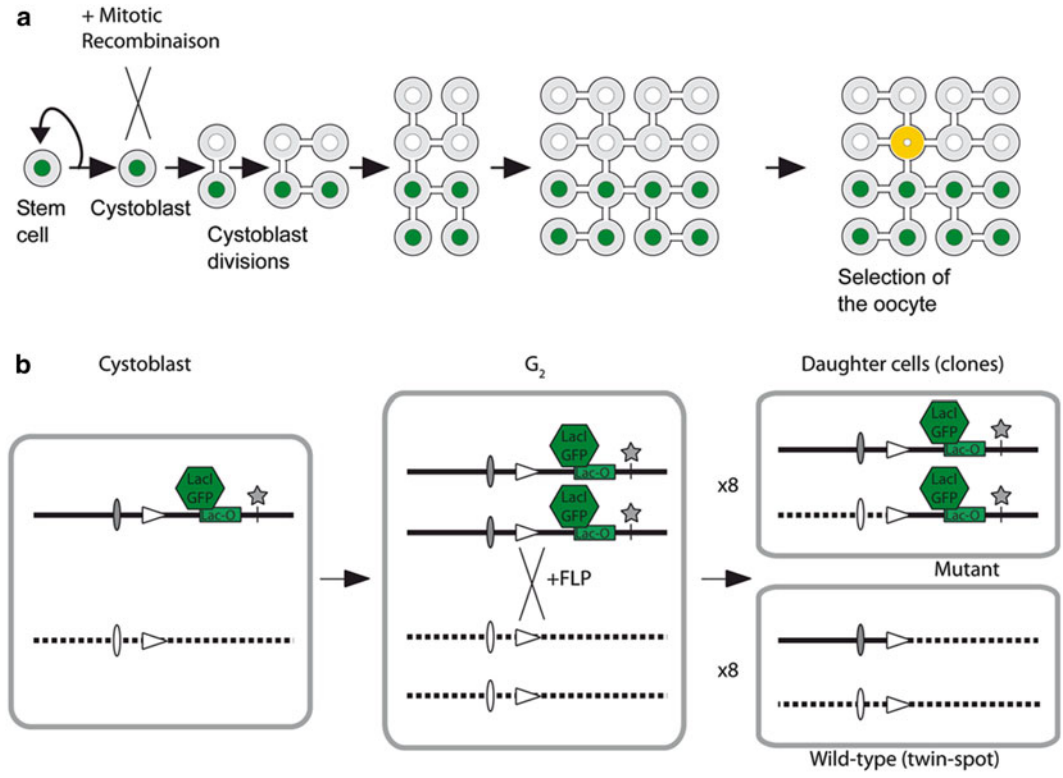

Fig. 5 Generation of mosaics in the germline cyst. (**a**) Mitotic recombination during the first division of a heterozygous cystoblast results in a mosaic cyst made of eight wild-type cells (*white*) and eight mutant cells (*green*), while recombination in the germline stem cell divisions generates clonal germline cysts (not shown). In such mosaics, the oocyte nucleus can be either wild type or mutant. (**b**) Generation of mosaics with the lacO/GFP-LacI system. Before mitotic recombination, a parental cell has an arm of each of two homologous chromosomes: one carrying the mutation (*star*) in *cis* to the *lacO* transgene, as well as the GFP-LacI transgene (not shown), and the other arm carries the wild-type allele. All cells exhibit nuclear GFP-LacI fluorescence, and discrete fluorescent foci are visible in the nuclei of cells with the *lacO* transgene. Heterozygous females exhibit a single focus of GFP in the oocyte nucleus and multiple foci in the polyploid nurse cells. Activation of the FLP recombinase induces recombination between the two FRT sites presents on homologous chromosomes before mitosis. After the mitotic division, the mother cell has a 50 % chance of giving rise to a daughter cell homozygous for the mutation and exhibiting two GFP foci. The other daughter cell is homozygous for the wild-type allele and is lacking the GFP focus

directly by the presence of two clear foci of GFP fluorescence within the oocyte nucleus [37]. However, when using this method, it must be kept in mind that proteins can diffuse through cytoplasmic bridges, consequently the absence of a phenotype in a mutant cell could be due to a contribution from the neighboring wild-type cells.

1.2.6 Production of Clones in Ovarian Somatic Cells

The FLP/FRT system can be equally used to induce homozygous mutant clones in somatic cells. The main limitation is that these cells have to be mitotically active to induce mitotic recombination.

In the adult ovary, the terminal filament cells, cap cells and escort cells are not dividing. To generate mutant clones in these cell lineages, one has to induce recombination during the previous larval stages. However, these different cell types often share some common progenitors, so it can be difficult to induce mutant clones in only one cell type [38]. Follicle stem cells divide throughout adult life and follicle cells also divide until stage 6. Clonal analysis is thus easier in these cell types. However, as in the case of germ cells, cytokinesis remains incomplete in most follicle cells. Follicle cells thus remain connected by small ring canals, through which markers and proteins can diffuse [39]. This should be taken into account when analyzing the cell autonomy of a given phenotype [40]. Furthermore, different types of follicle cells also share some common ancestors and it can be difficult to induce clones in only one cell type. For example, stalk cells and polar cells have a common progenitor very early on in the germarium.

Here, mutant cells are identified by the absence of markers. One should be careful that the absence of markers is not due to the absence of the whole cell. Mechanical damage during dissection can induce holes in the epithelium, which look like mitotic clones because of the absence of dominant markers [41]. Similar types of damage can also be caused by pipetting up and down the ovaries before immunostaining. We thus strongly advise not to use this method of dissection.

1.2.7 Clonal Misexpression: Flip-Out and MARCM Techniques

The advent of the Gal4/UAS system has introduced the ability to misexpress or overexpress genes in specific groups of cells [38]. Despite an ever-increasing number of promoters driving Gal4 expression, clonal expression in a very restricted number of cells is difficult to achieve. It is now possible to combine the FLP/FRT system with the Gal4/UAS system to create genetic mosaics in germline and somatic cells.

The Flip-out technique allows the induction of constitutive expression of one or several transgenes in single cells or clones of cells [42]. The expression of the transgene is switched on by the excision of a "FLPout" cassette, inserted between the transgene and its promoter. The removal of the FLPout cassette, containing the transcriptional termination site, leads to the fusion of the promoter to the coding sequence of the transgene and consequently to its expression (Fig. 6). For example, the ubiquitous *actin5c* (Act5C) or *tubulin1α* (tub1α) promoters are commonly used (*see* ref. 25 for a list of useful promoters to study oogenesis). The FLPout cassette, flanked on both sides by an FRT sequence, contains a marker gene (e.g., yellow, CD2) and a transcriptional termination site (polyA signal). Since these two FRT sites are orientated in the same direction, FLP-mediated recombination will lead to the excision of the FLPout cassette. This "FLPout" event is induced and adjusted through the timing and levels of FLP expression.

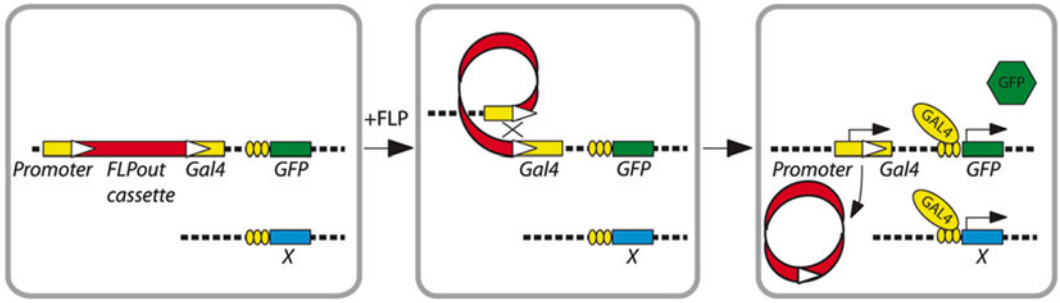

Fig. 6 The FLPout-Gal4 technique. Before recombination, a parental cell has a chromosome carrying one FLPout cassette. Activation of the FLP recombinase induces recombination between two flanking FRT sites, leading to the release of the cassette and thus to the expression of the Gal4 transgene under the exogenous promoter. GAL4 will in turn activate UAS-regulated transgenes, including UAS-driven marker genes (such as GFP). This technique also allows the expression of multiple UAS-transgenes at the same time

Eventually, since the single FRT site obtained after the excision fuses the promoter to the coding sequence of the transgene, the induced transgene expression is transmitted to the progeny of the cells that underwent the FLPout event. As the founder FLPout cell, the FLPout progeny can be identified by the absence of the FLP-out-cassette markers. In most experiments, FLP is expressed under the heat-shock-inducible promoter hsp70 [42, 43]. The timing and strength of the heat shock modulate "FLPout clone formation". Whereas early clone induction generally results in larger clones, the strength of the heat shock influences the number of cells that undergo a FLPout event. The FLPout system has been combined with the Gal4/UAS system. This "FLPout-Gal4 system" combination allows the ubiquitous expression of the Gal4 transcription factor after the FLPout event [44, 45]. Clones expressing Gal4 will in turn activate any UAS-transgene present. Therefore, these Gal4-expressing clones can be positively marked, for example, by the presence of a UAS-GFP or UAS-lacZ construct.

With the regular FLP/FRT system, homozygous clones are identified by the lack of a dominant marker. As previously described, these clones may sometimes be difficult to distinguish from a complete absence of mutant cells. One way to circumvent this problem is to mark positively the homozygous mutant cells. It is possible using a method called MARCM (mosaic analysis with a repressible cell marker), which relies on the combination of the FLP/FRT system, the activator Gal4/UAS system and its repressor Gal80 (Fig. 7). Before recombination, Gal80 inhibits the activity of the Gal4 transcription factor, whose respective transgenes are located on each arm of the same chromosome. A FRT site is located proximal to the ubiquitously expressed *tubP*-Gal80 transgene. On the homologous FRT chromosome, a mutation under study is located

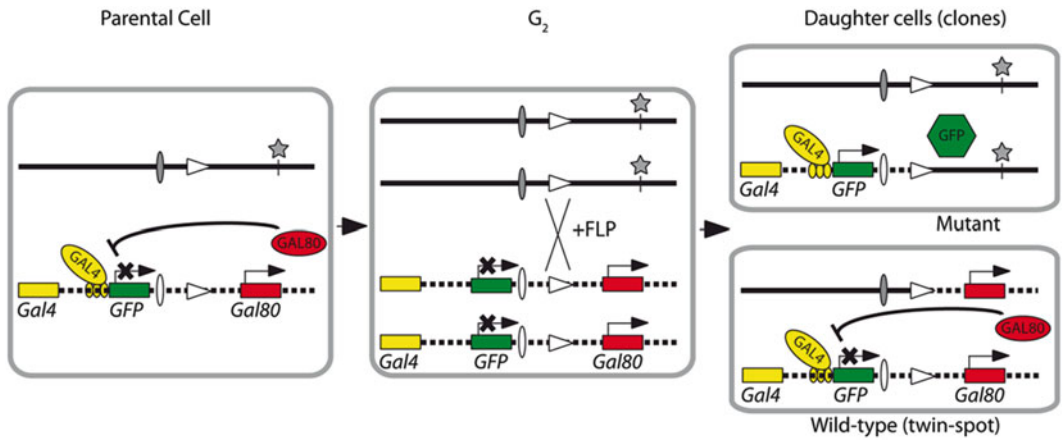

Fig. 7 Mitotic recombination with the MARCM system. Before mitotic recombination, a parental cell has one chromosome carrying a mutation (*star*) and the homologous chromosome carrying the wild type allele and a transgene expressing the Gal80 repressor. For convenience the Gal4 gene, which is driven by a constitutive promoter, and the UAS marker gene are drawn on the same chromosome; however, they can also be located on different chromosomes. Activation of the FLP recombinase induces recombination between the two FRT sites present on homologous chromosomes before mitosis. After the mitotic division, the mother cell has a 50 % chance of giving rise to a daughter cell homozygous for the mutation and lacking the Gal80 repressor transgene. In the absence of GAL80, GAL4 can drive the expression of a UAS-marker transgene (e.g., GFP) in the homozygous mutant cell. The other daughter cell is homozygous for the wild-type allele (giving rise to the "twin-spot") and is expressing two copies of the Gal80 repressor transgene

on the same FRT chromosome arm. After FLP/FRT induced recombination, both copies of the Gal80 transgenes have 50 % chance to segregate into one of the daughter cells. Consequently, in the twin cell, the mutation is homozygous, the Gal4 activity is recovered, and genes downstream of UAS sequences become expressed (e.g., UAS-marker transgene UAS-GFP or UAS-lacZ). This technique also allows the expression of a UAS-transgene in a marked cell clone that is accompanied by a wild-type sister clone for comparison. Importantly, this system offers the possibility to drive, in addition to the marker, other UAS-transgenes in the mutant clone.

This technique is mostly used in somatic cells. It has not been used in germline cells to our knowledge. It is theoretically possible to use it in germline cells with some modifications: (1) UAS sequences have to be UASp which work in germ cells [46]; (2) the Gal4 activator should **not** be a chimaera with VP16, as it is often the case with germline drivers such as nanos-Gal4::VP16. Indeed, the repressor Gal80 binds the activating part of Gal4, but does not recognize VP16.

1.2.8 Screens

The power and efficiency of the FLP/FRT system has allowed using this technique not only to study the function of single genes but also to interrogate functionally the entire genome for novel

genes involved in the formation of a mature egg. Genetic screens have been performed using the FLP/FRT system either in the germline or in somatic cells. Flies carrying FRT chromosomes are directly mutagenized and random mutations are induced on FRT chromosomes. Homozygous cells are then generated either in the germline or in somatic cells. The study of ovarian development was previously limited to female sterile mutations. Instead, these mosaic screens have allowed the identification of many lethal genes, which were required to complete oogenesis. The most commonly used mutagen with FRT chromosomes is the alkylating agent EMS, which makes mostly point mutations in the genome. Random insertions of P-elements are impossible to use because the FRT insertion are themselves P-based transgenes; and the mobilization of P-elements in the genome would also trigger the mobilization of FRT insertions. Instead, existing collections of P-element insertions have been recombined onto FRT chromosome corresponding to their insertion site. It is however possible to use PiggyBac mutagenesis directly on FRT chromosome as the two transposons do not use the same transposase [47].

In germ cells, genetic screens have been performed with the OvoD1 system to score for late phenotypes (after stage 6) and with GFP for genes involved in the early steps of oogenesis [48]. Indeed, recent studies have shown that key developmental decisions, such as the selection, polarization, or localization of the oocyte (the future egg cell) are made during the very early steps of oogenesis, before the arrest caused by the *ovoD1* mutation (reviewed in ref. 3). To uncover novel genes involved during these early stages, a mosaic genetic screen for mutations causing an early arrest of oogenesis have been performed using the FLP/FRT system [49, 50]. The morphology of arrested egg chambers was sufficient to discriminate several phenotypic classes without any staining procedures [50].

2 Materials

2.1 Fly Stocks: FLP, FRT, and Balancer Chromosomes

The Bloomington Stock Center maintains a wide variety of FLP and FRT chromosomes with many combinations of markers and mutations (http://flystocks.bio.indiana.edu/). Many more are available from the laboratories that generated the initial mutants. The list in Table 1 is a starting point for available FRT chromosomes carrying neo, GFP, RFP markers and also *ovoD1* mutations (*see* Table 1). Table 2 is a starting point for FLP lines (*see* Table 2). The Bloomington Stock Center also keeps useful balancer chromosomes: CyO, y+ for the second chromosome, TM6B, Tb or TM6B, y+ for the third chromosome, and T(2;3) SM6a; TM6B, Tb (a translocation between SM6a and TM6B, which segregates the second and third chromosomes together).

Table 1
FRT lines to induce somatic and/or germline clones

Name	Marker	Map	OvoD	GFP	RFP	Arm-Z
X						
101	w^+	14A-B	+	+		
18A	ry^+neo^+	18A		+		+
9-2	w^+	18E	+ ovoD2	+		
19A	ry^+neo^+	19A	+ ovoD1-18	+	+	
2L						
40A	ry^+neo^+	40A	+ ovoD1-18	+	+	+
2R						
G13	w^+	42B	+ ovoD1-18	+		
42D	ry^+neo^+	42D			+	+
43D	ry^+neo^+	43D				+
3L						
2A	w^+	79D-F	+ ovoD1-18	+	+	
80B	ry^+neo^+	80B			+	+
3R						
82B	ry^+neo^+	82B	+ ovoD1-18	+	+	+

2.2 Reagents, Buffers and Equipment

1. Phosphate buffered saline (1× PBS) or Schneider Medium.
2. PBT: 1× PBS with 0.2 % Triton™ X-100. Store at 4 °C for up to 1 week.
3. Fix Solution: 1× PBS with 4 % paraformaldehyde (PFA).
4. Methanol 100 %.
5. Block Solution: PBT and 10 % BSA (*see* **Note 2**). Store at 4 °C.
6. The Developmental Hybridoma Studies Bank (DSHB) produces and sells many monoclonal antibodies relevant for clonal analysis (Myc, GFP, beta-Galactosidase) at a low price (http://dshb.biology.uiowa.edu). Similar antibodies are also commercially available.
7. Halocarbon oil 10S (Voltalef, VWR).
8. Standard fly food.
9. G418 (Geneticin/neomycin; Invitogen, cat. no. (11811).

Table 2
FLP lines to induce somatic and/or germline clones

Name	Chromosome	Efficiency
{hsFLP1}	X	+ [26]
{hsFLP12}	X	+++ [43]
{hsFLP22}	X	+++ [43]
{hsFLP38}	2	++ [16]
{hsFLP86E}	3	++ [16]
{betaTub85D-FLP}1	X	ND
{ovo-FLP.R}	X	ND
{ovo-FLP.R}	2	ND
{ovo-FLP.R}	3	ND
{UAS-FLP.Exel}1	X	ND
{UAS-FLP.Exel}3	3	ND
{3XUAS-FLPG5.PEST}	X	ND
{3XUAS-FLPG5.PEST}	2	ND
{20XUAS-FLPG5.PEST}	X	ND
{20XUAS-FLPG5.PEST}	2	ND
{20XUAS-FLPG5.PEST}	3	ND
{UASp-FLP.G}1	X	ND
{UASp-FLP.G}3	3	ND
{UAS-FLP.MB}	X	ND
{UAS-FLP1.D}	2	ND
{UAS-FLP1.D}	3	ND

10. 25 °C fly culture incubator.
11. Temperature-adjustable water bath tank (or 37 °C bacteria incubator).
12. Dissecting microscope.
13. Dissecting tools: three-well dissecting dishes, fine forceps, tungsten needles.
14. Table top rotator for 1.5 ml tubes.
15. Microscope glass slides (22 × 40 mm, 0.17 mm thickness) and coverslips (18 × 18 mm, 0.17 mm thickness).
16. Mounting Medium: Glycerol, Cityfluor, or VECTASHIELD.
17. Epifluorescence or confocal microscope to analyze ovaries.

3 Methods

The methods described here are used in female ovaries, though they can also be used for male testis. Before starting a mosaic analysis, we suggest you to read some general advices on how to set up your crosses (*see* **Note 3**). The control samples should be treated exactly in the same conditions as those of the experimental samples. The first step is to generate flies bearing the mutation of interest recombined onto the appropriate FRT chromosome. Germline clones can then be induced using the FRT-OvoD1 system to study late oogenesis stage or the FRT-GFP system to study early stages as well as follicle cells. The most common method to induce expression of the FLP is to use heat-shock inducible promoter. For advice on heat-shock duration and timing *see* **Note 1**. It is also possible to perform double mutant mosaic analysis (*see* **Note 4**), mosaic analysis of mutations located proximal to FRT insertions or located on chromosome 4 (*see* **Note 5**). Unfortunately, it is also possible that you do not get clones in some case (*see* **Note 6**).

3.1 Construct a Chromosome with Both an FRT Site and a Mutation (m^-)

There are two types of FRT insertions with different selection markers (*see* Table 1). The first category is a FRT insertion with a mini-*white* (*w*) marker. The FRT insertion can then be followed by red pigmentation of the eye. Both the FRT insertion and the mutation of interest need to be in a *w* background to follow the FRT insertion. The second category of FRT insertions contains a Neomycin-resistant cassette and a *rosy* (*ry*) transgene. The FRT insertion can be followed by the ry^+ cassette if all flies are in an *ry* background. The ry^+ cassette can be difficult to score so it is advised to use the accompanying Neomycin-resistant cassette. If Neomycin/G418 is added to the fly food, only the larvae containing the *neo*-cassette will survive. FRT-bearing larvae are thus positively selected. The *neomycin* gene is under the control of a heat-shock promoter, therefore 37 °C heat-shocks can improve significantly the survival rate.

A third method to follow the FRT insertions is to use PCR primers to amplify directly the FRT sequences. This method works for both categories of FRT sites (*see* **Note 7**).

3.1.1 Recombining a Mutation onto FRT on an Autosome

As an example, the following steps describe how to proceed with a mutation (m−) located on the right arm of the second chromosome (*see* **Note 7**).

1. Set up the cross on neomycin/G418-containing fly food using 8–10 virgin heterozygous females and 3–5 males with the appropriate balancer at 25 °C:

   ♀ *w;* m^-*/P[*ry^+*;hs-neo;FRT]42D* × ♂ *w; Sco/CyO*

2. Transfer parental flies daily into a new vial with freshly prepared G418-containing food.

3. Perform the heat shock treatment on the offspring at 1–3 days of age, at 37 °C for 1 h, to drive the expression of *hs-neo*.
4. After hatching, select single *w* males and cross them individually to a balancer stock (such as *w*; *Sco/CyO*) to establish independent recombinant lines. The number of independent stocks needed to be established depends on the genetic distance between your mutation of interest and the FRT insertion. Usually, when the mutation is on the other half of the chromosome arm, 30 stocks are sufficient. One can go up to 200 lines when the mutation is very close to the FRT site. Each of these lines can then be tested for the presence of the mutation, either by crossing it to another allele of the same gene or a deficiency uncovering the region. The obtained genotype is: *w;* m$^-$*,P[ry+;hs-neo;FRT]42D/CyO*.

3.1.2 Recombining a Mutation onto FRT on X Chromosome

As an example, the following steps describe how to proceed with a mutation (m–) located on the long left arm of the X chromosome (*see* **Note 7**).

1. Set up a cross on neomycin/G418-containing media using 8–10 virgin heterozygous females and 3–5 males with the appropriate balancer at 25 °C:

   ♀ m$^-$*/P[ry$^+$;hs-neo;FRT]18A* × ♂ *Y/FM7*

2. Transfer parental flies daily into a new vial with freshly prepared G418-containing food.
3. Perform the heat shock treatment on the offspring at 1–3 days of age, at 37 °C for 1 h, to drive the expression of *hs-neo*.
4. After hatching, select single *FM7* females and cross them individually to a balancer stock male (such as *Y/FM7*) to establish independent recombinant lines:

   ♀ m$^-$*, P[ry$^+$;hs-neo;FRT]18A/FM7* × ♂*Y/FM7*

   The obtained genotype is: *w;* m$^-$*, P[ry$^+$;hs-neo;FRT]18A/FM7*

   - Cross the resulting m$^-$*, P[ry$^+$;hs-neo;FRT]18A/Y male* with m$^-$*/FM7* females:

     ♀ m$^-$*/FM7* × ♂ m$^-$*, P[ry$^+$;hs-neo;FRT]18A/Y*

   - If in the progeny m$^-$/m$^-$*, P[ry+;hs-neo;FRT]18A* females exhibit the expected m$^-$ homozygous phenotype, then the above corresponding recombinant line contains both the FRT and m$^-$ on the X chromosome.

3.2 Generating Germline Clones with the FRT/OvoD1 System

The following steps describe, as an example, how to proceed with a mutation (m$^-$) located on the left arm of the second chromosome (*see* **Note 8**).

1. Produce by standard crosses female flies that are heterozygous for the mutation under study and the *ovo^{D1}* chromosome by

crossing ovo^{D1} males to females that have the mutation balanced and present distal to an FRT site on that chromosome arm. The ovo^{D1} can only be brought in by males.

2. Set up the cross using 8–10 virgin heterozygous females and 3–5 males at 25 °C.

♀ *w;* m⁻, *FRT-40A/CyO*×♂ *hs*-FLP/Y; ovo^{D1}, *FRT-40A/CyO*

3. Perform the heat shock treatment on these offspring at 1–3 days of age, to drive the expression of the FLP recombinase. Females of the following genotype should be dissected:

♀ *hs*-FLP/+; m⁻, *FRT-40A*/ovo^{D1}, *FRT-40A*

3.3 Generating Germline Clones with the FRT/GFP System

The following steps describe, as an example, how to proceed with a mutation (m⁻) located on the left arm of the second chromosome.

1. Produce by standard crosses female flies that are heterozygous for the mutation under study and the GFP-FRT chromosome by crossing GFP-FRT males to females that have the mutation balanced and on an FRT chromosome arm. In this case, the cross can be done in both directions, by bringing in the mutation either by males or females. When using a lethal mutation on the X chromosome, the mutation can only be introduced by females.
2. Set up the cross using 8–10 virgin heterozygous females and 3–5 males at 25 °C.

♀ *w;* m⁻, *FRT-40A/CyO*×♂ *hs*-FLP/Y; *ubi*-GFP, *FRT-40A/CyO*

3. Perform the heat shock treatment on these offspring at 1–3 days of age, to drive the expression of the FLP recombinase. Females of the following genotype should be dissected:

♀ *hs*-FLP/+; m⁻, *FRT-40A*/*ubi*-GFP, *FRT-40A*

3.4 Generating Mutant Somatic Clones with the FRT/GFP System

The procedure to generate somatic clones with the FRT/GFP system is exactly the same as for germline clones (*see* Subheading 3.3). The main parameter to be adjusted is the timing of the heat-shock. It is possible to hit the FSCs when heat-shocking the third instar larvae using the same procedure as for germline clones. However, FSCs are still actively dividing at the adult stage, so heat-shocks can also be performed on adult female. It is also possible to generate small clones by inducing recombination while the follicle cells are still dividing before stage 6. These clones are however transient and the flies should be dissected only a few days after recombination. *See* Subheading 1.2.3 for specific considerations when analyzing mosaics in somatic cells.

3.5 Overexpressing a Candidate Gene (X) in GFP-Marked Mutant (m^-) Clones

As mentioned above, the MARCM technique has been used only in somatic cells to our knowledge. Here, we describe its use in follicular cells (*see* **Note 9**).

1. Produce by standard crosses flies with the following genotype:

   ♀ *y, w, hs*-FLP/+; *actin*-GAL4, *UAS*-EGFP/ *UAS-geneX; FRT82B, tub*-GAL80/*FRT82B*

2. Perform the heat shock either on larvae or adults, depending on your developmental stage of interest.

3.6 Antibody Staining of Ovaries

1. Dissect the ovaries in 1× PBS or Schneider Medium with tungsten needles (*see* **Note 10**).
2. Fix the ovaries in Fix Solution with rocking for 20 min.

2′. Optional: Wash 3× in methanol, the ovaries can then be stored at −20 °C, if required.

3. Wash 10 min in 1× PBS.
4. Permeabilize for 30 min in 1× PBT.

4′. Optional: Incubate the ovaries in Blocking Solution for 1 h.

5. Wash 3× 10 min with 1× PBS.
6. Add 200–500 µl of the primary antibody in 1× PBS. Incubate overnight, with rocking at room temperature (usually 20 h).
7. Aspirate the primary antibody and recycle it.
8. Wash 4× 30 min with 1× PBS with rocking.
9. Add the secondary antibody in 1× PBS (usually at 1/200 final concentration).
10. Incubate for 2–4 h with rocking at room temperature.
11. Aspirate the secondary solution and wash 3× 10 min in 1× PBS.
12. Proceed to staining for Phalloidin, DAPI (1/500) or Hoechst (1/500) during the wash.
13. Mount in one of several types of Mounting Medium: Glycerol, Cityfluor, or VectaShield.

3.7 Live Imaging of Ovaries

1. Dissect the ovaries in a drop of halocarbon oil (*see* **Note 10**).
2. Remove the muscular sheath around each ovariole.
3. Pull a line of parallel germaria thus making them stick to coverslips in the oil.
4. Put two late stage egg chambers on each side of this line, just making it easier to find the germarium and to position the coverslip on top of the microscope stage.

4 Notes

1. The efficiency of recombination depends on each FRT insertion and the levels of expression of the FLP [26]. In general, there is not much choice for the FRT insertions available for a given mutation. However, the efficiency of recombination does vary for different FRT insertions. The levels of *hs*-FLP can also vary greatly from one line to another (*see* Table 2). Very efficient FLP could be due to multiple insertions of the same *hs*-FLP transgene on the same chromosome. For each FLP line, it is possible to control the levels of FLP with two parameters: (1) temperature and (2) duration of each shock. The maximal and usual temperature is 37 °C, but FLP can be induced already at 29 °C. An example of a strong heat-shock regime to induce germline clones with the FRT-OvoD1 system is 2 h of heat-shock at 37 °C once per day for 3 consecutive days. This strong regime is used during genetic screens when lots of clones need to be induced in each individual.

   It is important to keep track of the number and duration of heat-shocks for each vial. This can be written directly on the vial or on the plug (date of crosses/date of first heat-shock/numbers of heat-shock).

   It has been worked out that third instar larvae (when they start crawling up the vial) is the best stage of development to induce germline clones. Since the heat-shock promoter is ubiquitous, clones will be induced in any dividing cells of third instar larvae. However, at this time, the future GSCs are actively dividing, while cells in imaginal discs have mostly stopped dividing. Therefore, although this procedure enriches for the number of clones in germ cells, it is not restricted to germ cells.

   If a mutation is detrimental to GSCs viability, it is advised to limit recombination to the adult stage. Indeed, GSCs are still dividing at the adult stage (every 24 h on average) and mitotic recombination is still possible. The probability of inducing mosaics will be however lower than during the larval stage. On the other hand, if the mutation under study induces a rapid loss of GSCs, mutant GSCs can have already disappeared at the adult stage if recombination is induced in third instar larvae.

   In follicle cells, inducing clones at the adult stage is more efficient than in germ cells, and can be used routinely. It is also possible to use UAS-FLP transgenes and Gal4 drivers that are expressed in FSCs or in a subpopulations of follicle cells such as border cells [52, 53].

   Heat shocks can be given in either a 37 °C water bath or an air incubator. Water baths are slightly more efficient in the transduction of heat. However, when large number of vials

needs to be heat-shocked simultaneously (during a genetic screen for example), an air incubator is a good alternative. Fly food tends to dry a bit more in an air incubator, so it is a good idea to add some water.

2. The species from which the serum is derived is not important when using highly specific primary and secondary antibodies. We routinely add sodium azide (0.02 %) to ensure that there will be no microbial growth.
3. Even a light regime of heat-shocks can be detrimental to a fly's health, and more larvae or adult flies will die than in non-heat-shocked vials. One should be careful to set up crosses with more adults than regular crosses in order to obtain more larvae per vial for heat-shocks. Larvae are also more resistant than adult flies to long heat-shocks. Although the focus of this chapter is on ovaries, and it is important to keep males in the same vials as the females, because the presence of males stimulate oogenesis.
4. It is possible to induce clones homozygous for two different mutations. The easiest case is when both mutations can be recombined onto the same chromosome arm. A single marked FRT chromosome can then be used as in regular clonal analysis.

   A second case is when the two mutations are on different chromosomes. One can either use two FRT chromosomes with the same marker such as GFP. The homozygous double mutant cells will be identified by the complete lack of GFP, but single mutant cells for any of the two mutations cannot be distinguished. One can also used two different markers, one FRT-GFP and one FRT-LacZ or RFP. Alternatively, one can also use antibody staining against one of the mutated genes if the corresponding protein is completely absent [54]. Double homozygous mutant cells can be identified by the lack of both markers and the protein.

   A third case is when both mutations are on the same chromosome but on different chromosome arms. Special FRT chromosomes need to be used carrying two FRT insertions on both sides of centromeres. Such chromosomes can be found at the Bloomington Stock Center. For an example, *see* ref. 47.
5. The regular FLP/FRT system cannot be used to analyze mosaics for genes located between an FRT insertion and a centromere or for genes located on the fourth chromosome. One alternative is to construct a transgene that is able to rescue completely the mutation of interest, and to recombine this transgene onto a FRT chromosome. Homozygous mutant cells will be induced by the absence of the rescue cassette in a background completely homozygous for the mutation of interest.

6. It is possible that no clones will be identified in the recombining females, even when following the protocol carefully. If this occurs, it is suggested to check whether: (1) There is a FRT insertion recombined with the mutation of interest. This can be done by PCR or by inducing clones in the eye disc with eyeless-FLP; (2) The dominant marker is present and expressed as it should be on the marker chromosome. One can dissect the FRT-marker stock without crosses or heat-shocks to test for the presence of the marker; (3) The mutation is cell-lethal. Homozygous clones may be induced, but could disappear as mutant cells either die or are expelled from the tissue. The presence of "twin-spot" cells is an indication that recombination events have taken place, but that homozygous cells have disappeared. You can then adjust the clone induction procedure and dissect quickly after the clone induction (*see* **Note 1**).
7. As controls during the positive selection, take flies from the corresponding *hs-neo* :FRT (the parents of the original cross) line into one vial with G418, and follow the same procedure. DO NOT use FRT 101, 18E (also called 9-2), 42B (also called G13), or 2A FRT strains as positive controls, since these FRTs do not contain a *neo* resistance gene. In practice, the *hs-neo* can be leaky in many strains. Heat-shocks are thus not always required for survival. Transfer the recombined adults to a new vial before the next generation begins to hatch. When the above recombinant lines hatch, check the corresponding controls. If flies emerged from the negative control vial, you cannot be confident that the selection worked efficiently. Different choices are then available:
   - Induce clones with *ey*-FLP to validate the presence of the FRT chromosome. It is easy to check if clones have been induced in the eye without any dissection or staining procedure.
   - Screen for the presence of the FRT by PCR. This second option can be a good choice if the mutation of interest is more than ~20 map units from the FRT site because it is likely that many of the flies recovered are good recombinants. (Map unit positions of genes can be found in the gene reports in Flybase). Single-fly DNA preps for PCR protocol [51] works well to amplify FRT sequences. FRT primers are:

   Sense sequence: TGAAGTTCCTATACTTTCTAGAGAATA GGAACTTC

   Antisense sequence: GAAGTTCCTATTCTCTAGAAAGTA TAGGAACTTCA
8. As a control, dissect females with the same genotypes from vials, which have NOT been heat-shocked. It will confirm that OvoD1 is working correctly and that the genotypes of the flies in the cross are correct.

9. As for the FLP-FRT lines, the FLPout and FLPout-Gal4 lines may show leaky expression, and control experiments without FLP induction are strongly advised for misexpression studies. This method eliminates possible artifacts due to dissection (*see* Subheading 1.2.4) when whole cells detached from the epithelium. However, one should still be careful of communication between follicle cells by small ring canals, either for the interpretation of loss-of-function experiments, but also for diffusion of markers and/or overexpressed proteins.
10. Before dissection, put the females for one night on fly food supplemented with yeast to get healthy, enlarged ovaries.

Acknowledgments

T.R. is supported by an FRM Ingenieur Fellowship (n° ING 20140129247), and the J.R.H. lab is funded by CNRS, Ville de Paris, and FSER (Schlumberger).

References

1. Spradling AC (1993) Developmental genetics of oogenesis. In: Bate M, Martinez-Arias A (eds) The development of *Drosophila melanogaster*. Cold Spring Harbor Laboratory Press, New York, pp 1–70
2. Lin H, Yue L, Spradling AC (1994) The *Drosophila* fusome, a germline-specific organelle, contains membrane skeletal proteins and functions in cyst formation. Development 120:947–956
3. Huynh JR, St Johnston D (2004) The origin of asymmetry: early polarisation of the *Drosophila* germline cyst and oocyte. Curr Biol 14: R438–R449
4. Castagnetti S, Hentze MW, Ephrussi A et al (2000) Control of oskar mRNA translation by Bruno in a novel cell-free system from *Drosophila* ovaries. Development 127:1063–1068
5. Keyes L, Spradling A (1997) The *Drosophila* gene *fs(2)cup* interacts without to define a cytoplasmic pathway required for the structure and function of germ-line chromosomes. Development 124:1419–1431
6. Lantz V, Chang J, Horabin J et al (1994) The *Drosophila orb* RNA-binding protein is required for the formation of the egg chamber and establishment of polarity. Genes Dev 8:598–613
7. Suter B, Romberg LM, Steward R (1989) Bicaudal-D, a *Drosophila* gene involved in developmental asymmetry: localized transcript accumulation in ovaries and sequence similarity to myosin heavy chain tail domains. Genes Dev 3:1957–1968
8. van Eeden FJ, Palacios IM, Petronczki M et al (2001) Barentsz is essential for the posterior localization of *oskar* mRNA and colocalizes with it to the posterior pole. J Cell Biol 154: 511–523
9. Wharton RP, Struhl G (1989) Structure of the *Drosophila* BicaudalD protein and its role in localizing the posterior determinant nanos. Cell 59:881–892
10. Bolivar J, Huynh JR, Lopez-Schier H et al (2001) Centrosome migration into the *Drosophila* oocyte is independent of BicD and egl, and of the organisation of the microtubule cytoskeleton. Development 128:1889–1897
11. Grieder NC, de Cuevas M, Spradling AC (2000) The fusome organizes the microtubule network during oocyte differentiation in *Drosophila*. Development 127:4253–4264
12. Mahowald A, Strassheim JM (1970) Intercellular migration of the centrioles in the germarium of *Drosophila melanogaster*. J Cell Biol 45:306–320
13. Huynh JR, St Johnston D (2000) The role of BicD, Egl, Orb and the microtubules in the restriction of meiosis to the *Drosophila* oocyte. Development 127:2785–2794
14. Carpenter A (1975) Electron microscopy of meiosis in *Drosophila melanogaster* females.

I Structure, arrangement, and temporal change of the synaptonemal complex in wild-type. Chromosoma 51:157–182

15. Cox RT, Spradling AC (2003) A Balbiani body and the fusome mediate mitochondrial inheritance during *Drosophila* oogenesis. Development 130:1579–1590
16. Chou TB, Perrimon N (1992) Use of a yeast site-specific recombinase to produce female germline chimeras in *Drosophila*. Genetics 131:643
17. Metzger D, Chambon P (2001) Site- and time-specific gene targeting in the mouse. Methods 24:71
18. Orban PC, Chui D, Marth JD (1992) Tissue- and site-specific DNA recombination in transgenic mice. Proc Natl Acad Sci U S A 89:6861
19. Sauer B, Henderson N (1988) The cyclization of linear DNA in *Escherichia coli* by site-specific recombination. Gene 70:331–341
20. Xu T, Rubin GM (1993) Analysis of genetic mosaics in developing and adult *Drosophila* tissues. Development 117:1223–1237
21. Andrews BJ, Proteau GA, Beatty LG et al (1985) The FLP recombinase of the 2 micron circle DNA of yeast: interaction with its target sequences. Cell 40:795–803
22. Jayaram M (1985) Two-micrometer circle site-specific recombination: the minimal substrate and the possible role of flanking sequences. Proc Natl Acad Sci U S A 82:5875
23. Branda CS, Dymecki SM (2004) Talking about a revolution: the impact of site-specific recombinases on genetic analyses in mice. Dev Cell 6:7–28
24. Sauer B (1994) Site-specific recombination: developments and applications. Curr Opin Biotechnol 5:521–527
25. Hudson AM, Cooley A (2014) Methods for studying oogenesis. Methods 68:207–217
26. Golic KG, Lindquist S (1989) The FLP recombinase of yeast catalyzes site-specific recombination in the *Drosophila* genome. Cell 59: 499–509
27. Nakano M et al (2001) Efficient gene activation in cultured mammalian cells mediated by FLP recombinase-expressing recombinant adenovirus. Nucleic Acids Res 29:E40
28. Heidmann D, Lehner CF (2001) Reduction of Cre recombinase toxicity in proliferating *Drosophila* cells by estrogen-dependent activity regulation. Dev Genes Evol 211:458–465
29. Chou TB, Perrimon N (1996) The autosomal FLP-DFS technique for generating germline mosaics in *Drosophila melanogaster*. Genetics 144:1673–1679
30. Perrimon N (1984) Clonal analysis of dominant female-sterile, germline-dependent mutations in *Drosophila melanogater*. Genetics 108:927–939
31. Chou TB, Noll E, Perrimon N (1993) Autosomal P[ovoD1] dominant female-sterile insertions in *Drosophila* and their use in generating germ-line chimeras. Development 119: 1359–1369
32. Jordan P, Karess R (1997) Myosin light chain-activating phosphorylation sites are required for oogenesis in *Drosophila*. J Cell Biol 139:1805–1819
33. Xie T, Spradling AC (1998) decapentaplegic is essential for the maintenance and division of germline stem cells in the *Drosophila* ovary. Cell 94:251–260
34. Robinett CC, Straight A, Li G et al (1996) In vivo localization of DNA sequences and visualization of large-scale chromatin organization using lac operator/repressor recognition. J Cell Biol 135:1685–1700
35. Straight AF, Belmont AS, Robinett CC et al (1996) GFP tagging of budding yeast chromosomes reveals that protein-protein interactions can mediate sister chromatid cohesion. Curr Biol 6:1599–1608
36. Vazquez J, Belmont AS, Sedat JW (2001) Multiple regimes of constrained chromosome motion are regulated in the interphase *Drosophila* nucleus. Curr Biol 11:1227–1239
37. Caceres L, Nilson LA (2005) Production of gurken in the nurse cells is sufficient for axis determination in the *Drosophila* oocyte. Development 132:2345–2353
38. López-Onieva L, Fernández-Miñán A, González-Reyes A (2008) Jak/Stat signalling in niche support cells regulates dpp transcription to control germline stem cell maintenance in the *Drosophila* ovary. Development 135:533–540
39. Airoldi SJ, McLean PF, Shimada Y et al (2011) Intercellular protein movement in syncytial *Drosophila* follicle cells. J Cell Sci 124: 4077–4086
40. McLean PF, Cooley L (2013) Protein equilibration through somatic ring canals in *Drosophila*. Science 340:1445–1447
41. Haack T, Bergstralh D, St Johnston D (2013) Damage to the *Drosophila* follicle cell epithelium produces "false clones" with apparent polarity phenotypes. Biol Open 2(12): 1313–1320
42. Brand A, Perrimon N (1993) Targeted gene expression as a means of altering cell fates and generating dominant phenotypes. Development 118:401–415

43. Struhl G, Basler K (1993) Organizing activity of wingless protein in *Drosophila*. Cell 72: 527–540
44. Ito K, Awano W, Suzuki K, Hiromi Y, Yamamoto D (1997) The *Drosophila* mushroom body is a quadruple structure of clonal units each of which contains a virtually identical set of neurones and glial cells. Development 124:761
45. Pignoni F, Zipursky SL (1997) Induction of *Drosophila* eye development by decapentaplegic. Development 124:271
46. Rorth P (1998) Gal4 in the *Drosophila* female germline. Mech Dev 78:113–118
47. Mathieu J, Sung HH, Pugieux C et al (2007) A sensitized PiggyBac-based screen for regulators of border cell migration in *Drosophila*. Genetics 176:1579–1590
48. Martin SG, Leclerc V, Smith-Litiere K et al (2003) The identification of novel genes required for *Drosophila* anteroposterior axis formation in a germline clone screen using GFP-Staufen. Development 130:4201–4215
49. Barbosa V, Kimm N, Lehmann R (2007) A maternal screen for genes regulating *Drosophila* oocyte polarity uncovers new steps in meiotic progression. Genetics 176:1967–1977
50. Jagut M, Mihaila-Bodart L, Molla-Herman A et al (2013) A mosaic genetic screen for genes involved in the early steps of *Drosophila* oogenesis. G3 (Bethesda) 3:409–425
51. Gloor GB, Preston CR, Johnson-Schlitz DM et al (1993) Type I repressors of P element mobility. Genetics 135:81–95
52. Duffy JB, Harrison DA, Perrimon N (1998) Identifying loci required for follicular patterning using directed mosaics. Development 125: 2263–2271
53. Liu Y, Montell DJ (1999) Identification of mutations that cause cell migration defects in mosaic clones. Development 126:1869–1878
54. Becam IE, Tanentzapf G, Lepesant JA et al (2005) Integrin-independent repression of cadherin transcription by talin during axis formation in *Drosophila*. Nat Cell Biol 7: 510–516
55. Miller A (1950) The internal anatomy and histology of imago of *Drosophila melanogaster*. In: Demerec M (ed) Biology of *Drosophila*. Wiley, New York, pp 424–444

Chapter 4

Genetic Mosaic Analysis of Stem Cell Lineages in the *Drosophila* Ovary

Kaitlin M. Laws and Daniela Drummond-Barbosa

Abstract

Genetic mosaic analyses represent an invaluable approach for the study of stem cell lineages in the *Drosophila* ovary. The generation of readily identifiable, homozygous mutant cells in the context of wild-type ovarian tissues within intact organisms allows the pinpointing of cellular requirements for gene function, which is particularly important for understanding the physiological control of stem cells and their progeny. Here, we provide a step-by-step guide to the generation and analysis of genetically mosaic ovaries using flippase (FLP)/*FLP recognition target* (*FRT*)-mediated recombination in adult *Drosophila melanogaster*, with a focus on the processes of oogenesis that are controlled by diet-dependent factors.

Key words Oogenesis, Clonal analysis, Genetic mosaics, *FLP/FRT*, Germline stem cell, Follicle stem cell, Follicle cell, *Drosophila*

1 Introduction

The ease of genetic mosaic generation in *Drosophila melanogaster* has allowed significant advances in understanding multiple aspects of stem cell biology and other processes during oogenesis [1, 2]. Genetic mosaic analyses, which typically involve the generation of identifiable, genetically distinct clones of cells within the context of wild-type tissue, allow the tracing of cell lineages, determining exact cells in which gene function is required, and distinguishing between cell autonomous and non-cell autonomous roles for genes. Genetic mosaics afford the added advantage of circumventing the lethality of mutations in essential genes, thereby uncovering their roles in later developmental stages.

Methods for the generation of mosaic animals have evolved over the years from technically challenging experimental manipulations involving transplantation to the use of sophisticated genetic tools that facilitate mitotic recombination. In the classic quail–chicken chimera example, cells transplanted from quail embryos were distinguished from those of the host chicken embryo by the

Diana P. Bratu and Gerard P. McNeil (eds.), *Drosophila Oogenesis: Methods and Protocols*, Methods in Molecular Biology, vol. 1328, DOI 10.1007/978-1-4939-2851-4_4,

dense regions of heterochromatin in their nuclei, permitting the mapping of their fate during development [3]. In *Drosophila melanogaster*, transplantation of pole cells allowed the removal of gene function exclusively from the germline [4], and transplantation of imaginal discs elucidated the tissue-autonomous and environmental factors influencing their developmental fate [5]. X-ray-induced mitotic recombination was useful in generating clones of mutant cells for the purpose of addressing cell autonomy of gene function [6]. With the advent of molecular tools for inducible, site-specific mitotic recombination taking advantage of the yeast-derived flippase (FLP)/*FLP recognition target* (*FRT*) system [7], the use of genetic mosaic analysis in *Drosophila* has become commonplace.

Genetic mosaic analyses are very versatile. Typically, genetic mosaics are generated in the context of heterozygous organisms that carry *FRT* sequences at the base of specific chromosome arms. One chromosome arm carries a mutation of interest, while its homolog has a wild-type allele of the corresponding gene and a readily identifiable marker, such as a ubiquitously expressed transgene encoding green fluorescent protein (GFP) or β-galactosidase (β-gal). In addition, a transgene encoding FLP under the control of a heat-shock inducible or tissue-specific promoter is present *in trans*. Once FLP expression is induced—for example, by heat-shocking the organism at a specific point during development or adulthood—cells can undergo FLP-mediated mitotic recombination through homologous *FRT* sequences, potentially generating unequal sister chromatids (Fig. 1a). As sister chromatids segregate during mitosis, a homozygous mutant cell lacking the GFP (or β-gal) marker might be generated, forming a clone of GFP-negative mutant cells as it subsequently undergoes cell division rounds (Fig. 1b–g). It should be noted, however, that numerous variations of this technique have been developed, involving the generation of positively marked mutant clones, clones for overexpression of transgenes or RNA hairpins for RNA interference, or wild-type clones for lineage tracing analysis [8–10].

Fig. 1 (continued) The marker (*orange box*) is a constitutively expressed transgene encoding GFP or β-gal. (**b**) A mosaic ovariole containing previtellogenic (*asterisk*) and vitellogenic (*arrowhead*) follicles with GFP-negative germline cysts. (**c**) In a mosaic germarium, a GFP-negative GSC (*arrowhead*) gives rise to GFP-negative progeny. (**d**) A GSC loss event. GFP-negative germline cysts are present, but the original GFP-negative GSC is absent. (**e**) The FSC is located immediately anterior to the 2a/2b border, and it is recognizable as the anterior-most cell (*arrowhead*) in a GFP-negative follicle cell clone. (In region 2a, individual 16-cell cysts do not fill entire diameter of germarium, whereas in region 2b, lens-shaped 16-cell cysts span the breadth of germarium.) (**f**) When the FSC is lost, GFP-negative follicle cells can be detected, but the most anterior follicle cells are far posterior to 2a/2b. (**g**) A transient clone (*dashed line*) in a follicle cell monolayer provides an indirect readout for follicle cell proliferation. Absence of GFP (*green*) indicates marker-negative cells; 1B1 (*red*) labels fusomes and follicle cell membranes; Lamin C (LamC, *red*) labels cap cell nuclear envelopes; DAPI (*blue*) labels nuclei. Scale bars represent 10 μm. Images in (**c**–**f**) are shown at the same magnification

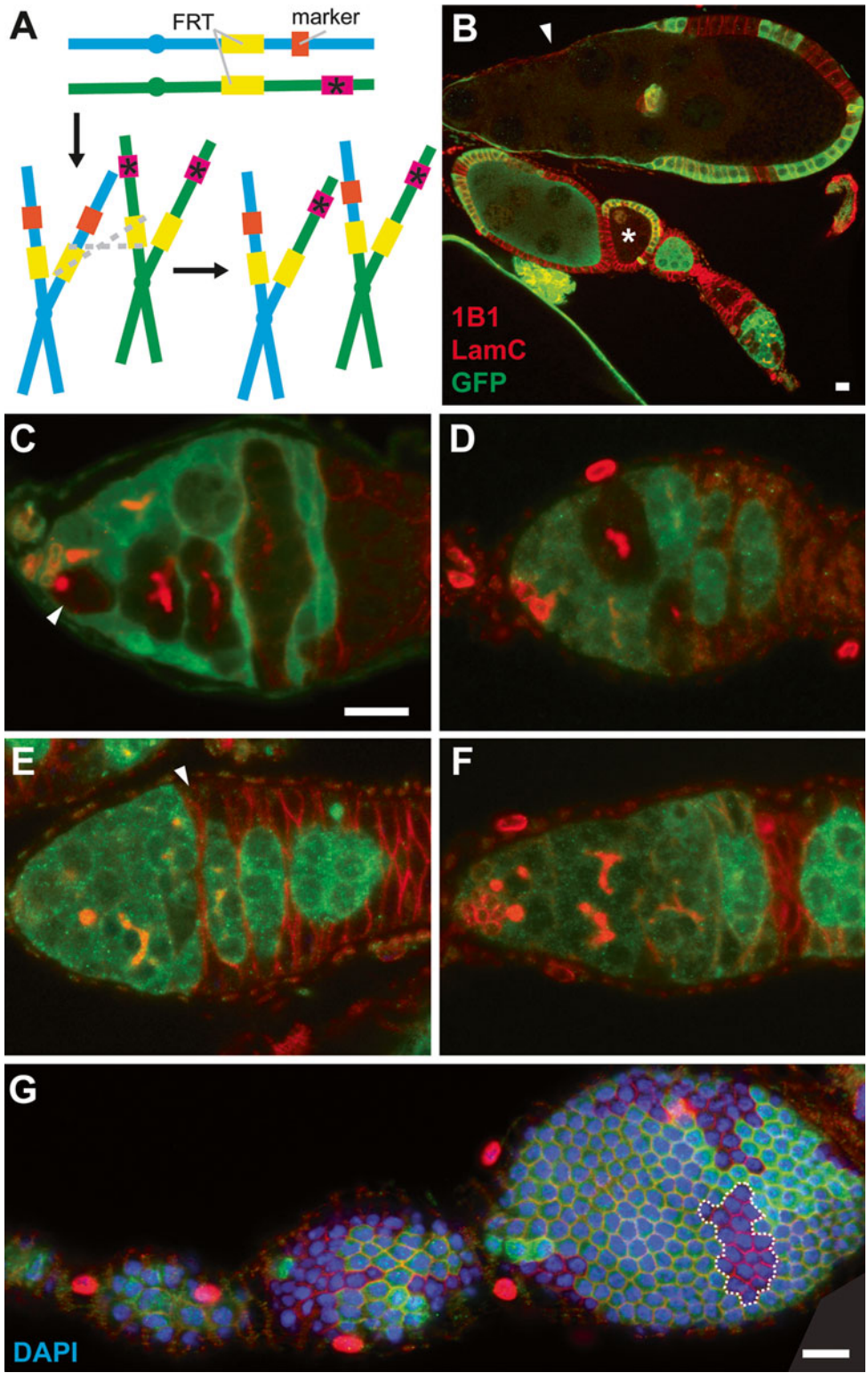

Fig. 1 Confocal images of genetic mosaic ovarioles and germaria. (**a**) GFP- or β-gal-negative mutant cells can be generated as unequal sister chromatids, produced as a result of FLP/*FRT*-mediated mitotic recombination (*grey dashed lines*), segregate during mitosis. The mutant allele is indicated by a *pink box* and an *asterisk*.

The focus of this chapter is how genetic mosaic analysis using adult-generated negatively marked clones of cells in the germline or follicle cell lineage can be used to study a number of processes during *Drosophila* oogenesis that are known to be controlled by dietary conditions. Previous studies in our laboratory using this type of analysis have led to the identification of specific cells that require various nutrient-sensing or hormonal pathway components, allowing us to distinguish between direct versus indirect roles of systemic factors in controlling multiple distinct processes, including germline stem cell (GSC) and follicle stem cell (FSC) maintenance or proliferation, germline cyst growth and development, follicle cell proliferation, and vitellogenesis [11–17]. The described protocol represents a detailed guide to strain generation, FLP/*FRT*-mediated clonal induction, ovary dissection and immunostaining, and data analysis.

2 Materials

2.1 Drosophila Strains and Culture Conditions

1. Suitable *Drosophila* strains (*see* **Note 1**), including mutant stock of interest, heat-shock inducible flippase (*hs-Flp*) (*see* **Note 2**), *FRT* insertion on appropriate chromosome arm (*see* **Note 3**), and a corresponding *FRT* insertion recombined to a ubiquitously expressed marker, such as *ubi-GFP* or *arm-lacZ* (for GFP or β-gal expression, respectively).
2. G418, an aminoglycoside antibiotic, diluted in dH_2O to appropriate concentration, according to specific *FRT* insertion (*see* **Note 4**).
3. Standard fly culture medium in a plugged vial.
4. Dry active yeast, such as used in baking.
5. Wet yeast paste: ~20 g active dry yeast thoroughly mixed into ~35 ml of dH_2O to the consistency of smooth peanut butter (*see* **Note 5**).
6. Water bath set at 37 °C.
7. Vinyl-coated lead weight ring (or other weight of approximately 500 g).
8. Kimwipes.
9. Plastic rack for fly vials.
10. Dissecting pin or thin spatula.

2.2 Dissection and Immunostaining of Ovaries

1. 1.5 ml microfuge tubes (*see* **Note 6**).
2. Glass or plexiglass dissection dish.
3. Kimwipes.
4. Glass Pasteur pipette and bulb.

5. Phosphate buffered saline (PBS).
6. Grace's Insect Medium.
7. 3 % bovine serum albumin (BSA) prepared in dH_2O.
8. Washing Solution: 0.1 % Triton™ X-100 in PBS (*see* **Note 7**).
9. Blocking Solution: 5 % BSA, 0.1 % Triton™ X-100, 5 % normal goat serum in PBS (*see* **Note 8**).
10. Fixation Solution: 5.3 % formaldehyde in Grace's Insect Medium, prepared from 16 % formaldehyde (*see* **Note 9**).
11. Primary antibodies: mouse anti-1B1 (Adducin-related protein; Developmental Studies Hybridoma Bank, DSHB), mouse anti-Lamin C (DSHB); chicken anti-GFP (Abcam) or chicken anti-β-gal (Abcam).
12. Secondary antibodies: anti-mouse Alexa Fluor 568 or 633 and anti-chicken Alexa Fluor 488 (Life Technologies).
13. Click-It Kit (Invitrogen), for EdU incorporation assay (*see* **Note 10**).
14. 4′,6-diamidino-2-phenylindole (DAPI), for staining DNA.
15. Microscope glass slides and coverslips.
16. Weights of approximately 120 g, for flattening mounted samples.
17. Stereomicroscope.
18. Two pairs of sharpened forceps.
19. Tungsten needle and/or 27-gauge needle and syringe.
20. Nutator, for rotation of sample during fixation, washing, and immunostaining procedures.

2.3 Image Acquisition and Analysis

1. Confocal microscope or equivalent microscopy setup.
2. Image analysis software (such as ImageJ).

3 Methods

Overall, setting of the standard crosses to obtain control and experimental genotypes and performing the heat shock protocol described below take approximately 2 weeks if starting from expanded, healthy fly stocks. Following the final heat-shock, the timing of dissection for clonal analysis is a crucial variable for the appropriate interpretation of results, as discussed in Subheading 3.3.

3.1 Drosophila Strains and Culture Conditions

1. Generate a recombinant fly stock containing both the proximal *FRT* insertion and the mutant allele of interest on the same chromosome arm through standard crosses. *FRT* transgenes may carry different selection markers, but the majority include the *neoR* marker (*see* **Notes 4** and **11**). To select for flies carry-

ing the *neoR*-containing *FRT* among progeny resulting from recombination cross (*see* **Note 12**), maintain the cross on food treated with a G418 solution of appropriate concentration (*see* **Note 13**). Crosses should be transferred to fresh food every 2 days, such that the resulting progeny will be raised on G418 and thereby selected for the presence of the *FRT* insertion. Individual progeny should subsequently be screened for the presence of the mutant allele of interest for identification of flies carrying the recombinant chromosome and balanced as a stock.

2. Generate flies of control and experimental genotypes (*see* **Note 14**) through standard crosses. At 0–2 days after eclosion (*see* **Note 15**), transfer females of appropriate genotypes along with sibling males to vials especially prepared for heat shock. These vials should include half of a folded Kimwipe directly covering the food surface to prevent the flies from sticking to it during heat shock.
3. Place flies in heat shock vials in a plastic rack, spreading vials out to allow easy water flow between them. Heat shock flies in the 37 °C water bath, placing the weight on top of the vials to keep the rack underwater, and maintaining the appropriate water level to ensure that flies are confined to the submerged portion of the vial. Heat shock should be conducted for 1 h × 2/day (*see* **Note 16**), for 3 consecutive days (*see* **Note 17**).
4. Following the final heat shock, transfer flies to vials supplemented with wet yeast paste, adding new males to the vials if some have died during heat shock. Transfer flies to vials containing fresh wet yeast daily until dissection. When selecting time points for dissection, consider the perdurance of both the marker used (*see* **Note 18**) and the protein of interest. Dissection time points up to 10 days after heat shock will include both transient and permanent clones [18] (*see* **Note 19**), which is an important consideration when interpreting the data. Multiple time points are typically included in the analyses.

3.2 Dissection and Immunostaining of Ovaries

1. Prepare eppendorf tubes for the dissected ovaries by filling them with a 3 % BSA solution (*see* **Note 20**).
2. Using a Pasteur pipette, transfer Grace's Insect Medium to a dissection dish (*see* **Note 21**).
3. Anesthetize the flies using CO_2 and select females for dissection. Pick up the females one at a time by gently pinching the thorax with sharp forceps.
4. Submerge each female in a dissection well filled with Grace's Insect Medium under a stereomicroscope. While holding females by the thorax, use the second pair of forceps to carefully pinch and pull away the posterior of the abdomen (at approximately two segments from the end). Ovaries should

come out easily; otherwise, they can be pushed out of the abdomen.

5. Tease apart the anterior halves of ovarioles using a sharp tungsten needle or a fine-gauge needle in a syringe (*see* **Note 22**). Immobilize ovaries by holding on to their posterior end using a pair of forceps and run the tungsten needle between ovarioles to tear the muscle sheath away from the anterior half.
6. Before transferring dissected ovaries to eppendorf tubes, remove the BSA solution from eppendorf tubes using a pasteur pipette, and discard the solution. This will also serve to coat the pipette with BSA and prevent ovaries from sticking to the glass. Use this coated pipette to transfer the dissected ovaries to the eppendorf tube.
7. Repeat this process for all genotypes, minimizing the time between dissection and fixation. Ideally, the time between dissection and fixation should not exceed 30 min.
8. Fix the ovaries in freshly prepared Fixation Solution for 13 min with rotation on a nutator at room temperature (*see* **Note 23**).
9. Rinse the ovaries 3× in Washing Solution by letting ovaries settle to bottom of the tube, then repeatedly changing the buffer. Wash 4 × 15 min on a nutator at room temperature (*see* **Note 24**).
10. Block the ovaries in Blocking Solution for at least 3 h at room temperature or overnight at 4 °C on a nutator (*see* **Note 25**).
11. Stain the ovaries with primary antibodies diluted in Blocking Solution: anti-1B1 (1:10), anti-Lamin C (1:100), and anti-GFP (1:2000). Primary antibody incubation times range from 3 h at room temperature to overnight at 4 °C on a nutator.
12. Wash the samples 4 × 15 min in Washing Solution rocking on a nutator (*see* **Note 26**).
13. Stain the ovaries with secondary antibodies (anti-mouse Alexa Fluor 568 and anti-chicken Alexa Fluor 488) diluted 1:200 in blocking solution and protected from light by covering with aluminum foil. Secondary antibody incubation times range from 1 to 5 h at room temperature on a nutator.
14. Stain the sample for 10 min with 0.5 μg/ml DAPI in Washing Solution at room temperature, protected from light, on a nutator.
15. Wash the sample for at least 4 × 15 min in Washing Solution at room temperature, protected from light by covering with aluminum foil, on a nutator.
16. Remove the Washing Solution and add a small volume of the mounting medium of choice. (We use either Vectashield or 90 % glycerol containing 20 mg/ml *n*-propyl gallate). Gently and thoroughly mix the ovarioles with mounting medium using

a pasteur pipette. The samples will keep at 4 °C in the dark in mounting medium for extended periods of time (*see* **Note 27**).

17. To mount the samples, transfer the samples mixed with mounting medium onto a glass slide under a stereomicroscope. Using a pair of tungsten needles, carefully separate the large late stage egg chambers from the ovarioles and remove them from the slide. (For details on the staging of ovarian follicles, *see* ref. 19) The presence of large egg chambers on the slide will prevent the germaria from being sufficiently flattened by the mounting process, making it difficult to image them. Using tungsten needles, gently distribute the ovarioles away from each other prior to adding the coverslip.
18. Add a glass coverslip, cover it with a Kimwipe, and apply gentle pressure to the sample using a weight. This will flatten the ovarioles to facilitate imaging (*see* **Note 28**). Seal the coverslip using nail polish. Sealed, the mounted slides will keep for extended periods of time at 4 °C in the dark.

3.3 Image Acquisition and Analysis

Several general considerations in genetic mosaic analysis are crucial for accurate data interpretation. For example, perdurance of the protein of interest after removal of the cognate gene through mitotic recombination will depend on the stability of the protein and corresponding mRNA. Similarly, visualization of mutant cells will depend on the perdurance of GFP or β-gal markers. Finally, the marker expression level and the frequency of clone induction will vary depending on the specific marker and *FRT* insertions used for the experiments, respectively.

The types of images required vary depending on the type of analysis being conducted. We find it more efficient to acquire images for one type of analysis at a time rather than acquiring all types of images during the same microscopy sessions because the image acquisition mode may vary according to type of analysis. One should also be careful to avoid the analysis of damaged ovarioles (*see* ref. 20) or those where immunostaining did not work well. The most common types of analyses performed in our lab are described below, starting with germline analyses involving ovarioles followed by those focused on the germarium, and ending with analyses of the follicle cell lineage.

3.3.1 Follicle Growth and Survival

1. The growth and survival of GFP (or β-gal)-negative mutant germline cysts within developing follicles is assessed relative to flanking follicles containing GFP-positive cysts within the same ovariole (Fig. 1b, asterisk; Fig. 2a). In control mosaic ovarioles,

Fig. 2 (continued) (**c**) Permanent clones arising from an identifiable GFP-negative FSC in the germarium (*left*) or without a GFP-negative FSC (*right*), which indicates a loss event. (**d**) Transient (*left*) and permanent (*middle*) follicle cell clones are imaged in single planes for quantification of follicle cell proliferation by clone size or EdU incorporation frequency, respectively. Cross-sections of follicle cell clones (*right*) in the ovariole are often visible during germline cyst analyses

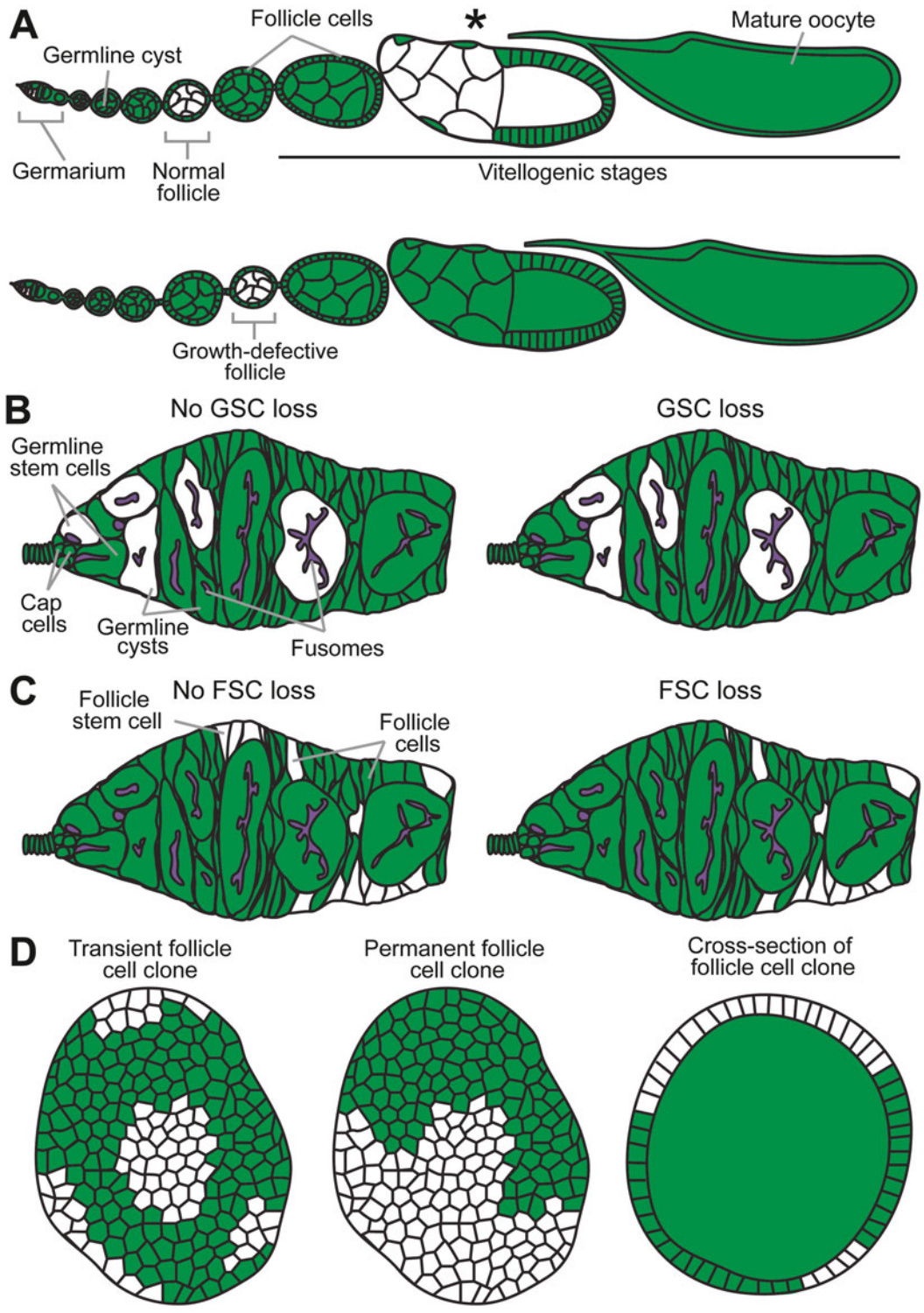

Fig. 2 Diagrams of potential genetic mosaic analysis outcomes. (**a**) *Top*: A normal ovariole containing previtellogenic ("normal follicle") and vitellogenic (*asterisk*) follicles with GFP-negative germline cysts. *Bottom*: A follicle containing a GFP-negative cyst showing a delay in growth, readily apparent in comparison to neighboring wild-type follicles. (**b**) A permanent clone derived from an identifiable GFP-negative GSC (*left*) populates the germarium (*left*). A recent GSC loss event is recognizable by the presence of GFP-negative germline cystoblasts/cysts within a mosaic germarium without the original GFP-negative mother GSC (*right*).

GFP-negative follicles are larger than anterior and smaller than posterior flanking follicles. A deviation from this pattern in the experimental mosaics can reflect either a defect in cyst growth or premature death of the cyst. These two possibilities can be distinguished by co-staining ovaries with an apoptosis marker. Several dozens of ovarioles should be analyzed per genotype at 10 days after the last heat shock. (For more precise quantification of the extent of cyst growth delay or overgrowth, *see* refs. 16 and 17).

3.3.2 Progression Through Vitellogenesis

1. Vitellogenesis begins at stage 8 of oogenesis [19, 21]. To assess the progression of mutant cysts through vitellogenesis, we quantify the fraction of ovarioles that contain a GFP-negative vitellogenic cyst in control versus mutant mosaic ovarioles (Fig. 1b, arrowhead; Fig. 2a, asterisk). Do not include any "artificially truncated" ovarioles (i.e., in which vitellogenic cysts have been inadvertently removed from the ovariole during dissection or mounting) in the analysis. Although degenerating vitellogenic egg chambers with pyknotic nuclei may also be directly detected in mosaic ovarioles, it is not possible to reliably score such egg chambers as GFP-negative or -positive. The ideal number of ovarioles scored per genotype will depend on the penetrance of the phenotype, but, at a minimum, several dozen should be analyzed at 10 days after heat shock.
2. An alternative method for quantifying a vitellogenesis block involves exclusively analyzing mosaic ovarioles in which the entire germline is homozygous mutant, and scoring what percentage of the ovarioles have vitellogenic versus dying follicles, in relation to equivalent control mosaics. Samples sizes, however, will be inevitably small, given the rarity of mosaic ovarioles containing a fully mutant germline.

3.3.3 GSC Maintenance

1. Method I: measuring the occurrence of directly observable GSC loss events. In germaria where all transient clones have exited the germaria [18], all GFP-negative cystoblasts and germline cysts will have arisen from a GFP-negative GSC (Fig. 1c, arrowhead; Fig. 2b). To quantify GSC loss, we count the number of germaria that contain GFP-negative GSCs along with their GFP-negative progeny (Figs. 1c and 2b, left), versus similar germaria in which the original GFP-negative GSCs have been lost (i.e., the presence of GFP-negative germline cysts/cystoblasts in the absence of a GFP-negative GSC indicates that the GSC was lost from the niche) (Figs. 1d and 2b, right) (*see* **Note 29**). The number of germaria showing a GSC loss event as a fraction of all germaria containing a mosaic germline can be directly compared among different control and experimental mosaics. This approach provides a snapshot

of the GSC loss events, and a single time point (e.g., 7–10 days after the last heat-shock) can be informative when comparing control and mutant mosaic germaria. A subtle GSC loss phenotype may not become apparent unless many germline mosaic germaria are analyzed, but approximately 100 germaria per genotype represents a reasonable sample size.

2. Method II: calculating the fraction of ovarioles carrying GFP-negative GSCs over time. Quantify the number of germaria containing at least one GFP-negative GSC as a percentage of the total number of germaria in the sample (*see* **Note 30**). This proportion is sensitive to the recombination frequency of the *FRT*, so changes in the fraction of ovarioles containing GFP-negative GSCs should be tracked over time (e.g., 4–7 days, 2, 3, and 4 weeks after heat shock) in control and mutant mosaic germaria. Due to potential variability in the frequency of initial FLP/*FRT*-mediated recombination events, larger samples sizes (several hundred germaria per genotype per time point) allow more reliable measurements.

3.3.4 FSC Maintenance

1. Currently, no reliable markers exist for FSCs, and they can only be unambiguously identified using a combination of criteria, including lineage tracing, morphology and position within germaria. Briefly, FSCs are the anterior-most somatic cells within follicle cell clones immediately anterior to the 2a/2b junction of the germarium (Fig. 1e, arrowhead; Fig. 2c, left). Follicle cells differ from more anteriorly located somatic cells, escort cells, by nuclear and cellular morphology [23]. The same general strategy described above to measure GSC loss can be used for FSCs (Figs. 1e, f, and 2c), with similar timing and sample size considerations.

3.3.5 Early Cyst Development

1. The number of early progeny of GFP-negative GSCs at different stages of development can be readily quantified in germaria containing at least one GFP-negative GSC. Germline cysts are staged by the morphology of their fusomes [24] (Figs. 1c and 2b). After counting the numbers of GFP-negative cystoblasts, and 2-, 4-, 8-, and 16-cell cysts present within each germarium, those numbers are normalized to the number of GFP-negative GSCs within that same germarium. By comparing the average number of different early GFP-negative GSC progeny present in control versus mutant mosaic germaria, it is possible to detect changes in the relative frequencies of various stages, which can be the result of stage-specific delay, arrest or death of germline cysts. Alternatively, the relative distribution of early germline stages can be compared between GFP-negative versus GFP-positive GSC progeny within the same population of germaria of a given genotype, which has the advantage of

minimizing any potential influence of genotypic background on the analyses. Analyzing several dozens of mosaic germaria per genotype at 7–10 days after heat shock should be sufficient to reveal differences in cyst distribution.

3.3.6 GSC Proliferation

1. To directly measure the frequency of GSCs in S phase, quantify the total number of mutant, GFP-negative GSCs that have incorporated the thymidine analog EdU as a percentage of all GFP-negative GSCs observed (*see* **Note 31**). This number can be compared to either incorporation of EdU in neighboring, marker-positive GSCs, or in marker-negative GSCs in control mosaics. Although this is a labor-intensive process, it is recommended to score several hundred of the GFP-negative GSCs per genotype for reliable results, unless differences in proliferation rates are enormous and readily apparent.
2. An indirect (and less labor intensive) readout of GSC proliferation is the number of progeny per GSC present in each germarium. Comparing the number of cystoblasts and germline cysts per GFP-negative versus GFP-positive GSCs is a relative measure of the number of GSC divisions in the recent past, as long as problems with cystoblast/cyst survival are ruled out (*see* Subheading 3.3.5).

3.3.7 FSC Proliferation

As for GSCs, FSC proliferation can be detected by EdU incorporation. In this case, lineage analysis is used to identify FSCs as described above, and the number of EdU-positive FSCs as a fraction of all GFP-negative FSCs is compared between mutant and control mosaic germaria. As for GSC proliferation analysis, sample sizes should be large.

3.3.8 Follicle Cell Proliferation

1. The proliferation of follicle cells can also be directly measured by quantifying the number of EdU-positive follicle cells as a fraction of all GFP-negative follicle cells analyzed during mitotic stages of follicle development (egg chamber stages 2–6; [19]). The percentage of EdU-positive follicle cells within the population of GFP-negative follicle cells can be compared to that of GFP-positive follicle cells within the same mutant mosaic ovarioles or to that of GFP-negative follicle cells in control mosaic ovarioles (Fig. 2d). Dozens of ovarioles should be scored at 10 days after heat shock.
2. Alternatively, transient follicle cell clone size (e.g., 3 days after heat shock) quantification may serve as a readout for follicle cell proliferation during mitotically dividing stages (egg chamber stages 2–6; [19]). GFP-negative clones should be compared in mutant and control mosaic ovarioles (Fig. 1g, dashed outline; Fig. 2d, *left*). One caveat of this approach, however, is that other factors (such as cell death or elimination) can also influence clone size. Dozens of clones should be analyzed per genotype.

4 Notes

1. Many of the necessary strains can be obtained from the Bloomington *Drosophila* Stock Center at Indiana University (www.flystocks.bio.indiana.edu).
2. Rather than employing *hs-Flp*, one could drive a *UAS-Flp* transgene in a spatially restricted pattern using a Gal4 line with a specific expression pattern [9], although this eliminates temporal control.
3. *FRT* insertion should map to the same chromosome arm as the mutation of interest, which should be distal to the *FRT*.
4. The concentration of G418 is calculated based on the active concentration of the drug and the level of resistance conferred by expression of the *neomycin resistance* (*neoR*) transgene in different *FRT* insertion lines. The G418 concentration should therefore be optimized for each specific *FRT* insertion, using appropriate positive and negative controls to ensure appropriate selection. For example, flies carrying one copy of the *FRT82B* insertion survive when raised on food treated with 30 mg/ml of active G418, while all control wild type flies die.
5. The consistency of yeast paste may change over time. We recommend storing prepared yeast paste at 4 °C, covered with Parafilm.
6. While 1.5 ml microtubes are usually used, smaller tubes may be used to conserve antibody, especially when ovary size is significantly reduced.
7. Immunostaining for the fusome marker 1B1 works best when Triton™ X-100 is used, whereas for an alternate fusome marker, α-spectrin, we recommend Tween-20 instead.
8. The same detergent should be used in the washing and blocking solutions.
9. 16 % FA keeps for 1 week at 4 °C after being opened, after which fixation quality deteriorates. Fixation conditions must be optimized for each antibody, but antibodies described in this protocol work reproducibly well under these fixation conditions.
10. If using the Click-It EdU incorporation kit, the Alexa Fluor 633 secondary antibody should be used instead of Alexa Fluor 568, which has a similar emission spectrum to the Click-It conjugate. The manufacturer's instructions should be used to visualize EdU.
11. Different *FRT* insertions vary in levels of *neoR* expression, which is controlled by a heat-shock inducible promoter. While the leakiness of the promoter is often sufficient for selection on G418-treated fly food at room temperature, it is sometimes

necessary to periodically heat-shock flies at 37 °C during the drug treatment for robust expression of *neoR* (e.g., *FRT80B*) and effective selection.

12. The "recombination cross" is the cross between females carrying the *FRT* chromosome in *trans* to the mutation of interest and balancer males.
13. To prepare the fly food for G418 selection, etch a checkerboard pattern onto the surface of the preprepared food using a dissecting needle or thin spatula, and then apply 200 μl of G418 solution. Dry food completely under a fume hood before transferring the crosses to the vials.
14. Experimental genotypes should carry the *FRT* insertion recombined to the mutant allele in *trans* to a corresponding wild-type *FRT* chromosome carrying a GFP or β-gal marker, in addition to the *hs-Flp* transgene on a separate chromosome. Control genotypes are virtually identical, with the exception that no mutant allele is present, such that marker-negative clones will be wild type.
15. To induce clones in the ovarian GSC niche, *Drosophila* should be heat shocked in the late larval and early pupal stages [14] rather than in adult stages.
16. Heat shocks should ideally be 8–12 h apart.
17. Between heat shocks, transfer flies to regular fly food supplemented with dry yeast.
18. For example, we find that perdurance of GFP makes the identification of negatively marked GSCs difficult until 4 days after the last heat shock.
19. Transient clones are derived from mitotic recombination occurring within individual dividing progeny of the stem cells (which further divide to form clones) and, as oogenesis progresses, they disappear. In contrast, permanent clones are derived from a stem cell, and tend therefore to be much longer lasting than transient clones.
20. Reagents and freshly dissected ovaries can be kept at room temperature or on ice, depending on which particular cellular proteins or structures will be visualized by immunostaining. For example, if an EdU incorporation assay will be performed, all reagents and dissected ovaries should be kept at room temperature.
21. Placing a black background under the dissecting dish helps with visualization of the ovaries during dissection and mounting.
22. For assays conducted on unfixed tissue (e.g., EdU incorporation), or for the visualization of intact terminal filament structures, do not tease ovarioles apart at this stage. In these

cases, ovarioles can be teased apart following fixation by returning them to the dissection plate with Wash Buffer.

23. Optimal fixation and staining conditions depend on the antibody being used and should be established prior to conducting this analysis. These conditions work well for the antibodies noted in this protocol, which are routinely used in our laboratory.
24. Once the Fixation Solution has been thoroughly rinsed from the sample, washes are very flexible. Depending on the antigen being detected, the sample can remain in Wash Solution for up to 2 weeks at 4 °C.
25. Samples can remain in Blocking Solution for extended periods of time at 4 °C.
26. After the samples have been stained with primary antibody, they can be stored in washing solution for extended periods of time at 4 °C.
27. Labile epitopes and the Click-it reaction used to detect EdU incorporation are exceptions and should be imaged as soon as possible.
28. The extent to which ovarioles should be flattened varies depending on the type of analysis to be conducted. For example, to obtain good single-plane images of the follicle epithelium, additional weight (up to double) may be necessary. Conversely, samples lacking vitellogenic stages (such as those from flies on a poor diet) will be more easily flattened.
29. GSCs can be unambiguously identified by the presence of a stereotypically shaped, 1B1-positive fusome juxtaposed to the Lamin C-positive niche [22].
30. The percentage of ovarioles containing GFP-negative GSCs sometimes increase from early to later time points, possibly due to some GFP perdurance at early time points.
31. An increase in the percentage of EdU incorporation of GSCs could reflect either an increase in proliferation rates or a slower S phase. To distinguish between these possibilities, it is necessary to employ a secondary method of analysis (e.g., the use of a different cell cycle marker, such as the mitosis marker phosphorylated histone H3, or a direct comparison between the numbers of GSC progeny).

Acknowledgements

We are grateful to members of the Drummond-Barbosa lab for critical comments during the preparation of this manuscript. This work was supported by National Institutes of Health (NIH) grant R01 GM069875 (D.D.B.). K.L. was supported by NIH training grant T32CA009110.

References

1. Perrimon N (1998) Creating mosaics in *Drosophila*. Int J Dev Biol 42:243–247
2. Theodosiou NA, Xu T (1998) Use of FLP/FRT system to study *Drosophila* development. Methods 14:355–365
3. Le Lievre CS, Le Douarin NM (1975) Mesenchymal derivatives of the neural crest: analysis of chimaeric quail and chick embryos. J Embryol Exp Morphol 34:125–154
4. Lehmann R, Nusslein-Volhard C (1987) hunchback, a gene required for segmentation of an anterior and posterior region of the *Drosophila* embryo. Dev Biol 119:402–417
5. Hadorn E (1968) Transdetermination in cells. Sci Am 219:110–114 passim
6. Simon MA, Bowtell DD, Dodson GS et al (1991) Ras1 and a putative guanine nucleotide exchange factor perform crucial steps in signaling by the sevenless protein tyrosine kinase. Cell 67:701–716
7. Xu T, Rubin GM (1993) Analysis of genetic mosaics in developing and adult *Drosophila* tissues. Development 117:1223–1237
8. Lee T, Luo L (2001) Mosaic analysis with a repressible cell marker (MARCM) for *Drosophila* neural development. Trends Neurosci 24:251–254
9. Evans CJ, Olson JM, Ngo KT et al (2009) G-TRACE: rapid Gal4-based cell lineage analysis in *Drosophila*. Nat Methods 6:603–605
10. Struhl G, Basler K (1993) Organizing activity of wingless protein in *Drosophila*. Cell 72:527–540
11. Ables ET, Drummond-Barbosa D (2010) The steroid hormone ecdysone functions with intrinsic chromatin remodeling factors to control female germline stem cells in *Drosophila*. Cell Stem Cell 7:581–592
12. Ables ET, Drummond-Barbosa D (2013) Cyclin E controls *Drosophila* female germline stem cell maintenance independently of its role in proliferation by modulating responsiveness to niche signals. Development 140:530–540
13. Hsu HJ, Drummond-Barbosa D (2009) Insulin levels control female germline stem cell maintenance via the niche in *Drosophila*. Proc Natl Acad Sci U S A 106:1117–1121
14. Hsu HJ, Drummond-Barbosa D (2011) Insulin signals control the competence of the *Drosophila* female germline stem cell niche to respond to Notch ligands. Dev Biol 350:290–300
15. Hsu HJ, LaFever L, Drummond-Barbosa D (2008) Diet controls normal and tumorous germline stem cells via insulin-dependent and -independent mechanisms in *Drosophila*. Dev Biol 313:700–712
16. LaFever L, Drummond-Barbosa D (2005) Direct control of germline stem cell division and cyst growth by neural insulin in *Drosophila*. Science 309:1071–1073
17. LaFever L, Feoktistov A, Hsu HJ et al (2010) Specific roles of Target of rapamycin in the control of stem cells and their progeny in the *Drosophila* ovary. Development 137:2117–2126
18. Margolis J, Spradling A (1995) Identification and behavior of epithelial stem cells in the *Drosophila* ovary. Development 121: 3797–3807
19. Spradling AC (1993) Developmental genetics of oogenesis. In: Bate M (ed) The development of *Drosophila melanogaster*. Cold Spring Harbor Laboratory Press, Plainview, NY
20. Haack T, Bergstralh DT, St Johnston D (2013) Damage to the *Drosophila* follicle cell epithelium produces "false clones" with apparent polarity phenotypes. Biol Open 2:1313–1320
21. Cummings MR, Brown NM, King RC (1971) The cytology of the vitellogenic stages of oogenesis in *Drosophila melanogaster*. 3. Formation of the vitelline membrane. Z Zellforsch Mikrosk Anat 118:482–492
22. Xie T, Spradling AC (2000) A niche maintaining germ line stem cells in the *Drosophila* ovary. Science 290:328–330
23. Sahai-Hernandez P, Castanieto A, Nystul TG (2012) *Drosophila* models of epithelial stem cells and their niches. Wiley Interdiscip Rev Dev Biol 1:447–457
24. de Cuevas M, Spradling AC (1998) Morphogenesis of the *Drosophila* fusome and its implications for oocyte specification. Development 125:2781–2789

Chapter 5

Culturing *Drosophila* Egg Chambers and Investigating Developmental Processes Through Live Imaging

Lathiena Manning and Michelle Starz-Gaiano

Abstract

Drosophila oogenesis provides many examples of essential processes in development. A myriad of genetic tools combined with recent advances in culturing egg chambers ex vivo has revealed several surprising mechanisms that govern how this tissue develops, and which could not have been determined in fixed tissues. Here we describe a straightforward protocol for dissecting ovaries, culturing egg chambers, and observing egg development in real time by fluorescent microscopy. This technique is suitable for observation of early- or late-stage egg development, and can be adapted to study a variety of cellular, molecular, or developmental processes. Ongoing analysis of oogenesis in living egg chambers has tremendous potential for discovery of new developmental mechanisms.

Key words *Drosophila melanogaster* oogenesis, Live imaging, Ex vivo egg culturing, Fluorescent microscopy, Developmental genetics, Cell migration, Morphogenesis

1 Introduction

The advent of live, fluorescent imaging of cells and tissues has revolutionized our ability to understand cell biology and the events that occur during development [1–3]. The *Drosophila* ovary is small and transparent, making it straightforward to culture and image. Additionally, ovaries are amenable to a variety of genetic manipulations, which enables targeted investigations of the genes controlling development. The combination of mutant analysis and live imaging provides much greater detail on molecular functions. Several recent reviews detail oogenesis comprehensively, including [4–6]. Eggs mature along a structure called an ovariole, resembling a string of beads. Each egg chamber is comprised of a small number of cell types: 1 oocyte, 15 large nurse cells that support oocyte growth, and 600–1000 follicle cells that surround the germline cells.

While the architecture of the egg chamber is relatively simple, the regulatory systems that coordinate tissue development are

Diana P. Bratu and Gerard P. McNeil (eds.), *Drosophila Oogenesis: Methods and Protocols*, Methods in Molecular Biology, vol. 1328, DOI 10.1007/978-1-4939-2851-4_5,

quite complex. The ovary provides examples of many different kinds of developmental processes, including stem cell regulation, RNA localization, tissue morphogenesis, and cell migration, and insights into all of these have been made possible by direct observation of cell behaviors in their natural environments by live imaging (Table 1). Among the striking discoveries, researchers have found that proteins can traffic between intercellular ring canals throughout this tissue [22, 32], that the oblong egg architecture requires molecular corseting through ECM and actinomyosin contraction waves [18, 23], that stem cells interact with each other and niche cells [30], and that clusters of migratory cells move by cycling leader cells [10–12]. Undoubtedly, additional live imaging studies will yield further insights into oogenesis as well as conserved developmental mechanisms more generally.

Here, we provide a straightforward protocol for imaging cellular events during oogenesis on a conventional compound fluorescent microscope. While it would be ideal to image eggs within the mother, this is not possible due to opacity of the cuticle and the massive movements of the ovary that occur to promote egg laying. Thus, developing eggs must be dissected from the female flies and cultured ex vivo. We first describe a method for dissection of the ovary out of the female and into ovarioles. Although microdissection is challenging at first, practice makes this methodology accessible to researchers at all experience levels. Egg chambers are then placed in a culturing chamber suitable for imaging. While short-term imaging of older egg chambers in air-permeable halocarbon oil was known to work [24, 25, 27], recent discoveries enabled optimization of culture conditions for longer term egg development [10–12, 19, 21, 28]. In particular, addition of insulin and careful regulation of the media pH made this possible. A checkpoint between stages 9 and 10 of oogenesis still prevents

Table 1
Areas of study that have applied live imaging techniques during oogenesis

Category of study	References
Cargo transport-RNA localization	[7–9]
Cell migration	[10–17]
Cytoskeleton	[18–20]
Mitochondrial dynamics	[21]
Morphogenesis	[22–26]
Protocols/tools	[13, 17, 27–29]
Stem cell regulation	[30, 31]

observations of egg chambers transitioning through all of oogenesis [1], perhaps due to hormonal signals or massive growth at the middle stages, which could require import of nutrients not provided in the culture media. However, early stages can be observed for up to 14 h [30], and older stages can routinely be cultured for 4–6 h without developmental defects [12, 28, 29].

The protocol described here is suitable for investigation of events at multiple developmental time points. We provide tables with characterized, genetically tagged markers that have been used for different purposes, and we detail stains and dyes that enable observation of subcellular structures. We describe methodology for fluorescent imaging on a standard upright compound microscope equipped with a digital camera and time-lapse acquisition software, and suggest tips for alternative imaging systems. Thus, this basic protocol can be adapted for various purposes to characterize fundamental processes in oogenesis.

2 Materials

2.1 Dissection and Culturing Solutions

1. Schneider's medium.
2. Dissection medium: To Schneider's medium add fetal bovine serum to 15 % (v/v) and 0.6× penicillin/streptomycin. Filter sterilize and store at 4 °C (*see* **Note 1**).
3. Live imaging medium: Add 1 μl of concentrated HCl (caustic—use caution) to 1 ml of dH_2O. Using this, add bovine insulin to prepare a stock solution of 10 mg/ml. Add insulin stock solution to an aliquot of 1 ml of the dissection medium to a final concentration of 200 μg/ml (*see* **Note 2**). Prepare 2 ml of the dissection medium if using fluorescent dyes or labels.
4. Fluorescent dyes: Dilute each dye separately to its final concentration in 0.5 ml of live imaging medium. We use 2 μg/ml of Hoechst 33342 DNA dye and 9 μM of FM 4-64. Additional dyes/stains have been successfully imaged in living egg chambers (Table 2).

2.2 Ovary Dissection

1. "Fly station": Stereomicroscope with top-down illumination (*see* **Note 3**) and a CO_2 blow gun and pad for anesthetizing flies.
2. Dumont #5 Forceps (*see* **Note 4**).
3. One glass depression dish/slide(s) with two cavities or two slides with one depression each. One cavity is needed for dissection and the other is used to place ovaries in after dissection to separate them from the fly carcass and unwanted tissues/debris that can contaminate the media.

Table 2
Fluorescent dyes used for live imaging of oogenesis

Fluorescent dye	Localization	Concentration	Excitation wavelength (nm)	Source	References
FM 4-64	Cell membrane	9 μM	515	Life Technologies	[10, 11, 26]
Hoechst 33342	Nucleus	2 μg/ml	350	Life Technologies	M.S.G. [47]
MitoTracker-GreenFM	Mitochondria	1:1000	488	Life Technologies	[21]
Vybrant DiO	Nucleus	1:200	488	Life Technologies	M.S.G. unpublished
SYTO Green Fluorescent Nucleic Acid Stains	Nucleus	1:400	488	Life Technologies	M.S.G. unpublished

2.3 Live Imaging

1. Air-permeable culture dish Lumox® Dish 50 (Sarstedt) (*see* **Note 5**) that can fit on the stage of a compound, live-imaging microscope (*see* **Note 6**).
2. 22×40 mm^2 glass cover slips, one cut with a diamond knife or broken into 3–4 narrow strips that will be used as "feet" to hold up the top cover slip and prevent it from crushing the samples. The top cover slip size depends on the culture dish size.
3. Halocarbon oil.

3 Methods

3.1 Dissection of Ovaries

1. To "fatten" flies: Transfer 5–15 female flies (2–4 days old) of the appropriate genotype (*see* Table 3 for select, characterized transgenic lines with fluorescent reporters used in egg chambers) and a few males to a fresh fly food vial with added active dry yeast. Use cotton as a plug for the vials, and add a few drops of water to the cotton to keep the humidity high.
2. Put the vial with the desired flies in a 25 or 29 °C incubator for 14–16 h for stages 8–10 egg chambers (temperature and incubation time are dependent on genotype and desired stages for imaging; *see* **Note 7**).
3. At the fly station, pipet a few drops of dissection medium (without insulin) to fill each of the two cavities in a glass depression slide. The medium in the depression slide can be at room temperature. Gather the remaining materials at the fly station, and keep the live imaging medium on ice.

Table 3
Representative fluorescent reporter lines that genetically label cells for live imaging

Fluorescent reporter line	Labeled structure(s)	Stage observed	References (source if different)
Mito-GFP	Mitochondria	Germarium	[21, 33] (Carnegie Protein Trap Library)
Jupiter-GFP	Microtubules of germline stem cells	Germarium	[30, 34]
UAS-Tubulin-GFP	Escort cells	Germarium	[30] (G. Struhl)
His2Av-mRFP	All nuclei	Germarium, 5–9	[23, 30] (Bloomington *Drosophila* Stock Center (BDSC))
Wcd::GFP/GFP	Germline stem cells	Germarium	[35]
Df31-GFP	All nuclei	Germarium	[30, 33]
Vkg-GFP	Basal surface of follicle cells	5–9	[23, 33, 35] (Carnegie Protein Trap Library)
Myristoylated-mRFP	Follicle cells	5–9	[23]
Indy-GFP	Cell membrane	5–9	[23] (J. Lipsick)
PACT-GFP	Centrioles	5–10	[7, 36]
Sas-4-GFP	Centrioles	5–10	[7, 37]
Cam-RFP	Cell membrane	5–10	[7, 38]
Cnn-GFP	Pericentriolar material	5–10	[7, 39]
Msn-YFP	Basal surface of follicle cells	6	[26] (*Drosophila* Genetic Resource Center (DGRC))
Me31B-GFP	Germline	8–10	[27] (S. Kobayashi)
Tau-GFP	Microtubules of oocyte and nurse cells	8–13	[3, 9, 12, 27] (D. St Johnston)
Osk:MCP-GFP	Oocyte	9	[3, 7] (D. St Johnston)
Ub-GFP-Pav-KLP	Ring canals	9–10	[22, 40]
Sqh-GFP	Cell membrane and myosin II	9–10	[14, 41]
EB1-GFP	Microtubule plus ends	9–10	[12, 42]
UAS-GFP-Paxillin	Focal adhesions	9–10	[18] (BDSC)
α-catenin-GFP	Cell membrane	9–10	[11] (DGRC)
ubi-NLS-GFP or dsRed	Nuclei	9–10	[10–12, 43] (BDSC)
Slbo-Lifeact-FP	Actin in border cells	9–10	[13]
UAS-Photo-activatable GFP	Under Gal4 and light control	9–10	[22, 32, 44]
Staufen-GFP	Oocyte	9–13	[9] (D. St Johnston)
E-Cadherin-GFP	Cell membrane	9–15	[18, 25, 45] (E. F. Wieschaus)
Moesin-GFP	Cell membrane	10–14	[18, 24, 28] (BDSC)
MCP-GFP/RFP	Tagged RNAs	11–13	[9]

The table represents a sample of transgenic lines used to investigate various aspects of *Drosophila* oogenesis. Published results showed expression at the stages indicated

4. Anesthetize the flies using CO_2 and place them on a CO_2 pad. Sort the females from the males, and arrange the females with wings down and anterior to the left.
5. Hold the forceps in each hand at a slight angle, resting the hinge end against the base of the first finger. With the left hand, grasp a female at the top of the abdomen, near the thorax (*see* **Note 8**) (Fig. 1a). Submerge the abdomen of the fly into the dissection media in the depression slide.
6. With the right-hand forceps, grasp the ventral posterior end of the abdomen and pierce through the cuticle. Gently pull to the right, which should liberate ovaries and some internal organs (*see* **Note 9**). Carefully separate ovaries from other tissues, and place them into fresh media in a depression slide (Fig. 1b). Discard the carcass and wipe the forceps off on a tissue.
7. Repeat until at least 3–4 female flies are dissected. Discard the males.
8. Gently remove the dissection media by pipetting 20 μl at a time with a P20 pipettor. Watch through the microscope to avoid removing any ovaries or ovarioles. Add several drops of live imaging medium to the ovaries. Live imaging medium should be kept on ice during the dissections, but the depression slide and ovaries can stay at room temperature.

3.2 Dissection of Ovaries into Ovarioles

1. With the left forceps, hold an ovary at the posterior end (near the largest egg chambers). Some older egg chambers will be crushed. With the right (dominant-hand) forceps, pinch an egg chamber near the narrow anterior end of the ovary, nearest to germarium (Fig. 1c) (*see* **Note 10**).
2. Slowly and steadily, pull an ovariole chain out of the ovary sheath (*see* **Note 11**). Egg chambers of different stages, connected by stalks (Figs. 1c, d), will be visible. Continue to dissect out ovarioles individually until all desired egg chambers are removed (*see* **Note 12**).
3. Remove any undesired egg chambers or debris with forceps from the depression slide and discard into other medium or a tissue (*see* Fig. 1d for an overview of egg chamber stages) (*see* **Note 13**).
4. Carefully aspirate the live imaging medium using a P20 pipettor and discard. Look through the microscope to avoid pipetting up any ovariole chains or egg chambers (*see* **Note 14**). Repeat until most media is removed, but retain some in the depression cavity to prevent drying of the ovarioles (*see* **Note 15**).
5. Gently add 200 μl of live imaging medium or medium supplemented with a fluorescent dye. For Hoechst 33342 nuclear staining, incubate the ovariole chains in media and dye for

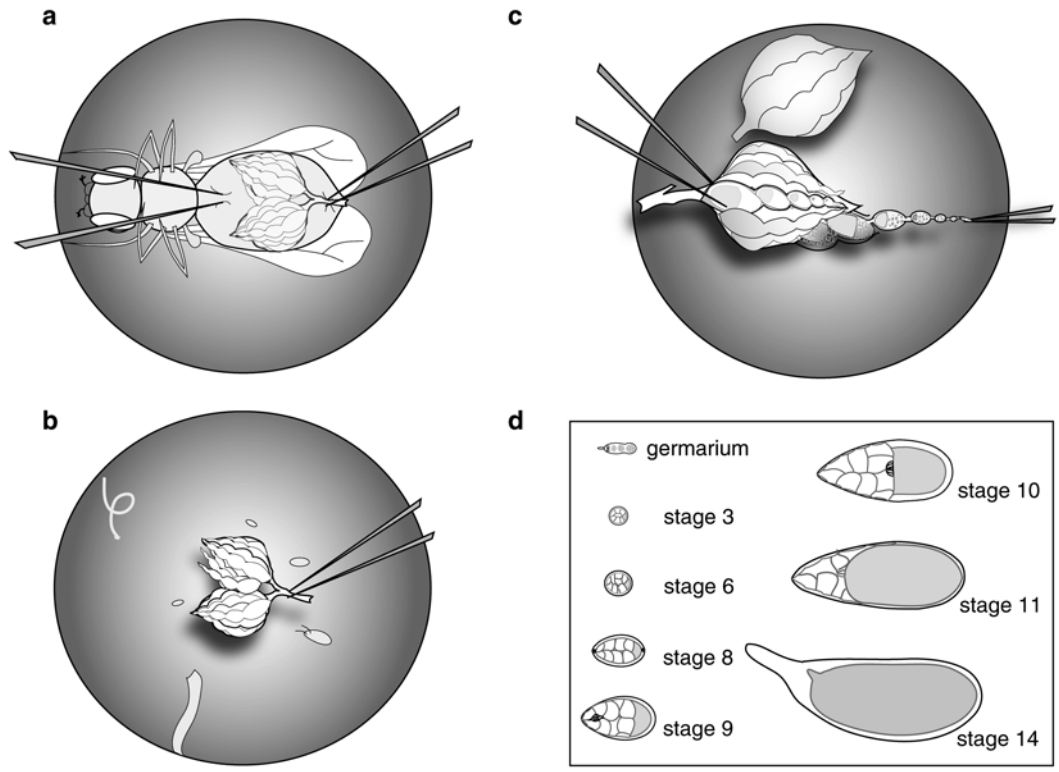

Fig. 1 Depiction detailing *Drosophila melanogaster* ovary and ovariole dissection. (**a**) Ventral view of a female fly with the anterior facing left. Left-hand forceps, held at an angle, grasp the female at the abdomen. Right-hand forceps pierce the cuticle at the abdomen posterior and pinch the oviduct. This would be reversed for left-handed researchers. (**b**) The ovaries have been gently pulled out of the abdomen of the fly and should be transferred to a new cavity of a depression slide with fresh media to protect them from lysed cells and debris. (**c**) One ovary (depicted at higher magnification than in **b**) is held at the posterior end with the left forceps, while the right forceps grasp young egg chambers, near the germarium. As the young egg chamber is steadily pulled to the right, an ovariole chain is liberated from the ovary sheath. Stalks between egg chambers can be seen when the ovariole is free from the sheath; otherwise egg chambers are pressed together, as seen in the ovary. (**d**) Depiction of multiple stages of oogenesis with the anterior facing left and posterior facing right. Stages are indicated

10 min, and then carefully remove the solution (*see* **Note 16**). If no dyes are being used, remove the media after incubation for a few minutes and proceed to **step 7**.

6. Add 200 μl of live imaging medium supplemented with a second label or dye. For the membrane marker FM 4-64, incubate the ovariole chains with the supplemented media for 5 min. Then, carefully remove the solution (*see* **Note 16**).
7. Gently add 200 μl of live imaging medium to the ovarioles. Take care to submerge all the ovarioles. Prepare a chamber for live imaging.

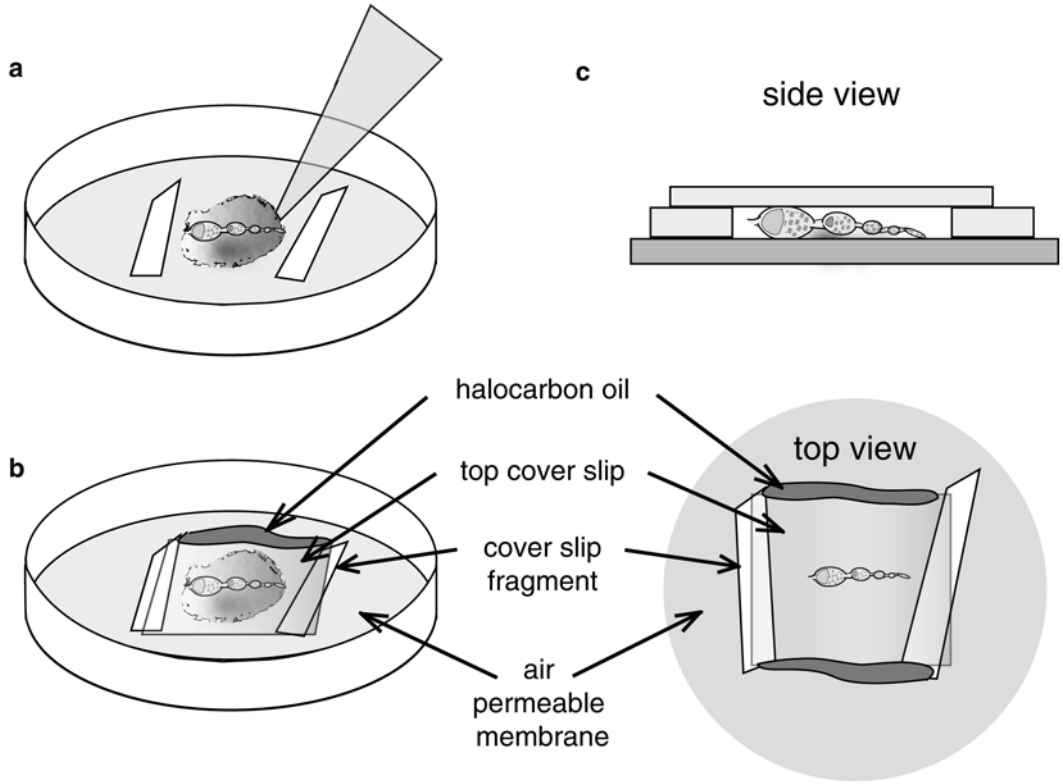

Fig. 2 Assembly of a long-term live imaging chamber. (**a**) Two pieces of a broken glass cover slip are placed on a culturing dish with enough space to allow for egg chambers. Cover slip pieces act as a platform to hold up the top cover slip and prevent crushing the egg chambers (as shown in **c**). Using a pipettor, egg chambers in live imaging media are transferred to the dish between the cover slip pieces. (**b**) Gently place a 22×40 mm^2 cover slip onto the cover slip fragments to cover the egg chambers. Pipette a small amount of halocarbon oil (*darker gray*) along the top side of the cover slip and repeat on the bottom side (not shown). (**c**) *Top*: Side view of the completed live imaging chamber. *Bottom*: Top view of the completed live imaging chamber

3.3 Mounting of Egg Chambers for Long-Term Live Imaging

1. For imaging on an upright microscope, prepare a Lumox® culture dish for mounting egg chambers (for other cases, *see* **Note 17**). Wrap a 22×40 mm^2 glass cover slip in a Kimwipe tissue and break into two or three strips. Place the two pieces onto the membrane of a culture dish, creating a space for egg chambers approximately 1 cm apart (Fig. 2a) (*see* **Note 18**). This acts as a platform for the top cover slip to prevent crushing the ovarioles. Add a few microliters of live imaging media at the base of the cover slips, to make them stay in place.
2. Cut off the end of a 200 µl pipette tip with a clean razor blade. Slowly pipet 50 µl of the ovarioles in live imaging medium and transfer to the culture dish in the space between the two pieces of cover slip, avoiding the creation of bubbles.
3. Slowly and gently place a 22×40 mm^2 cover slip on top of the cover slip pieces to cover the egg chambers (Fig. 2b, c).

Handle carefully and do not apply any pressure to the cover slip (*see* **Note 19**).

4. Pipet halocarbon oil around the two sides of the perimeter of the cover slip to prevent evaporation of the media (Fig. 2b, c).

3.4 Imaging of Egg Chambers

1. Place the live imaging chamber on the stage of a compound fluorescent microscope (*see* **Note 17**). Choose the desired objective, taking care not to touch the live imaging chamber (*see* **Note 20**).
2. Scan through the ovarioles using white light illumination, until a desired egg chamber is selected (*see* **Note 21**). Avoid any egg chamber with abnormal appearance or damage, even if the damage is far from the cells of interest.
3. Select the time-lapse function on the microscope. Test the exposure times for all channels (*see* **Note 22**).
4. Select the appropriate interval time and duration for the experiment (*see* **Note 23**).
5. Start the automated time-lapse imaging, and check the focal plane, camera exposure times, and developmental progression every 10–15 min. *See* Fig. 3 for an example of normal development of a stage 9 egg chamber. Pause the time-lapse acquisitions and adjust the focus or exposure times if needed (*see* **Note 24**), or choose a new specimen if development is not proceeding normally (*see* **Note 25**).

4 Notes

1. Sterilized dissection medium can be kept in the cold for up to a month. If stored, swirl the medium to check for contaminants (which would look cloudy and settle to the bottom) prior to use. Sera concentrations range from 10 to 20 % [10, 18, 19, 25, 28]. Sera quality sometimes varies by batches. Some laboratories have had success with alternative media, such as EBR or Ringers [19, 21], but we have found that the pH of the medium is the most important factor; it must be near pH 6.9–7.0. Alternatively, some laboratories image with egg chambers directly in halocarbon oil [7, 12, 27, 29, 35].
2. Insulin stock solutions can be stored at –20 °C and stored for 2–3 days or two freeze-thaw cycles. Live imaging medium should be made fresh for best egg chamber viability. The pH of the final medium should be correct with addition of insulin, but test it if in doubt. If the pH is higher than 7.1, discard it and remake the medium.
3. For a stereomicroscope setup, we prefer adjustable gooseneck lights and a black base for optimally viewing white ovaries.

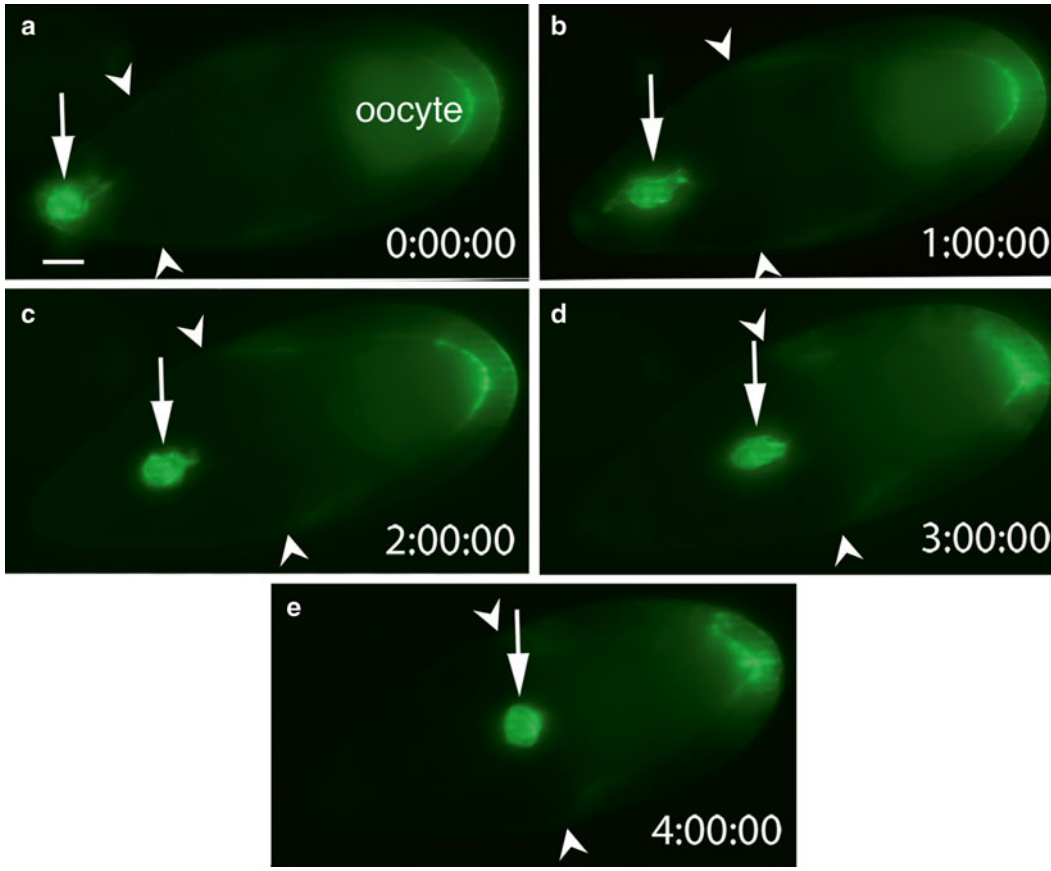

Fig. 3 Live imaging of border cell migration in stage 9 egg chambers. (**a**–**e**) Time-lapse series of fluorescent images of a stage 9 egg chamber. At stage 9, border cells detach from the anterior epithelium (*left*) and migrate as a cluster towards the oocyte located at the egg chamber posterior. *Arrows* indicate the border cell cluster; *arrowheads* indicate the anterior-most columnar follicle cells; and times are indicated in hours. Scale bar is 20 μm. Note the normal movements of the border cells and outer follicle cells as development proceeds

4. Sharp fine-tipped forceps are essential for precise ovariole dissection to prevent egg chamber damage. We use #5 forceps with a tip diameter of 0.05×0.02 mm made of Dumostar alloy for strength and durability, and always store the forceps clean and dry, with a tip protector. Forceps tips should close evenly. Bent tips can often be repaired by bending under the dissection microscope, and dull tips can sometimes be sharpened to an acceptable point by using a wet sharpening stone.
5. This protocol is optimized for Sarstedt Lumox dishes, which have an air-permeable bottom membrane that does not interfere with fluorescent illumination of specimens. These dishes can be reused several times by washing them out with mild detergent and rinsing with ethanol, as long as the membrane is not damaged. Several laboratories have had success imaging

egg chambers mounted on glass-bottom culture slides/dishes, such as those from ibidi or MakTek [29, 30].

6. Stage adaptors designed to fit a small culture dish (35–50 mm), instead of a standard slide, are ideal for securing the Lumox dish while imaging. If an adaptor is not available, the dish can be placed atop a glass slide on a standard stage. For other culture chambers, a different adaptor may be necessary.
7. For general purposes, overnight incubation of females on yeast paste at 25 °C is appropriate because the yeast stimulates egg production. A 14–16-h incubation results in many stage 8–10 egg chambers at the time of dissection, but this can vary by other environmental conditions. If younger egg chambers are desired, shorter incubation times or colder incubation temperature would be needed; conversely, a longer time spent at 25 °C will produce more older egg chambers. If Gal4 lines are being used, we incubate flies at 29 °C to increase Gal4 activity and gene expression.
8. This protocol is written for a right-handed researcher for the purpose of clarity, but can easily be reversed for someone who is left-handed.
9. Often the ovaries will be pulled out intact as a pair, or one at a time, and can be easily recognized and separated from other tissues. However, if the flies have not been sufficiently fattened, very small ovaries can be hard to distinguish from other organs. Sometimes the abdomen breaks off entirely, and must be filleted open or squeezed to liberate the ovaries. It is also important at this step to avoid breaking the gut and releasing its contents—if this occurs, the media will become cloudy in appearance, and it is important to wash ovaries off gently with additional dissection medium.
10. The main method described is optimized for middle to late oogenesis stages. To image germaria, do NOT grasp the anteriormost tip of the ovaries. Instead, hold the ovaries in the left hand, and grasp one or two egg chambers towards the center with the right hand. Slowly peel the ovarioles apart towards the right. Other methods, such as teasing, have been employed.
11. As ovarioles are pulled out of the muscle sheath, they will deform and pop back into shape. The stalks between egg chambers should be apparent (Fig. 1c). It is important to pull on only one or two ovarioles at a time or they will not be liberated from the sheath. While imaging through the muscle sheath is possible, it results in movements during imaging. Live imaging tends to be more successful using egg chambers that have not been mishandled. Even small scrapes or bumps can disrupt development, so it is critical to manipulate the ovarioles by contacting the stages that are not to be imaged.

It may also help to press the forceps gently against the bottom of the depression well to stabilize them.

12. Careful ovariole dissections can be a time-consuming process. It is beneficial to minimize the time spent here, to improve the length of live imaging. Thus, we recommend practicing these steps prior to an imaging experiment. Also, for initial experiments, dissect only a small number of ovarioles while keeping in mind that not all egg chambers will be at the desired stage(s).
13. If the egg chambers of interest are of an early developmental time point, it is important to remove late-stage egg chambers to prevent excess consumption of medium and to allow for better mounting of the small egg chambers.
14. To avoid pipetting the desired ovarioles, swirl the depression slide and let the contents settle to collect ovarioles in the center of the well. Then, aspirate from the top side of the depression well.
15. Egg chambers must not be allowed to dry out, or they will die. The medium can evaporate quickly given the small volumes and the heat from the light of the microscope. Proceed quickly to the next step.
16. Incubation times for fluorescent markers vary by dye, application, and the egg chamber stage of interest, and should be determined empirically. The suggested times are for imaging mid-oogenesis stages, particularly to see border cell migration.
17. For short-term imaging (less than 30 min), ovarioles can be mounted in air-permeable halocarbon oil on a glass slide or cover slip [7, 12, 27, 29, 35]. For mounting for imaging on an inverted microscope, a top cover slip is not necessary. In this case, place egg chambers in media on a slide or dish that has a glass cover slip bottom [7, 29, 30] (*see* **Note 5** for other culture dishes).
18. Take care not to puncture the permeable membrane of the imaging dish.
19. Handle the cover slip by the edges, or with a forceps, so no fingerprints are left on it, which would interfere with imaging. Do not press down on the egg chambers, as they could be crushed or deformed and not develop well. Try to avoid trapping small air bubbles under the cover slip.
20. For imaging border cell migration or overall egg chamber development during mid-oogenesis, a 20× air objective is usually sufficient. To image with an oil objective, it is helpful to have the cover slip fragments closer together to hold up the top cover slip and reduce pressure on the samples.
21. It is important to avoid excessive exposure to fluorescent light to prevent phototoxic effects. We recommend first finding the

correct stages using transmitted light illumination with phase-contrast or DIC capabilities, and then briefly examining the fluorescent markers to identify the desired samples/stages. Be aware that the oocyte displays some autofluorescence [28, 29]. We often mark the location of several possible samples before deciding which are the best ones. Do not choose to image egg chambers that are touching other specimens, or in contact with an air bubble, as these will not develop well. While it is possible with an automated X–Y stage to image multiple egg chambers at once, this can cause the specimens to change positions if they are in live imaging medium.

22. If using more than one fluorescent channel, select lower exposure times to prevent phototoxicity. Intensities may change during long-term imaging, but many imaging platforms allow the user to pause and change the exposure times during the time course. For standard experiments, we use a 20× objective on an epifluorescent microscope (Zeiss AxioImager Z1) equipped with filters to reduce heat and a motorized stage that can be controlled through a computer (Zeiss AxioVision software). As a guideline, we recommend total exposure times to be limited to 600 ms. There is a trade-off between exposure times and number of total images captured, or length of the experiment. For optical sections, we use a structural interference system (Zeiss Apotome), but confocal microscopy is a good alternative if the scanning speed is fast. Optical sectioning may require longer total exposure times, so development may proceed better if the total number of images is small. Spinning disc and two-photon imaging systems dramatically reduce phototoxicity, but may also reduce signal intensity. For discussion of different imaging methodologies, *see* [46].

23. Interval times between image acquisitions will vary based on the application and stage of the egg chamber. If long exposure times are required, we recommend longer intervals between image acquisitions. If short intervals are necessary, the specimen may not survive as long. We routinely acquire images at 3- or 5-min intervals for a duration of 4–5 h.

24. Several problems are common in the early stages of time-lapse imaging. Drastic changes in focal plane may signal swelling of the specimen or sinking of the bottom membrane. Adjust the focal plane as needed. If the egg chamber is drifting out of the field of view, the stage may be uneven or there may be a gap in the seal of halocarbon oil, allowing slow evaporation. This may be corrected by adjusting the live imaging chamber accordingly.

    In the case other problems arise, a new specimen is often required. If the egg chamber swells or bursts, the media may be imbalanced or evaporating. If egg chamber shrinks in size, the

egg chamber has likely died, or the media may be imbalanced. A new culture may be needed in these cases. If irregularities in development become obvious, the egg chamber has likely been damaged, and should be replaced with a different one for imaging. If the egg chamber is not developing at all after 30 min, test another specimen. Multiple specimens not developing can indicate a problem with the media. If egg chambers are not developing, try a pilot experiment with less frequent image capture to reduce phototoxicity and demonstrate that culture conditions are working. It is advantageous to identify several possible samples to image at the beginning, and record their locations on the stage, to minimize time spent switching to a new sample later.

25. To assess if mid- to late oogenesis is progressing normally, look for growth of the oocyte, rearrangement of outer follicle cells, border cell migration, cytoplasmic streaming from the nurse cells, and normal spatiotemporal appearance of fluorescent reporters (Fig. 3).

Acknowledgements

This work was funded in part by a Department of Education Grant, Graduate Assistance in the Areas of National Need (GAANN) training fellowship (P200A120017), and by an NIGMS Initiative for Maximizing Student Development Grant (2 R25-GM55036), IMSD Meyerhoff Graduate Fellowship, to L.M. and a National Science Foundation CAREER Award (IOS-1054422) to M.S.G. We appreciate helpful comments on the manuscript from Dr. N. Sanchez-Alberola, G. Wunderlin, E. Desai, and D. DiMercurio, and we thank Dr. J. McDonald and Dr. A.C.C. Jang for sharing culturing information.

References

1. He L, Wang X, Montell DJ (2011) Shining light on *Drosophila* oogenesis: live imaging of egg development. Curr Opin Genet Dev 21:612–619
2. Mavrakis M, Pourquie O, Lecuit T (2010) Lighting up developmental mechanisms: how fluorescence imaging heralded a new era. Development 137:373–387
3. Parton RM, Valles AM, Dobbie IM et al (2010) Live cell imaging in *Drosophila melanogaster*. Cold Spring Harb Protoc 2010:pdb.top75
4. Hudson AM, Cooley L (2014) Methods for studying oogenesis. Methods 68:207–217
5. Bastock R, St. Johnston D (2008) *Drosophila* oogenesis. Curr Biol 18:R1082–R1087
6. Horne-Badovinac S, Bilder D (2005) Mass transit: epithelial morphogenesis in the *Drosophila* egg chamber. Dev Dyn 232: 559–574
7. Zhao T, Graham OS, Raposo A et al (2012) Growing microtubules push the oocyte nucleus to polarize the *Drosophila* dorsal-ventral axis. Science 336:999–1003
8. Forrest KM, Gavis ER (2003) Live imaging of endogenous RNA reveals a diffusion and entrapment mechanism for *nanos* mRNA localization in *Drosophila*. Curr Biol 13:1159–1168

9. Weil TT, Forrest KM, Gavis ER (2006) Localization of *bicoid* mRNA in late oocytes is maintained by continual active transport. Dev Cell 11:251–262
10. Bianco A, Poukkula M, Cliffe A et al (2007) Two distinct modes of guidance signalling during collective migration of border cells. Nature 448:362–365
11. Prasad M, Montell DJ (2007) Cellular and molecular mechanisms of border cell migration analyzed using time-lapse live-cell imaging. Dev Cell 12:997–1005
12. Tekotte H, Tollervey D, Davis I (2007) Imaging the migrating border cell cluster in living *Drosophila* egg chambers. Dev Dyn 236:2818–2824
13. Cai D, Chen SC, Prasad M et al (2014) Mechanical feedback through E-cadherin promotes direction sensing during collective cell migration. Cell 157:1146–1159
14. Majumder P, Aranjuez G, Amick J et al (2012) Par-1 controls myosin-II activity through myosin phosphatase to regulate border cell migration. Curr Biol 22:363–372
15. Starz-Gaiano M, Melani M, Wang X et al (2008) Feedback inhibition of Jak/STAT signaling by apontic is required to limit an invasive cell population. Dev Cell 14:726–738
16. Ramel D, Wang X, Laflamme C et al (2013) Rab11 regulates cell-cell communication during collective cell movements. Nat Cell Biol 15:317–324
17. Wang X, He L, Wu YI et al (2010) Light-mediated activation reveals a key role for Rac in collective guidance of cell movement in vivo. Nat Cell Biol 12:591–597
18. He L, Wang X, Tang HL et al (2010) Tissue elongation requires oscillating contractions of a basal actomyosin network. Nat Cell Biol 12:1133–1142
19. Spracklen AJ, Fagan TN, Lovander KE et al (2014) The pros and cons of common actin labeling tools for visualizing actin dynamics during *Drosophila* oogenesis. Dev Biol 393:209–226
20. Ferreira T, Prudencio P, Martinho RG (2014) *Drosophila* protein kinase N (Pkn) is a negative regulator of actin-myosin activity during oogenesis. Dev Biol 394:277–291
21. Cox RT, Spradling AC (2003) A Balbiani body and the fusome mediate mitochondrial inheritance during *Drosophila* oogenesis. Development 130:1579–1590
22. McLean PF, Cooley L (2013) Protein equilibration through somatic ring canals in *Drosophila*. Science 340:1445–1447
23. Haigo SL, Bilder D (2011) Global tissue revolutions in a morphogenetic movement controlling elongation. Science 331: 1071–1074
24. Dorman JB, James KE, Fraser SE et al (2004) bullwinkle is required for epithelial morphogenesis during *Drosophila* oogenesis. Dev Biol 267:320–341
25. Osterfield M, Du X, Schüpbach T et al (2013) Three-dimensional epithelial morphogenesis in the developing *Drosophila* egg. Dev Cell 24:400–410
26. Lewellyn L, Cetera M, Horne-Badovinac S (2013) Misshapen decreases integrin levels to promote epithelial motility and planar polarity in *Drosophila*. J Cell Biol 200:721–729
27. Weil TT, Parton RM, Davis I (2012) Preparing individual *Drosophila* egg chambers for live imaging. J Vis Exp (60): e3679
28. Prasad M, Jang AC, Starz-Gaiano M et al (2007) A protocol for culturing *Drosophila melanogaster* stage 9 egg chambers for live imaging. Nat Protoc 2:2467–2473
29. Pokrywka NJ (2013) Live imaging of GFP-labeled proteins in *Drosophila* oocytes. J Vis Exp (73): 50044
30. Morris LX, Spradling AC (2011) Long-term live imaging provides new insight into stem cell regulation and germline-soma coordination in the *Drosophila* ovary. Development 138: 2207–2215
31. Snapp EL, Iida T, Frescas D et al (2004) The fusome mediates intercellular endoplasmic reticulum connectivity in *Drosophila* ovarian cysts. Mol Biol Cell 15:4512–4521
32. Airoldi SJ, McLean PF, Shimada Y et al (2011) Intercellular protein movement in syncytial *Drosophila* follicle cells. J Cell Sci 124: 4077–4086
33. Buszczak M, Paterno S, Lighthouse D et al (2007) The carnegie protein trap library: a versatile tool for *Drosophila* developmental studies. Genetics 175:1505–1531
34. Karpova N, Bobinnec Y, Fouix S et al (2006) Jupiter, a new *Drosophila* protein associated with microtubules. Cell Motil Cytoskeleton 63:301–312
35. Fichelson P, Moch C, Ivanovitch K et al (2009) Live-imaging of single stem cells within their niche reveals that a U3snoRNP component segregates asymmetrically and is required for self-renewal in *Drosophila*. Nat Cell Biol 11:685–693
36. Martinez-Campos M, Basto R, Baker J et al (2004) The *Drosophila* pericentrin-like protein is essential for cilia/flagella function, but

appears to be dispensable for mitosis. J Cell Biol 165:673–683

37. Peel N, Stevens NR, Basto R et al (2007) Overexpressing centriole-replication proteins in vivo induces centriole overduplication and de novo formation. Curr Biol 17:834–843
38. Morin X, Daneman R, Zavortink M et al (2001) A protein trap strategy to detect GFP-tagged proteins expressed from their endogenous loci in *Drosophila*. Proc Natl Acad Sci U S A 98:15050–15055
39. Conduit PT, Brunk K, Dobbelaere J et al (2010) Centrioles regulate centrosome size by controlling the rate of Cnn incorporation into the PCM. Curr Biol 20:2178–2186
40. Minestrini G, Mathe E, Glover DM (2002) Domains of the Pavarotti kinesin-like protein that direct its subcellular distribution: effects of mislocalisation on the tubulin and actin cytoskeleton during *Drosophila* oogenesis. J Cell Sci 115(4):725–736
41. Royou A, Field C, Sisson JC et al (2004) Reassessing the role and dynamics of nonmuscle myosin II during furrow formation in early *Drosophila* embryos. Mol Biol Cell 15(2): 838–850
42. Shimada Y, Yonemura S, Ohkura H et al (2006) Polarized transport of Frizzled along the planar microtubule arrays in *Drosophila* wing epithelium. Dev Cell 10:209–222
43. Cliffe A, Poukkula M, Rørth P (2009) Culturing *Drosophila* egg chambers and imaging border cell migration. Nat Protoc 10:289
44. Datta SR, Vasconcelos ML, Ruta V et al (2008) The *Drosophila* pheromone cVA activates a sexually dimorphic neural circuit. Nature 452:473–477
45. Huang J, Zhou W, Dong W et al (2009) Directed, efficient, and versatile modifications of the *Drosophila* genome by genomic engineering. Proc Natl Acad Sci 106(20): 8284–8289
46. Davis I, Parton RM (2006) Selection of appropriate imaging equipment and methodology for live cell imaging in *Drosophila*. CSH Protoc doi:10.1101/pdb.ip21
47. Stonko D, Manning L, Starz-Gaiano M, Peercy B (2015) A force-based biophysical model of collective cell migration in a three-dimensional, heterogeneous environment. PLoS One. 10(4):e0122799

Chapter 6

Border Cell Migration: A Model System for Live Imaging and Genetic Analysis of Collective Cell Movement

Mohit Prasad, Xiaobo Wang, Li He, Danfeng Cai, and Denise J. Montell

Abstract

Border cell migration in the *Drosophila* ovary has emerged as a genetically tractable model for studying collective cell movement. Over many years border cell migration was exclusively studied in fixed samples due to the inability to culture stage 9 egg chambers in vitro. Although culturing late-stage egg chambers was long feasible, stage 9 egg chambers survived only briefly outside the female body. We identified culture conditions that support stage 9 egg chamber development and sustain complete migration of border cells ex vivo. This protocol enables one to compare the dynamics of egg chamber development in wild-type and mutant egg chambers using time-lapse microscopy and taking advantage of a multiposition microscope with a motorized imaging stage. In addition, this protocol has been successfully used in combination with fluorescence resonance energy transfer biosensors, photo-activatable proteins, and pharmacological agents and can be used with wide-field or confocal microscopes in either an upright or an inverted configuration.

Key words Border cell migration, *Drosophila* stage 9 egg chambers, Organ culture, Collective cell migration, Time-lapse live imaging

1 Introduction

Collective cell migration refers to the concerted movement of a group of cells. Unlike single moving cells such as fibroblasts or fish keratinocytes, collectively migrating cells maintain some level of adhesion among themselves during movement [1, 2]. Though this kind of cellular movement is characteristic of several physiological processes during embryonic development [3], wound healing, and tumor metastasis [1], it has been studied less extensively than the movements of single cells. Recently, a number of model systems have emerged for the study of collective movement using the powerful combination of genetic manipulations and live imaging [4, 5]. One of these, border cell migration in the *Drosophila* ovary, is the focus of this chapter.

Drosophila females bear a pair of ovaries within the abdomen (Fig. 1). Each ovary consists of 15–20 strings of egg chambers of

Diana P. Bratu and Gerard P. McNeil (eds.), *Drosophila Oogenesis: Methods and Protocols*, Methods in Molecular Biology, vol. 1328, DOI 10.1007/978-1-4939-2851-4_6,

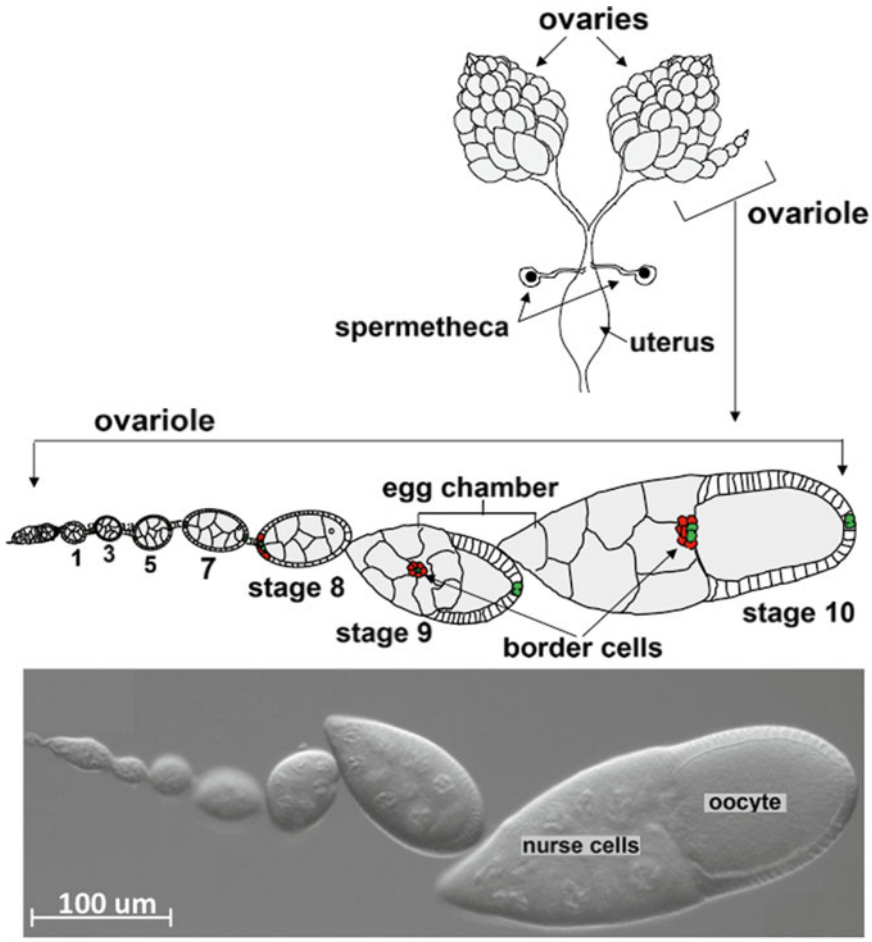

Fig. 1 Anatomy of the *Drosophila* ovary. *Top*—Schematic drawing of a pair of ovaries dissected from female fruit fly. A schematic drawing of an enlarged single ovariole containing egg chambers of the indicate stages of development. *Bottom*—DIC image of an ovariole with similar stages of egg chamber development

increasing stages of maturity, called the ovarioles. At the tip of each ovariole resides the germarium, which contains germline and somatic stem cells and their immediate progeny. Egg chambers assemble in the germarium when somatic follicle cells surround a cyst of 16 interconnected germline cells, one of which develops into the oocyte while the other 15 differentiate as support cells called nurse cells [6]. Egg chambers bud off from the germarium and then grow and progress through 14 developmental stages of *Drosophila* oogenesis [7]. Unlike the germ line cells, follicle cells continue to undergo mitotic divisions until stage 6 when they switch to endoreplication without cytokinesis [8]. During early oogenesis at each end of each egg chamber a pair of specialized follicle cells differentiates into the polar cells [9]. The polar cells secrete a cytokine, Unpaired (Upd), which activates JAK-STAT signaling in nearby follicle cells [10]. In late stage 8 and early stage 9, anterior

follicle cells (4–6 in number) that perceive the highest level of JAK-STAT signal round up [11, 12]. These cells are the border cells.

One or two of the cells extend protrusions in between the nurse cells. Some of these protrusions retract right away but sooner or later a protrusion attaches stably to the nurse cells and the border cell cluster detaches from the other follicle cells and from the basement membrane that surrounds the egg chamber [13, 14]. The border cells migrate directly down the center of the egg chamber toward the oocyte, in response to secreted signals. One such signal is the PDGF- and VEGF-related factor 1 (PVF1), which binds to a receptor tyrosine kinase, PVR, expressed on the border cells [15, 16]. PVR functions redundantly with epidermal growth factor receptor (EGFR) [15]. Three ligands for the EGFR are expressed in the oocyte [16, 17], Spitz, Keren, and Gurken, all of which are TGFα homologs. *Spitz* and *keren* mRNAs are distributed throughout the oocyte at stage 9 and these two ligands can redirect border cells when either one is misexpressed [16]. Thus, these ligands promote migration of the border cells to the oocyte. When the border cells get very close to the oocyte, they turn and move toward the dorsal side [17] (Movie 1). *Grk* mRNA and protein are restricted to the dorsal/anterior corner of the oocyte and promote the dorsal turn [17]. It is unlikely that border cells sense Grk until they get near the oocyte because there is no dorsal bias to the migration before that point [16]. Moreover, when Grk is expressed ectopically it is not sufficient to redirect border cells during the posterior migration [16].

The border cells cover a distance of approximately 150–200 μm in 4–6 h [13]. Their migration speed is variable and is faster in the beginning and slower near the end [14, 18]. In the migrating cluster, individual border cells can change relative position within the group, while the polar cells remain in the center [13, 14]. Until 2007, border cell migration was studied exclusively in fixed tissue due to the lack of suitable culture conditions for stage 9 egg chambers. Recently, we identified the culture conditions and subsequently optimized the imaging conditions for capturing the complete migration while minimizing phototoxicity [13] (Movie 1). This protocol has enabled more detailed phenotypic analysis and use of pharmacological agents, fluorescence resonance energy transfer (FRET) probes, and photo-activatable proteins [12, 19, 20]. In addition, this protocol can be used for studying other aspects of oogenesis including epithelial morphogenesis of follicle cells [21], RNA localization in the oocyte [22], actin dynamics in nurse cells [23, 24], and stem cell division in the germarium [24]. Key features of the protocol are optimization of pH and addition of insulin, which may generally enhance cultures of *Drosophila* tissues including imaginal discs. Longer term cultures (>6 h) may require perfusion systems to allow medium exchange.

2 Materials

2.1 Culture Reagents and Equipment

1. *Drosophila* Schneider's medium (*Drosophila* S2 Medium) supplemented with 20 % fetal bovine serum (FBS).
2. Insulin: A 10 mg/ml stock solution was prepared in acidified water (*see* **Note 1**) and used to supplement the culture media to a final concentration of 0.2 mg/ml.
3. (Optional) FM4-64 lipophilic dye dissolved in dH_2O or DMSO (*see* **Note 2**) used for labeling plasma membranes of all cells.
4. A fluorescent reporter that marks the border cells, e.g., *slbo*-GAL4; UAS-mCD8GFP [25, 26] or *slbo*-GAL4; UAS-MoesinGFP [13].
5. (Optional) Streptomycin/penicillin 10,000 U/ml of penicillin G–sodium, 10,000 mg/ml streptomycin sulfate in 0.85 % saline.
6. Lumox® dish (50 mm) (Sarstedt).
7. Cover slip glasses: 22×22 mm^2, thickness: 0.13–0.17 mm.
8. Steriflip®-GP, 0.22 μm filter (EMD Millipore SCGP00525).
9. Two pairs of forceps (Dumostar forceps #5) and a dissecting microscope.
10. Concavity dissection slides.
11. Fine-Tip Transfer Pipettes.
12. Halocarbon oil 27.
13. (Optional) Poly-D-lysine, 10 mg/ml in PBS.
14. Dry baker's yeast.
15. Heat-filter KG1 (Chroma Technologies).
16. BG38 IR suppression filter (Chroma Technologies).
17. Neutral-density filters (ND 0.3) (Chroma Technologies).
18. Wide-field microscope: We use a Zeiss Axio Imager upright epifluorescence microscope and Plan-Apochromat 20×/0.8 N.A. dry objective. Illumination source is X-Cite 120 metal halide lamp. Filter cube sets: BP470/40, FT495, BP525/50 for Alexa 488/GFP and BP550/25, FT570, BP605/70 for Alexa 568/DsRed.
19. Confocal microscope: We use a Zeiss 510-Meta inverted confocal microscope and Plan-Apochromat 63×/1.4 N.A. oil objective with argon (488 nm) and HeNe (542 nm) lasers. Filter sets are for FITC and TRITC.

2.2 Preparation of Culture Medium

1. *Drosophila* S2 medium was supplemented with 20 % FBS (needed) and 0.6× streptomycin/penicillin (optional). Sterilize it by passing through a 0.22 μm filter.

2. The final pH of the medium was adjusted to 6.85–6.95. Verify the pH of the medium before every use (*see* **Note 3**).
3. Supplement with insulin to a final concentration of 0.2 mg/ml. Henceforth, the medium with all the supplements would be referred to as complete medium.
4. (Optional) FM4-64 dye can be used at a final concentration of 9 μM to stain plasma membranes of all cells.

3 Methods

3.1 Preparing Poly-D-Lysine-Coated Cover Slips (Optional)

Take 5–10 cover slips (22×22 mm^2), wash with MilliQ H_2O, and dry. Cover the cover slips evenly with approximately 200 μl of 2 mg/ml of poly-D-lysine in PBS and dry them completely in a 37 °C oven. Rinse cover slips in flowing tap H_2O and subsequently rinse with MilliQ H_2O and then dry at room temperature.

3.2 Preparing Female Flies for Dissection

Transfer 5–10 females (2–4 days old) of the desired genotype along with 3–4 males into a new fly vial with fresh fly food, a small amount of baker's yeast, and incubate at 25 °C for 14–18 h (*see* **Note 4**).

3.3 Dissection of Ovaries to Egg Chambers

1. Anesthetize female flies on a CO_2 pad.
2. Fill the cavity of the dissection slide with complete medium and place the slide under the dissecting microscope.
3. Transfer one anesthetized fly to the slide using forceps.
4. Gently hold the thorax or upper abdomen of the immobile fly using a pair of forceps, submerge it in the medium, while with another pair of forceps grasp and peel off a bit of abdominal cuticle at the middle of the abdomen (Fig. 2a).
5. This reveals a large pair of ovaries, which are white and opaque after overnight fattening. Grasp the base of the ovaries (the common oviduct) and pull them away from the rest of the fly and into the medium (Fig. 2b). Remove the carcass using the forceps and discard it on a dampened Kimwipe. Keep the ovaries covered in medium at all times.
6. Repeat this process for all female flies, accumulating the ovaries in the complete medium on the dissection slide. Handle the ovaries very gently (*see* **Note 5**).
7. With one pair of forceps, hold the posterior part of a single ovary. Use another pair of forceps to gently grasp the anterior tip of the ovary (Fig. 2c) (older egg chambers reside at the posterior while the germarium and early-stage egg chambers occupy the anterior tip).

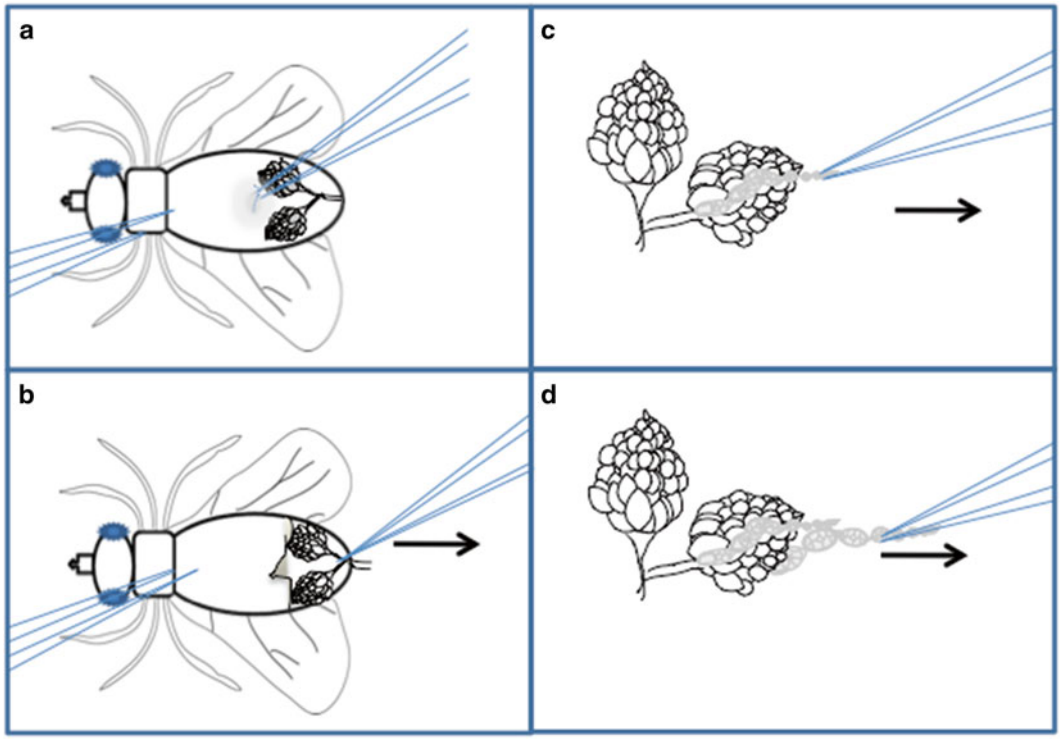

Fig. 2 Ovary dissection technique: Schematic representation of egg chamber dissection. (**a**) The female fly should be immobilized on its back using the left forceps. The right forceps are used to pinch the soft cuticle of the ventral side of the abdomen. (**b**) Pull the cuticle toward the right (*arrow*), revealing the ovaries. Grasp the common oviduct with the right forceps and pull to the right (*arrow*) to free the ovaries from the carcass. (**c**) Immobilize the ovary pair by pinching the oviduct using the left forceps. Use the right forceps to grasp the tip of an ovariole and slowly pull to the right (*arrow*). (**d**) Repeat until multiple ovarioles have been freed from the sheath

8. Gently pull the ovarioles out of the muscular sheath around ovary. Strings and sometimes individual egg chambers will pop out of the muscle sheath (Fig. 2c, d). Repeat this action until you get 5–10 stage 9 egg chambers. Never touch the stage 9 egg chambers directly with the forceps! You can pull on early- or very-late-stage egg chambers such that stage 9 chambers get isolated (*see* **Note 5**).
9. Use a plastic fine-tip transfer pipette to transfer egg chambers to a 500 µl Eppendorf tube. After the egg chambers settle down, aspirate old medium and replace with 300 µl fresh complete medium.
10. Break a 22×22 mm^2 cover slip into two halves (spacers). Align them 1 cm apart on a Lumox® dish and immobilize them with 5 µl complete medium under each of them.

11. Transfer 55 μl complete media with egg chambers between two cover slip spacers.
12. Carefully cover the samples with another 22×22 mm^2 cover slip. Cover slip should land on two spacers. Avoid bubbles (*see* **Note 6**).
13. Remove excess media from around the cover slips with Kimwipe so that egg chambers just barely move when you gently rock the Lumox® dish. Take care not to compress the egg chambers.
14. Seal every edge of the cover slips with a thin layer of halocarbon oil 27 (~20 μl in total) to minimize evaporation of the media during imaging (*see* **Note 7**).
15. For the upright microscope, the glass spacers and cover slips are mounted on the top of Lumox® dish; for the inverted microscope, the sample is mounted on the bottom of the dish.

3.4 Time-Lapse Imaging of the Egg Chambers

1. Transfer the Lumox® dish to a microscope stage equipped with a petri dish holder.
2. Set up the center of the Lumox® dish as a reference point. Move to a location on the dish, identify an egg chamber of the desired stage, and mark its coordinates. Repeat this step for other locations, avoiding egg chambers that have abnormal morphology (i.e., uneven follicle cell layer). In addition, avoid choosing egg chambers that are located near a germarium. The inherent pulsating movement of germarium might move the egg chamber during imaging.
3. Lower the light intensity using 25 % neutral density filter. Include KG1 and BG38 filters to suppress heating of the sample (*see* **Note 8**). When imaging more than one egg chamber at a time, mark the position of the center of each border cell cluster and identify the correct exposure for each channel and each egg chamber. Try not to exceed 150 ms for each channel. With this exposure setting one can collect 16 z-sections, 1.25 μm apart at 20× magnification, for each channel. Egg chambers generally tolerate a time interval of 2.25 min between successive frames when imaging four egg chambers with 16 z-sections for each of the two channels.
4. Start time-lapse image acquisition. Use modest speed of the mobile stage. We have successfully used an Axiocam MRm camera mounted on a Zeiss Axioimager (upright, wide field) microscope with 20× magnification for 5–6 h. Higher magnification, such as 40×, can be used for shorter total imaging times.
5. During acquisition, it is necessary to refocus on the border cells as they move. In addition, look for signs of normal develop-

ment such as egg chamber growth, outer follicle cell rearrangement, dynamic changes in gene expression (e.g., expression of the *slow border cell* enhancer in centripetal cells), and of course border cell movement.

6. The Lumox® dish can be reused as long as the film base is intact. After the experiment, carefully remove the cover slips and wash away the halocarbon oil by rinsing several times with Windex cleaner and then thoroughly with H_2O.
7. After imaging, one can process the images in different ways depending on the software available. Movie 1 shows a maximal intensity projection of the 16 z-slices over the entire time interval of acquisition.

4 Notes

1. Insulin powder dissolves in slightly acidic condition. For preparing acidic H_2O, dilute 1 μl of concentrated HCl in 1 ml of MilliQ H_2O.
2. If using DMSO for dissolving FM4-64, the final dilution of DMSO in complete medium should be 1:1000. A higher concentration of DMSO impedes border cell migration.
3. The pH of the medium is critical for the experiment. Low pH impedes border cell migration and high pH leads to early degeneration of the egg chamber.
4. The age of the female fly is very important. The ovaries of newly hatched flies do not fatten very well, while the ovaries of older fly have large number of mature egg chambers.
5. Gentle handling of the ovaries is critical as even inconspicuous damage to egg chambers inhibits border cell migration.
6. While lowering the cover slip onto the medium with egg chambers, one needs to be very careful that the ends of the cover slip should land on the spacer to avoid any damage to the egg chambers.
7. Do not use nail polish.
8. The addition of a heat-filter KG, infrared suppression filter (BG38), and 25 % neutral density filter suppresses phototoxicity to the sample during long-term imaging.

Acknowledgements

This work was supported by the National Institute of General Medical Sciences grant GM73164 to D.J.M.

References

1. Ilina O, Friedl P (2009) Mechanisms of collective cell migration at a glance. J Cell Sci 122:3203–3208
2. Aman A, Piotrowski T (2010) Cell migration during morphogenesis. Dev Biol 341:20–33
3. Weijer CJ (2009) Collective cell migration in development. J Cell Sci 122:3215–3223
4. Lopez-Schier H (2010) Fly fishing for collective cell migration. Curr Opin Genet Dev 20:428–432
5. Rorth P (2009) Collective cell migration. Annu Rev Cell Dev Biol 25:407–429
6. Spradling AC (1993) Developmental genetics of oogenesis. In: Bate M, Martinez-Arias A (eds) The development of *Drosophila melanogaster*, vol 1. Cold Spring Harbor Press, Cold Spring Harbor, NY, pp 1–70
7. King RC (1970) Ovarian development in *Drosophila melanogaster*. Academic, New York, NY
8. Edgar BA, Orr-Weaver TL (2001) Endoreplication cell cycles-more for less. Cell 105:297–306
9. Ruohola H, Bremer KA, Baker D et al (1991) Role of neurogenic genes in establishment of follicle cell fate and oocyte polarity during oogenesis in *Drosophila*. Cell 66:433–449
10. Silver DL, Montell DJ (2001) Paracrine signaling through the JAK/STAT pathway activates invasive behavior of ovarian epithelial cells in *Drosophila*. Cell 107:831–841
11. Montell DJ, Rorth P, Spradling AC (1992) Slow border cells, a locus required for a developmentally regulated cell-migration during oogenesis, encodes *Drosophila* C/Ebp. Cell 71:51–62
12. Starz-Gaiano M, Melani M, Wang XB et al (2008) Feedback inhibition of JAK/STAT signaling by apontic is required to limit an invasive cell population (vol 14, pg 726, 2008). Dev Cell 15:330
13. Prasad M, Montell DJ (2007) Cellular and molecular mechanisms of border cell migration analyzed using time-lapse live-cell imaging. Dev Cell 12:997–1005
14. Bianco A, Poukkula M, Cliffe A et al (2007) Two distinct modes of guidance signalling during collective migration of border cells. Nature 448:362–365
15. Duchek P, Somogyi K, Jekely G et al (2001) Guidance of cell migration by the *Drosophila* PDGF/VEGF receptor. Cell 107:17–26
16. McDonald JA, Pinheiro EM, Kadlec L et al (2006) Multiple EGFR ligands participate in guiding migrating border cells. Dev Biol 296:94–103
17. Duchek P, Rorth P (2001) Guidance of cell migration by EGF receptor signaling during *Drosophila* oogenesis. Science 291:131–133
18. Prasad M, Jang AC, Starz-Gaiano M et al (2007) A protocol for culturing *Drosophila melanogaster* stage 9 egg chambers for live imaging. Nat Protoc 2:2467–2473
19. Wang X, He L, Wu YI et al (2010) Light-mediated activation reveals a key role for Rac in collective guidance of cell movement in vivo. Nat Cell Biol 12:591–597
20. Cai D, Chen S-C, Prasad M et al (2014) Mechanical feedback through E-cadherin promotes direction sensing during collective cell migration. Cell 157:1146–1159
21. Horne-Badovinac S, Bilder D (2005) Mass transit: epithelial morphogenesis in the *Drosophila* egg chamber. Dev Dyn 232:559–574
22. Grunert S, St. Johnston D (1996) RNA localization and the development of asymmetry during *Drosophila* oogenesis. Curr Opin Genet Dev 6:395–402
23. Hudson AM, Cooley L (2002) Understanding the function of actin-binding proteins through genetic analysis of *Drosophila* oogenesis. Annu Rev Genet 36:455–488
24. Morris LX, Spradling AC (2011) Long-term live imaging provides new insight into stem cell regulation and germline-soma coordination in the *Drosophila* ovary. Development 138: 2207–2215
25. Rorth P, Szabo K, Bailey A et al (1998) Systematic gain-of-function genetics in *Drosophila*. Development 125:1049–1057
26. Wang X, Bo J, Bridges T et al (2006) Analysis of cell migration using whole-genome expression profiling of migratory cells in the *Drosophila* ovary. Dev Cell 10:483–495

Chapter 7

Visualizing Microtubule Networks During *Drosophila* Oogenesis Using Fixed and Live Imaging

Kevin Legent, Nicolas Tissot, and Antoine Guichet

Abstract

The microtubule cytoskeleton is a plastic network of polarized cables. These polymers of tubulin provide orientated routes for the dynamic transport of cytoplasmic molecules and organelles, through which cell polarity is established and maintained. The role of microtubule-mediated transport in the asymmetric localization of axis polarity determinants, in the *Drosophila* oocyte, has been the subject of extensive studies in the past years. However, imaging the distribution of microtubule fibers in a large cell, where vitellogenesis ensures the uptake of a thick and hazy yolk, presents a series of technical challenges. This chapter briefly reviews some of these aspects and describes two methods designed to circumvent these difficulties. We provide a detailed protocol for the visualization by immunohistochemistry of the three-dimensional organization of tubulin cables in the oocyte. Additionally, we detail the stepwise procedure for the live imaging of microtubule dynamics and network remodeling, using fluorescently labeled microtubule-associated proteins.

Key words Microtubule, Tubulin, MAP, +TIP, *Drosophila*, Oogenesis, Live imaging, Dynamics, Jupiter, EB1

1 Introduction

The microtubule (MT) cytoskeleton forms a dynamic network of polarized cables that provide orientated routes for the cytoplasmic transport of molecules and organelles [1]. These MTs are polymerized heterodimers of α and β-tubulin that undergo a series of post-translational modifications, and are associated with a wide variety of MT-associated proteins (MAPs) and molecular motors, which ensure the functional diversity among MT cables [2, 3]. Tubulin polymerization, which extends MTs in a polarized manner from their (−) end towards their (+) end, is a reversible process that also ensures network plasticity [4]. This organelle is involved in countless cellular functions including division, migration, and cell polarization. Indeed, the asymmetric distribution of cellular components

Diana P. Bratu and Gerard P. McNeil (eds.), *Drosophila Oogenesis: Methods and Protocols*, Methods in Molecular Biology, vol. 1328, DOI 10.1007/978-1-4939-2851-4_7,

is essential for the structure and the function of both individual cells and tissues such as epithelia. This cell polarity is established through the orchestrated distribution of specific cortical components near or at the plasma membrane [5]. This process involves the MT-dependent transport of cargoes such as proteins, or messenger RNAs subsequently translated in situ, but also specific organelles and vesicles that ensure the trafficking of transmembrane proteins and lipids [6, 7].

Drosophila oogenesis provides an excellent model system in which to study the MT functions in polarized transport and tissue morphogenesis [8]. Each ovarian egg chamber is a functional unit composed of 16 interconnected clonal germ cells (the oocyte and its 15 supporting nurse cells) that form a cyst, ensheathed in a monostratified epithelium of follicle cells [9, 10]. MT-associated transport is essential for oocyte specification, its growth, and stepwise polarization which involves the asymmetric localization and anchoring of several transcripts encoding axis determinants of the embryo and future developing fly [11]. During a critical period, between stages 6 and 9 of oogenesis, the oocyte undergoes a series of morphological changes and symmetry-breaking events, including a dual interplay between dynamic rearrangements of the MT networks [12] and the migration of the nucleus to an anterior-dorsal position [13–16]. This polarization process also involves the MT-dependent localization of the mRNA of the anterior determinant *bicoid* (*bcd*) to the anterior margin of the oocyte [17], the posterior accumulation of the transcripts of the posterior determinant *oskar* (*osk*) [18], and the transport of the dorsal determinant *gurken* (*grk*) to the anterior-dorsal cortex of the oocyte, in close vicinity to the nucleus [19, 20].

The strict dependency of asymmetry establishment on MT-mediated transport renders paramount a thorough analysis of the MT network organization and dynamics. A large part of our understanding of the mechanisms underlying MT-dependent polarization of the egg chamber, and particularly of the oocyte, was gained from elegant experiments that took advantage of MAPs, molecular motors, or cargoes as readouts for network architecture and MT-directed transports in vivo. A number of techniques and various experimental strategies have yielded complementary observations. A detailed 3D confocal analysis of fixed egg chambers in which MTs are decorated with anti-kinesin heavy-chain (Khc) antibodies has allowed the identification of a complex network with at least two perpendicular MT subsets. Bundles of MTs with a dorsal-ventral orientation persist throughout mid-oogenesis (stages 6–9), while a second network displays an anterior-posterior orientation that undergoes dynamic rearrangements during these stages [15].

The combined 2D live imaging of transgenic flies expressing the fluorescently labeled MT-binding protein Tau (that marks all MTs), the end-binding protein EB1 [a MT (+) end tracking

protein, or "+TIP"], and the RNA-binding protein Staufen (actively transported towards the posterior of the oocyte) have made clear that the MT network in the oocyte is highly dynamic and organized with a biased polarity that increases towards the posterior [21].

Considerable advances have also stemmed from the development of the mRNA-MS2/MS2CP-FP tagging system. This technique, in which RNAs containing MS2-binding sites are labeled by the MS2 coat protein fused to a fluorescent reporter, permits live imaging of mRNAs in vivo [22]. It has been used, for instance, to demonstrate that *osk*-containing particles in the *Drosophila* oocyte are actively shuttled along MTs, with a biased polarity towards the posterior, and largely through kinesin-mediated transport [23, 24].

Live imaging of tagged reporters that associate either directly or indirectly with the MT network is thus essential when studying rapidly evolving processes such as MT dynamics and provides valuable information complementary to immunohistochemistry on fixed tissues. However, less emphasis has been brought upon the direct visualization of tubulins in the network of MT cables, particularly in the oocyte. Indeed, MT analysis in large egg chambers, past stage 8, is hindered by a number of structural features that impair the detection of polymerized tubulins by standard immunohistochemistry. Antibody penetration suffers from titration in the MT-rich follicle cells that form a 10–15 μm thick epithelium that surrounds the oocyte [15]. Additionally, the process of vitellogenesis and yolk deposition into the oocyte, with the progressive uptake and storage of massive amounts of protein/glycogen-rich particles and lipid droplets in the ooplasm, reduces antibody penetration. The continuous growth of the oocyte (e.g., approximately 30×50 μm by stage 8) also decreases the optical resolution in deeper confocal sections [25]. It is also likely that the thickness and viscosity of the yolk and the encapsulation of the oocyte in the follicular epithelium prevent efficient clearance of its content in free cytoplasmic tubulin by detergents, thus titrating the amount of antibodies available for the detection of MT cables. Moreover, MT stability also appears to decrease in classical solutions such as phosphate buffer saline (PBS) and paraformaldehyde (PFA)-based fixatives [26]. As a whole, classical immuno-detection of tubulins in fixed oocytes may suffer from low antibody penetration, reduced accessibility of the antigens, and artifacts prior to fixation [27].

The following protocol details a procedure our laboratory has previously adapted [15] from a method developed to preserve the cytoarchitecture in cells in which antibody penetration is reduced [26]. Our combined use of Britton-Robinson buffer (BRB)-based solutions, increased amounts of detergent, and methanol fixation allows improved immuno-detection of MT-associated tubulins in fixed *Drosophila* egg chambers.

However, direct detection of tubulins with antibodies is not suitable for the live imaging of MT networks. Interestingly, transgenic flies constitutively expressing fluorescently labeled tubulins have been successfully used to image MT networks in the oocyte and follicle cells, during early oogenesis [28]. However, these decorated MT cables are poorly visible in oocytes of later stages [29], where large stocks of free cytoplasmic tubulin may prevent fiber detection. Alternatively, fluorescently labeled MT-binding proteins have proven more reliable [21]. Thus we further provide a protocol we have optimized for the live imaging of MT dynamics during *Drosophila* oogenesis. We have taken advantage of publicly available transgenic strains expressing fluorescently tagged MAPs, to follow either short-term elongation dynamics, or long-term morphogenetic remodeling of the MT networks. Optimal microscope configurations and egg chamber maintenance in Voltalef 10S oil, which is permeable to oxygen and has suitable optical properties [22], have allowed us to image living egg chambers for up to 90 min before degeneration. The following sections provide a detailed explanation of the steps required to carry out these imaging techniques both in fixed and live tissues.

2 Materials

2.1 Drosophila Stocks and Mating

1. Wild-type strains such as *Canton S*, *Oregon R*, or the commonly used w^{1118} mutant.
2. Jupiter is a MAP that binds MTs along their entire length. The protein-trap insertion line *P{PTT-un1}JupiterGFP* contains an exon-like GFP in the first intron of the gene *jupiter*, and decorates MTs uniformly in vivo [30].
3. EB1 is a +TIP MAP that decorates extending MTs, and forms dynamic comets in vivo [31]. The transgenic line w^{1118}; *P{w[+mC]=GAL4::VP16-nos.UTR}CG6325*^{MVD1},*P{UASp-EB1::GFP}* allows the expression of GFP-tagged EB1, under the control of the *nanos* (*nos*) regulatory sequences [32], specifically and very early on in the *germarium* in the female germline. EB1::GFP expression is milder in later vitellogenic stages.
4. Thick yeast paste: Prepare from active dry yeast powder mixed with distilled water. Deposit a chunk of paste with the tip of a spatula, on the surface of the fly food to keep it moist (*see* **Note 1**).

2.2 Dissection

1. A pair of fine forceps (e.g., Dumont #55) (Fig. 1b).
2. A pair of stainless steel-made fine needles (0.1 mm diameter, e.g., Morpho minucies No 20) bent into a hook using forceps, and mounted on a micro dissecting needle holders (Fig. 1e) (*see* **Note 2**).

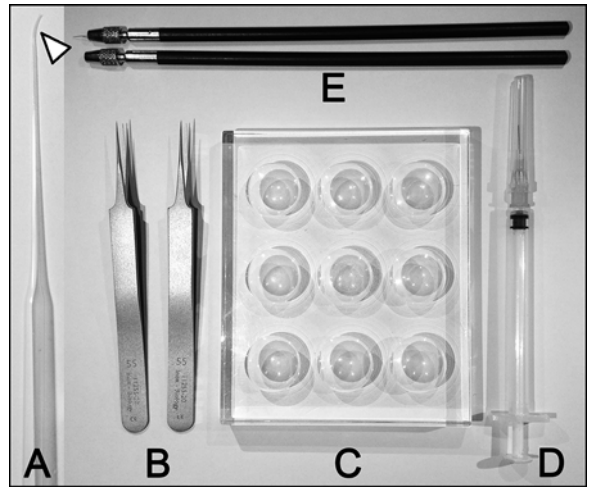

Fig. 1 Materials for dissecting and staining *Drosophila* ovaries. (**A**) A Pasteur pipette tapered into a distal bend (*arrowhead*). (**B**) A pair of Dumont #55 fine forceps. (**C**) A 9-well watch glass dish. (**D**) A 0.5 ml syringe. (**E**) Microdissecting needles and holders

3. A 9-well watch glass-type dish (Fig. 1c).
4. Regular microcentrifuge tubes and thin-wall PCR vials.
5. A 0.5 ml syringe (Fig. 1d).
6. A glass Pasteur pipette, tapered into a distal bend, with a benzene burner (Fig. 1a).
7. Microscope glass slides (superfrost 26 × 75 × 1 mm).
8. Glass cover slips (24 × 40 × 0.17 mm).
9. Nail polish.
10. A binocular microscope equipped with a dark baseplate.
11. A duster-like gas spray.

2.3 Solutions

1. BRB80: 80 mM PIPES, pH 6.8, 1 mM $MgCl_2$, 1 mM EGTA (*see* **Note 3**).
2. BRB80-T: 1 % Triton™X-100 (v/v) in BRB.
3. Methanol (*see* **Note 4**).
4. Ethanol (70 % (v/v) in dH_2O).
5. 1× PBS: 137 mM NaCl, 2.7 mM KCl, 10 mM Na_2HPO_4, 1.8 mM KH_2PO_4, stored at 4 °C.
6. PBST: 0.1 % Tween (v/v) in 1× PBS.
7. PBST freshly supplemented with 2 % (w/v) bovine serum albumin (BSA, Fraction V). Aliquots of a 10 % (w/v) BSA solution, in BRB or PBS, can be stored at −20 °C.

8. Voltalef 10S oil (refractive index $n = 1.410$).
9. Glycerol-based antifadent/anti-bleaching mounting media (e.g., Citifluor AF2).
10. Immersion oil (refractive index $n = 1.515$).

2.4 Antisera

1. Primary antibody: Mouse monoclonal anti-α-Tubulin Clone B-5-1-2 (Sigma). Immunogen: *Strongylocentrotus purpuratus* (sea urchin) sperm axonemes.
2. Alternative antibodies: Mouse monoclonal anti-α-Tubulin Clone DM1A (Sigma, Immunogen: Purified chick brain Tubulin). FITC-conjugated mouse monoclonal anti-α-Tubulin Clone DM1A (Sigma, Immunogen: Purified chick brain Tubulin). Rabbit polyclonal anti-Kinesin heavy chain (Cytoskeleton, Immunogen: Purified *Drosophila* Kinesin heavy chain).
3. Secondary antibody: AlexaFluor 488 chicken anti-mouse IgG (H + L).

2.5 Microscopy Hardware

1. A confocal laser scanning microscope (LSM), inverted or upright, equipped with standard detectors for regular imaging of fixed samples (e.g., a Zeiss LSM 710).
2. A spinning disc confocal microscope equipped with a CCD camera for live imaging (e.g., Yokogawa CSU-X1 spinning disc coupled to a Nikon Eclipse Ti microscope and a Coolsnap HQ2 CCD camera). Alternatively, a laser scanning confocal microscope equipped with highly sensitive detectors can be used for live imaging (e.g., GaAsP detectors). An inverted microscope is better suited for live imaging following our protocol.

3 Methods

3.1 Imaging MTs in Fixed Ovarioles

1. In food vials containing fresh yeast, cross 10–15 freshly hatched females with 3–5 males of the desired genotype (Subheading 2.1, **item 1**). For 2–3 days prior to dissection, allow the flies to feed on yeast for their ovaries to fatten up.
2. Anesthetize the flies on a pad, with constant carbon dioxide flow.
3. Under the dissection microscope, pick up each female individually with a pair of forceps, holding it gently halfway down the thorax, dorsal-side up. Submerge it in a watch glass well filled with 100–200 µl of BRB80 at room temperature (*see* **Note 5**).
4. Grab the fly thorax with one pair of tweezers, chop off its head, and uncap the lower dorsal abdominal cuticle around the A4–A5 segmental boundary, with another pair of forceps (*see* **Note 6**).

5. Isolate and detach the pair of teardrop-shaped ovaries, which can fill up to 2/3rd of the female abdomen, and should be readily available upon cuticle removal (*see* **Note 7**).
6. Transfer the pair of ovaries in a well filled with fresh BRB80 at room temperature.
7. Repeat **steps 3–6**, a few times for 10 min, until you collect around 15 pairs of ovaries.
8. For each ovary, while holding the posterior end with a forceps, tease apart the ovarioles by running a hooked needle in between them, towards the *germarium* at the anterior end of the ovary (*see* **Note 8**).
9. Transfer the ovaries into a 1.5 ml centrifuge tube containing 200 µl of pre-warmed BRB80-T. Incubate at 25 °C for 1 h in a water bath without agitation (s*ee* **Note 9**).
10. Carefully remove the BRB80-T with a tapered Pasteur pipette while leaving the pellet of ovaries untouched.
11. Resuspend the ovaries in 500 µl of methanol chilled to –20 °C. Fix at –20 °C for 15 min (*see* **Notes 10–12**).
12. Discard the methanol and rinse the ovaries 2× in PBST. Briefly spin down (1 s) the methanol-soaked ovaries as they tend to keep afloat in PBST at first.
13. Wash 2 × 10 min in PBST at room temperature.
14. Rehydrate the tissues overnight (15 h) in PBST, at 4 °C without agitation (*see* **Note 13**).
15. Transfer the ovaries into a 200 µl PCR-type vial (*see* **Note 14**).
16. Pre-adsorb the ovaries in 100 µl PBST supplemented with 2 % BSA (w/v), rocking for 1 h at room temperature.
17. Add the desired primary antisera and incubate overnight at 4 °C on a nutator. In our hands, mouse monoclonal anti-α-Tubulin Clone B-5-1-2 can be used at 1:100, and allows immunolabeling of the *Drosophila* ovarian MT networks.
18. Wash 3 × 10 min in PBST at room temperature, and incubate on a nutator with the secondary antibody diluted in PBST, supplemented with 2 % BSA, for either 3 h at room temperature or overnight at 4 °C, in the dark. In our hands, AlexaFluor 488 chicken anti-mouse IgG (H + L) can be successfully used at 1:500. Wash 3 × 10 min in PBST at room temperature (*see* **Note 15**).
19. Several mounting strategies can be used, including the following one. Transfer the ovaries into a watch glass filled with PBST. Under a dissecting microscope, with low-angle incident light, use fine needles to carefully isolate the relevant ovarioles containing egg chambers of the desired stages. Whenever possible, discard very late stages and large eggs that may hinder the proper mounting of the preparation.

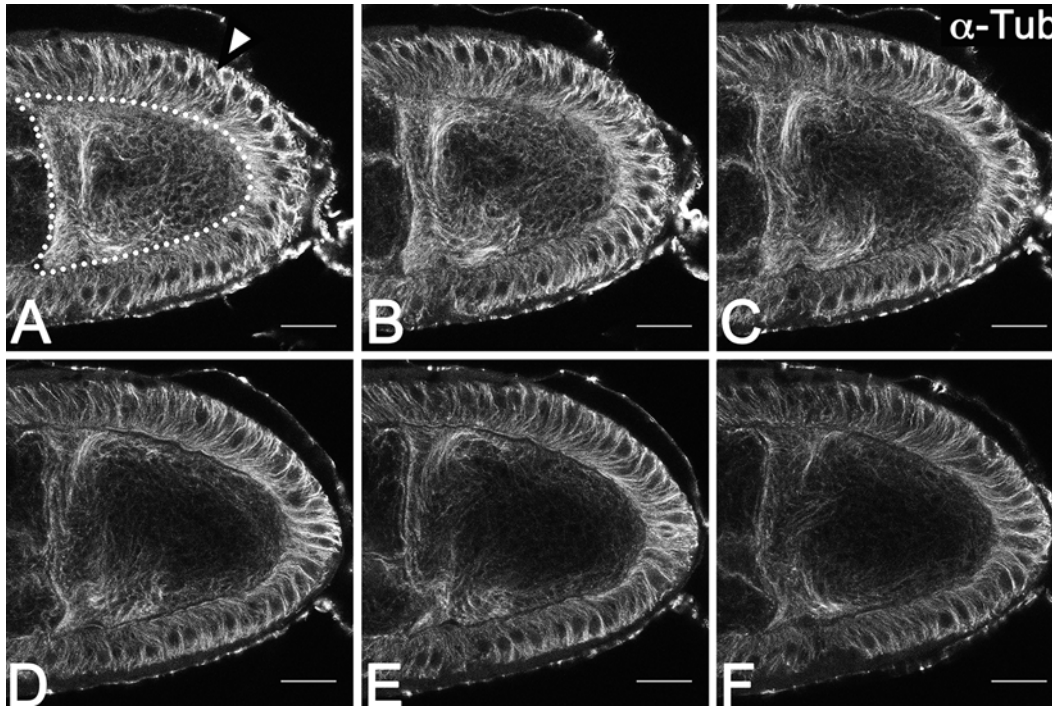

Fig. 2 MT organization during *Drosophila* mid-oogenesis. All six panels (**a**–**f**) illustrate a stack of confocal z-sections of a stage-9 egg chamber from a w^{1118} female, stained with the B-5-1-2 anti-α-Tubulin, antibody. Voxel depth is 1.175 mm. In (**a**), a *dashed line* delineates the oocyte. The *arrowhead* indicates the surrounding epithelium of follicle cells. Follicle cells exhibit MT bundles with a strong apical-basal orientation. MT fibers in the oocyte form a more complex network that varies substantially between confocal planes. Scale bar is 20 μm

20. Ovarioles can now be pipetted out of the well, and onto a clean slide in a minimal volume of PBST. Excessive liquid may be removed off the slide with the help of a 0.5 ml syringe. Quickly cover the ovarioles with a few drops of a glycerol-based mounting medium, before they may dry out. Carefully place a cover slip and seal it on the slide with nail polish.
21. Egg chambers can be screened with 10× magnification and imaged with a confocal microscope and suitable 20×, 40×, or 63× objective lenses, using standard procedures (Fig. 2).

3.2 Imaging MTs in Live Ovarioles

The following protocol is designed to image MT dynamics in live ovarioles, particularly up to stage 9 of oogenesis. Past that stage, only superficial MTs in the oocyte can be imaged due to light diffusion and absorption by the thick and hazy yolk. Short-term elongation dynamics can be followed using EB1::GFP, a fluorescently tagged +TIP MAP which specifically labels the +end of extending MTs, and thus indicates the polarity of the MT network [31]. In addition, long-term morphogenetic remodeling of the MT network can be followed using the MAP Jupiter::GFP which

uniformly decorates MTs along their entire length. It should be mentioned that Jupiter does not provide any information about the network polarity [30].

1. Dissect one pair of ovaries of the desired genotype (Subheading 2.1, **item 2** or **3**) according to Subheading 3.1, **steps 1–5**, except for BRB80, which shall be replaced with a few drops of Voltalef 10S oil (*see* **Note 16**).
2. Clean a 0.17 mm thick cover slip with 70 % ethanol, wipe it with dry soft paper, dust it with a gas duster, and add two drops of Voltalef 10S oil on one side (*see* **Note 17**).
3. Transfer the ovaries onto the cover slip in the oil. Pull on the anterior tip of the ovarioles with tweezers (or needles) to detach and isolate them individually [33] (*see* **Note 18**).
4. For each string containing egg chambers of interest, if stages past 10–11 are still attached, use needles to tear apart and remove these larger chambers, in order to allow relevant cysts to fall into closer contact with the cover slip (*see* **Note 19**).
5. Dust the lens-facing side of the cover slip with the gas spray and set it up directly on the microscope stage (*see* **Note 20**).
6. In order to visualize the MTs, one can use a confocal laser scanning microscope (LSM) equipped with highly sensitive detectors to improve the signal-to-noise ratio. This optical solution produces sharp optical sections that help reducing the contribution of out-of-focus light to the image. Images are acquired sequentially. (We use a Zeiss LSM 780 confocal microscope with GaAsP detectors.) One can also use a spinning disc confocal microscope equipped with a CCD camera. Imaging multiple points simultaneously increases the acquisition speed. However, optical resolution in deeper confocal sections is decreased, which limits imaging large oocytes (stages 8 and higher). (We use a Yokogawa CSU-X1 spinning disc coupled to a Nikon Eclipse Ti microscope and a CoolSNAP HQ2 CCD camera.)
7. Use objectives with maximal numerical aperture (NA), specifically corrected for the desired cover slip thickness. (We use a 60× objective, NA = 1.4, adjusted for 0.17 mm thick cover slips.) (*See* **Note 21**.)
8. Adjust the microscope settings to obtain the highest resolution. With a confocal microscope, pixel size is adjusted to 80 nm, and the GaAsP channel PMT gain is set to 800 V approximately. The pinhole is set to 1 Airy unit but may be slightly more open if the signal is too dim. This option allows an increase in signal detection, at the expense of resolution, while avoiding stronger photobleaching of the sample. With a spinning disc microscope, the camera is set to binning 1 × 1,

with an exposure time typically between 150 and 500 ms, depending on the intensity of the fluorescence signal.
For GFP-tagged MAPs such as EB1::GFP and Jupiter::GFP, a 488 nm laser is used to excite the fluorophores.

9. Quickly screen the samples to locate egg chambers of interest. Avoid spending too much time at this step since the lifetime of ovaries in Voltalef 10S oil will not extend beyond 90 min.
10. When imaging the MT network, at least one image every 2 s is required for the tracking of individual fibers in the network. A higher frequency is possible whenever the signal is strong enough, but significant photobleaching can quickly alter the recording. With time steps of 500 ms, the fluorescence signal may vanish in less than 5 min. Taking a picture every 2 s, for 5–20 min, allows imaging approximately 4–18 independent egg chambers on the same slide, during the life-span of the sample.

    Indeed, a 5-min-long movie of EB1::GFP-expressing oocytes provides enough material to extract time-lapse series of a few seconds that allow the tracking of individual MTs +ends (Fig. 3).

    To image MT network remodeling over longer periods, a lower frequency of acquisition helps reducing photobleaching, but will not allow the tracking of individual fibers. Figure 4 shows the reorganization of MT networks labeled with Jupiter::GFP, in a stage-6 oocyte, over the course of 20 min. Note that Jupiter does not indicate the polarity of extending MT fibers.

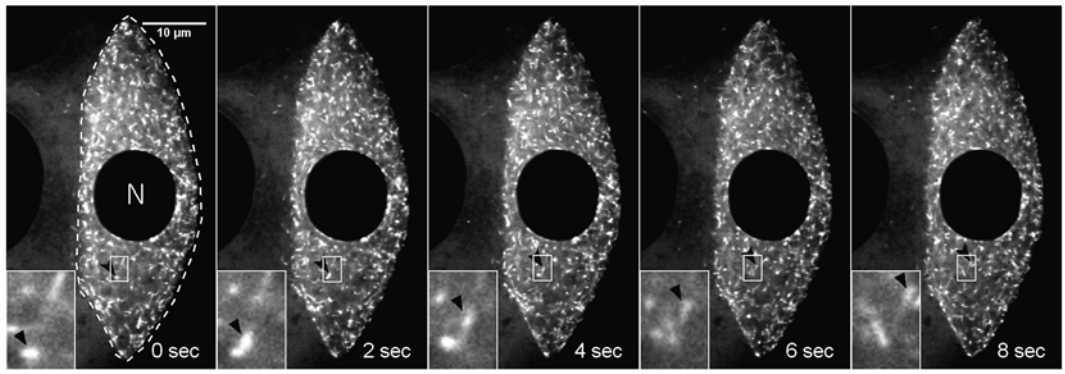

Fig. 3 Short-term MT dynamics. All five panels illustrate an 8-s-long time-lapse series of a single confocal plane. Images represent time points from a 5-min-long movie of a stage-6 *Drosophila* oocyte of the following genotype: *nos-Gal4*, *UASp-EB1::GFP*. One image was acquired every 2 s on a spinning disc confocal microscope. Posterior is to the right. A *dashed line* delineates the oocyte. N: oocyte nucleus. *Inset*: the *black arrowhead* shows the temporal tracking of an extending MT comet, labeled with the +TIP MAP, EB1::GFP

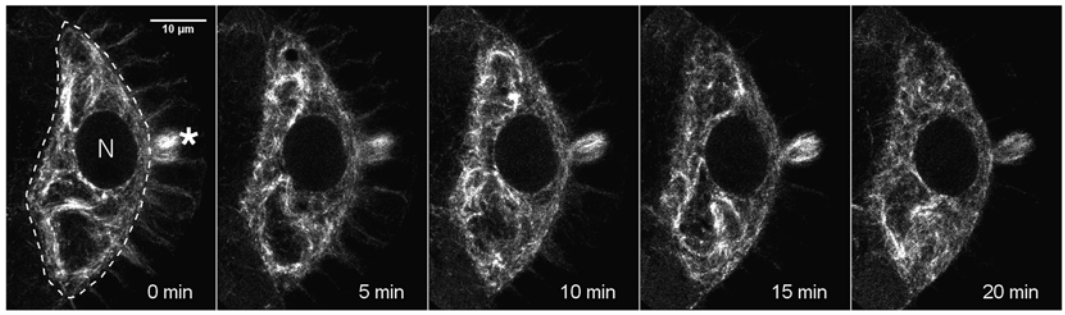

Fig. 4 Remodeling of the MT network during *Drosophila* mid-oogenesis. All 5 panels illustrate time points of a 20-min-long movie of a single confocal plane in a stage-6 *Drosophila* oocyte expressing Jupiter::GFP. One image was acquired every 2 s with a laser scanning confocal microscope. Snapshots of every 5 min are displayed. Posterior is to the right. A *dashed line* delineates the oocyte. N: oocyte nucleus. The GFP-tagged MAP Jupiter decorates MT cables along their entire length and illustrates the overall structural reorganization of the MT network in the oocyte over longer periods of time. The *asterisk* points to the two posterior polar follicle cells where Jupiter::GFP accumulates at high levels

11. Post-processing possibilities: Acquired images may be further processed using deconvolution, which can improve image resolution by up to 10 %. (Images presented in Figs. 3 and 4 have not been deconvoluted or modified post-acquisition.)

    Potential photobleaching of the samples can also be corrected in the application ImageJ, with algorithms such as Bleach Correction from EMBL.

    Additionally, MT dynamics can be analyzed with software such as the "+TIP tracker" module of "U-track" developed in the Danuser lab (http://lccb.hms.harvard.edu/software.html), or the "PIVlab" module developed for Matlab (Mathworks), by William Thielicke and Prof Eize J. Stamhuis.

4 Notes

1. Yeast paste deposited exclusively on the plastic wall of the vial will dry out too quickly.
2. Alternatively these can be mounted on 200 µl pipette tips.
3. BRB80 is an alternative recipe of the BRB. It is usually kept as a 5× stock at 4 °C.
4. Aliquots of 200 µl are stored at −20 °C. Methanol is toxic; handle with gloves and discard in dedicated containers.
5. Allow all solutions to warm up prior to their use. MTs are sensitive to cold shocks that induce their depolymerization. Also avoid the use of PBS in which MTs are unstable [15].

6. Fly wings are large hydrophobic structures. Their optional removal prior to ovaries dissection can help the fly sink into BRB80.
7. Maintaining both ovaries attached to the female oviduct (and uterus) provides a convenient handle for subsequent transfers.
8. A most careful combing of the ovarioles is essential for good penetration of subsequent solutions. Ovariole dissociation by pipetting the sample up and down several times in a pipette tip should be avoided. This method has been shown to induce mechanical damage to the ovaries and is likely to alter cell polarity and cytoarchitecture, particularly prior to fixation [34].
9. This step is designed to extract the oocyte cytoplasm, most importantly in vitellus-containing egg chambers past stage 8, where antibody penetration is severely reduced. Amounts of free unpolymerized cytosolic tubulin should also be decreased, while anchored proteins are retained and the cytoskeleton architecture is largely preserved.
10. A dedicated rack previously stored at –20 °C also improves the rapid cooling of the ovary-containing centrifuge tube.
11. Other *Drosophila* tissues, such as imaginal discs, cannot undergo harsh treatments such as 1 % Triton™X-100 extraction, followed by methanol fixation. Instead, dissect in BRB80 and fix with freshly thawed 4 % PFA in BRB80, for 25 min at room temperature. Wash 3×10 min in PBST at room temperature. This procedure allows for MT preservation and subsequent detection.
12. Methanol fixation does not preserve the native quaternary conformation of the filamentous actin polymer, and precludes the use of phalloidin to visualize the actin cytoskeleton. Anti-actin antibodies can be used instead. However, after methanol fixation, other antigens may no longer be recognized [35].
13. Rehydration for 2 h at 4 °C, followed by 2 h at room temperature, also works, but to a lesser extent.
14. Decreasing the working volume helps reducing the amount of precious antibodies used for immunohistochemistry. Transparent polypropylene thin walls ensure pipetting accuracy during the subsequent rounds of incubations and washes. These vials are particularly convenient when only a few ovaries of a given genotype can be collected at once, and inadvertent loss is to be avoided.
15. When necessary, MT labeling with primary antibodies conjugated with a fluorescent dye can be alternatively chosen in order to avoid the subsequent use of secondary antibodies. In our hands, FITC-conjugated mouse monoclonal anti-a-Tubulin Clone DM1A can be used.

16. Voltalef 10S oil is a low-viscosity polychlorotrifluoroethylene (PCTFE) oil permeable to gas exchange, which prevents dehydration and hypoxia. Importantly, its refractive index (1.410) is relatively close to the ones of the glass cover slip (1.523) and the immersion oil for the Zeiss objectives we use (1.515). Its use improves the matching of refractive indices along the path of the light and ensures limited spherical aberrations and improved optical resolution.
17. A pipette tip dipped in oil provides enough of it.
18. A string containing the *germarium* and egg chambers up to stages 9–10 can easily be recovered. However later stages are larger and often detach from the ovariole.
19. Minimizing the distance between the sample and the objective lens helps improving signal detection by reducing absorption and light diffusion.
20. Adjust the slide holder tightly, but pay attention not to bend the cover slip, which may cause optical aberrations and a decrease in the resolution.
21. A mismatch between the objective correction and the cover slip type will poorly correct spherical aberrations and decrease the optical resolution.

Acknowledgments

The manuscript was improved by the critical comments of Véronique Brodu and Alain Debec. This work was supported by the Centre National de la Recherche Scientifique (CNRS), the Ligue Nationale Contre le Cancer (LNCC, Grant RS11/75-34 to A.G.), and the Fondation ARC pour la Recherche sur le Cancer (ARC, Grant SL220100601358 to A.G.). K.L. is a fellow of the LNCC (GB/MA/IQ-10594). N.T. is a fellow of France-BioImaging.

References

1. Gross SP (2004) Hither and yon: a review of bi-directional microtubule-based transport. Phys Biol 1:R1–R11
2. Janke C (2014) The tubulin code: molecular components, readout mechanisms, and functions. J Cell Biol 206:461–472
3. Marx A, Muller J, Mandelkow EM et al (2006) Interaction of kinesin motors, microtubules, and MAPs. J Muscle Res Cell Motil 27: 125–137
4. Gardner MK, Zanic M, Howard J (2013) Microtubule catastrophe and rescue. Curr Opin Cell Biol 25:14–22
5. St. Johnston D, Ahringer J (2010) Cell polarity in eggs and epithelia: parallels and diversity. Cell 141:757–774
6. Sugioka K, Sawa H (2012) Formation and functions of asymmetric microtubule organization in polarized cells. Curr Opin Cell Biol 24:517–525
7. Siegrist SE, Doe CQ (2007) Microtubule-induced cortical cell polarity. Genes Dev 21: 483–496
8. Steinhauer J, Kalderon D (2006) Microtubule polarity and axis formation in the *Drosophila* oocyte. Dev Dyn 235:1455–1468

9. Spradling A (1993) Developmental genetics of oogenesis. In: Martinez-Arias A, Bate M (eds) The development of *Drosophila melanogaster*. Cold Spring Harbor Laboratory Press, Cold Spring Harbor, NY, pp 1–70
10. Horne-Badovinac S, Bilder D (2005) Mass transit: epithelial morphogenesis in the *Drosophila* egg chamber. Dev Dyn 232:559–574
11. Kugler JM, Lasko P (2009) Localization, anchoring and translational control of oskar, gurken, bicoid and nanos mRNA during *Drosophila* oogenesis. Fly (Austin) 3:15–28
12. Theurkauf WE, Smiley S, Wong ML et al (1992) Reorganization of the cytoskeleton during *Drosophila* oogenesis: implications for axis specification and intercellular transport. Development 115:923–936
13. Guichet A, Peri F, Roth S (2001) Stable anterior anchoring of the oocyte nucleus is required to establish dorsoventral polarity of the *Drosophila* egg. Dev Biol 237:93–106
14. Januschke J, Gervais L, Dass S et al (2002) Polar transport in the *Drosophila* oocyte requires Dynein and Kinesin I cooperation. Curr Biol 12:1971–1981
15. Januschke J, Gervais L, Gillet L et al (2006) The centrosome-nucleus complex and microtubule organization in the *Drosophila* oocyte. Development 133:129–139
16. Zhao T, Graham OS, Raposo A et al (2012) Growing microtubules push the oocyte nucleus to polarize the *Drosophila* dorsal-ventral axis. Science 336:999–1003
17. Berleth T, Burri M, Thoma G et al (1988) The role of localization of bicoid RNA in organizing the anterior pattern of the *Drosophila* embryo. EMBO J 7:1749–1756
18. Ephrussi A, Dickinson LK, Lehmann R (1991) Oskar organizes the germ plasm and directs localization of the posterior determinant nanos. Cell 66:37–50
19. Riechmann V, Ephrussi A (2001) Axis formation during *Drosophila* oogenesis. Curr Opin Genet Dev 11:374–383
20. Neuman-Silberberg FS, Schupbach T (1993) The *Drosophila* dorsoventral patterning gene gurken produces a dorsally localized RNA and encodes a TGF alpha-like protein. Cell 75: 165–174
21. Parton RM, Hamilton RS, Ball G et al (2011) A PAR-1-dependent orientation gradient of dynamic microtubules directs posterior cargo transport in the *Drosophila* oocyte. J Cell Biol 194:121–135
22. Belaya K, St. Johnston D (2011) Using the mRNA-MS2/MS2CP-FP system to study mRNA transport during *Drosophila* oogenesis. In: Gerst JE (ed) RNA detection and visualization. Methods and protocols. Humana Press, Hatfield, pp 265–283
23. Zimyanin VL, Belaya K, Pecreaux J et al (2008) In vivo imaging of *oskar* mRNA transport reveals the mechanism of posterior localization. Cell 134:843–853
24. Becalska AN, Gavis ER (2009) Lighting up mRNA localization in *Drosophila* oogenesis. Development 136:2493–2503
25. Parton RM, Valles AM, Dobbie IM et al (2010) Live cell imaging in *Drosophila melanogaster*. Cold Spring Harb Protoc 2010:pdb. top75
26. Pizon V, Iakovenko A, Van Der Ven PF et al (2002) Transient association of titin and myosin with microtubules in nascent myofibrils directed by the MURF2 RING-finger protein. J Cell Sci 115:4469–4482
27. Hudson AM, Cooley L (2014) Methods for studying oogenesis. Methods 68:207–217
28. Grieder NC, de Cuevas M, Spradling AC (2000) The fusome organizes the microtubule network during oocyte differentiation in *Drosophila*. Development 127:4253–4264
29. Baffet AD, Benoit B, Januschke J et al (2012) *Drosophila* tubulin-binding cofactor B is required for microtubule network formation and for cell polarity. Mol Biol Cell 23: 3591–3601
30. Karpova N, Bobinnec Y, Fouix S et al (2006) Jupiter, a new *Drosophila* protein associated with microtubules. Cell Motil Cytoskeleton 63:301–312
31. Rebollo E, Sampaio P, Januschke J et al (2007) Functionally unequal centrosomes drive spindle orientation in asymmetrically dividing *Drosophila* neural stem cells. Dev Cell 12: 467–474
32. Van Doren M, Williamson AL, Lehmann R (1998) Regulation of zygotic gene expression in *Drosophila* primordial germ cells. Curr Biol 8:243–246
33. Prasad M, Jang AC, Starz-Gaiano M et al (2007) A protocol for culturing *Drosophila melanogaster* stage 9 egg chambers for live imaging. Nat Protoc 2:2467–2473
34. Haack T, Bergstralh DT, St. Johnston D (2013) Damage to the *Drosophila* follicle cell epithelium produces "false clones" with apparent polarity phenotypes. Biol Open 2: 1313–1320
35. Small J, Rottner K, Hahne P et al (1999) Visualising the actin cytoskeleton. Microsc Res Tech 47:3–17

Chapter 8

Visualization of Actin Cytoskeletal Dynamics in Fixed and Live *Drosophila* Egg Chambers

Christopher M. Groen and Tina L. Tootle

Abstract

Visualization of actin cytoskeletal dynamics is critical for understanding the spatial and temporal regulation of actin remodeling. *Drosophila* oogenesis provides an excellent model system for visualizing the actin cytoskeleton. Here, we present methods for imaging the actin cytoskeleton in *Drosophila* egg chambers in both fixed samples by phalloidin staining and in live egg chambers using transgenic actin labeling tools.

Key words Actin cytoskeleton, Oogenesis, Nurse cells, Microscopy, *Drosophila*

1 Introduction

Drosophila oogenesis is an ideal system to study actin cytoskeletal dynamics. Each ovary is comprised of approximately 15 ovarioles—chains of developing egg chambers or follicles. *Drosophila* oogenesis consists of 14 morphologically defined stages [1]. Mid-to-late-stage oogenesis (stage 10B–stage 13) requires the activities of numerous actin-binding proteins to mediate dynamic actin remodeling within the 15 germline-derived support or nurse cells [2]. This remodeling is necessary for the completion of oogenesis and, ultimately, female fertility. As the nurse cells are very large, these cells are an excellent system for visualizing the actin cytoskeleton in both live and fixed samples.

Fixed imaging of the actin cytoskeleton using phalloidin to label actin filaments allows for a detailed analysis of the spatial and temporal regulation of actin remodeling during mid-to-late oogenesis. Formation of cytoplasmic actin bundles begins during stage 10B in the four posterior nurse cells along the nurse cell/oocyte boundary. Actin bundles then form throughout the remaining nurse cells by the end of stage 10B [3] (Fig. 1). Additionally, the cortical actin network just beneath the nurse cell membranes is strengthened at this time. This specific pattern of spatial and

Diana P. Bratu and Gerard P. McNeil (eds.), *Drosophila Oogenesis: Methods and Protocols*, Methods in Molecular Biology, vol. 1328, DOI 10.1007/978-1-4939-2851-4_8,

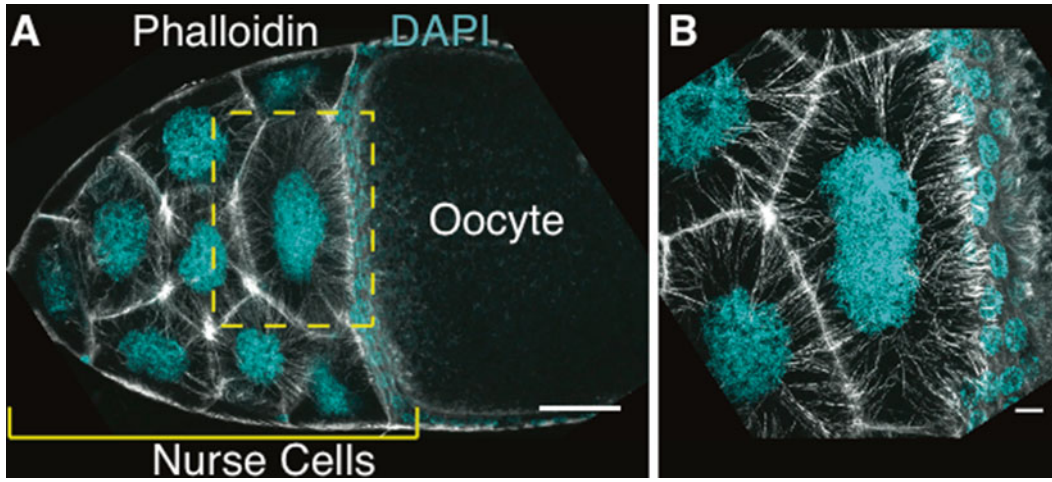

Fig. 1 Actin visualization in a stage 10B egg chamber. Maximum projections of 3–5 confocal slices of a late stage 10B egg chamber stained with phalloidin (actin, *white*) and DAPI (DNA, *cyan*). (**a**) Image taken with a 20× objective. Scale bar is 50 μm. (**b**) Image taken with a 63× objective. Scale bar is 10 μm. Nurse cells in late stage 10B egg chambers exhibit a robust network of radially aligned actin filament bundles that form at the nurse cell membranes and extend inwards towards the nucleus. The cortical actin is also strengthened during this stage of oogenesis

temporal regulation of actin remodeling provides a system for understanding how actin dynamics are regulated. For example, imaging of fixed samples can highlight defects in actin remodeling even at a relatively low magnification (20× objectives) [4].

Here, we describe two protocols for visualizing filamentous actin in fixed samples by phalloidin staining. The first, standard protocol (Subheading 3.1) works well for imaging the robust actin bundle network of stage 10B and later egg chambers. However, some less stable actin structures are formed in developing egg chambers and require a fixation protocol that stabilizes actin filaments [5, 6]. The actin fixation protocol detailed in Subheading 3.2 enhances stabilization of the less robust actin filament structures for better visualization than the standard fixed imaging protocol. The choice of method will depend upon the actin structures being analyzed.

The genetic tools available in *Drosophila* enable in vivo live imaging of actin cytoskeletal dynamics. Actin can be labeled directly via GFP or RFP tags on any of the six *Drosophila* actins (available at the Bloomington *Drosophila* Stock Center) [7]. Indirect actin labeling tools are also available for expression in the germline [8–11], including LifeAct [12], Utrophin [13], and Ftractin [14]. The actin filaments formed during mid-to-late oogenesis in live egg chambers can be visualized by expression of these UASp transgenic insertion lines with germline-specific GAL4 lines [15] (matα, oskar, nanos, matα-geneswitch). Although expression of some of these actin

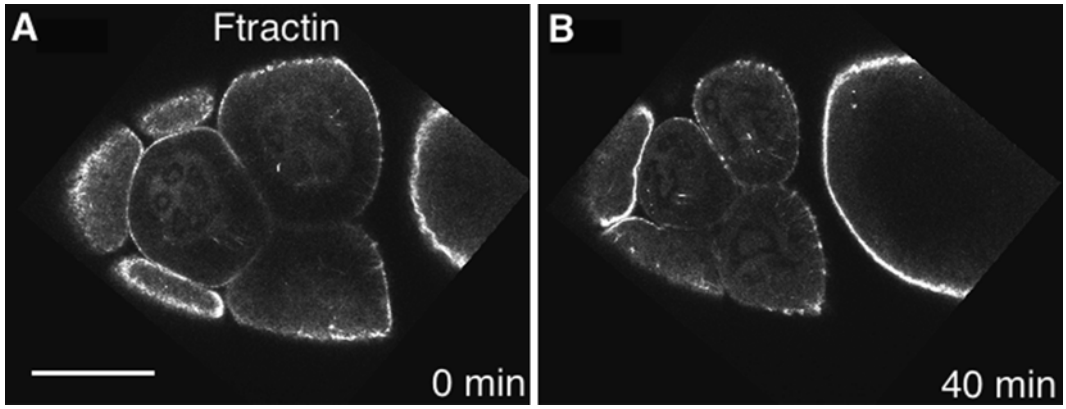

Fig. 2 Live imaging time course of a stage 10B egg chamber expressing Ftractin-tdTomato. (**a**) Image captured at $t=0$ min (stage 10B) and (**b**) 40 min (stage 11). Scale bar is 50 μm. Actin bundles labeled with Ftractin are observable in a live egg chamber as it progresses from late stage 10B to 11 and begins to undergo nurse cell dumping

labeling tools is known to cause defects, low expression of Utrophin or strong expression of Ftractin (Fig. 2) can be used to visualize the actin cytoskeleton live with minimal defects [8]. Additionally, live egg chambers can be maintained in a simple culture media for several hours while oogenesis progresses [16–19]. Therefore, the dynamics of actin remodeling can be observed in a single egg chamber as late-stage oogenesis is completed.

Here, we present methods for both short-term and long-term live imaging. Subheading 3.3, which is intended for short-term imaging, utilizes a simple liquid culture media throughout dissection and imaging. However, egg chambers may shift position in a liquid media, particularly as nurse cell dumping occurs. If a long-term time course of imaging or multipoint short-term imaging is desired, egg chambers can be embedded in an agarose media to prevent movement (Subheading 3.4).

2 Materials

2.1 Solutions

1. Wet yeast paste: 50 g active dry yeast mixed with 90 ml of ddH_2O, stored at 4 °C (*see* **Note 1**).
2. Grace's Insect Culture Medium. Store at 4 °C.
3. In vitro egg maturation (IVEM) medium: 10 % fetal bovine serum (FBS, heat inactivated) in Grace's Insect Culture Medium plus 1× penicillin/streptomycin. Prepare fresh before each use.
4. 20 % Paraformaldehyde (PFA): Prepare in fume hood. Dissolve 0.496 g of $Na_2CO_3 \cdot H_2O$ in ~800 ml of dH_2O. Add 200 g of paraformaldehyde. Heat, with stirring, to ~80 °C to get the

paraformaldehyde into solution. Bring to a final volume of 1 l with dH_2O. Filter through Whatman filter paper (#1) to remove the sludge. Store at room temperature (*see* **Notes 2** and **3**).

5. 1× Phosphate-buffered saline (1× PBS): 135 mM NaCl, 3.2 mM Na_2HPO_4, 1.3 mM KCl, 0.5 mM KH_2PO_4, pH 7.4.
6. Actin fixative [5, 6]: 4 % paraformaldehyde (diluted from 20 % solution in 1× PBS), 2 % Triton™ X-100, 1 U/ml fluorescent phalloidin (*see* **Notes 2**, **3**, and **4**).
7. Antibody wash: 0.1 % bovine serum albumin, 0.1 % Triton X-100 in 1× PBS.
8. Triton antibody wash: 0.1 % bovine serum albumin, 0.2 % Triton X-100 in 1× PBS.
9. Phenylenediamine solution: 50 mg phenylenediamine, 4.4 ml of dH_2O, 500 µl of 10× PBS. Vortex to dissolve. Bring to pH 9.0 with 1 N NaOH.
10. Phenylenediamine mounting medium [20]: 5 ml of glycerol, 4 ml of dH_2O, 1.0 ml of phenylenediamine solution. Aliquot rapidly in 200 µl volumes and store at −80 °C (*see* **Note 5**).
11. Embedding agarose: Prepare a low-melt agarose working solution (this can be kept for ~1 week in aliquots at 4 °C) with a 1 % (w/v) solution of low-melt agarose in Grace's Insect Culture Medium. Heat to 65 °C to liquefy. Mix molten agarose 1:1 with 42 °C 2× IVEM medium (20 % FBS and 2× penicillin/streptomycin in Grace's Insect Culture Medium). Keep this embedding agarose at 42 °C to keep it in its liquid state.

2.2 Dissection Materials

1. Gas-permeable fly pad.
2. CO_2 source.
3. Forceps (#5 Dumont).
4. Sharpened Tungsten dissection needles [21].
5. Pin vises and supplied needles.
6. Nine-well spot plates for dissection.
7. A dark surface (i.e., a piece of black plexiglass).
8. Pasteur pipets and pulled Pasteur pipets [16] (*see* **Note 6**).
9. Cover slip bottom dishes (MatTek Corporation, 35 mM, cover slip thickness will depend on the microscope objective used).
10. Glass slides.
11. Cover slips (cover slip thickness will depend on the microscope objective used).
12. Nail polish.
13. Dissecting microscope.
14. 0.5 ml microcentrifuge tubes.

15. Kimwipes.
16. Nutator.
17. Aluminum foil.

2.3 Antibodies/ Fluorophore Conjugates

1. Alexa488-, rhodamine-, or Alexa647-phalloidin.
2. DAPI.

3 Methods

3.1 Fixed Imaging

1. Collect newly enclosed adult flies of interest (males and females) (*see* **Note 7**).
2. Feed the flies with a dab of wet yeast paste daily for 3–4 days (*see* **Note 8**).
3. Warm Grace's Medium to room temperature before beginning the dissection (*see* **Note 9**).
4. Put the flies to sleep under CO_2 gas.
5. Fill a dissection well (9-well spot plate, etc.) with Grace's Medium, place on a dark surface (i.e., a piece of black plexiglass), and submerge a female fly in the dissection well.
6. Remove the whole ovaries using two pairs of forceps.
7. Use a sharpened dissection needle to separate the individual ovarioles for approximately the anterior third of the length of the ovary (separate between the clear egg chambers while leaving the white/opaque egg chambers at the posterior of the ovariole more closely packed; Fig. 3).
8. Transfer the ovaries to a 0.5 ml tube with Grace's Medium (*see* **Note 10**). Do not let the ovaries dry out.
9. Prepare enough 4 % PFA solution (20 % PFA diluted in Grace's Medium) to have 300 μl per sample.
10. Remove all the Grace's Medium with a pulled pipet and rapidly add 300 μl of a freshly diluted 4 % paraformaldehyde solution. Incubate for 10 min at room temperature on a nutator (*see* **Notes 11** and **12**).
11. Remove the fixative using a pulled pipet (*see* **Note 3**) and rinse with antibody wash.
12. Wash the ovaries 6 × 10 min with ~300 μl of antibody wash at room temperature on a nutator (*see* **Note 13**).
13. Dilute the desired primary antibody and phalloidin (1:250–1:500 dilution) in Antibody wash solution. Make enough for 300 μl per sample (*see* **Note 14**).

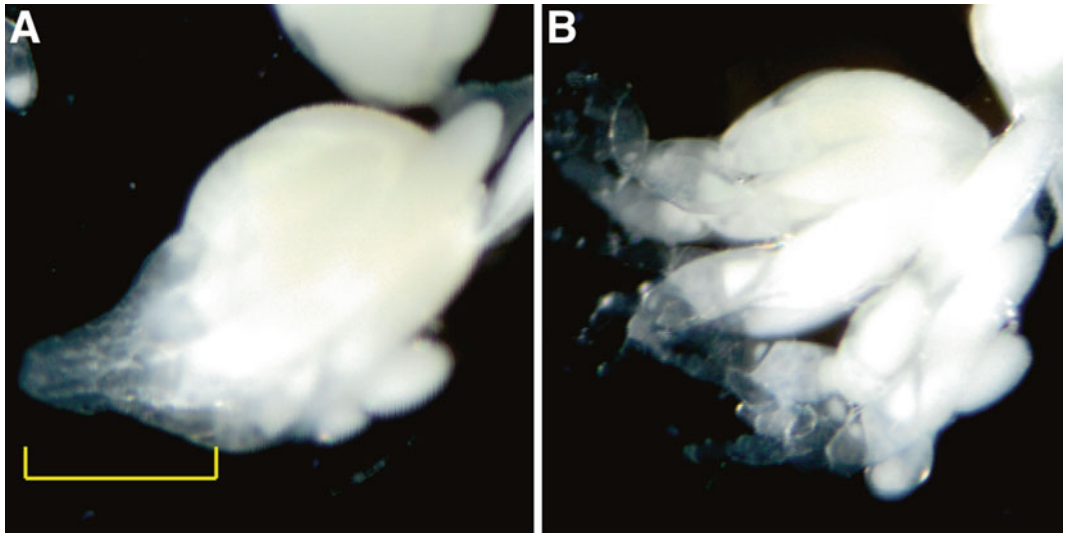

Fig. 3 Images of a dissected ovary before and after teasing the ovarioles apart. (**a**) Intact pair of ovaries. *Yellow* bracket indicates area of the ovary to be teased apart. (**b**) Pair of ovaries after sharpened dissection needles were used to separate the ovarioles over the anterior 1/3 of each ovary. Teasing the ovarioles apart prior to fixation is necessary to fully fix the sample and to allow staining reagents to evenly label the tissue

14. Completely remove the final wash (using a pulled pipet) and add 300 μl of the primary antibody/phalloidin mix to each sample. Incubate the samples at room temperature for 2–4 h or at 4 °C overnight on a nutator covered with aluminum foil (*see* **Notes 15** and **16**).
15. Wash the ovaries 6 × 10 min with ~300 μl of antibody wash at room temperature on a nutator covered with aluminum foil (*see* **Note 13**).
16. If a primary antibody was used in addition to phalloidin, incubate in the secondary antibody (make sure to select a fluorophore different than the phalloidin conjugate); otherwise proceed to **step 18**. Dilute the secondary antibody in ~300 μl of antibody wash, including phalloidin again. Completely remove the final wash (using a pulled pipet) and add ~300 μl of secondary antibody solution per sample. Incubate the samples at room temperature for 2–4 h or at 4 °C overnight on a nutator covered with aluminum foil (*see* **Note 16**).
17. Wash the ovaries 6 × 10 min with ~300 μl of antibody wash at room temperature on a nutator covered with aluminum foil (*see* **Note 13**).
18. If desired, the samples can be stained with DAPI to visualize DNA. Wash the samples at room temperature on a nutator for 10 min in 1× PBS containing DAPI at a 1:5000–1:10,000 dilution.
19. Rinse once with 1× PBS.

20. Store the ovaries in fresh 1× PBS. Samples can be stored at 4 °C or mounted immediately.
21. On a spare glass slide, place two separate drops of mounting media.
22. Pipet the mounting media onto the slide to be used for mounting.
23. Use forceps to move the stained ovaries into the first drop of mounting media on the spare slide, and then move the ovaries to the second drop. Then, place the ovaries in mounting media on a glass slide to be mounted (*see* **Note 17**).
24. Use sharpened dissection needles to separate individual ovarioles and egg chambers (*see* **Notes 5**, **18**, and **19**).
25. Apply the cover slip, invert the slide onto a Kimwipe, and apply gentle pressure to remove excess mounting media and to slightly squish the egg chambers for better imaging (*see* **Notes 20** and **21**).
26. If using a non-hardening mounting medium such as phenylenediamine, seal the cover slips using nail polish.
27. Store the slides in the dark at 4 °C (*see* **Note 22**).

3.2 Fixed Imaging for Stabilizing Actin Structure

1. Follow **steps 1–8** of Subheading 3.1.
2. Prepare enough actin fixative to have 300 μl per sample.
3. Remove the Grace's Medium completely with a pulled pipet and add 300 μl of actin fixative. Incubate for 10 min at room temperature on a nutator covered with aluminum foil (*see* **Notes 3**, **4**, and **15**).
4. Remove the fixative and rinse 2× with Triton antibody wash.
5. Wash the ovaries 3×10 min with ~300 μl of antibody wash supplemented with 1 U/ml fluorescent phalloidin at room temperature on a nutator covered with aluminum foil (*see* **Note 4**).
6. Wash the ovaries 3×10 min with ~300 μl of antibody wash at room temperature on a nutator protected covered with aluminum foil.
7. Follow **steps 13–27** of Subheading 3.1.

3.3 Short-Term Live Imaging

1. Collect and feed the flies as described in Subheading 3.1, **steps 1** and **2**.
2. Prepare a fresh aliquot of IVEM medium and warm to room temperature (*see* **Note 23**).
3. Dissect the ovaries as described in Subheading 3.1, **steps 4–6**, using IVEM medium in the dissection well instead of Grace's Medium. Move the ovaries quickly away from the debris (*see* **Note 24**).
4. Use two dissection needles to isolate individual egg chambers of the desired stage (*see* **Note 25**).

5. Pipet the egg chambers and a small drop of IVEM medium onto a cover slip bottom dish. If desired, a cover slip can be placed on top of the egg chambers to limit their movement and push the egg chambers to the bottom cover slip (*see* **Note 26**).
6. Egg chambers are now ready for imaging on an inverted confocal microscope (*see* **Note 27**).
7. Stage 10B or later egg chambers prepared in this manner will complete oocyte development. Time course imaging is feasible for several hours to capture the actin remodeling of stages 10B through 13 (Fig. 2) (*see* **Note 28**).

3.4 Long-Term Live Imaging

1. Collect and feed the flies as described in Subheading 3.1, **steps 1** and **2**.
2. Follow **step 2** of Subheading 3.3.
3. Melt the low-melt agarose working solution in a 65 °C heat block.
4. Keep the melted low-melt agarose working solution liquid (incubate in a 42 °C heat block) and warm the 2× IVEM medium in a 42 °C heat block.
5. Mix the 2× IVEM medium and the low-melt agarose working solution 1:1 to make the embedding medium and return to the 42 °C heat block.
6. Follow **steps 3** and **4** of Subheading 3.3.
7. Pipet ~200–300 µl of the embedding agarose onto the cover slip portion of a cover slip bottom dish (*see* **Note 29**).
8. Transfer isolated egg chambers to the embedding agarose using a Pasteur pipet (keep egg chambers at the end of the pipet, submerge the end into the agarose, and let the egg chambers fall into the agarose by gravity).
9. Adjust the location of the egg chambers using a dissection needle as necessary. Embedding agarose will solidify and hold the egg chambers in place.
10. Cover the solidified embedding agarose with IVEM medium.
11. Image on an inverted confocal microscope as discussed in Subheading 3.3, **steps 6** and 7.

4 Notes

1. Wet yeast paste consistency should be adjusted to be between a thick solid and a runny liquid, by either adding more ddH_2O or more active dry yeast, respectively.
2. Other fixative options: commercially available paraformaldehyde and formaldehyde (dilute to a 4 % working concentration).

3. Formaldehyde and paraformaldehyde are highly toxic. Always handle with care and the appropriate personal protective equipment. Follow all hazardous waste disposal guidelines.
4. Phalloidin is highly toxic. Always wear appropriate protective equipment when handling solutions containing phalloidin.
5. Mounting media will turn brown if left for too long at room temperature. Do not use mounting media if it has turned dark brown (light brown is fine).
6. Heat the thin portion of a 9″ Pasteur pipette over a Bunsen burner. As soon as the glass begins to soften, quickly move the pipette out of the flame and pull into a fine tube. Break off the end to produce a very thin pipet tip. Use eye protection as glass fragments may fly off.
7. The age of the females at the time of dissection can affect ovary quality and overall female fertility. Thus, it is important to be consistent with the age of dissected females. Remove all of the old adult flies from the vials 1 day before collecting flies so that all of the collected adults are approximately the same age (within ~24 h).
8. Feeding the flies with wet yeast paste daily for 3–4 days is important for the development of large ovaries and a good distribution of stages.
9. Do not use cold media or place ovaries in the cold until they are fixed. Actin filaments are disrupted by cold temperatures. Allowing the Grace's Medium to incubate at room temperature for 30 min is sufficient.
10. Some antibodies will work better if the staining is performed in 1.5 ml microcentrifuge tube. Staining conditions have to be optimized for each reagent.
11. The timing of the fixation can vary depending on the fixative and antibodies being used. For example, some antibodies work better if the fixation is 15 min with diluted 37 % formaldehyde.
12. Ovaries will not move in the tube during fixation. Ensure that all ovaries are submerged in fixative. During the washes and antibody incubation the ovaries will move freely within the microcentrifuge tube.
13. Antibody washes can be left on the ovaries for longer than 10 min if needed, with the exception of the first wash following fixation. This wash should only be 10 min so that any residual fixative is rapidly removed.
14. If the antibody is precious, smaller volumes of the primary antibody/phalloidin mix can be used. However, ovary staining will tend to be more uneven with smaller volumes.

15. Always keep solutions containing fluorophores and ovary samples stained with fluorescent reagents protected from light to avoid photobleaching the samples by covering with aluminum foil.
16. Primary and secondary antibody staining can be performed at room temperature or at 4 °C. If the antibody step will be performed at room temperature, 2–4 h is sufficient. If the step is performed at 4 °C, samples should be stained overnight (minimum of 12 h). Some antibodies work better at lower temperatures for longer periods of time. Therefore, the staining conditions must be optimized for each reagent by comparing different incubation times/temperatures for each primary antibody to determine what works best for a particular reagent.
17. It is important to completely remove all of the PBS from the ovary samples before mounting the samples on slides. This can be accomplished by moving ovaries through puddles of mounting media on an extra slide before transferring the ovaries to the mounting media on the final slide. This step is critical for obtaining the appropriate refractive index for imaging.
18. Work quickly/efficiently when mounting samples to avoid exposing the samples to light for too long. If the samples are exposed to too much light, photobleaching can occur.
19. Other options for mounting media include VectaShield and ProLong Gold.
20. The amount of pressure applied to the cover slip during mounting is important to appropriately squish the egg chambers. Too much force will result in overly flattened egg chambers that appear distorted. Too little force will result in egg chambers too thick to image across their whole depth.
21. Take care to avoid shifting the cover slip once it has been placed on the slide. Egg chambers can be stretched/distorted if the cover slip is shifted while applying pressure.
22. Fluorescent signals from slides mounted in phenylenediamine mounting medium fade after ~4–6 months of storage at 4 °C. Samples mounted in ProLong Gold and VectaShield maintain their signal for considerably longer.
23. Stage 10B or later egg chambers will develop in culture using IVEM medium. Other culture medium is required for development of egg chambers earlier than stage 10B [18].
24. It is important to move the ovaries/egg chambers away from debris from the fly dissection as quickly as possible. Exposure to the contents of a punctured digestive tract, for example, will inhibit development.
25. For stage-specific isolation of egg chambers for live imaging, the slightly larger needles supplied with the pin vises are

recommended. These needles are less likely to puncture the live egg chambers than the sharpened tungsten needles.

26. Ovaries and egg chambers dissected in Grace's Medium tend to stick to glass pipets. To avoid this, pipet IVEM medium or a 3 % bovine serum albumin (BSA) solution up and down in the pipet prior to transferring tissues. This step will prevent the tissue from sticking.
27. When performing live imaging on egg chambers, scan speed, resolution, and laser power may have to be adjusted to prevent excessive damage to the living egg chambers. If the egg chambers will be imaged repeatedly over a time course, scan speed should be increased, while resolution and laser power should be decreased, so minimal damage is done.
28. Fluorescence recovery after photobleaching (FRAP) analysis can be performed on live egg chambers expressing actin-labeling tools. 50–100 iterations of 100 % laser power are typically sufficient to bleach an area of interest. A high scan speed and lower resolution are required to capture recovery of fluorescence.
29. Work quickly once the embedding medium has been placed in the cover slip bottom dish or the agarose will solidify before the egg chambers sink to the bottom. This issue will result in an inability to get a clear image by confocal microscopy.

Acknowledgements

We would like to thank Andrew Spracklen for his work on the live imaging protocols as well as the actin fixation protocol, and Ding Ye and Fang Lin for advice on using low-melt agarose to embed live egg chambers for imaging. This work was funded by National Science Foundation MCB-1158527.

References

1. Spradling AC (1993) Developmental genetics of oogenesis. In: Martinez-Arias B (ed) The development of *Drosophila melanogaster*. Cold Spring Harbor Laboratory Press, Cold Spring Harbor, NY, pp 1–70
2. Hudson AM, Cooley L (2002) Understanding the function of actin-binding proteins through genetic analysis of *Drosophila* oogenesis. Annu Rev Genet 36:455–488
3. Guild GM, Connelly PS, Shaw MK et al (1997) Actin filament cables in *Drosophila* nurse cells are composed of modules that slide passively past one another during dumping. J Cell Biol 138:783–797
4. Groen CM, Spracklen AJ, Fagan TN et al (2012) *Drosophila* Fascin is a novel downstream target of prostaglandin signaling during actin remodeling. Mol Biol Cell 23: 4567–4578
5. Frydman HM, Spradling AC (2001) The receptor-like tyrosine phosphatase Lar is required for epithelial planar polarity and for axis determination within *Drosophila* ovarian follicles. Development 128:3209–3220
6. Spracklen AJ, Kelpsch DJ, Chen X et al (2014) Prostaglandins temporally regulate cytoplasmic actin bundle formation during *Drosophila* oogenesis. Mol Biol Cell 25:397–411

7. Roper K, Mao Y, Brown NH (2005) Contribution of sequence variation in *Drosophila* actins to their incorporation into actin-based structures in vivo. J Cell Sci 118:3937–3948
8. Spracklen AJ, Fagan TN, Lovander KE et al (2014) The pros and cons of common actin labeling tools for visualizing actin dynamics during *Drosophila* oogenesis. Dev Biol 393:209–226
9. Huelsmann S, Ylanne J, Brown NH (2013) Filopodia-like actin cables position nuclei in association with perinuclear actin in *Drosophila* nurse cells. Dev Cell 26:604–615
10. Zanet J, Jayo A, Plaza S et al (2012) Fascin promotes filopodia formation independent of its role in actin bundling. J Cell Biol 197:477
11. Rauzi M, Lenne PF, Lecuit T (2010) Planar polarized actomyosin contractile flows control epithelial junction remodelling. Nature 468:1110–1114
12. Riedl J, Crevenna AH, Kessenbrock K et al (2008) Lifeact: a versatile marker to visualize F-actin. Nat Methods 5:605–607
13. Burkel BM, von Dassow G, Bement WM (2007) Versatile fluorescent probes for actin filaments based on the actin-binding domain of utrophin. Cell Motil Cytoskeleton 64:822–832
14. Johnson HW, Schell MJ (2009) Neuronal IP3 3-kinase is an F-actin-bundling protein: role in dendritic targeting and regulation of spine morphology. Mol Biol Cell 20:5166–5180
15. Brand AH, Perrimon N (1993) Targeted gene expression as a means of altering cell fates and generating dominant phenotypes. Development 118:401–415
16. Spracklen AJ, Tootle TL (2013) The utility of stage-specific mid-to-late *Drosophila* follicle isolation. J Vis Exp (82): 50493
17. Tootle TL, Spradling AC (2008) *Drosophila* Pxt: a cyclooxygenase-like facilitator of follicle maturation. Development 135:839–847
18. Prasad M, Jang AC, Starz-Gaiano M et al (2007) A protocol for culturing *Drosophila melanogaster* stage 9 egg chambers for live imaging. Nat Protoc 2:2467–2473
19. Prasad M, Montell DJ (2007) Cellular and molecular mechanisms of border cell migration analyzed using time-lapse live-cell imaging. Dev Cell 12:997–1005
20. Platt JL, Michael AF (1983) Retardation of fading and enhancement of intensity of immunofluorescence by p-phenylenediamine. J Histochem Cytochem 31:840–842
21. Brady J (1965) A simple technique for making very fine, durable dissecting needles by sharpening tungsten wire electrolytically. Bull World Health Organ 32:143–144

Chapter 9

Single-Molecule RNA In Situ Hybridization (smFISH) and Immunofluorescence (IF) in the *Drosophila* Egg Chamber

Livia V. Bayer, Mona Batish, Stephen K. Formel, and Diana P. Bratu

Abstract

Detection of nucleic acids in whole tissues has become key in our understanding of gene expression during development. In situ hybridization (ISH) has been an invaluable technique in the making of numerous discoveries. Most recently, the technical advance of using short, fluorescently labeled probes has allowed for the detection of single-mRNA molecules. Thus, quantification of RNA levels in single cells or even within subcellular regions is now possible without RNA isolation. In combination with the immunofluorescence (IF) technique, visualization of nucleic acids and associating proteins is achieved with higher resolution than ever before using light microscopy. Here we describe the steps implemented to achieve the visualization of individual messenger RNAs (mRNA) using single-molecule FISH (smFISH) probes, as well as detection of mRNA/protein (mRNP) complexes via smFISH in combination with IF.

Key words mRNA, mRNP, Stellaris™ probe, smFISH, Immunofluorescence, Egg chambers, Oogenesis, *Drosophila melanogaster*

1 Introduction

Fluorescence in situ hybridization (FISH) technology was developed to detect DNA or RNA in fixed tissue. Although mRNA expression levels can be assessed via RT-qPCR and Northern blotting after the RNA is isolated from the cells, the need for doing so without lysing the cells made FISH a much sought-after tool. After J.G. Gall and M.L. Pardue first described the "Formation and detection of RNA-DNA hybrid molecules in cytological preparations" in 1969, ISH became a workhorse for cell biologists [1]. Since that first experiment, in which DNA was detected via tritium-labeled RNA, there have been numerous developments in visualizing nucleic acids in fixed and live cells. Moreover, the versatility of probe sizes and tag labels enables for the application of this technique to various tissue types [2, 3].

Diana P. Bratu and Gerard P. McNeil (eds.), *Drosophila Oogenesis: Methods and Protocols*, Methods in Molecular Biology, vol. 1328, DOI 10.1007/978-1-4939-2851-4_9,

There are double- and single-stranded DNA probes, RNA probes, and synthetic oligonucleotides. The probes may be long or short, structured or "linear", each presenting different thermodynamic characteristics that are important for the recognition of a complementary target sequence. Longer probes (>50 nucleotides) usually present two major disadvantages: (1) they do not penetrate the tissue as efficiently as smaller probes do, and (2) they are more tolerant of a higher number of mismatches, thus making them less specific. Short probes support greater tissue penetration and target recognition, as well as increased stability. RNA probes, while excellent in creating highly stable RNA-RNA hybrids, are sensitive to RNase activity, which makes working with these probes challenging. Modifications of the nucleic acid backbone, such as 2′-*O*-methyl and locked nucleic acids (LNAs) during oligonucleotide synthesis, have offered numerous advantages, such as increased thermal stability and resistance to nucleases [4, 5]. The probes can also be designed to form secondary structures, which proved to enhance target specificity and expand the applications to live cells [6, 7].

The labeling scheme of probes has also improved. Today's probes are no longer labeled with radioactivity, but with compounds and chemical moieties that provide greater flexibility for visualizing nucleic acids in fixed cells (e.g., biotin, digoxigenin (DIG), and fluorescent dyes) [8, 9]. The label can be attached co- or post-synthesis: (1) it can be incorporated during oligonucleotide synthesis via modified nucleotides or (2) at the 5′ or 3′ ends of the oligo-probe. A disadvantage of using biotin or DIG tags is that they involve an intermediate step for detection of the probes. Alternatively, labeling the probes with a fluorescent molecule allows for a more immediate detection of the target, thus leading to their popularity in recent years. The group of R. Singer first described how fluorescently labeled oligonucleotide probes can reliably detect single molecules of β-actin mRNA in cultured cells. They generated five 50-nt-long probes, each containing five amino-modified thymidine residues, conjugated to a Cy3 fluorochrome, spaced every ten nucleotides [10]. This allowed very sensitive and direct detection of target mRNA. However, along with being expensive to synthesize, the background signal due to nonspecific binding of even one of the five probes was substantially high. The efforts to lower the cost and achieve enhanced specificity of single-copy mRNA detection were met by A. Raj et al. who most recently introduced a modified version of fluorescently labeled probes, known as "Stellaris™" or "smFISH" probes [11]. In this system, a set of oligo probes, each 20 nt long, labeled with a fluorophore at the 3′ terminus, is designed to specifically detect one mRNA molecule [12–14]. Under optimal conditions, a set specific for one target contains 48 oligos, but excellent signal can be achieved with as few as 30 probes and as many as 80 probes per target. The probes are designed to bind in close proximity to each other along

the length of the transcript and all probes have similar GC content so that most of the probes will bind optimally under the same hybridization conditions. The binding of this large number of probes gives a highly fluorescent diffraction spot while nonspecific binding of few probes or unbound probes only give diffused background. Being so small in size, these probes allow detection of target mRNA even in the presence of secondary structures in the transcript, bound mRNA-binding proteins, or ribosomes. The probes can be designed using an automated algorithm provided free of cost via the Biosearch Technologies website (www.biosearchtech.com) by simply inputting an mRNA's nucleotide sequence, followed by the selection of a desired fluorophore label. Red and far-red fluorophores are more desirable due to their minimal contributions to background autofluorescence of a cell [12]. These probes can therefore be used to visualize the expression and localization of single-copy transcripts, as well as measure gene expression during tissue development.

Furthermore, apart from understanding the localization pattern of mRNA, it is often desired to simultaneously identify the localization of proteins, particularly the proteins that are involved in mRNA transport and localization. The intracellular distribution of proteins is usually achieved by immunofluorescence (IF) using antibodies specific for the target protein and using a fluorescently conjugated secondary antibody for imaging. In this chapter, we offer detailed protocols on how to achieve excellent signal using the smFISH probes alone as well as in combination with immunostaining in *Drosophila* egg chambers. This protocol will enable simultaneous visualization of RNA and its associated proteins.

2 Materials

2.1 Isolation and Fixation of Ovaries

All reagents and buffers should be made using RNase-free DEPC-treated water and prepared in an RNase-free environment.

1. 5× Robb's medium: 500 mM HEPES pH 7.4, 275 mM potassium acetate, 200 mM sodium acetate, 500 mM sucrose, 50 mM glucose, 6 mM magnesium chloride, 5 mM calcium chloride. Store at −20°C.
2. 10× Phosphate-buffered saline (PBS): 1.37 M NaCl, 27 mM KCl, 100 mM Na_2HPO_4, 20 mM KH_2PO_4, pH 7.4.
3. Triton™ X-100.
4. Fixation wash buffer, 1× PBST: 1× PBS, 0.05 % Triton™ X-100.
5. 2× Oocyte buffer: 200 mM potassium cacodylate, pH 7.2, 200 mM sucrose, 80 mM potassium acetate, 20 mM sodium acetate, 20 mM EGTA.

6. 16 % paraformaldehyde (PFA) (EM grade).
7. Oocyte fixation solution: 4 % PFA, 1× oocyte buffer, 1× PBS (v/v: 1 part 16 % PFA, 2 parts 2× oocyte buffer, 1 part 1× PBS).
8. Two dissection forceps (Dumont #5 tweezers).
9. Deep-well concavity glass slide.
10. Dissection microscope.

2.2 Probe Hybridization

1. Deionized formamide. (Caution! Formamide is a teratogen and it should be handled in a chemical fume hood.)
2. 20× Saline-sodium citrate (SSC).
3. Hybridization buffer: 10 % dextran sulfate, 1 μg/μl *Escherichia coli* tRNA, 2 mM vanadyl ribonucleoside complex, 0.02 % RNase-free BSA, 10 % formamide, 2× SSC. Filter using 0.2 μm filters and store at −20 °C.
4. FISH wash buffer: 10 % formamide, 2× SSC in dH_2O.

2.3 Immunostaining

1. Bovine serum albumin (BSA) (*see* **Note 1**).
2. IF wash buffer: 2× SSC, 0.05 % Triton™ X-100 in dH_2O.

2.4 Mounting and Imaging

1. Microscope glass slides (22 × 75 mm^2; 1 mm thickness).
2. Microscope glass cover slips (22 × 40 mm^2 or 17 × 40 mm^2; 0.13–0.17 mm thickness).
3. Antifade Mounting Medium: ProLong Gold®.
4. Nail polish.
5. Fluorescent microscope with appropriate filter cubes or confocal microscope with appropriate lasers.

3 Methods

3.1 smFISH: RNA Fluorescence In Situ Hybridization with Single Molecule-Detecting Probes, Stellaris™

During *Drosophila* oogenesis, the nurse cells' polyploid nuclei provide large quantities of factors necessary for growth of the developing oocyte. While mRNAs can be translated in the nurse cells, several mRNAs are transported into the oocyte. For example, *bicoid*, *oskar*, and *gurken* mRNAs, each plays a crucial role in establishing the body axes of the future embryo. *bicoid* and *oskar* mRNAs encode proteins that determine the anterior-posterior axis, while *gurken* is necessary for the dorsal-ventral axis formation. *gurken* mRNA is detected at the oocyte posterior during early stages of development, and subsequently at the anterior-dorsal corner of the oocyte during later stages (Fig. 1). *oskar* mRNA is also transcribed early and localizes to the posterior of the oocyte by stage 9 (Fig. 1).

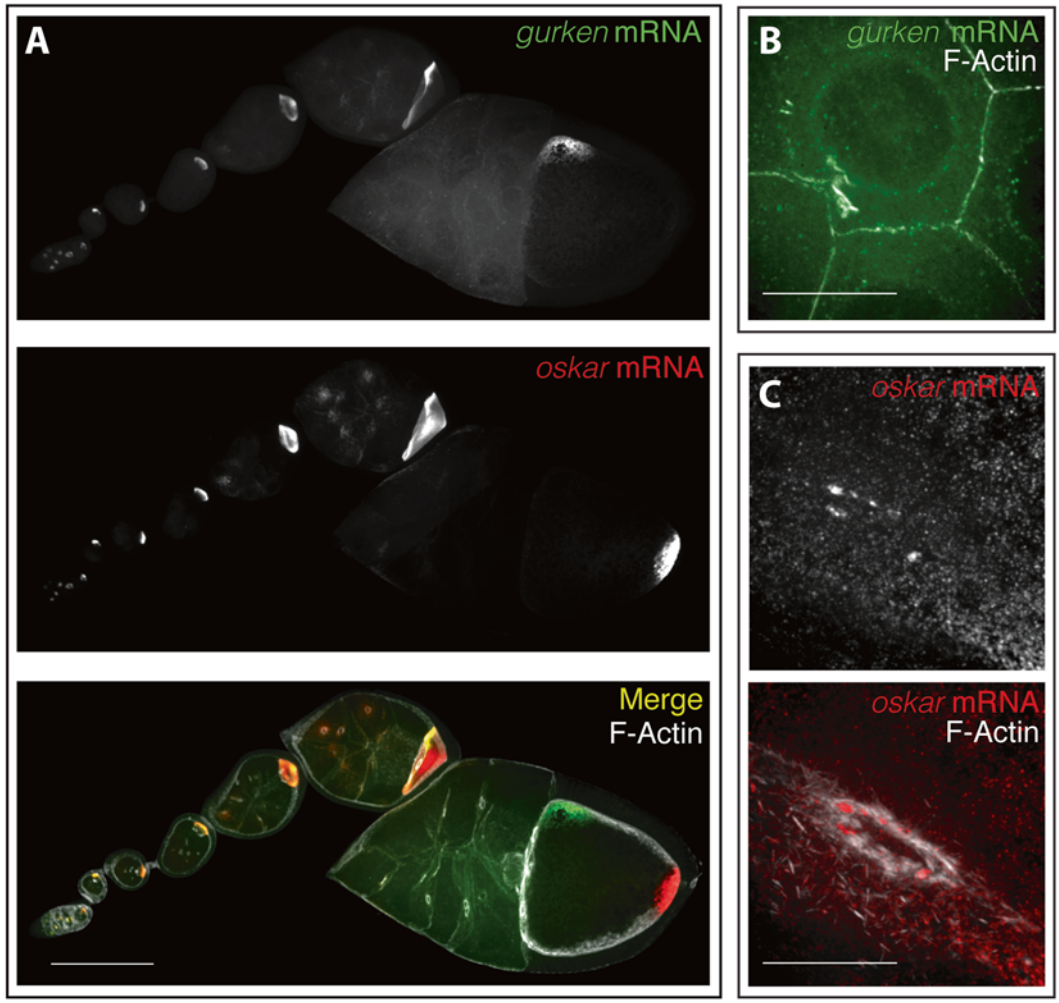

Fig. 1 Detection of mRNAs during oogenesis with smFISH probes. (**A**) Visualization of endogenous *gurken* mRNA (Cy5—*green*), and *oskar* mRNA (TMR—*red*) expression in a single-ovariole egg chamber chain, beginning in the germarium through stage 10 egg chambers. Phalloidin staining highlights the F-actin cytoskeleton (*white*). Images (13) were stitched together using ImageJ software [15], representing projections of 26–49 optical Z-slices at 0.5 μm steps. Scale bar is 100 μm. (**B**) Detection of *gurken* mRNA particles (Cy5—*green*) and F-actin (*white*) in nurse cells at higher magnification. The image represents a projection of 25 optical Z-slices at 0.2 μm steps. Scale bar is 20 μm. (**C**) Detection of *oskar* mRNA (TMR—*red*) and F-actin (*white*) particles around a ring canal at high magnification. Images represent projections of 11 optical Z-slices at 0.2 μm steps. Scale bar is 20 μm

Since the expression and localization of these mRNAs are tightly controlled during their transport into the oocyte, the egg chamber provides an excellent system to study mRNA regulation. This protocol describes the steps necessary to achieve single-molecule detection of multiple mRNAs simultaneously.

3.1.1 Dissection and Fixation of Ovaries

1. Collect and feed newly hatched female flies on fresh yeast paste for 2–4 days. Replenish with fresh yeast paste daily (*see* **Note 2**).
2. Build a dissection station by taping the dissecting slide directly onto a CO_2 pad. Add 1× Robb's medium to the concavity glass slide cavity (*see* **Note 3**).
3. Anesthetize the flies on the CO_2 pad and dissect out the ovaries. Collect them in the 1× Robb's medium (*see* **Note 4**).
4. Remove the extra tissue and organs that get dissected out with the ovaries and transfer the ovaries using a glass pipet into a 1.5 ml microcentrifuge tube.
5. Remove the Robb's medium and rinse with ~1 ml 1× PBS by inverting the tube two times, and then letting the ovaries settle down. Remove as much 1× PBS solution as possible.
6. Incubate for 15 min with ~400 μl of oocyte fixation solution with constant rocking (*see* **Note 5**).
7. Wash three times for 10 min with ~1 ml of 1× PBST with constant rocking. Allow the egg chambers to settle down between each wash (*see* **Note 6**).

3.1.2 Probe Hybridization

Day 1

1. Prehybridization: Wash one time for 10 min with ~1 ml of FISH wash buffer using constant rocking (*see* **Note 7**).
2. Allow the ovaries to settle and then transfer them back with a glass pipet into a concavity glass slide cavity placed onto the stage of a dissecting microscope.
3. Tweeze apart into individual ovarioles. Transfer them back to the 1.5 ml tube (*see* **Note 8**).
4. Prepare the smFISH solution by diluting the smFISH probes in hybridization buffer. The concentration of the probes should be experimentally determined; an appropriate starting concentration is 1 ng/μl (*see* **Note 9**).
5. Hybridization: Exchange the FISH wash buffer with the smFISH probe solution and incubate overnight at 37 °C in the dark without rocking (*see* **Note 10**). Protect the samples from light in all of the subsequent steps by covering with aluminum foil.

Day 2

6. Remove the smFISH probe solution and store it at 4 °C for future use (up to three experiments).
7. Wash the egg chambers three times for 10 min with ~1 ml of FISH wash buffer with constant rocking.

3.1.3 Mounting

1. Remove as much of the FISH wash buffer as possible.
2. Take a P100 pipette tip and cut off a few millimeters of the tip, thus creating a larger opening, aiding in adding the viscous mounting media over the egg chambers (~2× the volume of the egg chambers) (*see* **Note 11**).
3. Transfer the egg chambers in the mounting media to a glass slide spreading them across the middle section.
4. Under a dissecting microscope, use a tweezer to further spread the egg chambers across the slide, ensuring that they are not crowded in one area, and that each ovariole chain is well separated.
5. Gently place the cover slip on top and remove all excess medium via vacuum aspiration or dabbing with a Kimwipe (*see* **Note 12**).
6. Let the slides cure overnight at room temperature, and then store them in a dark place at 4 °C (*see* **Note 13**).

3.1.4 Imaging

1. Images may be acquired with a variety of fluorescence microscopes equipped with appropriate filter sets and a high resolving camera. We use a spinning disc CSU 10 Leica DM4000 confocal microscope setup that includes a Hamamatsu C9100-13 EMCCD, and diode lasers (491, 561, and 640 nm).

3.2 RNA smFISH Followed by Immunofluorescence Staining

Even though biochemical approaches are great for deciphering direct or indirect interactions between proteins and mRNAs, they offer very little information about the spatial context where these events take place in the tissue. Combining RNA smFISH with indirect immunofluorescence provides an excellent platform to analyze the spatial distribution of mRNAs and their regulatory proteins simultaneously (Fig. 2). While some of the previous combination FISH/IF protocols could take as long as 5 days, the use of smFISH allows simultaneous detection of RNA and protein in as little as 2 days. The two protocols of RNA hybridization and antibody staining done in either order have given similar results. Here, we describe a combined protocol for RNA smFISH and IF labeling, which can be used to detect multiple mRNAs and proteins in a single experiment.

3.2.1 Dissection and Fixation of the Ovaries

1. Follow the steps in Subheading 3.1.1 (*see* **Note 4**).

3.2.2 Probe Hybridization

1. Follow the steps in Subheading 3.1.2 until **step 5** (*see* **Notes 8** and **10**).
2. Wash one time for 10 min with ~1 ml of 10 % formamide in 2× SSC with constant rocking.

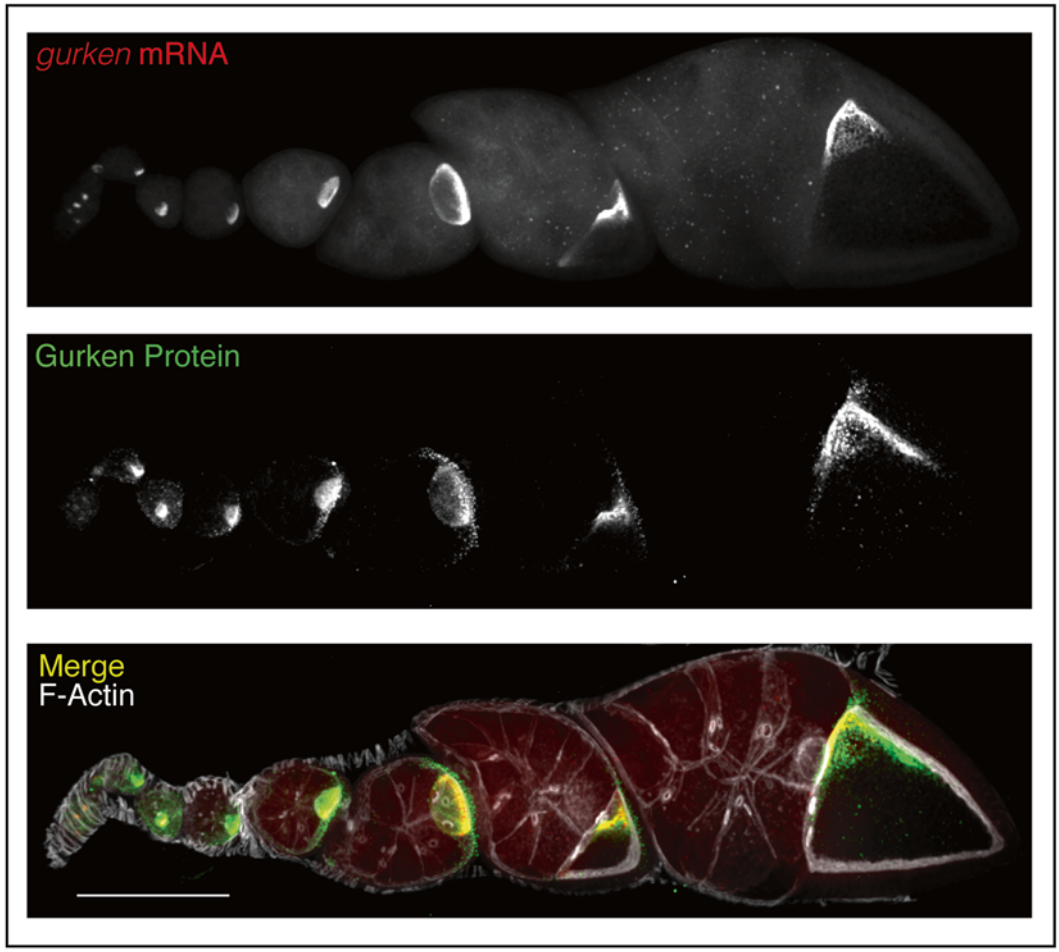

Fig. 2 Co-detection of mRNA and protein via smFISH-IF. Visualization of endogenous *gurken* mRNA (Cy5—*red*) localization and Gurken protein (Alexa Fluor 488—*green*) expression, beginning in the germarium through stage 10 egg chambers. Phalloidin staining depicts the F-actin cytoskeleton (*white*). Images (6) were stitched together using ImageJ software [15] and represent projections of 27–70 optical Z-slices at 0.5 μm steps. Scale bar is 100 μm

3.2.3 Antibody Incubation

1. Permeabilize the egg chambers with 1 % Triton™ X-100 in 2× SSC and simultaneously block with 1 % BSA for 2 h with constant rocking. Exchange this solution twice during the incubation (*see* **Note 14**).
2. Rinse two times with ~1 ml of 2× SSC.
3. Prepare the primary antibody solution in 2× SSC and Triton™ X-100 according to previously established optimal concentrations of the particular primary antibody and detergent (*see* **Notes 15** and **16**).
4. Remove the 2× SSC and incubate in primary antibody solution overnight at 4 °C with constant rocking (*see* **Note 17**).

Day 3

5. Remove the primary antibody solution and wash three times for 10 min with ~1 ml of IF wash buffer (*see* **Note 16**).
6. If a directly labeled primary antibody is used, proceed to Subheading 3.2.4 for mounting and imaging; if a secondary antibody is necessary, continue with **step 7**.
7. Prepare the secondary antibody solution in 2× SSC and 0.1 % Triton™ X-100 (*see* **Notes 15**, **16**, and **18**).
8. Incubate with secondary antibody solution for 2–4 h at room temperature with constant rocking.
9. Remove the secondary antibody solution and wash three times for 10 min with ~1 ml of IF wash buffer.

3.2.4 Mounting and Imaging

1. Follow the steps in Subheadings 3.1.3 and 3.1.4.

3.3 Immunofluorescence Staining Followed by RNA smFISH

3.3.1 Dissection and Fixation of the Ovaries

1. Follow **steps 1**–**7** in Subheading 3.1.1 (*see* **Note 3**).

3.3.2 Antibody Incubation

Day 1–2

1. Follow **steps 1**–**8** in Subheading 3.2.3 for antibody incubation.
2. Remove the secondary antibody, and wash one time for 10 min with IF wash buffer.
3. Fix with oocyte fixation solution for 10 min. This step will cross-link the antibodies and the antibody signal will not be lost during the subsequent probe hybridizations.
4. Wash two times for 10 min with FISH wash buffer.

3.3.3 Probe Hybridization

1. Follow **steps 1**–**7** in Subheading 3.1.2.

3.3.4 Mounting and Imaging

Day 3

1. Follow the steps in Subheadings 3.1.3 and 3.1.4.

4 Notes

1. Contaminating nucleases present in BSA may lead to a decrease of the signal. Switching to nuclease-free ultrapure non-acetylated BSA can alleviate this problem.

2. Add a few males to the vials to ensure that the flies are not virgins.
3. If a white surface fly pad is used, insert a small piece of used, but clean, exposed film (dark color) underneath the dissecting slide in order to provide greater contrast when transferring the ovaries onto the slide.
4. It is important that the ovaries do not incubate in the Robb's medium longer than 15 min. Proceed to the next step as quickly as possible. 10–15 ovaries are sufficient for one FISH experiment; use 15–20 ovaries for a combined FISH-IF protocol.
5. Keep the samples protected from light in all subsequent steps when a fluorescently tagged protein is expressed in the egg chambers. With multiple samples, fix each sample immediately; do not let them sit in Robb's medium or PBS for an extended period of time. Oocyte fixation solution should be made separately and mixed well before it is added to the oocytes.
6. After removing the fixative, the ovaries may stick together in the PBST; gently flick the bottom of the tubes until the ovaries are separated. Samples can stay in PBST longer than 10 min. When multiple samples are being fixed sequentially, synchronize them at this step and maintain this synchronization for the remainder of the protocol.
7. The prehybridization wash must contain the same percentage of formamide as the hybridization solution.
8. Secure the ovaries with one tweezer. Using the tip of the other tweezer, comb from the birth canal toward the germarium to completely separate the ovarioles. Ovaries should stay in this buffer no longer than ~15 min. After returning the ovaries to the 1.5 ml tube, allow them to settle for at least 1 min, as the smallest egg chambers take longer to settle and may not be visible by eye. Separating the ovarioles is slightly different for the combined smFISH-IF experiments. Using the same combing motion as above, DO NOT separate the ovarioles completely. It is advantageous to keep the ovarioles connected near the birth canal to minimize the loss of the smaller chambers over the many subsequent steps. When finished tweezing, each ovary should look like a spread-out bunch of bananas.
9. Efficient hybridization of probes to their target depends on three key parameters: probe concentration, temperature, and formamide concentration. Probe concentration should be the first parameter adjusted for signal optimization; optimization of the probe concentration allows for the maintenance of similar conditions between experiments. Although increasing the temperature and formamide concentration leads to a higher stringency, it can also lead to false negatives.

10. Immerse 15–20 ovaries in 30 μl of the probe solution, and mix it by flicking the bottom of the tube gently. Do not vortex. The incubation period can be as short as 2 h for adequate signal generation, and thus, in the combined FISH-IF experiments, the protocol may be performed in just 2 days. More than one RNA can be detected simultaneously when using multiple probes labeled with different fluorophores.
11. Cut a pipet tip off at a slight diagonal, not straight across; this will ensure removal of all the contents from the tube. Too much medium may lead to the shifting of egg chamber distribution on the glass slide when covering with the cover glass, while too little medium may result in the formation of air bubbles. About 45 μl of mounting media is sufficient for 20 pairs of WT ovaries.
12. Push the cover slip down very lightly while using the dissecting scope to check how much the smaller egg chambers are floating. If the egg chambers are shifting, push down the cover slip a little bit more and remove the excess media again. Repeat until the movement of the germarium is minimal. Extra care has to be taken not to push down too hard, as that could lead to the tearing or bursting of the larger egg chambers; remove as many of the later stage egg chambers if the younger stages and the germarium are the desired stages to be imaged.
13. Seal the edges with nail polish for long-term storage at 4 °C.
14. Triton™ X-100 is a nonionic detergent that can aid in antibody penetration into the tissue and the reduction of nonspecific binding due to hydrophobic interactions of the molecules. BSA is used as a blocking agent to reduce possible background signal.
15. Antibody concentration should be experimentally determined starting with the concentration recommended in the manufacturer's instructions. The concentration of the detergent should be optimized for each antibody in a range of 0.05–0.5 %; an appropriate starting concentration is 0.1 %. Use between 250 and 500 μl of solution.
16. Nonspecific binding can be reduced by adding 0.1 % BSA to the antibody and IF wash buffer solutions.
17. Some primary antibodies bind better at room temperature; check the manufacturer's instructions, or test experimentally.
18. The secondary antibody is usually diluted 1:1000; however, consult the manufacturer's instructions for recommended working dilutions.

Acknowledgements

We would like to thank the members of the Bratu lab for constructive criticism during the preparation of this manuscript. LVB, SKF and DPB were supported by NSF CAREER award to DPB. The Gurken 1D12 antibody, developed at the California Institute of Technology, was obtained from the Developmental Studies Hybridoma Bank, created by the NICHD of the NIH and maintained at The University of Iowa, Department of Biology, Iowa City, IA.

References

1. Gall JG, Pardue ML (1969) Formation and detection of RNA-DNA hybrid molecules in cytological preparations. Proc Natl Acad Sci U S A 63:378–383
2. Wetmur JG (1991) DNA probes: applications of the principles of nucleic acid hybridization. Crit Rev Biochem Mol Biol 26:227–259
3. Boutorine AS, Novopashina DS, Krasheninina OA et al (2013) Fluorescent probes for nucleic Acid visualization in fixed and live cells. Molecules 18:15357–15397
4. Beaucage SL, Iyer RP (1992) Advances in the Synthesis of Oligonucleotides by the Phosphoramidite Approach. Tetrahedron 48: 2223–2311
5. Roget A, Bazin H, Teoule R (1989) Synthesis and use of labelled nucleoside phosphoramidite building blocks bearing a reporter group: biotinyl, dinitrophenyl, pyrenyl and dansyl. Nucleic Acids Res 17:7643–7651
6. Tyagi S, Bratu DP, Kramer FR (1998) Multicolor molecular beacons for allele discrimination. Nat Biotechnol 16:49–53
7. Tyagi S, Kramer FR (1996) Molecular beacons: probes that fluoresce upon hybridization. Nat Biotechnol 14:303–308
8. Bauman JG, Wiegant J, Borst P et al (1980) A new method for fluorescence microscopical localization of specific DNA sequences by in situ hybridization of fluorochrome-labelled RNA. Exp Cell Res 128:485–490
9. Raap AK, van de Corput MP, Vervenne RA et al (1995) Ultra-sensitive FISH using peroxidase-mediated deposition of biotin- or fluorochrome tyramides. Hum Mol Genet 4:529–534
10. Femino AM, Fay FS, Fogarty K et al (1998) Visualization of single RNA transcripts in situ. Science 280:585
11. Raj A, van den Bogaard P, Rifkin SA et al (2008) Imaging individual mRNA molecules using multiple singly labeled probes. Nat Methods 5:877–879
12. Raj A, Tyagi S (2010) Detection of individual endogenous RNA transcripts in situ using multiple singly labeled probes. Methods Enzymol 472:365–386
13. Batish M, Raj A, Tyagi S (2011) Single molecule imaging of RNA in situ. Methods Mol Biol 714:3–13
14. Little SC, Tkacik G, Kneeland TB et al (2011) The formation of the Bicoid morphogen gradient requires protein movement from anteriorly localized mRNA. PLoS Biol 9:e1000596
15. Preibisch S, Saalfeld S, Tomancak P (2009) Globally optimal stitching of tiled 3D microscopic image acquisitions. Bioinformatics 25: 1463–1465

Chapter 10

Fluorescent In Situ Hybridization of Nuclear Bodies in *Drosophila melanogaster* Ovaries

Zehra F. Nizami, Ji-Long Liu, and Joseph G. Gall

Abstract

Fluorescent in situ hybridization (FISH) is a technique for determining the cytological localization of RNA or DNA molecules. There are many approaches available for generating in situ hybridization probes and conducting the subsequent hybridization steps. Here, we describe a simple and reliable FISH method to label small RNAs (200–500 nucleotides in length) that are enriched in nuclear bodies in *Drosophila melanogaster* ovaries, such as Cajal bodies (CBs) and histone locus bodies (HLBs). This technique can also be applied to other *Drosophila* tissues, and to abundant mRNAs such as histone transcripts.

Key words Fluorescence in situ hybridization (FISH), Small nuclear RNAs (snRNAs), Small Cajal body-specific RNAs (scaRNAs), Cajal bodies (CBs), Histone locus bodies (HLBs), *Drosophila* ovaries

1 Introduction

The nucleus of a cell is organized into non membrane-bound compartments such as CBs and HLBs, which are enriched in factors involved in pre-mRNA processing [1]. These bodies can be identified based on their molecular composition, either by antibody staining to label proteins or in situ hybridization to label RNAs. When labeling nuclear bodies, it is important to examine more than one marker because there can be situations when a particular protein or RNA is simultaneously enriched in two or more distinct classes of nuclear bodies. For example, coilin is a protein that has been widely used as a molecular marker of CBs, but in certain *Drosophila* tissues and at various stages of oogenesis, it is also enriched in HLBs [2]. As such, there is presently no one antibody that robustly and reliably acts as a unique marker of *Drosophila* CBs without some prior characterization of the tissue. In contrast, there are small RNAs in these bodies (200–500 nucleotides in length) that are uniquely localized. These include small Cajal body-specific RNAs (scaRNAs) and spliceosomal U small nuclear RNAs

Diana P. Bratu and Gerard P. McNeil (eds.), *Drosophila Oogenesis: Methods and Protocols*, Methods in Molecular Biology, vol. 1328, DOI 10.1007/978-1-4939-2851-4_10, © Springer Science+Business Media New York 2015

(snRNAs) that are enriched in CBs, and the U7 snRNA that is enriched in HLBs [3].

To label these small RNAs in CBs and HLBs, we use the simple and reliable FISH method described here. The simplicity lies in the generation of directly labeled fluorescent probes, which enables one to skip downstream labeling and amplification steps and proceed directly from hybridization to mounting the specimen. The reliability of the method stems from the cytological concentration of the target RNAs in foci such as CBs and HLBs.

In this protocol, we detail the specific methodology for FISH to RNA targets in CBs and HLBs in whole mount *Drosophila* ovaries [3] (Fig. 1). This protocol may be applied without modification to other *Drosophila* tissues and tissues from other organisms such as *Xenopus* ovaries. Furthermore, abundant mRNAs such as histone transcripts (Fig. 2) and localized mRNAs, such as the oskar transcripts that occur at the posterior pole of *Drosophila* eggs, can be labeled with this method. Thus the user may try this protocol as a rapid first pass to examine mRNA localization before attempting more lengthy or costly techniques, such as nonfluorescent haptens (digoxigenin or biotin), chemical amplification methods such as tyramide signal amplification, or single molecule FISH.

2 Materials

2.1 Generating the Template DNA for In Vitro Transcription

1. Optional: pGEM T-easy vector (Promega).
2. Standard PCR reagents: usually included in a kit containing a DNA polymerase, dNTPs, and reaction buffers.

2.2 In Vitro Transcription Reaction

1. Nuclease-free or ultra pure water. Available commercially, or can be prepared chemically with DEPC as follows. DEPC-treated dH_2O: Mix 2 ml of DEPC (diethyl pyrocarbonate) in 1 l of dH_2O. Shake vigorously. Let sit in a hood for 1 h. Autoclave to inactivate the remaining DEPC.
2. QIAquick PCR purification kit (Qiagen).
3. 20 mM CTP–ATP–GTP solution: Combine 4 μl each of 100 mM CTP, 100 mM ATP, and 100 mM GTP with 8 μl of dH_2O.

Fig. 1 (continued) The *arrows* label CBs and the *arrowheads* label HLBs. *Dotted white lines* indicate nuclei enlarged in panels **i–l**. (**g**, **i**, **j**) Oregon-R flies are wild-type for CBs and HLBs. (**h**, **k**, **l**) *WDR79MB10832/10832* flies are WDR79 protein-null mutants that lack CBs [5]. There are multiple HLBs in these nurse cells because the histone gene loci are dispersed due to loss of polyteny at this stage in development [6]. Cytoplasmic U7 snRNA bodies are U bodies [7]. Scale bar is 10 μm. Nuclear DNA was counterstained with DAPI (*gray*). Images are maximum intensity *z*-projections of multiple 0.5–1 μm optical sections obtained with a confocal microscope. Wild type and mutant specimens were treated identically and images were collected and processed with the same parameters

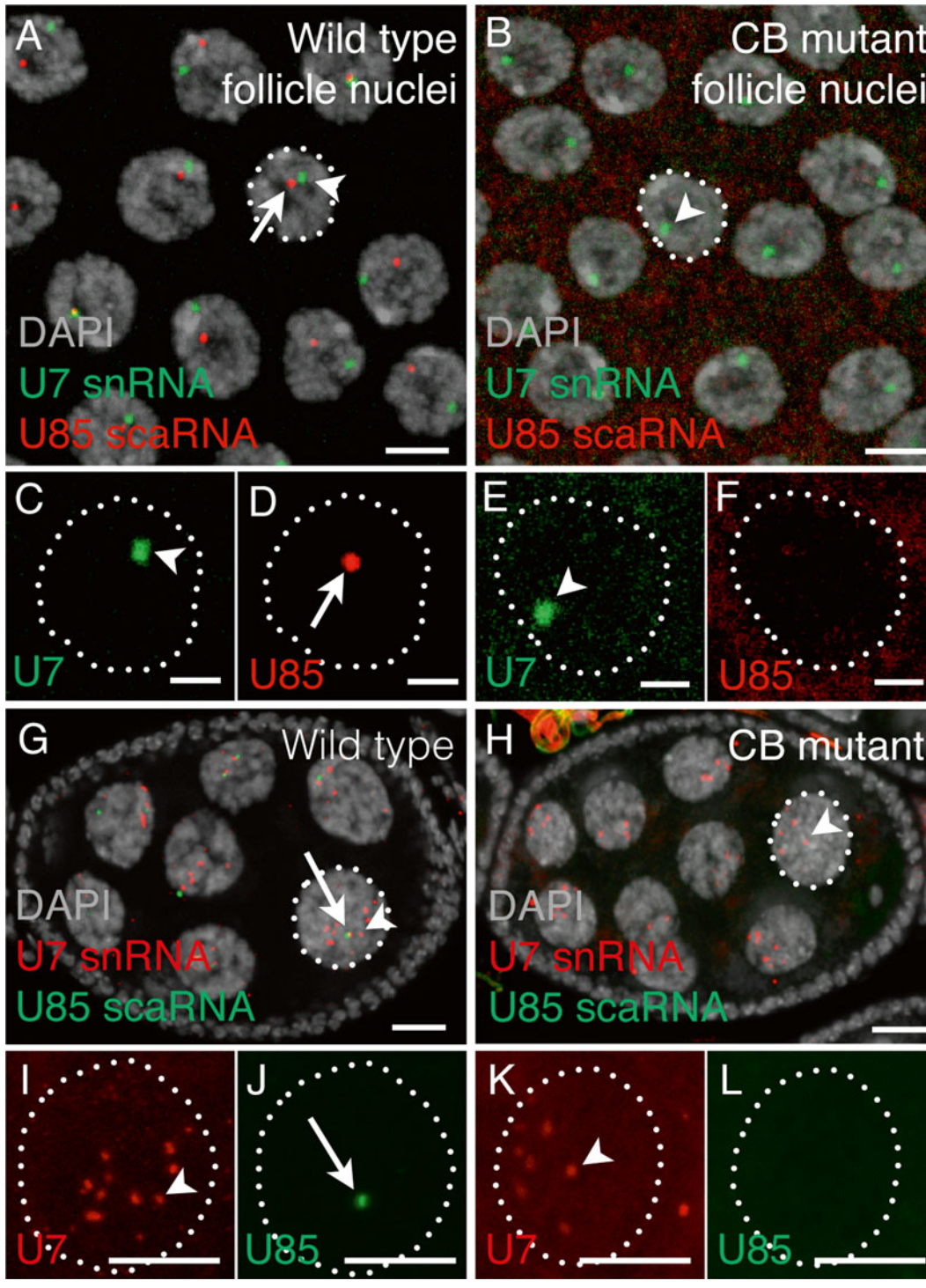

Fig. 1 FISH using U85 scaRNA (CB marker) and U7 snRNA (HLB marker) in wild-type and CB mutant *Drosophila* ovaries. (**a**–**f**) Follicle (somatic cell) nuclei from stage 8 egg chambers labeled with an Alexa-488 U7 snRNA antisense probe (Alexa-488, *green*) and a Cy5 U85 scaRNA antisense probe (Cy5, pseudo-colored red). The *arrows* label CBs and the *arrowheads* label HLBs. *Dotted white lines* indicate nuclei enlarged in panels **c**–**f**. (**a**, **c**, **d**) *y w* flies are wild-type for CBs and HLBs. (**b**, **e**, **f**) *Coilin199/199* flies are coilin protein null mutants that lack CBs [4]. (**g**–**l**) Stage 6 egg chambers showing germline nurse cell nuclei labeled with a Cy3 U7 snRNA antisense probe (Cy3, red) and a Cy5 U85 scaRNA antisense probe (Cy5, pseudo-colored green).

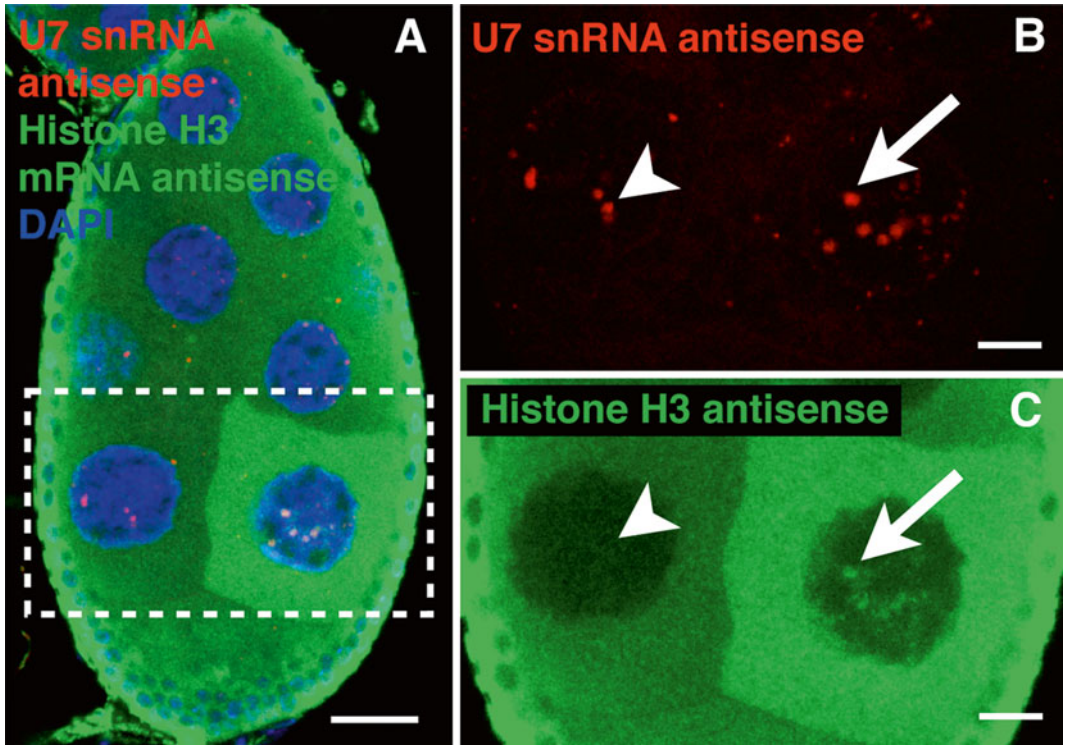

Fig. 2 FISH used to target histone H3 mRNA transcripts and U7 snRNA in a stage 7 wild-type and mutant *Drosophila* egg chamber. (**a**) U7 snRNA antisense probe (Cy3, *red*) labels HLBs in all nurse cell nuclei, whereas histone H3 mRNA antisense probe (Cy5, *green*) labels one nurse cell more prominently than other nurse cells. Because histone transcription is replication dependent, these nurse cells accumulate histone transcripts at different times due to their asynchronous endocycles [8]. (**b** and **c**) Enlarged images of the nurse cells from the *white box* shown in panel (**a**). (**b**) U7 snRNA antisense probe (*red*). (**c**) Histone H3 mRNA antisense probe (*green*). The histone H3 mRNA antisense probe is sensitive enough to detect cytoplasmic histone mRNA, as well as nascent transcripts at the histone locus in the transcribing nurse cell (*arrow*). In contrast, transcripts are not detected at HLBs in the other nurse cells (*arrowhead*), indicating that they are either not actively transcribing histone transcripts or the technique is not sensitive enough to detect them at this stage in the endocycle. Scale bar is 10 μm. Nuclear DNA was counterstained with DAPI (*blue*). The image is a maximum intensity *z*-projection of multiple 0.5–1 μm optical sections obtained with a confocal microscope

4. 10 mM UTP solution: Dilute the 100 mM UTP stock 1:10 in dH_2O.
5. Fluorescent UTP or fluorescent CTP (*see* **Note 1**).
6. RNasin ribonuclease inhibitor.
7. T3, T7, or SP6 RNA polymerase.
8. 5× transcription buffer (usually included with RNA polymerase).
9. DNAse I.
10. 250 mM EDTA: Dissolve 9.3 g of Na_2-EDTA·$2H_2O$ in approximately 80 ml of dH_2O. Adjust the pH to 8.0 with 10 N NaOH (EDTA will not dissolve until pH is increased). Make up to 100 ml with dH_2O. Autoclave.

11. GE Illustra MicroSpin G-50 Columns.

2.3 In Situ Hybridization of Whole-Mount Drosophila Ovaries

1. Grace's Insect Medium (FBS-free).
2. Fine jeweler's forceps.
3. Tungsten needles.
4. Dissecting microscope.
5. 20 % paraformaldehyde (PFA): Weigh out 200 g PFA in a hood. Weigh out 0.5 g $Na_2CO_3 \cdot H_2O$. Set a hot plate stirrer in the hood. Add Na_2CO_3 to ~800 ml dH_2O. Stir. Then add 200 g PFA. Heat and stir to ~80 °C to get it into solution. Make up to 1 l with dH_2O. Filter it through Whatman filter paper #1 in the hood since sometimes there is a lot of sludge. This stock is stable for many months at room temperature.
6. 4 % PFA in Grace's Insect Medium: Dilute 20 % PFA to 4 % in Grace's Insect Medium.
7. 5 % acetic acid (optional): Dilute v/v from glacial acetic acid.
8. 20× phosphate buffered saline (PBS): 160 g NaCl, 4 g KCl, 12.2 g Na_2HPO_4 anhydrous, 4 g KH_2PO_4 in 1 l of dH_2O.
9. 1× PBS: Dilute 1:20 with dH_2O from a 20× stock.
10. In situ mix: Combine 25 ml of 50 % formamide, 12.5 ml of 20× SSC, 0.5 ml of 5 mg/ml heparin, 0.5 ml of 50 mg/ml yeast tRNA, 0.9 ml of 0.5 M citric acid, pH 6, 0.75 ml of 20 % Triton™ X-100, and 9.85 ml nuclease-free H_2O to make a final volume of 50 ml.
11. Formamide.
12. 20× SSC: Dissolve 175.3 g NaCl and 88.25 g sodium citrate ($Na_3C_6H_5O_7 \cdot 2H_2O$) in 1 l of dH_2O, pH to 7.2 with 1 N HCl.
13. Heparin: Make a 5 mg/ml solution in dH_2O.
14. Yeast tRNA (Roche, USA, Catalog # 10109517001): Make a 50 mg/ml solution in dH_2O.
15. 0.5 M citric acid, pH 6: Dissolve 14.8 g citric acid ($C_6H_5O_7Na_3 \cdot 2H_2O$) in 100 ml of dH_2O (adjust to pH 6.0).
16. Triton™ X-100.
17. 10 μg/ml DAPI (4′,6-diamidino-2-phenylindole dihydrochloride): Dilute from 3.3 μg/μl stock in 70 % ethanol (stock can be stored in dark at 4 °C). The working stock (10 μg/ml) should be stored at room temperature in a dark bottle.

2.4 Mounting Labeled Tissue

1. Microscope glass slides and coverslips.
2. Phenylenediamine Stock Solution: Add 50 mg of phenylenediamine and 250 μl 20× PBS to 4.7 ml of dH_2O. Vortex to dissolve. Bring to pH 9.0 with 1 N NaOH. Store at –70 °C.

3. Mounting Medium: Mix 5 ml of glycerol, 4 ml of dH_2O and 1 ml of 10 mg/ml phenylenediamine Stock Solution. Aliquot rapidly to tubes on dry ice before storing at −70 °C.
4. Optional: Commercially available Mounting Media: ProLong Gold, Diamond antifade reagent, or VECTASHIELD.
5. Nail polish.

3 Methods

Create an RNAse-free environment by using autoclaved tips and reagents, and nuclease-free or DEPC-treated dH_2O in reactions. For suggestions in designing controls for this protocol, *see* **Note 2**. This protocol may be adapted to include immunostaining and FISH simultaneously or to target DNA loci instead of RNA as described below.

3.1 Generation of the Template DNA for In Vitro Transcription

There are at least four options for obtaining the template DNA required to generate single-stranded RNA probes by in vitro transcription (*see* **Note 3**).

1. Obtain previously cloned plasmid DNA for use as standard markers, such as U7 snRNA for HLBs and U85 scaRNA for CBs [3] (*see* **Note 4**).
2. Clone the target genes for these standard markers into a vector containing T3, T7, or SP6 RNA polymerase promoters (*see* **Note 5**).
3. PCR amplify the target genes with oligos containing T3, T7, or SP6 RNA polymerase promoter sequences as overhangs (*see* **Note 6**).
4. Generate short RNA probes (15–65 nucleotides in length) from a synthetic DNA oligo that contains a T3, T7, or SP6 RNA polymerase promoter sequence at the 5′ end of a short template DNA sequence for the target gene (*see* **Note 7**).

3.2 In Vitro Transcription of the Directly Labeled Fluorescent RNA Probes

1. If using plasmid DNA as a template, linearize with the appropriate restriction enzyme and purify the DNA before proceeding with the in vitro transcription reaction (*see* **Note 8**).
2. Combine the reagents for the in vitro transcription reaction in a 1.7 ml centrifuge tube in the following order: 2 μl of 20 mM CTP–ATP–GTP, 1.5 μl of 10 mM UTP, 5 μl of 1 mM fluorescent UTP, 1 μl of 40 mM RNAsin, 4 μl of 5× transcription buffer, 3.5 μl of nuclease-free H_2O, 2 μl DNA (1 μg plasmid DNA or 100 ng PCR product), 1 μl of 50 U/μl enzyme (T3, T7, or SP6 polymerase) for a total volume of 20 μl. Assemble the reaction at room temperature, making sure to keep the

RNA polymerase, NTPs, and RNase inhibitor on ice until use (*see* **Note 9**).

3. Mix well by tapping or vortex briefly. Pulse-spin. Incubate at 37 °C for 1.5–3 h.
4. Remove the template DNA by adding 1 μl of DNase I (dilute the stock solution 1:10 in DNase I buffer). Incubate at 37 °C for 10–20 min.
5. Inactivate the enzymes by adding 2 μl of 250 mM EDTA and incubating at 65 °C for 10–20 min.
6. Purify the RNA using a Sephadex column such as GE Illustra G50 spin columns, following manufacturer's instructions (*see* **Note 10**).
7. Analyze the probes by UV spectrophotometry and gel electrophoresis. Test 1 μl of the in vitro transcribed RNA on a NanoDrop spectrophotometer to determine RNA concentration (the concentration should be approximately 300 ng/μl). Test 1 μl of the RNA on a denaturing agarose gel to verify the quality and length of the RNA (the RNA should run as a single band).
8. Store the probes at −20 °C (can be kept for many years). Working solutions of the 10× probe in the in situ mix can be kept at −20 °C for at least several months.

3.3 In Situ Hybridization of Whole-Mount Drosophila Ovaries

1. Dissect out *Drosophila* adult ovaries in a physiological saline solution such as Grace's Insect Medium (*see* **Notes 11** and **12**).
2. Fix ovaries for 10 min in 4 % PFA in Grace's Insect Medium at room temperature. While in the fixative, comb through the ovaries with fine forceps or tungsten needles to separate the ovarioles (*see* **Notes 13** and **14**).
3. Remove the PFA and wash 5 min at room temperature in 1× PBS (*see* **Note 15**).
4. Add 100 μl of 5 % Triton™ X-100 to the PBS before transferring egg chambers to a 500 μl microfuge tube using a cut off pipette tip (*see* **Note 16**).
5. Remove the PBS and wash the tissue for at least 10 min with 100 μl of in situ mix at room temperature.
6. Prepare the probe mix by diluting the probe (to empirically determined final concentration) and DAPI (to final concentration of 1 μg/ml) in the in situ mix (*see* **Note 17**). One can use as little as 10 μl of probe per sample in a microfuge tube. Remove the in situ mix and replace it with probe mix. Ensure that the tissue is completely submerged in probe and tap the tube well to mix.

7. Incubate the probe with the specimen at 42 °C for 6–16 h (*see* **Note 18**).
8. Remove the probe and wash for at least 10 min with 100 µl of in situ mix with 1 µg/ml DAPI at room temperature (*see* **Note 19**).

3.4 Mounting Labeled Tissue

1. Remove the in situ mix and replace it with 15 µl of Mounting Medium (*see* **Note 20**).
2. Pipette the tissue onto a microscope glass slide and distribute the ovarioles evenly with forceps under a dissecting microscope.
3. Add a 22 × 22 mm^2 glass coverslip. To prevent egg chambers from being squashed, support the corners of the coverslip with a small amount of Vaseline or a Vaseline–paraffin wax mixture (melt equal weights of commercial Vaseline and paraffin wax, cool and store for use). Seal coverslip with commercial nail polish.

3.5 Combining Immunostaining and FISH

To perform the two methods simultaneously, modify the protocol in Subheading 3.3 as described below.

1. After fixation (**step 4**), proceed to a standard immunostaining protocol [3]. For a standard procedure, stain the tissue in primary and secondary antibodies overnight at room temperature.
2. Post-fix the tissue for 5 min at room temperature in 4 % PFA in 1× PBS.
3. Wash 2 × 5 min in 100 µl of 1× PBS at room temperature.
4. Continue with the FISH protocol starting at **step 5** (blocking in in situ mix) (*see* **Note 21**).

3.6 To Hybridize to DNA Instead of RNA

Adapt the protocol in Subheading 3.3 to include steps to denature the target DNA as described below.

1. At **step 6**, denature the probe at 80 °C for 5 min and quench on ice until use.
2. At **step 7** (hybridizing the probe to the specimen), denature the probe together with the specimen at 85 °C for 15 min before shifting to 42 °C for 6–16 h for hybridization (*see* **Note 22**).

4 Notes

1. There are several choices for fluorescent UTP or CTP with different excitation/emissions (in parentheses). These include ChromaTide Alexa Fluor 488-5-UTP (490/520), Aminoallyl-UTP-ATTO-488 (501/523), Cy5-UTP (5 mM stock: use 1 µl/20 µl per reaction) (649/670), Cy3-CTP (550/570), and Alexa Fluor 546-14-UTP (555/570).

2. This FISH protocol allows the user to employ multiple useful and biologically meaningful controls. To test the specificity of the antisense probe, use a sense probe as a negative control (*see* **Note 3**) or hybridize the probe in a null mutant fly (for viable alleles) or inducible clonal mutant (for lethal alleles). For CB markers, use CB mutant flies such as the coilin or WDR79 protein-null flies [4, 5]. For the HLB marker U7 snRNA, use the U7 snRNA null mutant fly [9]. To control for proper identification of a nuclear body, label with two or more markers. If the markers are RNA targets, label FISH probes with fluorescent nucleotides with nonoverlapping spectra (such as Alexa 488 and Cy3). If labeling both a protein and an RNA target simultaneously, adapt the protocol as in Subheading 3.5.
3. In vitro transcribed single-stranded RNA probes are advantageous because one can generate strand-specific probes from the same cloned template DNA: one antisense probe that hybridizes to the target RNA and one sense probe that acts as a control for nonspecific hybridization. Additionally, single-stranded probes do not require extensive denaturing steps like double-stranded RNA or DNA probes. A possible disadvantage of RNA probes is that they are less stable than DNA probes, but in our experience, when properly stored at −20 °C, they can be kept for many years.
4. Our lab has standard CB and HLB markers cloned and ready for distribution upon request [3]. We typically use the U85 scaRNA as a CB marker and the U7 snRNA as an HLB marker. scaRNAs are the best markers for CBs because they are highly enriched in these bodies. CBs are not present in all cell types, and tend to be absent in undifferentiated cells such as stem cells or embryonic cells [2]. Spliceosomal U snRNAs and U7 snRNA are also present in cytoplasmic U bodies [7].
5. Because the RNA components of CBs and HLBs are generally short RNAs derived from intronless genes (such as scaRNAs and snRNAs), the target genes can be easily amplified by PCR from genomic DNA and cloned into a TA cloning vector such as Promega's pGEM T-easy vector (contains T7 and SP6 phage RNA polymerase promoters). It is also straightforward to amplify the target gene by RT-PCR from total RNA. The short length of snRNAs and scaRNAs (<500 nt) makes them ideal for in situ hybridization probes because they readily penetrate whole tissues. If cloning into vectors that lack a T3, T7, or SP6 phage RNA polymerase promoter sequence, one can design oligos to include these sequences as a 5′ overhang (Fig. 3). The sequences to append the 5′ end of the oligos are: GCTAATACGACTCACTATA**G**GG for T7, GCAATTAACCCTCACTAAA**G**GG for T3, and

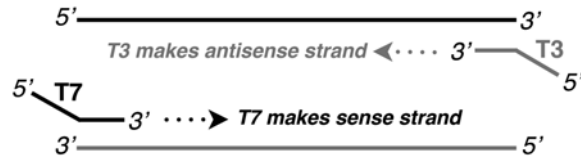

Fig. 3 A schematic of the oligo design for incorporating RNA polymerase promoter sequences into template DNA for in vitro transcription. The target genes sense strand is shown in *black* and the antisense strand in *gray*. The RNA polymerase promoters (T3, T7, or SP6) can be included as a 5′ overhang in the oligo design. To make an antisense probe, design the oligo to contain the reverse complement sequence (*short gray line*) downstream of the polymerase promoter (*gray overhang line* containing T3 RNA polymerase promoter sequence as an example). To make a sense probe, design the oligo to contain the coding sequence (*short black line*) downstream of the polymerase promoter (*black overhang line* containing T7 RNA polymerase promoter sequence as an example)

GCATTTAGGTGACACTATA**G**A for SP6. The bold **G** in the above sequences represents the +1 nucleotide (start of transcription).

6. In vitro transcribed probes can also be made directly from a PCR product, provided that one includes an RNA polymerase promoter at the 5′ end of the oligo (Fig. 3). This is a quick and useful technique when screening for CB or HLB markers. One should sequence the PCR product to make sure that there are no other templates in the reaction, and it is best to clone the product into a vector for long-term storage.
7. Generating a short probe from a synthetic DNA oligo allows one to skip any PCR and cloning steps and works well for standard CB and HLB targets. The disadvantage to this method is the cost of synthesizing DNA oligos to include both the RNA polymerase promoter and the template sequence. Design the DNA oligo to contain 15–65 nt of target DNA template sequence downstream of a T3, T7, or SP6 RNA polymerase promoter (*see* **Note 5** and Fig. 3). Modify the in vitro transcription reaction in Subheading 3.2, **step 2** to include an antisense oligo against the T3, T7, or SP6 RNA polymerase phage promoter. By pairing these oligos together, one generates the double-stranded DNA template necessary for the phage RNA polymerase to function.
8. Template DNA can be purified by standard alcohol precipitation techniques, or can be rapidly purified using columns such as Qiagen's QIAquick PCR purification kit (can also be used for restriction enzyme reactions).
9. The choice of a fluorescently conjugated nucleotide will depend on the lasers available for imaging the tissue. There are several fluorophores that we have found particularly bright and useful

(*see* **Note 1**). One should select nonoverlapping emission spectra when performing 2-color or 3-color FISH. Note that some of the fluorophores are conjugated to CTP rather than UTP, so the in vitro reaction has to be adjusted accordingly (to modulate the ratio of the unlabeled to the labeled nucleotide).

10. A probe that has effectively incorporated the fluorescently conjugated nucleotide will have a hue corresponding to the color of the emission spectrum (for example, Alexa 488-UTP labeled probes will appear green).
11. The presence or absence of CBs and HLBs follows a stereotyped pattern during oogenesis [2]. However, the size, morphology, and number of non-membrane bound organelles can vary depending on the nutritional state of the animal [10, 11]. To ensure consistent analysis of nuclear bodies, it is best to dissect animals of similar age and genetic background raised on a standard food source. For example, collect 2 day-old flies and then supplement fly food with wet yeast for two additional days to stimulate ovary development.
12. The choice of solution used for dissection can affect the organization of the oocyte nucleus (germinal vesicle, GV). In salt solutions of low ionic concentration (below 10 mM), nuclear bodies are induced de novo, particularly in egg chambers that are damaged in the process of dissection [12]. Dissection in Grace's Insect Medium preserves the morphology of nuclear bodies observed in live tissues. Furthermore, rapid dissection (less than 5 min, before fixation) is preferable for preserving morphology and preventing RNA degradation.
13. Any standard dissection and fixation technique will suffice. For example, dissect tissues in small 35 mm × 10 mm petri dishes or well slides, and transfer them with forceps to a separate well or dish that contains 100 µl of fixative, prepared fresh from a 20 % PFA stock. *Drosophila* ovaries are sufficiently fixed in as little as 10 min. Longer fixation periods are not necessary to preserve ovary morphology, and have been generally avoided because of the possibility of reduced permeability of the tissue to probe.
14. For better preservation of RNA, add acetic acid to the fixative to a final concentration of 0.5–2.5 %. This improves the brightness of the FISH signal but leaves the tissue more brittle and prone to damage. Acetic acid is not essential when the RNA target is abundant or densely localized, as it is in CBs or HLBs. Moreover, fixation with acetic acid is generally not compatible with immunostaining.
15. If dissecting in small petri dishes, use enough 1× PBS to fill the dish (approximately 3 ml).
16. *Drosophila* tissues stick to plastic surfaces unless solutions contain a detergent. To achieve a more uniform penetration of

RNA probes into the tissues when examining younger egg chambers (up to stage 10), remove the more mature chambers at this point (stages 11–14).

17. Probes generated by in vitro transcription as described in Subheading 3.2 are generally at a concentration of 300 ng/μl. Probes against RNA targets that are concentrated in nuclear bodies such as CBs and HLBs can be diluted as much as 1000× for FISH. Probes against diffusely localized RNA or lower abundance RNA targets should be diluted only 20–200×. DAPI is added to the probe mix to provide a robust fluorescent counterstain for nuclear DNA. If using minimal volumes of probe mix, such as 10 μl/sample, remove all wash solution from the specimen before adding the probe.
18. An incubation temperature of 42 °C is appropriate for hybridization of RNA probes (in 50 % formamide) to RNA targets in situ. Individual probes can be tested for optimal hybridization in the range of 37–52 °C (the higher the temperature, the more stringent the hybridization conditions). One can complete the procedure in 1 day (6 h incubation) or opt for an overnight incubation (up to 16 h) to analyze the next day. Overnight incubations are preferred for lower abundance targets, but are not necessary for most CB or HLB markers. For hybridization to RNA targets, incubations longer than 16 h may diminish the signal intensity due to degradation of the RNA targets. When using shorter RNA probes (such as 30–80 nucleotides in length), the hybridization incubation time can be reduced to 30 min–2 h because shorter probes penetrate the tissue better.
19. This short wash step is sufficient for examining CB and HLB markers because the RNA targets are highly localized. If experiencing high background, begin troubleshooting by decreasing the concentration of the probe before increasing the number, duration and/or temperature of washes.
20. We mount specimens in a phenylenediamine solution, which is cost effective but turns brown in a few weeks, even at −20 °C. For permanent preparations use commercially available mounting media such as VECTASHIELD, ProLong Gold, or ProLong Diamond.
21. The FISH signal may be diminished due to degradation of target RNA during immunostaining steps. If so, one can adapt the FISH protocol by using the probe at a higher concentration, or conducting the antibody staining steps at 4 °C.
22. The temperature and duration for the denaturation step affects the morphology of the tissue. Other denaturation treatments that work include 80 °C for 10 min or 90 °C for 5 min. For hybridization to DNA targets, the incubation time can be

extended to several days because the DNA targets are more stable than RNA targets, and the RNA probes are stable under these conditions. Both sense and antisense probes will hybridize to target DNA; hybridizing to target DNA is a useful method to test the specificity of the sense probe. These directly labeled fluorescent probes are sensitive enough to robustly label large gene clusters such as the histone genes. Other gene loci have not yet been tested.

Acknowledgements

We thank Svetlana Deryusheva (Carnegie Institution for Science) for useful advice and enhancements to this protocol.

References

1. Nizami Z, Deryusheva S, Gall JG (2010) The Cajal body and histone locus body. Cold Spring Harb Perspect Biol 2:a000653.
2. Nizami ZF, Deryusheva S, Gall JG (2010) Cajal bodies and histone locus bodies in *Drosophila* and *Xenopus*. Cold Spring Harb Symp Quant Biol 75:313-320.
3. Liu J-L, Murphy C, Buszczak M et al. (2006) The *Drosophila melanogaster* Cajal body. J Cell Biol 172:875–884.
4. Liu J-L, Wu Z, Nizami Z et al. (2009) Coilin is essential for Cajal body organization in *Drosophila melanogaster*. Mol Biol Cell 20:1661–1670.
5. Deryusheva S, Gall JG (2013) Novel small Cajal-body-specific RNAs identified in *Drosophila*: probing guide RNA function. RNA 19:1802–1814.
6. Dej KJ, Spradling AC (1999) The endocycle controls nurse cell polytene chromosome structure during *Drosophila* oogenesis. Development 126:293–303.
7. Liu JL, Gall JG (2007) U bodies are cytoplasmic structures that contain uridine-rich small nuclear ribonucleoproteins and associate with P bodies. Proc Natl Acad Sci USA 104: 11655–11659.
8. White AE, Leslie ME, Calvi BR et al. (2007) Developmental and cell cycle regulation of the *Drosophila* histone locus body. Mol Biol Cell 18:2491–2502.
9. Godfrey AC, Kupsco JM, Burch BD et al. (2006) U7 snRNA mutations in *Drosophila* block histone pre-mRNA processing and disrupt oogenesis. RNA 12:396–409.
10. Buckingham M, Liu JL (2011) U bodies respond to nutrient stress in *Drosophila*. Exp Cell Res 317:2835–2844.
11. Shimada Y, Burn KM, Niwa R et al. (2011) Reversible response of protein localization and microtubule organization to nutrient stress during *Drosophila* early oogenesis. Dev Biol 355:250–262.
12. Singer AB, Gall JG (2011) An inducible nuclear body in the *Drosophila* germinal vesicle. Nucleus 2:403–409.

Chapter 11

Ultrastructural Analysis of *Drosophila* Ovaries by Electron Microscopy

Thomas R. Hurd, Carlos G. Sanchez, Felipe K. Teixeira, Chris Petzold, Kristen Dancel-Manning, Ju-Yu S. Wang, Ruth Lehmann, and Feng-Xia A. Liang

Abstract

The *Drosophila melanogaster* ovary is a powerful, genetically tractable system through which one can elucidate the principles underlying cellular function and organogenesis in vivo. In order to understand the intricate process of oogenesis at the subcellular level, microscopic analysis with the highest possible resolution is required. In this chapter, we describe the preparation of ovaries for ultrastructural analysis using transmission electron microscopy and focused ion beam scanning electron microscopy. We discuss and provide protocols for chemical fixation of *Drosophila* ovaries that facilitate optimal imaging with particular attention paid to preserving and resolving mitochondrial membrane morphology and structure.

Key words *Drosophila* ovary, Germline, Transmission electron microscopy (TEM), Mitochondria, Cristae, Focused ion beam scanning electron microscopy (FIB-SEM)

1 Introduction

Drosophila oogenesis is a widely used model for studying a range of biological processes including adult stem cell self-renewal, maintenance, and cell differentiation [1–3]. The wealth of genetic tools available and the ease with which *Drosophila* ovaries can be imaged make it a particularly attractive system to study these processes. Light microscopy of fixed ovaries is the most commonly used approach to study *Drosophila* oogenesis. In addition to examining protein expression and localization in fixed tissues, the dynamics of oogenesis are increasingly also being explored in real time by live confocal imaging, with fluorescent protein markers to follow proteins, and the bacterial phage MS2 coat proteins and its RNA binding motifs to follow RNAs [2, 4]. The simplicity of light microscopy coupled with the fact that it can be used to monitor changes live as they occur, account for its widespread use. However, not all cellular

Diana P. Bratu and Gerard P. McNeil (eds.), *Drosophila Oogenesis: Methods and Protocols*, Methods in Molecular Biology, vol. 1328, DOI 10.1007/978-1-4939-2851-4_11,

structures can be resolved by light microscopy. Electron microscopy (EM) in contrast permits much better resolution of most cellular structures by exploiting the far shorter de Broglie wavelength of the electron [5, 6]. To date, EM has proven to be an essential method for understanding key processes of oogenesis such as polar granule morphology and composition.

1.1 Electron Microscopy of Drosophila Oogenesis

The first EM studies of the *Drosophila* ovary were published in the late 1960s and early 1970s. These initial studies by M.R. Cummings and R.C. King [7, 8], and A.P. Mahowald [9] characterized many general aspects of the process. However, since then the focus of many ultrastructural studies has been on determining the structure and composition of a specialized cytoplasm, called the germ plasm, that forms at the posterior of the late stage oocytes, and which is both necessary and sufficient to generate germ cells in the developing embryo [10, 11]. Ultrastructural studies have shown that the germ plasm is enriched in mitochondria and large electron dense structures, termed polar granules [12] (Fig. 1). Further studies using EM have characterized when polar granules first form and how their shapes change during development and between species [13]. Immuno-EM has also been indispensible to determining the protein and RNA constituents of polar granules [13] (Fig. 1). The elucidation and characterization of the polar granule structure and composition with EM is just one example of how useful this method can be. Due in no small part to ultrastructural studies, we now have a much better understanding not only of germ plasm and germ granules, but also of many facets of *Drosophila* oogenesis.

1.2 Preparation of Drosophila Ovaries for Transmission Electron Microscopy

The most often used method to prepare *Drosophila* ovaries for transmission electron microscopy (TEM) is conventional chemical fixation [9, 14, 15]. Typically, ovaries are first fixed at either room temperature or 4 °C with glutaraldehyde to cross-link proteins, and subsequently with osmium tetroxide to preserves lipids, especially phospholipid membranes [6, 16–18]. Ovaries are then treated with organic solvents such as ethanol to remove water prior to embedment in a water-insoluble resin for subsequent sectioning [6, 16] (Fig. 2). An ultramicrotome is used to cut thin sections, which are subsequently stained with heavy metals to impart contrast for cell ultrastructure [6, 16] (Fig. 3).

The major limitation of chemical fixation methods is the slow rate of diffusion of fixatives into tissues [6, 16, 17]. This is particularly problematic for thick and/or poorly permeable tissues. While *Drosophila* germaria and early stage egg chambers are relatively small (~15 μm in width) and permeable, diffusion of fixative into later stage egg chambers is more problematic as they are larger (~140 μm in width and ~450 μm in length) and surrounded by a poorly permeable vitelline membrane [19]. An alternative method often used to circumvent these problems is high-pressure freezing

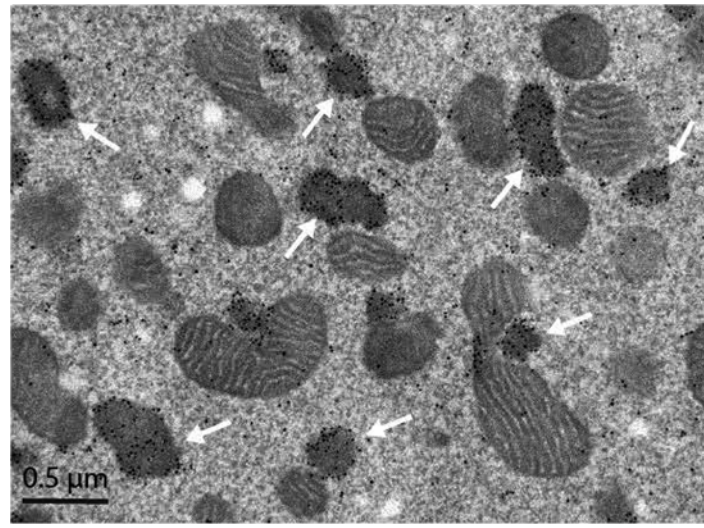

Fig. 1 Immuno-electron micrograph of germ plasm from a *Drosophila* embryo. Embryos were labeled with anti-Vasa serum. Polar granules are indicated with *arrows*. 15 nm gold particles are enriched in polar granules

and freeze-substitution (HPF-FS). In this method, cellular structures are rapidly immobilized prior to chemical fixation by freezing to −140 °C or below under high pressure [20, 21]. Although the rapid rate of immobilization often yields optimal near-native sample preservation, it requires expensive instrumentation, advance skills, and is not necessary to address many scientific questions. In general, for most biological applications, regular conventional chemical fixation yields satisfactory results [14, 15].

Standard chemical fixation methods preserve most structures in the ovary; however, inner mitochondrial membrane morphology is often not well maintained (Fig. 3a). To improve resolution of the inner mitochondria membrane, we have modified the standard chemical fixation protocol. We have found that decreasing the dehydration time and performing most processing steps at 4 °C greatly improves mitochondria membrane morphology (Fig. 3b). We have also found that including 0.1 % ruthenium red in the initial fixation reaction significantly improves the overall contrast of mitochondria. The modified chemical fixation protocol described in detail below yields improved resolution of intracellular membranous structures without the hassle and expense of HPF-FS sample preparation-based approaches.

1.3 Preparation of Drosophila Ovaries for Focused Ion Beam Scanning Electron Microscopy

EM is increasingly being used to determine the three-dimensional ultrastructure of cells and tissues. Traditionally this has been done by reconstruction of serial TEM sections or TEM tomography. Recently, however, focused ion beam scanning electron microscopy (FIB-SEM) has become a valuable technique to provide

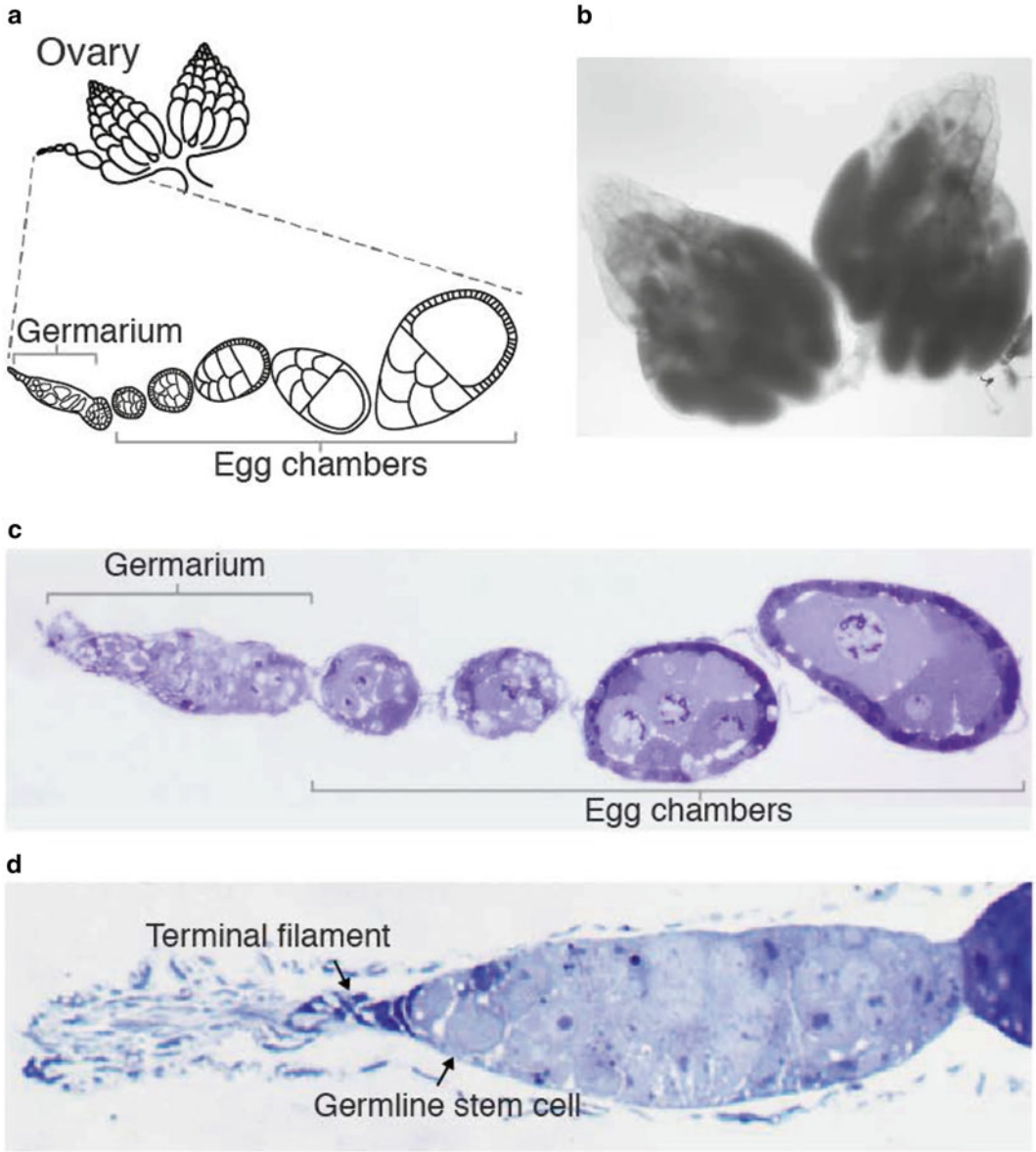

Fig. 2 The *Drosophila melanogaster* ovary. (**a**) Cartoon of oogenesis. (**b**) A pair of freshly dissected ovaries. (**c**) 500 nm Toluidine blue-stained thick sections of an ovariole and (**d**) a germarium

broad-spectrum resolution of large tissue volumes with high-resolution three-dimensional imaging. In this method, a focused ion beam is used to abrade the surface of the specimen exposing a new surface that is then imaged with a scanning electron beam. The repetition of this process generates a stack of successive images that can be compiled into a three-dimensional representation of the tissue being imaged. Automated ion milling and image acquisition make this method an increasingly powerful and efficient way

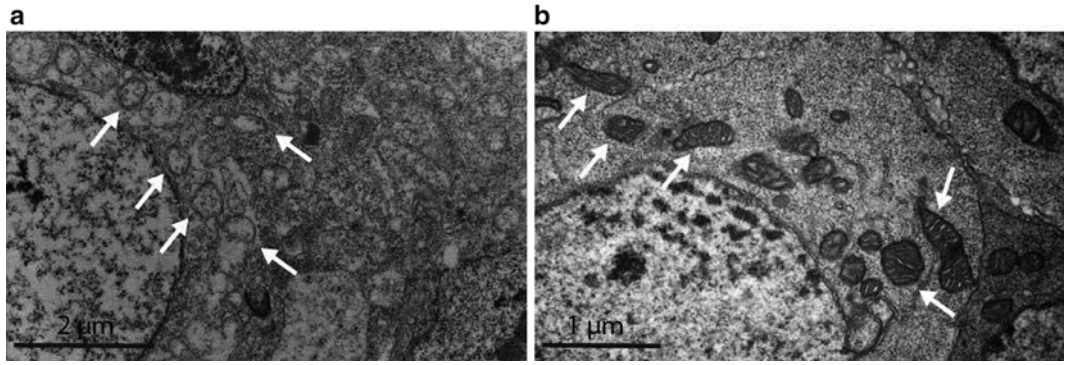

Fig. 3 Transmission electron micrographs of *Drosophila* ovaries prepared using different chemical fixation methods. (**a**) Conventional chemical fixation does not resolve inner mitochondrial membrane structure well. (**b**) A modified chemical fixation protocol greatly improves inner mitochondrial membrane structure. Mitochondria are indicated with *arrows*

to assess the three-dimensional structure of biological specimens at the ultrastructure level [22–24].

For FIB-SEM analysis, specimens are normally prepared using the chemical fixation OTO method [25]. In the last section of this chapter, we describe a modification of the OTO method with en bloc lead staining that improves preservation of *Drosophila* ovaries. With this method we are able to preserve and resolve cell membranes and mitochondrial structure (Fig. 4). This method should allow for detailed assessment of the three-dimensional ultrastructure of *Drosophila* ovaries.

2 Materials

All reagents should be made using ultrapure water (dH_2O, 18.2 MΩ cm at 25 °C). Solutions should be stored at room temperature unless otherwise indicated.

1. 0.2 M Sorenson's Phosphate Buffer (PB) stock solutions [16]:
   - 0.2 M Monobasic Stock Solution: 24 g sodium phosphate monobasic (NaH_2PO_4, MW 120 g/mol) dissolved in 1,000 ml of dH_2O. Filter the solution using filter paper, autoclave, and store at room temperature.
   - 0.2 M Dibasic Stock Solution: 53.65 g sodium phosphate dibasic heptahydrate ($Na_2HPO_4{\cdot}7H_2O$, MW 268.07 g/mol) dissolved in 1,000 ml of dH_2O. Filter the solution using filter paper, autoclave, and store at room temperature.
   - 0.2 M Sorenson's PB: Mix 9.5 ml of 0.2 M Monobasic Stock Solution and 40.5 ml of 0.2 M Dibasic Stock Solution to make 50 ml final volume.

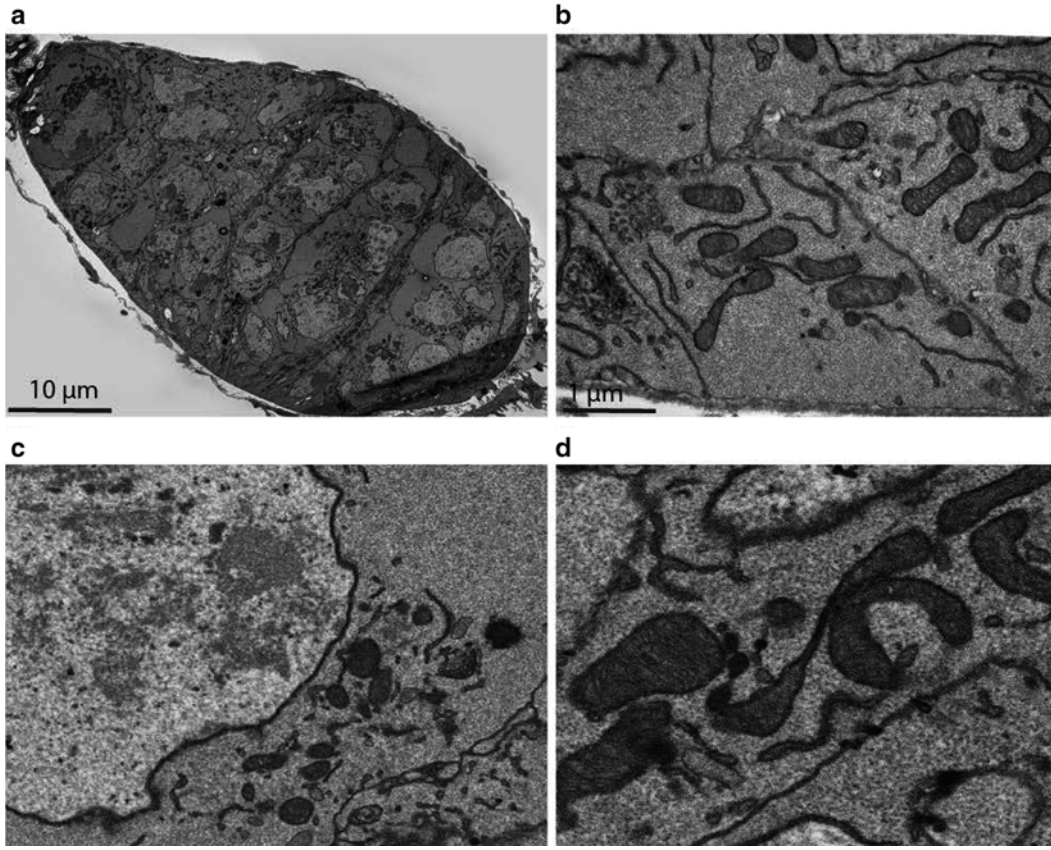

Fig. 4 The OTO method dramatically improves the contrast of *Drosophila* ovary cell membrane structure. (**a** and **b**) TEM images of a *Drosophila* germarium without post-section staining at low (**a**) and high (**b**) magnifications. (**c** and **d**) Comparable SEM micrographs

- 0.1 M Sorenson's PB: Add 25 ml of 0.2 M Sorenson's PB into 25 ml of dH_2O to make 50 ml final volume.

2. Fixative Working Solution: 2.5 % glutaraldehyde and 2 % paraformaldehyde in PB, pH 7.3, 10 ml in total volume (1 ml of EM grade 25 % glutaraldehyde, 1.25 ml of EM grade 16 % paraformaldehyde, 5 ml of 0.2 M Sorenson's PB, 2.75 ml of dH_2O). Adjust the pH to 7.3 if necessary.
3. Araldite 502 (Luft) [26]: Warm both Araldite 502 and DDSA in a 60 °C oven for 5 min; pour 27 ml of Araldite 502 and 23 ml of DDSA into a 50 ml Falcon tube and mix on a rotator for 30 min. Then add 1.5 ml of BDMA slowly and continue mixing for 30 min.
4. 1 % Toluidine Blue Staining Solution: 1 % toluidine blue in 1 % sodium borate (1.0 g of sodium borate into 100 ml dH_2O), protect from light.
   - Weight 1.0 g of toluidine blue on a top-loader balance being careful to avoid dispersing the stain. Add the stain to

100 ml 1 % sodium borate solution. Label and date, and shake daily for a week.

- Filter the staining solution using filter paper before using it.

5. Durcupan ACM hard recipe: Weight 11.4 g of single component A, 10 g of single component B, 0.3 g of single component C, and 0.05–0.1 g of single component D, mix thoroughly using a rotator.
6. Reynold's lead citrate.
7. 0.01 % TCH Solution: Weight 0.1 g of TCH (thiocarbohydrazide) and put it into 15 ml Falcon tube containing 10 ml of dH_2O. Place the tube in a 60 °C oven for 1 h. Agitate by swirling gently every 10 min to facilitate dissolving. Filter through a 0.22 μm Millipore syringe filter before use. The solution will precipitate at 4 °C.
8. Double-sided carbon tape.
9. Colloidal silver paint.
10. Slot grids.
11. SEM sample holder.
12. Gold/palladium.

3 Methods

3.1 Dissection

1. 12–24 h prior to analysis, fatten female *Drosophila melanogaster* in polystyrene vials (28.5 mm diameter) containing standard cornmeal molasses medium with active, granular yeast at 25 °C (*see* **Note 1**).
2. Anesthetize the *Drosophila* using carbon dioxide.
3. Remove the ovaries by grabbing the lower thorax of the fly with forceps and with a second set of forceps grab the lower abdomen and pull until the ovaries have separated from the rest of the fly (Fig. 2b).
4. Remove any addition cuticle or organs from the ovaries.

3.2 Conventional Fixation Method for TEM

3.2.1 Conventional Fixation and Embedding

1. Transfer the ovaries to a 2 ml small-capped glass vial or eppendorf tube containing 1 ml of fixative working solution, and fix 1 h at room temperature and then continue overnight at 4 °C.
2. Wash 3 × 5 min with 1 ml of 0.1 M Sorenson's PB at 4 °C.
3. Postfix for 1 h with 200 μl of 1 % OsO_4 in 0.1 M Sorenson's PB at 4 °C.
4. Wash 3 × 5 min with 1 ml of dH_2O at 4 °C.
5. En bloc stain 1 h with 200 μl of 1 % uranyl acetate in dH_2O at 4 °C.

6. Wash 3×5 min with 1 ml of dH_2O at 4 °C.
7. Dehydrate using 1 ml of each serial ethanol solution, starting by incubating with 30 % ethanol for 5 min at 4 °C.
8. Remove the medium and incubate for 5 min with 50 % ethanol at 4 °C.
9. Remove the medium and incubate for 5 min with 70 % ethanol at 4 °C.
10. Remove the medium and incubate for 5 min with 85 % ethanol at room temperature.
11. Remove the medium and incubate for 5 min with 95 % ethanol at room temperature.
12. Remove the medium and incubate 2×5 min with 100 % ethanol at room temperature.
13. Incubate 2×5 min with 100 % absolute ethanol at room temperature.
14. Incubate 2×10 min with a mixture of 1 part 100 % absolute ethanol to 1 part of Araldite 502 (without BDMA) at room temperature.
15. Incubate for 10 min with a mixture of 1 part 100 % ethanol to 2 parts Araldite 502 (without BDMA) at room temperature.
16. Incubate 3×10 min with pure Araldite 502 (without BDMA) at room temperature.
17. Infiltrate overnight with pure Araldite 502 (without BDMA) at room temperature.
18. Tease apart the ovarioles carefully using two insect pins (*see* **Note 2**).
19. Infiltrate for 1 h with pure Araldite 502 (with BDMA) at room temperature.
20. Transfer each ovary into a pyramid embedding mold (Fig. 5a) or flat embedding with BEEM® capsule (Fig. 5b). The polymerized pyramid block (Fig. 5a arrows) will be mounted onto

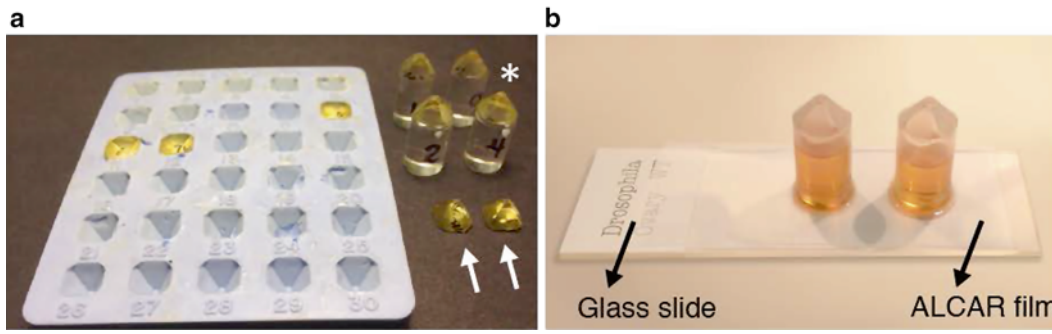

Fig. 5 *Drosophila* ovary embedding method. (**a**) Embedment with pyramid mold. (**b**) Flat embedment

the specimen stub with a specimen label affixed to it using epoxy glue (Fig. 5a star) (*see* **Note 3**). For flat embedding, place one or two ovaries onto glass slides covered with ACLAR embedding film, which makes it much easier to detach the block after polymerization. Place a BEEM® capsule (size 0) that is half filled with Araldite upside-down over the samples (Fig. 5b). Include a small label containing detailed sample information inside the BEEM® capsule for sample identification (*see* **Note 4**).

21. Move the embedded samples to 60 °C oven and polymerize for 48 h.

3.2.2 Sectioning and Staining

1. Trim the ovarioles around the area of interest, cut semi-thin sections (500 nm) on an ultramicrotome, and collect the sections using a beveled wooden applicator stick (*see* **Note 5**).
2. Transfer the samples to a drop of dH_2O on a glass slide.
3. Dry the glass slide on a 60 °C slide warmer and stain with 1 % toluidine blue to identify the area of interest, for example the germarium (Fig. 2c). The terminal filament structure (Fig. 2d) can be used to orient the germarium to facilitate the identification of the germline stem cells if necessary.
4. Collect the serial ultrathin sections (60 nm) on 0.25 % formvar [27] coated 1.0 × 2.0 mm slot copper grids (*see* **Note 6**).
5. Stain with (5 µl each grid) 3 % uranyl acetate in 50 % methanol for 20 min in the dark.
6. Stain with (5 µl each grid) Reynold's lead citrate for 5 min to further increase the contrast of the sample.
7. Acquire micrographs using a transmission electron microscope, in our case a Phillips CM-12 transmission electron microscope with Gatan 4k × 2.7k CCD camera and digital micrograph software.

3.3 FIB-SEM Sample Preparation

3.3.1 FIB-SEM Fixation and Embedding

The sample preparation for FIB-SEM was modified from Ellisman's OTO method [28]. Dissection (Subheading 3.1) and primary fixation (**steps 1** and **2** of Subheading 3.2.1) are the same as in conventional chemical fixation. An increase in sample contrast required for SEM is accomplished by the following steps:

1. Post-fix for 1 h with freshly made 1 % OsO_4 containing 1.5 % potassium ferrocyanide in 0.1 M Sorenson's PB at 4 °C.
2. Rinse 5 × 3 min with 1 ml of dH_2O at 4 °C.
3. Stain for 20 min with 0.01 % TCH Solution at room temperature.
4. Rinse 5 × 3 min with 1 ml of dH_2O at 4 °C.
5. Incubate for 30 min with 1 % OsO_4 in dH_2O at 4 °C.

6. Rinse 5 × 3 min with 1 ml of dH_2O at 4 °C.
7. En bloc stain with 1 % uranyl acetate in dH_2O (freshly diluted from a 3 % uranyl acetate stock) at 4 °C overnight.
8. Wash 5 × 3 min with 1 ml of dH_2O at 4 °C.
9. Dehydrate using ice-cold 30 %, 50 %, 70 %, 85 %, 95 %, 100 %, 100 % ethanol for 5 min each at 4 °C.
10. Incubate for 5 min with ice cold 100 % acetone.
11. Incubate for 5 min with 100 % acetone at room temperature.
12. Incubate for 2 h with Durcupan: 100 % acetone mix 1:3 (25 %) at room temperature.
13. Incubate for 2 h with Durcupan: 100 % acetone mix 1:1 (50 %) at room temperature.
14. Incubate for 2 h with Durcupan: 100 % acetone mix 3:1 (75 %) at room temperature.
15. Incubate with 100 % Durcupan overnight at room temperature.
16. Incubate for 2 h with fresh 100 % Durcupan at room temperature, and embed for 48 h at 60 °C.

3.3.2 FIB-SEM Sectioning

1. Trim and thin section samples on slot grids to identify the area of interest.
2. Mount the sample block on a SEM sample holder using double-sided carbon tape.
3. Use colloidal silver paint to electrically ground the exposed edges of the tissue block.
4. Sputter-coat the entire surface of the specimen with a thin layer of gold/palladium.
5. Image the sample using backscattered electron (BSE) mode in an FEI Helios Nanolab650 dual beam SEM. Record image after each round of ion beam milling using the SEM beam at 2 keV and 50 pA with a working distance of 4 mm.
6. Acquire data using the Auto Slice and View G3 software collecting two areas per sample simultaneously, with XY pixel size of 3.1 nm and Z step size of 10 nm, resulting in typical volumes of 6.3 μm × 6 μm × 0.5 μm.

4 Notes

1. *Drosophila melanogaster* often contains intracellular bacterial endosymbionts such as *Wolbachia*. We have found that it can be difficult to distinguish these from membrane-bound intracellular organelles such as mitochondria. We suggest either using strains that do not contain intracellular bacteria or

removing them prior to analysis with antibiotics such as tetracycline.

2. Ovarioles are easily damaged if ovaries are separated during sample processing. We therefore separate each ovary at the last step in pure resin in order to avoid damage due to physical manipulation prior to the tissue being properly fixed.
3. Embedment using pyramid mold may require the removal of small air bubbles. After transferring the ovary into the embedding mold, make sure the whole egg chambers are in the center and parallel to the bottom of the mold.
4. Separating polymerized Epon, Araldite, or Durcupan from glass can be troublesome. ACLAR film separates very easily from polymerized blocks and is therefore used as the sample surface, on top of which the BEEM® capsule is inverted. The glass slide serves only as a support for the ACLAR film, i.e., slide, ACLAR, sample, BEEM® capsule from bottom to top respectively.
5. To facilitate identification of an area of interest, it is often easiest to find an ovariole with a straight germarium and egg chambers (Fig. 2).
6. The shiny side of a slot grid is usually the flat side. However, this may vary by manufacturer. Grids should be placed with the flat side down on the formvar film to help prevent the formvar membrane from breaking. Also Parafilm should be used to pick up and store the grids. Newspaper or filter paper may break the film because of water absorption.

Acknowledgements

We would like to thank NYULMC OCS for the support to Microscopy Core, Edward Eng and William Rice from New York Structure Biology Center for the help of FIB-SEM imaging. TRH was supported by CIHR; FKT by EMBO and HFSP long-term fellowships; CS by NIH F31/HD080380. RL is an HHMI investigator and supported by NIH R01/R37HD41900.

References

1. Bastock R, St Johnston D (2008) *Drosophila* oogenesis. Curr Biol 18:R1082–R1087
2. He L, Wang X, Montell DJ (2011) Shining light on *Drosophila* oogenesis: live imaging of egg development. Curr Opin Genet Dev 21: 612–619
3. Horne-Badovinac S, Bilder D (2005) Mass transit: epithelial morphogenesis in the *Drosophila* egg chamber. Dev Dyn 232: 559–574
4. Forrest KM, Gavis ER (2003) Live imaging of endogenous RNA reveals a diffusion and entrapment mechanism for nanos mRNA localization in *Drosophila*. Curr Biol 13:1159–1168
5. Bozzola JJ, Lonnie D (1999) Electron microscopy, principles and techniques for biologists, 2nd edn. Jones and Bartlett, Sudbury, MA
6. Zhang S, Chen EH (2008) Ultrastructural analysis of myoblast fusion in *Drosophila*. Methods Mol Biol 475:275–297

7. Cummings MR, Brown NM, King RC (1971) The cytology of the vitellogenic stages of oogenesis in *Drosophila melanogaster*. 3. Formation of the vitelline membrane. Z Zellforsch Mikrosk Anat 118:482–492
8. Cummings MR, King RC (1970) Ultrastructural changes in nurse and follicle cells during late stages of oogenesis in *Drosophila melanogaster*. Z Zellforsch Mikrosk Anat 110:1–8
9. Mahowald AP (1972) Ultrastructural observations on oogenesis in *Drosophila*. J Morphol 137:29–48
10. Geigy R (1931) Action de l'ultra-violet sur le pole germinal dans l'oeuf de *Drosophila melanogaster* (Castration et mutabilite). Rev Suisse Zool 38:187–288
11. Illmensee K, Mahowald AP (1974) Transplantation of posterior polar plasm in *Drosophila*. Induction of germ cells at the anterior pole of the egg. Proc Natl Acad Sci U S A 71:1016–1020
12. Mahowald AP (1968) Polar granules of *Drosophila*. II. Ultrastructural changes during early embryogenesis. J Exp Zool 167: 237–261
13. Mahowald AP (2001) Assembly of the *Drosophila* germ plasm. Int Rev Cytol 203: 187–213
14. Mahowald AP, Strassheim JM (1970) Intercellular migration of centrioles in the germarium of *Drosophila melanogaster*. An electron microscopic study. J Cell Biol 45:306–320
15. Tazuke SI, Schulz C, Gilboa L et al (2002) A germline-specific gap junction protein required for survival of differentiating early germ cells. Development 129:2529–2539
16. Hayat MA (2000) Principles and techniques of electron microscopy biological applications, 4th edn. Cambridge University Press, Cambridge
17. Hopwood D (1969) Fixation of proteins by osmium tetroxide, potassium dichromate and potassium permanganate. Model experiments with bovine serum albumin and bovine gamma-globulin. Histochemie 18:250–260
18. Sabatini DD, Bensch K, Barrnett RJ (1963) Cytochemistry and electron microscopy. The preservation of cellular ultrastructure and enzymatic activity by aldehyde fixation. J Cell Biol 17:19–58
19. King RC (1970) Ovarian Development in *Drosophila melanogaster*. Academic Press, New York
20. Dahl R, Staehelin LA (1989) High-pressure freezing for the preservation of biological structure: theory and practice. J Electron Microsc Tech 13:165–174
21. Studer D, Humbel BM, Chiquet M (2008) Electron microscopy of high pressure frozen samples: bridging the gap between cellular ultrastructure and atomic resolution. Histochem Cell Biol 130:877–889
22. Bushby AJ, P'Ng KM, Young RD et al (2011) Imaging three-dimensional tissue architectures by focused ion beam scanning electron microscopy. Nat Protoc 6:845–858
23. Merchan-Perez A, Rodriguez JR, Alonso-Nanclares L et al (2009) Counting synapses using FIB/SEM microscopy: a true revolution for ultrastructural volume reconstruction. Front Neuroanat 3:18
24. Wei D, Jacobs S, Modla S et al (2012) High-resolution three-dimensional reconstruction of a whole yeast cell using focused-ion beam scanning electron microscopy. Biotechniques 53:41–48
25. Kelley RO, Dekker RA, Bluemink JG (1973) Ligand-mediated osmium binding: its application in coating biological specimens for scanning electron microscopy. J Ultrastruct Res 45:254–258
26. Luft JH (1961) Improvements in epoxy resin embedding methods. J Biophys Biochem Cytol 9:409–414
27. Slot JW, Geuze HJ (2007) Cryosectioning and immunolabeling. Nat Protoc 2:2480–2491
28. Wilke SA, Antonios JK, Bushong EA et al (2013) Deconstructing complexity: serial block-face electron microscopic analysis of the hippocampal mossy fiber synapse. J Neurosci 33:507–522

Chapter 12

Immuno-Electron Microscopy and Electron Microscopic In Situ Hybridization for Visualizing piRNA Biogenesis Bodies in *Drosophila* Ovaries

Shinsuke Shibata, Yukiko Murota, Yoshinori Nishimoto, Mana Yoshimura, Toshihiro Nagai, Hideyuki Okano, and Mikiko C. Siomi

Abstract

Immuno-electron microscopy and electron microscopic in situ hybridization are powerful tools to identify the precise subcellular localization of specific proteins and RNAs at the ultramicroscopic level. Here we describe detailed procedures for how to detect the precise location of a specific target labeled with both fluorescence and gold particles. Although they have been developed for the analysis of *Drosophila* ovarian somatic cells, these techniques are suitable for a wide range of biological applications including human, primate, and rodent analysis.

Key words Yb, Zuc, flam, PIWI-interacting RNAs, piRNAs, Electron microscopy, Immuno-electron microscopy, In situ hybridization, ISH, Electron microscopic in situ hybridization, EM-ISH, Fluorescence immunohistochemistry

1 Introduction

PIWI-interacting RNAs (piRNAs) are small noncoding RNAs enriched in animal gonads, where they repress transposons to maintain genome integrity. Loss of piRNAs causes a failure in germline development, resulting in infertility; thus, piRNAs are indispensable for the succession of animal life [1–3].

The majority of piRNAs have sequences antiparallel to transposon transcripts, and so have the potential to act as antisense oligonucleotides to silence them. However, piRNAs do not exhibit any enzymatic activities by themselves. Rather, piRNAs interact specifically with PIWI proteins to form piRNA-induced silencing complexes (piRISCs) and direct them to target transcripts through RNA–RNA base-pairings. Upon this, repression of transposons occurs at either the transcriptional or posttranscriptional levels, depending on the activity and/or the cellular localization of each

Diana P. Bratu and Gerard P. McNeil (eds.), *Drosophila Oogenesis: Methods and Protocols*, Methods in Molecular Biology, vol. 1328, DOI 10.1007/978-1-4939-2851-4_12,

PIWI protein. A subset of PIWI proteins contain an RNase-H-like endonuclease (Slicer) activity and induces posttranscriptional silencing (target RNA cleavage), whereas other PIWI members lack the nuclease activity, but collaborate with other factors to accomplish transcriptional silencing in the nucleus [4, 5].

Piwi (P-element induced wimpy testes) is one of three PIWI proteins expressed in *Drosophila*, and was originally identified as a factor necessary for germline stem cell renewal. Later, Piwi was shown to be associated with small RNAs called "repeat-associating small-interfering RNAs (rasiRNAs)" [6–8]. This association of PIWI proteins with rasiRNAs is a biological event conserved among many animal species. Thus, the alternative name "piRNAs" was given to rasiRNAs.

piRNAs originate primarily from intergenic piRNA clusters through the primary processing pathway, and are subsequently amplified by the Ping-Pong cycle, a reciprocal target RNA cleavage event that depends on the Slicer activity of PIWI proteins. Interestingly, the Ping-Pong cycle is germ cell-specific, meaning that somatic cells in the gonads lack the machinery, and therefore, they contain exclusively primary piRNAs. Such cell type-specific bias is also observed for PIWI expression, i.e., among all the PIWI members, Piwi is expressed in the somatic cells, whereas the germ cells express all PIWI proteins [3–5, 9].

The current model for primary piRNA biogenesis in *Drosophila* ovarian somatic cells (OSCs) shows that perinuclear Yb bodies are the center for processing primary piRNAs and piRISC formation [10, 11]. According to this model, nascent piRNA-free Piwi is localized at Yb bodies through association with Armitage, a DEAD-box RNA helicase. Piwi is then loaded with piRNA intermediates at Yb bodies, which are further processed by unknown factors. This sequential processing gives rise to mature piRISCs, which are then transported to the nucleus, the final destination of the silencing-capable effector complexes.

The notion that Yb bodies are the center for primary piRNA processing was further supported by the observation that many piRNA factors accumulate in these bodies. Depletion of the factors results in a severe primary piRNA loss, although Yb bodies are still present in the cells. However, loss of Yb protein, which consists of a DEAH-box RNA helicase and a Tudor domain, abolishes Yb bodies from the cells. Thus, Yb is the core factor for Yb body formation [10–15].

A recent study by Murota et al. showed that piRNA intermediates arising from the soma-specific piRNA cluster *flamenco* (*flam*) accumulate to perinuclear bodies adjacent to Yb bodies in OSCs and follicle cells in the ovaries [16]. Because of this, the non-membranous structures rich in *flam*-piRNA intermediates were termed Flam bodies. Interestingly, abolition of Yb's RNA-binding activity by introducing mutations into the DEAD-box helicase

domain disrupts not only Flam bodies but also Yb bodies. In parallel, crosslinking immunoprecipitation (CLIP) experiments showed that Yb protein directly associates with *flam*-piRNA intermediates. Based on these observations, a new model for primary piRNA biogenesis in OSCs was proposed: Yb directs the perinuclear localization of piRNA intermediates and piRNA factors to Flam bodies and Yb bodies, respectively, through direct binding to facilitate piRNA biogenesis and function. This also served to explain the requirement for Yb protein in the piRNA pathway.

In the study, Murota et al. performed RNA fluorescence in situ hybridization (RNA-FISH) to examine the cellular localization of *flam*-piRNA intermediates, and found that these RNAs accumulate to Flam bodies [16]. However, to obtain further and stronger support, Murota et al. also took an electron microscopy (EM) approach, through which they successfully showed that Flam bodies are *bona fide* cytoplasmic structures [16]. EM is a widely used method to analyze biological ultrastructure, including molecules, cells, and tissues from a variety of species. In EM, accelerated electrons can visualize subcellular structures with higher resolution than can be obtained by fluorescence microscopy because they have a wavelength shorter than that of visible light. Conventionally, the expression level and the specific location of proteins and RNAs in vivo are evaluated by fluorescence immunohistochemistry (IHC) and fluorescence in situ hybridization (FISH), respectively. Higher-resolution localization of proteins/RNAs can be obtained with immuno-EM (iEM) and EM-ISH [17, 18]. In addition to the high resolution, these approaches can be used to observe the adjacent subcellular organelles or microstructures such as mitochondria, endoplasmic reticulum, ribosomes, myelin lamellae, synapses, cilia, and a variety of molecules and fibers co-localized with the specific proteins or RNAs [16, 19–27].

Here, we describe the methods for how to carry out iEM and EM-ISH, both for cells and for tissues (Fig. 1). Briefly, for general EM analysis, cultured cells and tissues are fixed, dehydrated, embedded into plastic, ultrathin sectioned, and observed with EM (left column in Figs. 1 and 2). Cells and tissues are fixed moderately and the target protein is labeled with gold using a specific antibody to identify specific protein localization by iEM. Then, the samples undergo the next steps including additional EM fixation, a silver enhancement step (second column in Fig. 1) and transfer to the EM procedures (Fig. 3) [19–21, 23–27]. Cells and tissues are fixed and labeled with a tagged probe and a tag-recognizing antibody followed by the same procedures as for iEM (third column in Fig. 1) to visualize specific RNA location by EM-ISH (Fig. 4) [16, 22]. There are two common iEM procedures, designated pre-embedding and post-embedding iEM, which depend on the order of the antibody-staining and the resin-embedding steps (white-colored letters in Fig. 1). In this chapter, we focus on describing pre-embedding iEM.

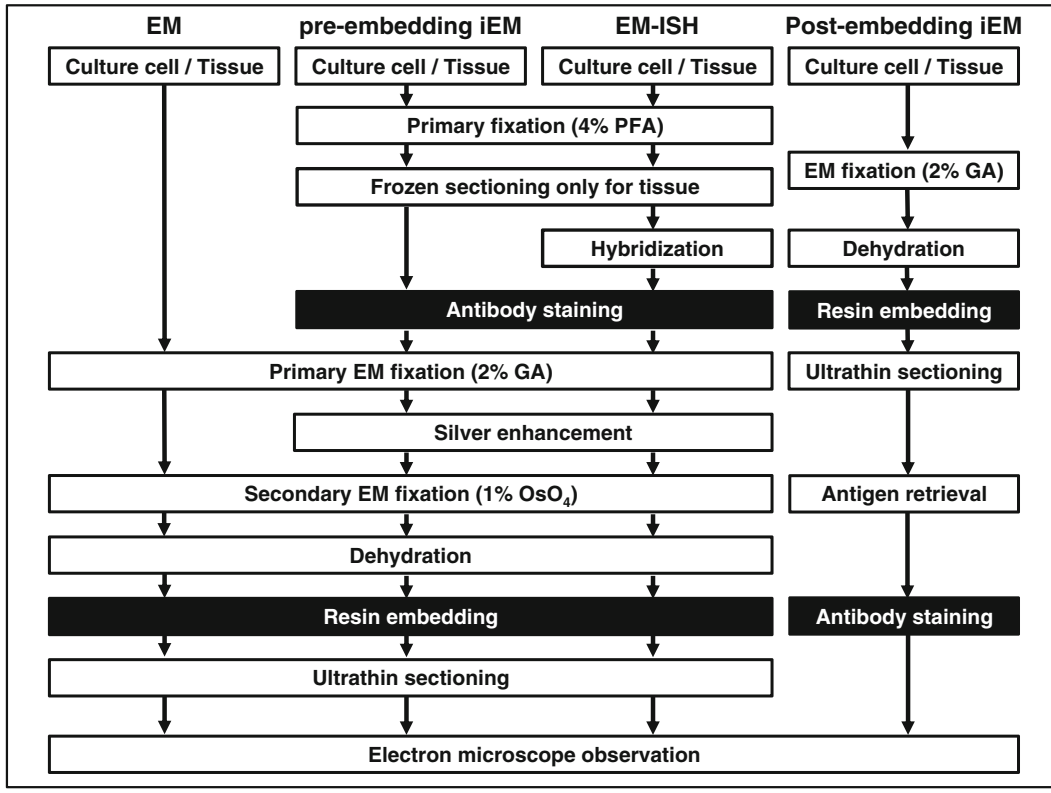

Fig. 1 Simplified flowchart of electron microscope analyses to identify protein and RNA localization. Sample preparation steps for general EM, pre-embedding iEM, EM-ISH, and post-embedding iEM. The detailed procedures for pre-embedding iEM and EM-ISH are described in the main text. Note that the EM-ISH procedure for tissue samples indicated in this flowchart is specific to mouse samples; however, the description in the text (Subheading 3.4) is specifically for fresh frozen samples including human biopsy or autopsy samples. Human tissue is not fixed initially, meaning that fresh frozen samples immediately after removal from the body should be stocked at −80 °C freezer, used for sectioning, then the EM-ISH procedure starts with fixation in 4 % PFA as indicated in the main text

In our special protocol, it is possible to detect protein/RNA localization with different levels of resolution, both by fluorescence microscopy and by EM [16, 22]. This is what is called correlative microscopic analysis, and it helps to supply additional information to that generated by fluorescence IHC (Figs. 3 and 4). The methods we have developed will enable increased understanding of physiological phenomena and can be applied to many aspects of in vivo biological analysis.

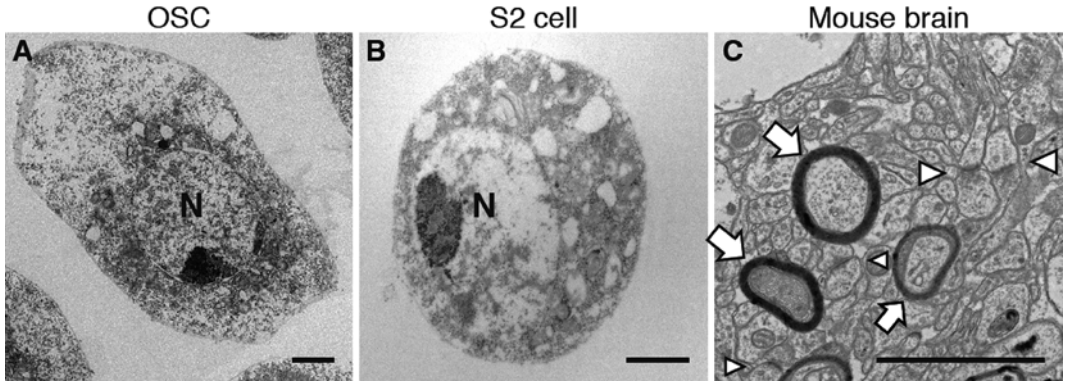

Fig. 2 Representative results from EM observation. Typical EM images of cultured cells from (**a**) *Drosophila* OSCs and (**b**) S2 cell lines. (**c**) Typical EM image from mouse brain cortical tissue. *N* nucleus, *arrows* myelinated neural fibers, *arrowheads* synapses. Scale bars are 2 μm

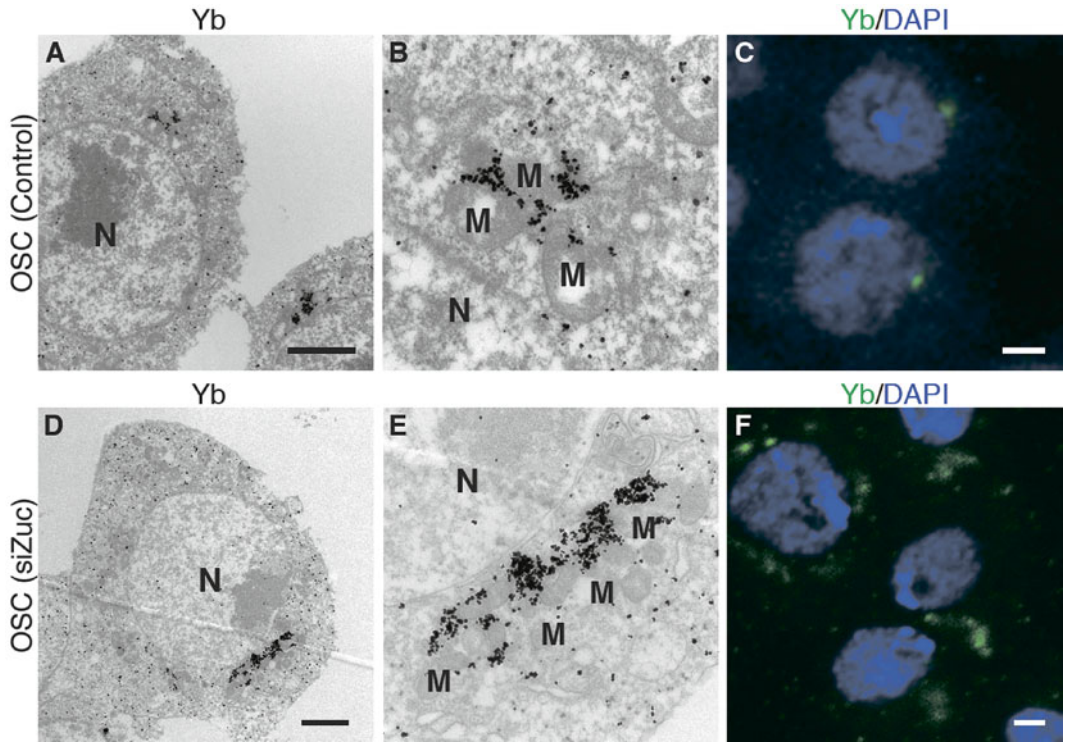

Fig. 3 Images from iEM and IHC experiments with anti-Yb antibodies. (**a**) The subcellular localization of the Yb protein is clearly shown by gold particles (*black dots*) in control OSCs. (**b**) Higher magnification of (**a**) demonstrates that the gold aggregation (Yb protein localization) is specifically detected adjacent to the mitochondria. (**c**) Fluorescence IHC enables visualization of a limited number of Yb aggregates in the OSC cytoplasm. (**d–f**) Yb aggregation was dramatically altered in *Zucchini* (*Zuc*)-knockdown OSCs (designated as siZuc), as evaluated with (**d**) low- and (**e**) high-magnification iEM; the corresponding fluorescence IHC image is indicated in (**f**). Detailed interpretation and procedures have been described previously [10, 11, 13, 28]. *N* nucleus, *M* mitochondria, *DAPI* nuclear stain. Scale bars are 2 μm

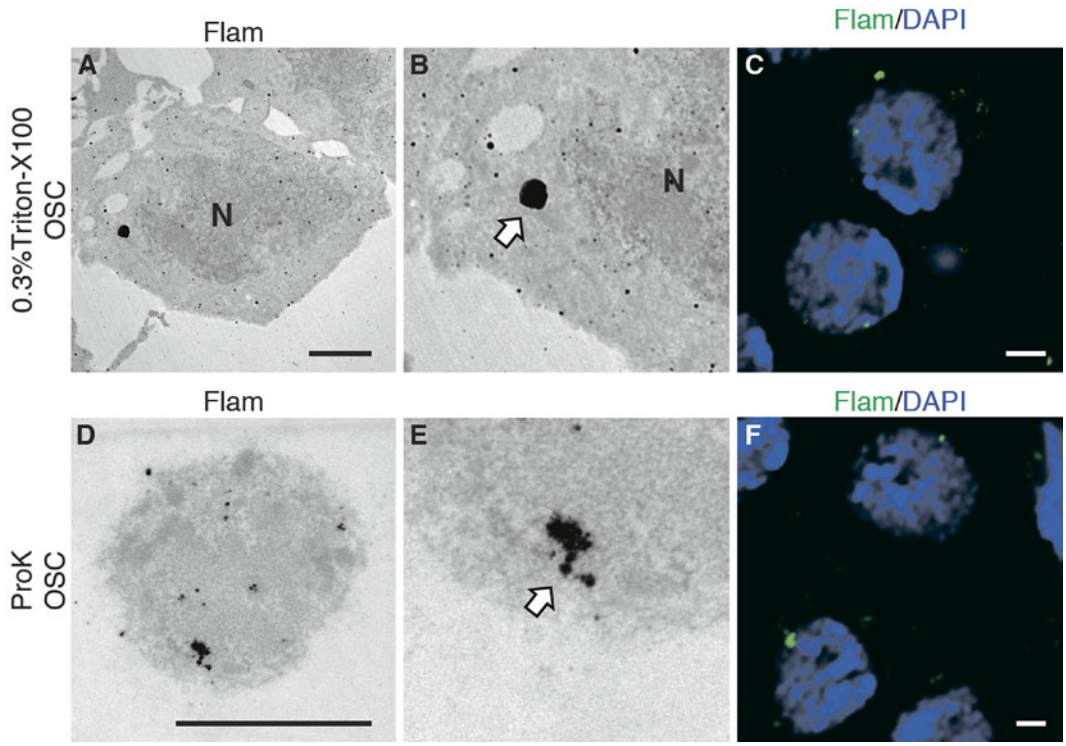

Fig. 4 EM-ISH and FISH images with a probe against *Flam*. (**a**) Subcellular aggregation of *Flam* noncoding RNAs is indicated by gold particles (*black dots*) in 0.3 % Triton X-100-treated control OSCs. (**b**) Higher magnification of (**a**) reveals a cytoplasmic localization. (**c**) Fluorescence IHC also shows cytoplasmic aggregation in OSCs. The EM-ISH images from Proteinase K (ProK)-treated OSCs were not clear due to membrane degradation (**d**, **e**), whereas the fluorescence IHC results (**f**) were quite similar to those from the Triton-treated sample (**c**). *N* nucleus, *DAPI* nuclear stain. Scale bars are 2 μm

2 Materials

2.1 iEM Analysis of Cultured Cells

1. *Drosophila* ovarian somatic cells (OSCs) [28] (*see* **Note 1**).
2. Chamber slide (four-well, glass- or plastic-bottomed) (*see* **Note 2**).
3. Paraformaldehyde (PFA), 16 %, EM grade.
4. 10× Phosphate-buffered Saline (PBS): 1.37 M NaCl, 27 mM KCl, 100 mM Na_2HPO_4, 20 mM KH_2PO_4, pH 7.4.
5. Saponin: a weak plant-derived detergent.
6. 0.1 M Phosphate Buffer (PB).
7. Block Ace.
8. Mouse anti-Yb monoclonal antibody [16].
9. Nanogold- and Alexa Fluor 488-conjugated anti-mouse antibody.
10. Glutaraldehyde: 25 % (EM grade).

Table 1
Composition of 100 % Epon plastic solution

Epon (g)	MNA (g)	EPOK-812 (g)	DDSA (g)	DMP-30 (ml)
200	54.0	102.6	43.8	2.2
180	48.6	92.3	39.4	2.0
160	43.2	82.1	35.0	1.8
140	37.8	71.8	30.7	1.5
120	32.4	61.6	26.3	1.3
110	29.7	56.4	24.1	1.2
100	27.0	51.3	21.9	1.1
90	24.3	46.2	19.7	1.0
80	21.6	41.0	17.5	0.9
70	18.9	35.9	15.3	0.8
60	16.2	30.8	13.1	0.7
50	13.5	25.7	11.0	0.6
40	10.8	20.5	8.8	0.4
30	8.1	15.4	6.6	0.3
20	5.4	10.3	4.4	0.2

See the text for details

11. HQ-Silver Enhancement kit.
12. 4 % osmium tetroxide (OsO_4).
13. Ethanol: 50, 70, 80, 90, and 100 % (*see* **Note 3**).
14. Acetone: 100 %.
15. QY-1: 99 % butyl glycidyl ether.
16. Epon Plastic Solution: Weigh MNA, EPOK-812, DDSA, and DMP-30 in a cup in the recommended proportions (Table 1) and mixed in a planetary centrifugal mixer for 3.5 min at 2,000 rpm (about 400×*g*) followed by deaeration for 1.5 min at 2,200 rpm (about 400×*g*) (*see* **Note 4**).
17. Planetary centrifugal mixer.
18. Glass slide mold (*see* **Note 5**).
19. Single-edged razor blade (*see* **Note 6**).
20. Cut-resistant gloves (*see* **Note 6**).
21. Diamond knife (2–3 mm width).
22. Copper grid (Veco Specimen Grids #100, 150, 200 mesh).
23. Grid stick.

24. Uranyl acetate: 2 %.
25. Lead citrate (Reynold's Solution).
26. Transmission electron microscope (TEM) or scanning electron microscope (SEM) (*see* **Note 7**).

2.2 iEM Analysis for Tissue

1. Sucrose (powder).
2. Frozen section compound.
3. Cryomold.
4. Liquid nitrogen (N_2).
5. Cryostat.
6. Matsunami adhesive silane (MAS)-coated glass slides (Matsunami glass, Japan) (*see* **Note 8**).

2.3 EM-ISH Analysis for Cells

1. PFA: powder.
2. 1× PBS, 0.1 M, pH 7.4.
3. 50× Denhardt's Solution.
4. Acetylation Buffer: 1.5 % triethanolamine, 0.25 % acetic anhydride, 0.25 % HCl.
5. 20× Saline Sodium Citrate Buffer (SSC): 3 M NaCl, 0.3 M $C_6H_5Na_3O_7{\cdot}2H_2O$ (trisodium citrate dihydrate), pH 7.0.
6. Prehybridization Solution: 50 % formamide, 2× SSC, 1× Denhardt's Solution, 10 mM EDTA, 100 μg/ml yeast tRNA, and 0.01 % Tween 20.
7. Hybridization Buffer: 50 % formamide, 2× SSC, 1× Denhardt's solution, 5 % dextran sulfate, 10 mM EDTA, 100 μg/ml yeast tRNA, and 0.01 % Tween 20.
8. Wash Buffer 1: 50 % formamide, 2× SSC, 0.01 % Tween 20.
9. NTET: 500 mM NaCl, 10 mM Tris–HCl, pH 8.0, 1 mM EDTA, 0.01 % Tween 20.
10. Wash Buffer 2: 2× SSC, 0.01 % Tween 20.
11. Wash Buffer 3: 0.2× SSC, 0.01 % Tween 20.
12. TBS-T: Tris-buffered saline (TBS) with 0.01 % Tween 20, pH 7.6.
13. 10× Blocking Reagent: 0.1 M maleate, 0.15 M NaCl.
14. Blocking Buffer: 1× Blocking Reagent in TBS-T.
15. 10× Fluorescein RNA Labeling Mix.
16. Rabbit anti-FITC (fluorescein isothiocyanate) antibody.
17. Nanogold- and fluorescence-conjugated anti-rabbit antibody.

2.4 EM-ISH Analysis for Tissue

1. MAS- or poly-l-lysine (PLL)-coated glass slides (*see* **Note 8**).
2. 0.2 N HCl.
3. Proteinase K (PCR grade).

4. Acetylation Solution: 1.5 % triethanolamine, 0.25 % acetic anhydride, 0.25 % HCl.
5. Prehybridization Solution: 50 % formamide, 2× SSC, 1× Denhardt's Solution, 10 mM EDTA, 100 μg/ml yeast tRNA, and 0.01 % Tween 20.
6. Hybridization Buffer: 50 % formamide, 2× SSC, 1× Denhardt's Solution, 5 % dextran sulfate, 10 mM EDTA, and 0.01 % Tween 20.
7. Wash Buffer 1: 50 % formamide, 2× SSC, and 0.01 % Tween 20.
8. RNase Solution: 10 μg/ml RNase A added to NTET.
9. Wash Buffer 2: 2× SSC with 0.01 % Tween 20.
10. Wash Buffer 3: 0.2× SSC with 0.01 % Tween 20.
11. TBS, pH 7.6.
12. Blocking Buffer: Blocking Reagent, 0.1 M maleate, 0.15 M NaCl, and 0.01 % Tween 20 in TBS.
13. DIG (digoxigenin)- or FITC-labeled probes.
14. Primary antibodies against DIG, FITC, and other specific targets.
15. Nanogold- and fluorescence-conjugated anti-rabbit antibody.

3 Methods

3.1 iEM Analysis for Culture Cells

The representative images with this iEM procedure are shown in Fig. 3. All steps are performed at room temperature unless otherwise indicated.

1. Culture the cells (*Drosophila* OSCs) in a slide chamber at an appropriate temperature (26–37 °C, usually 26 °C) [28].
2. Fix the cells with 4 % PFA in 0.1 M PBS, pH 7.4 for 20 min (*see* **Note 9**).
3. Wash 3 × 10 min with 0.1 M PB.
4. Incubate the cells for 1 h in 5 % Block Ace with 0.01 % saponin in 0.1 M PB.
5. Apply the primary antibody (mouse anti-Yb, 1:250 dilution) for 24 h at 4 °C.
6. Wash 12 × 10 min with 0.1 M PB.
7. Apply the nanogold- and Alexa Fluor 488-conjugated anti-mouse secondary antibody (1:100 dilution) for 24 h at 4 °C.
8. Wash 12 × 10 min with 0.1 M PB.
9. Images can be captured on a fluorescence microscope during the PB washes of **step 8** if desired (*see* **Note 10**).
10. Fix with 2.5 % glutaraldehyde.

11. Wash for 5 min with 0.1 M PB.
12. Wash 4 × 15 min with 50 mM HEPES Buffer, pH 5.8.
13. Wash 2 × 5 min with dH_2O.
14. Apply the silver enhancement solution from the HQ-Silver kit for 10 min in the dark room.
15. Wash 5 × 1 min with dH_2O in the dark room.
16. Wash for 5 min with 0.1 M PB.
17. Fix for 90 min with 1 % OsO_4 at 4 °C.
18. Dehydrate 2 × 5 min with 50 % ethanol at 4 °C.
19. Dehydrate 2 × 5 min with 70 % ethanol at 4 °C.
20. Dehydrate 2 × 5 min with 80 % ethanol at 4 °C.
21. Dehydrate 2 × 5 min with 90 % ethanol.
22. Dehydrate 2 × 5 min with 100 % ethanol.
23. Remove the line on the slide chamber glass, if necessary (*see* **Note 6**).
24. Apply the 100 % acetone for 5 min.
25. Apply the 100 % QY-1 2 × 5 min.
26. Apply the QY-1–Epon in a 1:1 ratio for 1 h.
27. Place the cells in 100 % Epon overnight.
28. Embed the glass slide in the silicon mold.
29. Incubate in 100 % Epon for 3 days (72 h) at 60 °C.
30. Store in a desiccator until dissection.
31. Remove the cells in Epon from the glass slides on top of a heat block at 120 °C.
32. Dissect the cells with an appropriate size (2 mm × 3 mm square).
33. Place the cells on a sectioning stage in a droplet of 100 % Epon.
34. Incubate overnight at 60 °C.
35. Store in a desiccator until sectioning.
36. Trim the block to an appropriate size (1 mm × 1.5 mm square).
37. Prepare the ultrathin sections (70 nm thick) with a diamond knife.
38. Collect the sections on a copper grid.
39. Dry the sections on the grid overnight.
40. Attach the copper grid to the grid stick for staining.
41. Incubate the sections in uranyl acetate for 10 min.
42. Wash the stick with the grids 3 × 1 min with dH_2O.
43. Incubate the sections in lead citrate for 10 min.

44. Wash the stick with the grids 3 × 1 min with dH_2O.
45. Remove the grid from the staining stick.
46. Dry the sections on the grid for 1 h.
47. Observe the cells by EM.

3.2 iEM Analysis for Tissue

1. Dissect out the target tissue.
2. Fix the tissue for about 10 h in 4 % PFA at 4 °C.
3. Incubate the tissue in 15 % sucrose in 0.1 M PB overnight at 4 °C.
4. Incubate the tissue in 30 % sucrose in 0.1 M PB overnight at 4 °C.
5. Immerse the tissue in cryocompound.
6. Freeze the tissue in an appropriate size cryomold with liquid N_2.
7. Prepare frozen 16–20 μm-thick sections of sample with a cryostat.
8. Dry the sections on glass slides for 1 h at 37 °C.
9. Wash the sections 3 × 10 min with 0.1 M PBS.
10. Incubate the sections in 5 % Block Ace with 0.01 % saponin in 0.1 M PB for 1 h.
11. Apply the primary antibody for 72 h at 4 °C.
12. Wash 10 × 10 min with 0.1 M PB.
13. Apply the nanogold-conjugated anti-mouse secondary antibody (1:100) for 24 h at 4 °C.
14. Continue the procedure with **step 8** in Subheading 3.1.

3.3 EM-ISH Analysis for Cells

The representative images with this EM-ISH procedure are shown in Fig. 4.

1. Culture the cells (*Drosophila* OSCs) in a PLL-coated four-well slide chamber at an appropriate temperature (26 °C) (*see* **Note 2**).
2. Fix the cells with 4 % PFA in 0.1 M RNase-free PBS, pH 7.4, overnight at 4 °C.
3. Wash for 5 min with RNase-free 0.1 M PBS.
4. Wash for 5 min with RNase-free dH_2O.
5. Apply 0.2 N HCl for 20 min.
6. Wash for 5 min with RNase-free dH_2O.
7. Incubate in pre-warmed 100 mM Tris–HCl, pH 8.0, 10 mM EDTA at 37 °C.
8. Incubate the section in 1.5 μg/ml Proteinase K at 37 °C for 1 min (*see* **Note 11**).
9. Place slides in 0.2 % glycine/PBS for 10 min.

10. Wash for 5 min with RNase-free 0.1 M PBS.
11. Fix the cells for 20 min with 4 % PFA in 0.1 M RNase-free PBS, pH 7.4.
12. Wash 2 × 5 min with RNase-free 0.1 M PBS.
13. Wash for 5 min with RNase-free dH_2O.
14. Incubate for 15 min with Acetylation Buffer.
15. Wash for 5 min with RNase-free dH_2O.
16. Dip for 5 min in 100 % ethanol.
17. Air-dry.
18. Incubate the cells in prehybridization solution at 55 °C for 1 h.
19. Incubate the cells with FITC-conjugated specific RNA probe (1 μg/ml) for 16 h at 55 °C in hybridization buffer (*see* **Note 12**).
20. Wash 2 × 30 min with Wash Buffer 1 at 55 °C.
21. Wash for 5 min with NTET at 37 °C.
22. Treat for 30 min with RNase A (100 μg/ml) in NTET at 37 °C.
23. Wash for 5 min with NTET at 37 °C.
24. Wash for 30 min with Wash Buffer 2 at 55 °C.
25. Wash for 30 min with Wash Buffer 3 at 55 °C.
26. Wash for 5 min with TBS-T.
27. Apply Blocking Buffer for 1 h.
28. Apply primary antibody (rabbit anti-FITC, 1:500 dilution) for 24 h at 4 °C.
29. Wash 12 × 10 min in 0.005 % saponin containing 0.1 M PB.
30. Apply the nanogold- and Alexa Fluor 488-conjugated anti-rabbit secondary antibody (1:100 dilution) for 24 h at 4 °C.
31. Continue the procedure with **step 8** in Subheading 3.1.

3.4 EM-ISH Analysis for Tissue

1. Prepare a fresh frozen tissue block.
2. Cut frozen sections (12–16 μm thick) with a cryostat and collect them on PLL- or MAS-coated glass slides.
3. Dry the sections for >2 h.
4. If the samples have been preserved in a −80 °C freezer, return them to room temperature without opening the slide case.
5. Edge each slide with silicon and dry it briefly.
6. Fix the tissues with 4 % PFA in RNase-free PBS for 30 min or at 4 °C overnight (use the latter for stronger fixation).
7. Wash the tissues for 5 min with RNase-free PBS.
8. Wash the tissues for 5 min with RNase-free dH_2O.

9. Apply 0.2 N HCl for 20 min, then briefly rinse with RNase-free dH_2O.
10. Incubate the section for 5 min in 3 μg/ml Proteinase K at 37 °C (*see* **Note 11**).
11. Transfer the slides slowly to a 0.2 % glycine/PBS solution and leave them for 10 min.
12. Wash for 5 min with RNase-free PBS, so as to not carry over any glycine to the next fixation step.
13. Post-fix for 20 min with 4 % PFA in RNase-free PBS.
14. Wash 2 × 5 min with RNase-free PBS.
15. Immerse briefly in RNase-free dH_2O, then incubate in Acetylation Solution.
16. Wash for 5 min with RNase-free dH_2O.
17. Dehydrate for 5 min with 100 % ethanol.
18. Dry the slides in a clean hood for 30 min.
19. Incubate the samples in prehybridization solution in a moisture chamber with swinging at 5 rpm at 55 °C for >30 min.
20. Hybridize with DIG- or FITC-labeled probes (final 2.5–10 μg/ml) in Hybridization Buffer in the moisture chamber with swinging at about 5 rpm at 55 °C for 16 h. To prevent the samples from drying up, cover the slides with a piece of Parafilm of the appropriate size.
21. Wash 2 × 30 min with Wash Buffer 1 at 55 °C.
22. Incubate for 15 min in NTET without RNase A at 37 °C.
23. Treat for 1 h with RNase A (10 μg/ml) in NTET at 37 °C.
24. Incubate the samples in NTET solution and leave them at 37 °C for 10 min. You can reuse the NTET solution from **step 22**.
25. Wash for 30 min with Wash Buffer 2 at 55 °C.
26. Wash for 30 min with Wash Buffer 3 at 55 °C.
27. Wash for 5 min in TBS-T.
28. Incubate for 30 min with Blocking Buffer.
29. Incubate the sections at 4 °C for 72 h with mouse anti-DIG (1:250 dilution) and rabbit anti-PSP1 (1:250 dilution) primary antibodies.
30. Wash 12 × 10 min in 0.005 % saponin containing 0.1 M PB at room temperature.
31. Incubate for 24 h at 4 °C with fluorescence- and nanogold-conjugated anti-mouse secondary antibodies (1:100) along with fluorescence-conjugated anti-rabbit secondary antibodies (1:800).
32. Continue the procedure with **step 8** in Subheading 3.1.

4 Notes

1. For this iEM approach, any cultured cells are suitable: for instance, primary cultured cells or cell lines from human, marmoset, or rodent. This procedure is focused on adhesive cells cultured in chamber slides; however, the method is also suitable for free-floating cells or explant tissue cultures.
2. Regarding the chamber slides, a chamber with four wells is the most suitable for embedding, rather than a chamber with one, two, or eight wells.
3. 50–80 % ethanol solutions are stored at 4 °C, whereas 90–100 % ethanol is stored at room temperature.
4. Preparation of the plastic solution usually follows the manufacturer's instructions.
5. The glass slide mold (microstar SNP-2) made of silicone should keep the glass slide or the chamber glass slide on the bottom of the mold until the resin has completely polymerized, to obtain an adequate thickness of plastic on the section.
6. A line-removal step using a single-edged razor blade is required for smooth removal of the resin-embedded cells from the slide chamber bottom, especially for chamber slides made of glass. This step is not necessary if using plastic-bottomed chamber slides. Lines from the PAP Pen or the Liquid Blocker for tissue sections should also be removed using a single-edged razor blade. Wear cut-resistant gloves for safety.
7. Both TEM and SEM are suitable for iEM and EM-ISH. For simplicity, this manuscript focuses on TEM. However, most of the materials and methods can be applied to various new serial-EM approaches, including the automated tape-collecting ultramicrotome-scanning electron microscope (ATUM-SEM), serial block face-scanning electron microscope (SBF-SEM), and the focused ion beam-scanning electron microscope (FIB-SEM).
8. Coating of the glass slides is critical for both iEM and EM-ISH to keep/remove the cells or tissue sections on the slides. Proteinase K or antigen-retrieval treatment will remove sections easily from a glass surface; however, the resin block preparation step requires a smooth peel-off (**steps 31–33** in Subheading 3.1). A PLL- or poly-l-ornithine-coated slide chamber is appropriate for cultured cells, and MAS- or PLL-coated glass slides are suitable for tissue samples.
9. For general EM analysis (without immunostaining), fix the cells and tissues with 2 % glutaraldehyde, wash 3 × 10 min with buffer and restart from the secondary EM fixation with OsO_4 (**step 17** in Subheading 3.1).

10. To capture the images with a fluorescence microscope, cover the cells/sections briefly with PB and carefully place a coverslip on top. An inverted microscope is not suitable because the coverslip will easily fall off.
11. The duration of the Proteinase K treatment step should be modified depending on the cell/tissue conditions (e.g., the cell type, fixation, and thickness of the sample). If the Proteinase K treatment is too strong to retain the normal membrane structure, reduce the concentration of Proteinase K solution, or substitute it with Triton™ X-100. As shown in Fig. 4, using Triton™ X-100 rather than Proteinase K better preserves the condition of the subcellular structures.
12. FITC-labeled RNA probes were prepared using RNA-labeling mixture and SP6 RNA polymerase according to the manufacturer's instructions. To prepare a probe specific for the flam locus, OSC genomic DNA was used as a template for PCR.

Acknowledgments

We are grateful to Dr. S. Nakagawa for providing insightful discussions and dedicated support to our project. We thank T. Yano at Electron microscope laboratory and G. Itai at Keio-med Open Access Facility for their special technical support and also thank all members of the Siomi and Okano laboratories for their invaluable comments. This work was supported by a Grant-in-Aid for Scientific Research from MEXT, Japan; a grant from Keio Gijuku Academic Development Funds to S.S.; and a grant from Brain Mapping by Integrated Neurotechnologies for Disease Studies (Brain/MINDS) to S.S. and H.O. The authors have no conflicts of interest to declare.

References

1. Siomi MC, Sato K, Pezic D et al (2011) PIWI-interacting small RNAs: the vanguard of genome defence. Nat Rev Mol Cell Biol 12:246–258
2. Juliano C, Wang J, Lin H (2011) Uniting germline and stem cells: the function of Piwi proteins and the piRNA pathway in diverse organisms. Annu Rev Genet 45:447–469
3. Ishizu H, Siomi H, Siomi MC (2012) Biology of PIWI-interacting RNAs: new insights into biogenesis and function inside and outside of germlines. Genes Dev 26:2361–2373
4. Malone CD, Brennecke J, Dus M et al (2009) Specialized piRNA pathways act in germline and somatic tissues of the *Drosophila* ovary. Cell 137:522–535
5. Brennecke J, Aravin AA, Stark A et al (2007) Discrete small RNA-generating loci as master regulators of transposon activity in *Drosophila*. Cell 128:1089–1103
6. Vagin VV, Sigova A, Li C et al (2006) A distinct small RNA pathway silences selfish genetic elements in the germline. Science 313: 320–324
7. Saito K, Nishida KM, Mori T et al (2006) Specific association of Piwi with rasiRNAs derived from retrotransposon and heterochromatic regions in the *Drosophila* genome. Genes Dev 20:2214–2222
8. Aravin A, Gaidatzis D, Pfeffer S et al (2006) A novel class of small RNAs bind to MILI protein in mouse testes. Nature 442:203–207

9. Gunawardane LS, Saito K, Nishida KM et al (2007) A slicer-mediated mechanism for repeat-associated siRNA 5′ end formation in *Drosophila*. Science 315:1587–1590
10. Saito K, Ishizu H, Komai M et al (2010) Roles for the Yb body components Armitage and Yb in primary piRNA biogenesis in *Drosophila*. Genes Dev 24:2493–2498
11. Olivieri D, Sykora MM, Sachidanandam R et al (2010) An in vivo RNAi assay identifies major genetic and cellular requirements for primary piRNA biogenesis in *Drosophila*. EMBO J 29:3301–3317
12. Handler D, Olivieri D, Novatchkova M et al (2011) A systematic analysis of *Drosophila* TUDOR domain-containing proteins identifies Vreteno and the Tdrd12 family as essential primary piRNA pathway factors. EMBO J 30: 3977–3993
13. Olivieri D, Senti KA, Subramanian S et al (2012) The cochaperone shutdown defines a group of biogenesis factors essential for all piRNA populations in *Drosophila*. Mol Cell 47:954–969
14. Qi H, Watanabe T, Ku HY et al (2011) The Yb body, a major site for Piwi-associated RNA biogenesis and a gateway for Piwi expression and transport to the nucleus in somatic cells. J Biol Chem 286:3789–3797
15. Szakmary A, Reedy M, Qi H et al (2009) The Yb protein defines a novel organelle and regulates male germline stem cell self-renewal in *Drosophila melanogaster*. J Cell Biol 185: 613–627
16. Murota Y, Ishizu H, Nakagawa S et al (2014) Yb integrates piRNA intermediates and processing factors into perinuclear bodies to enhance piRISC assembly. Cell Rep 8:103–113
17. Matsuno A, Nagashima T, Ohsugi Y et al (2000) Electron microscopic observation of intracellular expression of mRNA and its protein product: technical review on ultrastructural in situ hybridization and its combination with immunohistochemistry. Histol Histopathol 15:261–268
18. Herrera GA (1992) Ultrastructural immunolabeling: a general overview of techniques and applications. Ultrastruct Pathol 16:37–45
19. Zhang L, Kaneko S, Kikuchi K et al (2014) Rewiring of regenerated axons by combining treadmill training with semaphorin3A inhibition. Mol Brain 7:14
20. Takano M, Kawabata S, Komaki Y et al (2014) Inflammatory cascades mediate synapse elimination in spinal cord compression. J Neuroinflammation 11:40
21. Numasawa-Kuroiwa Y, Okada Y, Shibata S et al (2014) Involvement of ER stress in dysmyelination of Pelizaeus-Merzbacher disease with PLP1 missense mutations shown by iPSC-derived oligodendrocytes. Stem Cell Rep 2:648–661
22. Nishimoto Y, Nakagawa S, Hirose T et al (2013) The long non-coding RNA nuclear-enriched abundant transcript 1_2 induces paraspeckle formation in the motor neuron during the early phase of amyotrophic lateral sclerosis. Mol Brain 6:31
23. Takano M, Hikishima K, Fujiyoshi K et al (2012) MRI characterization of paranodal junction failure and related spinal cord changes in mice. PLoS One 7, e52904
24. Yasuda A, Tsuji O, Shibata S et al (2011) Significance of remyelination by neural stem/progenitor cells transplanted into the injured spinal cord. Stem Cells 29:1983–1994
25. Nagoshi N, Shibata S, Hamanoue M et al (2011) Schwann cell plasticity after spinal cord injury shown by neural crest lineage tracing. Glia 59:771–784
26. Tada H, Okano HJ, Takagi H et al (2010) Fbxo45, a novel ubiquitin ligase, regulates synaptic activity. J Biol Chem 285:3840–3849
27. Kumagai G, Okada Y, Yamane J et al (2009) Roles of ES cell-derived gliogenic neural stem/progenitor cells in functional recovery after spinal cord injury. PLoS One 4, e7706
28. Saito K (2014) RNAi and overexpression of genes in ovarian somatic cells. Methods Mol Biol 1093:25–33

Chapter 13

Visualizing Cytoophidia Expression in *Drosophila* Follicle Cells via Immunohistochemistry

Ömür Y. Tastan and Ji-Long Liu

Abstract

We describe a user-friendly immunohistochemical approach for the detection of protein localization in *Drosophila* ovaries, here focusing on CTP synthase. This approach mainly uses fluorescently labeled antibodies to detect single, double, or multiple antigens. We provide a step-by-step protocol with detailed notes and tips, a simplified method that can also be adapted to detect protein localization beyond *Drosophila* ovaries.

Key words *Drosophila*, Ovary, Antibody, Antigen, Immunohistochemistry, Follicle cell, Cytoophidium

1 Introduction

A pair of ovaries is the most prominent and easily found tissue in the abdomen of *Drosophila melanogaster* [1]. A female has a pair of ovaries that contain approximately 16 ovarioles, each of which continuously produces functional eggs. Egg chambers bud off and mature as they move along the ovarioles, reaching the posterior as mature eggs ready for fertilization. Oogenesis takes only around 7 or 8 days, depending on the temperature and availability of nutrition [2, 3]. *Drosophila* ovaries house a number of different cell populations, including germ cell lineage and follicular epithelium, which serve as excellent models for the study of different aspects of development [4].

Drosophila ovaries are particularly amenable to immunohistochemistry (IHC). IHC is a technique used to visualize the presence and location of proteins within tissues. In IHC, proteins are detected with antibodies that specifically bind to "epitopes" within the protein of interest. The advance of a fluorescent toolbox empowers IHC and many new approaches to detect protein localization and function [5]. In order to preserve these epitopes, tissues must be fixed prior to staining. Furthermore, in order for antibodies to penetrate the membranes, cells must be permeabilized with detergents. Depending on the nature of antibodies,

Diana P. Bratu and Gerard P. McNeil (eds.), *Drosophila Oogenesis: Methods and Protocols*, Methods in Molecular Biology, vol. 1328, DOI 10.1007/978-1-4939-2851-4_13,

IHC can be carried out with either a "two-step method" or "one-step method." In two-step IHC, the primary antibodies are not labeled with any fluorophores. Once the cells are fixed and permeabilized, a variety of primary antibodies can be mixed and put on the cells for the detection of different proteins (i.e., "the first step"). After primary antibody staining, adding secondary antibodies labeled with different fluorophores (i.e., "the second step") will make targeted proteins visible under either a fluorescent or a laser-scanning confocal microscope. In one-step IHC, primary antibodies are directly labeled with fluorophores that can be visualized either under a fluorescent or a laser-scanning confocal microscope. Combining with fluorescent proteins (such as green fluorescent protein, GFP [6], or mCherry), IHC can be used for detecting the spatial and temporal distributions of multiple proteins [7–11]. IHC can also be used in combination with fluorescence in situ hybridization (FISH) for detection of the relative localization of protein, RNA, and/or DNA [12, 13].

It was recently discovered that the enzyme CTP synthase forms filamentous subcellular structures (called cytoophidia) that are highly conserved from prokaryotes to eukaryotes [7, 14–16]. CTP synthase is expressed at moderate levels in *Drosophila* ovaries [17, 18]. It is cytoplasmic in the germarium and cytoophidium formation starts around stage 2 and the size of the cytoophidia seems to correlate with the cell size [7]. Two types of cytoophidia containing CTP synthase exist in nurse cells: macro-cytoophidia (those that are long and thick) and micro-cytoophidia (short and thin) [7]. Macro-cytoophidia and micro-cytoophidia coexist in *Drosophila* nurse cells and oocytes. The abundance of cytoophidia varies in different cells and tissues [7].

Here we describe an IHC protocol that we used routinely in our laboratory. Our aim was to make IHC as simple as possible. To this end, we have simplified the protocol by skipping some steps used in many other IHC protocols. For example, we do not wash the samples after staining with secondary antibodies and we do not add special mounting medium onto our slides. These changes seem to be against our intuition. However, our IHC results suggest that these changes work well. Furthermore, we have adapted this protocol to study other *Drosophila* tissues such as testes, gut, brain, various glands and imaginal discs in adult animals or larvae [7, 18], as well as to stain culture cells in mammals [19–21].

2 Materials

1. Tweezers (Dumont HP Tweezers 5 stainless steel. 0.10×0.06 mm^2 tip) (*see* **Note 1**).
2. Micro needles (angled stainless steel needles 0.25 mm diameter, 36 mm long) (*see* **Note 2**).

3. Disposable petri dish (35 mm) (*see* **Note 3**).
4. Grace's Insect Medium [22] (*see* **Note 4**).
5. Either paraformaldehyde (PFA) or 16 % formaldehyde (*see* **Note 5**).
6. Phosphate-buffered saline (1× PBS): 135 mM NaCl, 2.5 mM KCl, 4.3 mM Na_2HPO_4, and 1.5 mM KH_2PO_4, pH 7.2 (*see* **Note 6**).
7. Triton™ X-100 (*see* **Note 7**).
8. Horse serum (*see* **Note 8**).
9. PST (1×): 1× PBS, 0.3 % Triton™ X-100, 0.5 % horse serum (*see* **Note 9**).
10. Primary antibodies (*see* **Notes 10–14**).
11. Fluorescently labeled secondary antibodies (*see* **Notes 15** and **16**).
12. Vaseline (*see* **Note 17**).
13. Nail polish (*see* **Note 18**).
14. Glass slides.
15. Coverslips (*see* **Note 19**).

3 Methods

3.1 Preparing the Flies for Dissection

Two to three days before dissection, transfer the stocks into new vials with standard fly food. Tap the flies to the bottom and quickly add wet yeast paste on the inner wall of the new vials (*see* **Note 20**).

3.2 Dissection

1. Anesthetize the flies with CO_2.
2. Separate the flies by sex, discarding the males.
3. Separate the female flies into different groups by genotype.
4. Dissect the ovaries from each group in 3 ml of Grace's Insect medium (*see* **Note 4**) in a 35 mm petri dish at room temperature (Fig. 1a, b) (*see* **Notes 21** and **22**). Do this as quickly as possible without worrying about cleaning the accessory tissues (*see* **Note 23**).
5. Transfer the tissues to a 1.5 ml eppendorf tube using a 20 µl pipette (cut the pipette tip so that the opening is big enough to transfer the fly ovaries) (Fig. 1c, d) (*see* **Note 24**).
6. Remove as much liquid from the tube as possible.
7. In a fume hood, make a 4 % PFA solution by adding 50 µl of 16 % PFA into 150 µl of 1× PBS in a new 1.5 ml tube (*see* **Note 25**).
8. Add newly prepared 4 % PFA into the tube with the ovaries and incubate at room temperature for 10 min.

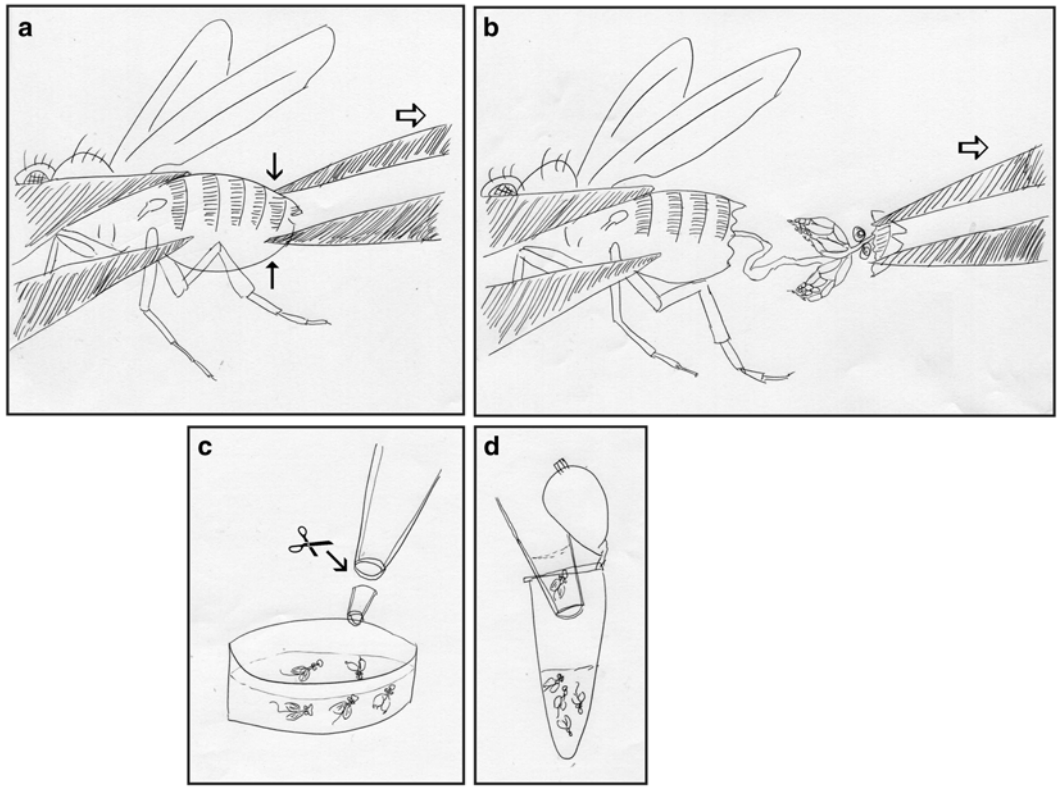

Fig. 1 Dissection of *Drosophila* ovaries. (**a**) Hold a female fly at her thorax and the anterior region of the abdomen with a pair of tweezers. Use the other pair of tweezers to pinch the segment (*solid arrows*) that is second to the most posterior segment, and then pull away from the flies main body (*open arrow*). (**b**) A pair of ovaries and accessory tissues can be easily removed from the flies' abdomen. (**c**) Cut a pipette tip with a blade or a pair of scissors and (**d**) transfer the ovaries and the attached accessory tissues from the dissecting petri dish into a 1.5 ml eppendorf tube

9. Remove as much of the 4 % PFA from the tube as possible (*see* **Note 26**).
10. Add 1 ml of PST to the tube. Remove the PST from the tube.
11. Add 1 ml of PST to the tube. Transfer the ovaries into a new petri dish.
12. Under the dissecting microscope, remove the accessory tissues from the ovaries (*see* **Note 27**).
13. Transfer the clean ovaries into a 500 μl microcentrifuge tube (cut the pipette tip to pipette up the ovaries).
14. Remove as much liquid as possible and then add 500 μl of PST.
15. Use the samples for immunostaining immediately or store them at 4 °C (*see* **Note 28**).

3.3 Immunostaining: Primary Antibody Incubation

1. Make the primary antibody mix for multiple tissue preparations. Target a final aliquot volume of 15 µl (*see* **Notes 29** and **30**).
2. Use 600 µl centrifuge tubes for immunostaining and transfer 2–5 pairs of ovaries into each tube.
3. Remove as much liquid as possible.
4. Add 15 µl of primary antibody mix to each tube.
5. Keep at room temperature overnight (*see* **Note 31**).

3.4 Immunostaining: Secondary Antibody Incubation

1. Make secondary antibody mix for multiple tissue preparations. Add a DNA dye (e.g., Hoechst or DAPI) to the secondary mix. Target a final aliquot volume of 15 µl (*see* **Notes 15** and **16).**
2. Remove as much of the primary antibody mix as possible.
3. Wash in 200 µl of 1× PST at room temperature (*see* **Note 32**).
4. Remove as much 1× PST as possible.
5. Add 15 µl of the secondary antibody mix per tube.
6. Keep at room temperature overnight (*see* **Note 31**).

3.5 Slide Preparation (~30 min Before Imaging)

1. Place a coverslip over paper towel (Fig. 2).
2. Put Vaseline on the four corners of the coverslip (*see* **Note 17**).
3. Transfer the ovaries in 12–15 µl of the secondary antibody mix onto the coverslip (*see* **Notes 33–36**).
4. Put a glass slide onto the coverslip and gently push the slide against the paper towel.
5. Flip the glass slide so the coverslip sits on the top of the glass slide.
6. Use a pipette tip to press the corners of the coverslip so that the liquid spreads evenly between the coverslip and the glass slide.
7. If there is extra liquid outside the coverslip region, gently wipe the liquid off with paper towel.
8. Seal the coverslip with nail polish (*see* **Note 37**).
9. Once the nail polish is dried (5–10 min), the slide is ready for microscopy (*see* **Notes 38** and **39**).

3.6 Confocal Microscopy

Images were taken with an objective (10×, 40× or 63×) on a fluorescence microscope or a laser-scanning confocal microscope (Fig. 3) (*see* **Notes 40** and **41**).

4 Notes

1. The tweezers used for dissection are very sharp and this helps to pull the bottom of the fly with precision preventing damage to the ovaries.

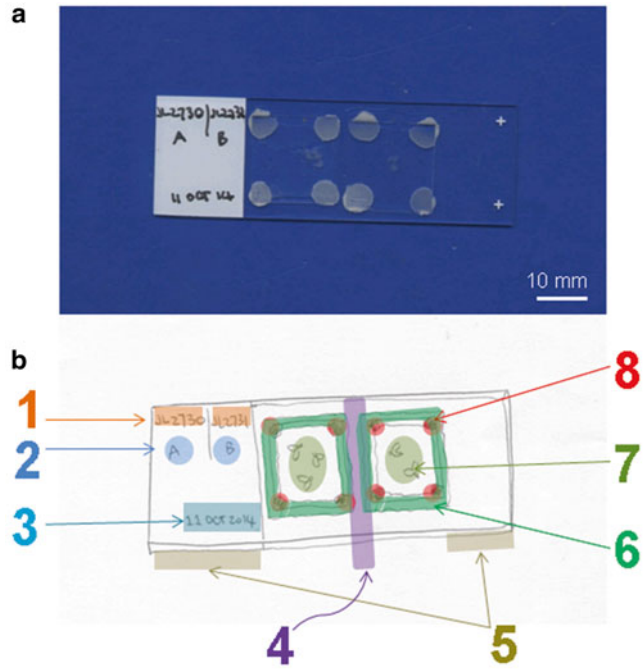

Fig. 2 Preparation of slides. (**a**) A slide with two coverslips. (**b**) The layout of the slide showing in (**a**). (*1*) Labels of the two coverslips showing on this slide. It is convenient to label the coverslips/samples continuously so each sample has a unique identification number in notebooks and digital files. (*2*) Labels of the two samples groups. Detailed information should be written in the notebook. (*3*) Date of slide preparation. (*4*) A gap between the two coverslips to avoid contamination from one another. (*5*) Sufficient space from the coverslips to the edges of the slide so samples are accessible for detection under microscopy. (*6*) Nail polish to seal coverslips. (*7*) Samples positioning at the center of the coverslips. (*8*) Vaseline at the corners of coverslips to protect samples from being squashed during scanning

2. A micro needle is useful for fine dissection, such as removing accessory tissues or combing the ovarioles after fixation.
3. We prefer to use a disposable petri dish for the dissection rather than a reusable glass dish.
4. It is important to dissect the tissues in a medium that mimics physiological conditions. By this standard, we chose Grace's insect medium. We strongly recommend not using PBS for the dissection step.
5. As regards whether to use paraformaldehyde or formaldehyde, in our experience this did not make much difference. Paraformaldehyde seems to be more durable at room temperature, and for this reason it was preferred. (a) Preparation of PFA: Open a vial of 16 % PFA, decant the contents into a

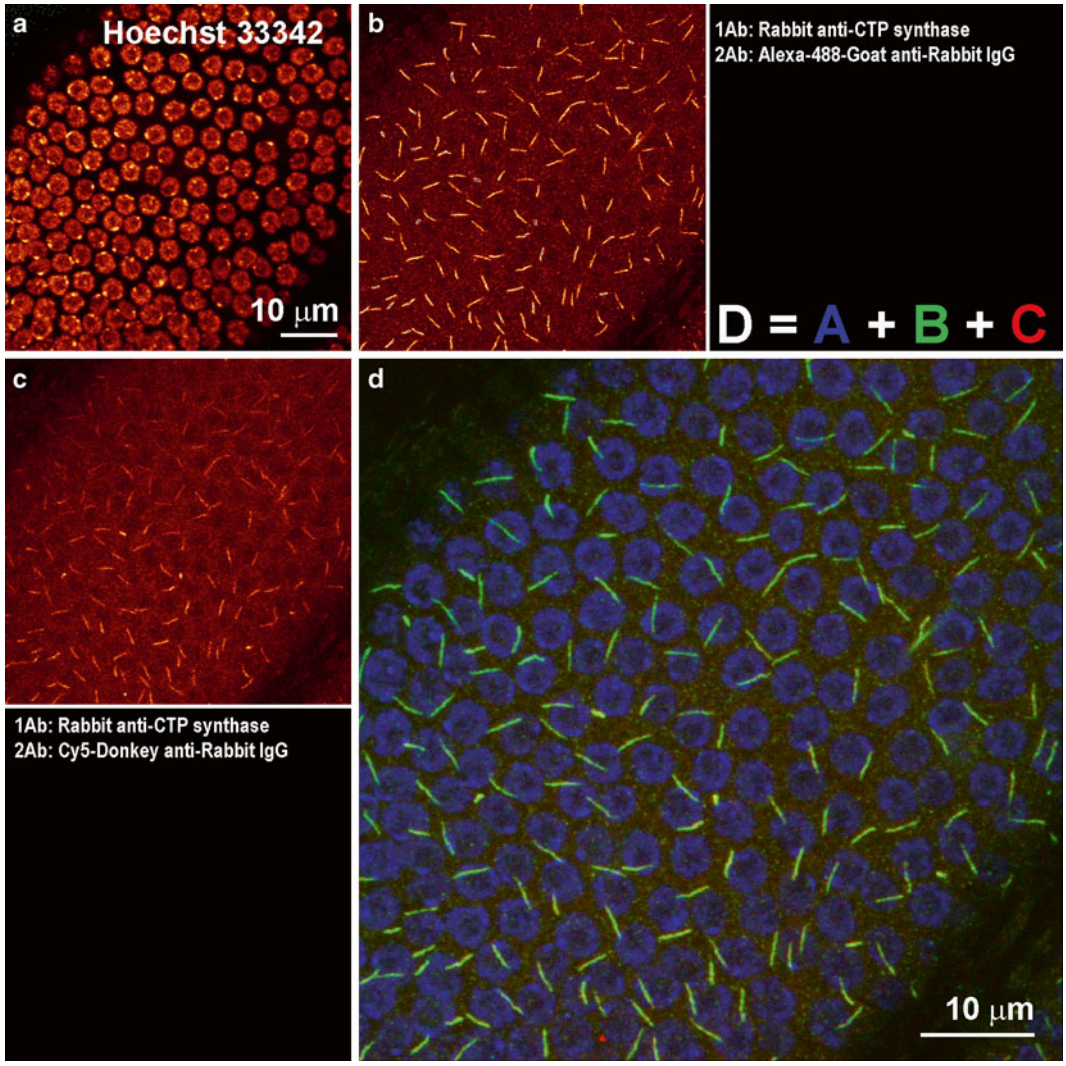

Fig. 3 *Drosophila* cytoophidia expression in the follicle cells monolayer. Images were taken under a Leica TCS SP5 II laser-scanning confocal microscope. (**a**) Follicle cell nuclei labeled with a DNA dye Hoechst 33342. (**b**, **c**) Cytoophidia, filamentous structures that contain CTP synthase [7]. The primary antibody used here is rabbit anti-CTP synthase and the secondary antibodies are Alexa 488 labeled goat anti-Rabbit IgG (**b**) and Cy5-labeled donkey anti-rabbit IgG (**c**). Note that although (**b**) and (**c**) show identical pattern, the signal showing in (**b**) is more intense and clearer than that in (**c**). Images in (**a**, **b,** and **c**) are shown in "glow-over display." (**d**) A merge image of (**a**, **b,** and **c**). Scale bar is 10 μm

15 ml falcon tube and store at room temperature. (b) Preparation of formaldehyde: Open a vial of 16 % formaldehyde, make 200 μl aliquots and store at −20 °C.

6. Use PBS Tablets for consistency. From a pack of 100 PBS tablets, each tablet makes 100 ml of 1× PBS. After dissolving the tablets in water, autoclave the 1× PBS solutions and store at room temperature. Alternatively, PBS can be prepared as a 20× stock.

7. Triton™ X-100 vs. Tween 20. Triton™-X 100 is the default detergent used in IHC. However, Tween 20 is a milder detergent, and in rare cases some antibodies tend to work only with Tween 20 in PST, and not with Triton™ X-100.
8. Powdered bovine serum albumin (BSA) vs horse serum. Both work similarly in blocking non-specific protein binding sites.
9. For 100 ml of PST, add 6 ml of 5 % Triton™ X-100 and 5 ml of 10 % horse serum into 89 ml of 1× PBS. PST may be stored at room temperature for several months.
10. The amount of the primary antibody needed is 10–15 μl, just enough to cover 2–5 pairs of ovaries. To accomplish this, we generate dilutions of primary antibodies and use these dilutions for the final primary antibody solutions (e.g., use 1 μl of 1:100 dilution in a 9.0 μl of PBT to achieve a 1:1000 final concentration.). If the original concentration of the antibody is known, the final concentration of the antibody used was normally 1 μg/ml.
11. The concentration of antibodies used for immunofluorescence is generally 10× higher than that used in Western blotting. For example, if the dilution for an anti-myc antibody is 1:10,000 for Western blotting, 1:1000 should be used as a starting point for immunofluorescence. Although this is a guideline, it may, however, not apply to all primary antibodies.
12. We generally make 10× stocks for primary and secondary antibodies. For example, if the optimal final concentration for an antibody is 1:1000, we will make 500 μl or 1 ml of a 1:100 dilution, that is, ten times the final concentration. We store 10× stocks at 4 °C.
13. Primary antibody concentration. Sometimes a lower amount may be more effective, and optimizing the primary antibody concentration for the first time can prove difficult. For a new antibody, the starting trial concentration for a polyclonal antibody may be higher (e.g., 1:250 or 1:500) than the concentration used for most antibodies (1:1000). After looking at our samples, we tend to decide whether to use less or more of the antibody. Generally, when there is no signal or a lot of background, one's instinctive reaction is to add more of the antibody. In contrast to this, however, what we found was that using a smaller quantity of a polyclonal antibody can increase signal quality. Sometimes, therefore, using a smaller quantity of primary antibody (increasing dilution from 1:1000 to 1:10,000) may give much better images with low background.
14. For staining multiple targeted proteins with multiple antibodies simultaneously, it is important to use primary antibodies raised from different species.
15. Antibodies arriving in powder form should be diluted in glycerol in accordance with the manufacturer's instructions.

16. Secondary antibodies may be labeled with fluorophores such as Alexa 488, Alexa 546, Cy3, Alexa 633, or Cy5 (Fig. 1). For the staining of multiple antibodies with different fluorophores, it is important to choose those with well separated spectra. For double labeling, we prefer the combination of Alexa 488 (or EGFP) and Cy5, along with staining the DNA with Hoechst 33342 or DAPI at the same time.
17. Vaseline is used to support the coverslip so the sample is not damaged during microscopy. We normally squeeze Vaseline into a 35-mm petri dish and let it dry for at least 3 days. The traditional method is to heat paraffin wax and Vaseline at a 1:1 ratio to make soft wax. However, for us, dried Vaseline has worked better than traditional soft wax, as well as being easier, cheaper, and simpler.
18. Any brand of nail polish will suffice, though our preference is for a cheap, transparent one.
19. We prefer 18×18 mm^2 coverslips.
20. Put 5–10 female flies together with 2–3 males in a vial with wet yeast paste on standard fly food and keep at 25 °C for 1–3 days. This ensures that the ovaries are fat and contain all developmental stages.
21. It is important to dissect flies at room temperature to maintain natural conditions for as long as possible prior to fixation. Once Grace's insect medium is removed from a fridge, pour it into a petri dish and wait for at least 10 min for the medium to warm up to room temperature. We have found that many proteins change their distribution pattern when the tissues are heat-shocked or cold-shocked before fixation.
22. The flies should be dissected one at a time with a pair of forceps/tweezers [4]. Pull the bottom of a single fly with one tweezer while holding the thorax of the fly with the other tweezer. Ideally, the ovaries will come out very easily. If not, push the ovaries out using the flat side of the tweezer (closed) while holding the fly at the thorax with the other tweezer.
23. Try to minimize the time between dissection and fixation.
24. It is easier to control pressure during tissue transfer with a 20 μl pipette than with a 200 μl pipette. This helps to avoid the tissues becoming stuck onto the walls of the tips during transfer. In addition, use pipette tips for the transfer of tissues only if the medium contains a detergent or serum.
25. When handling PFA, use gloves and a fume hood, as it is toxic. If no fume hood is available, ensure that the eppendorf tubes are closed once the PFA is added.
26. Used PFA should be kept in a capped bottle or a tightly closed container and disposed of appropriately.

27. After fixation and washing, the accessory tissues may be removed in the dissecting dish using tweezers. The ovaries can be opened up more using a pair of micro needles to allow penetration of the fixing solution. It is even possible to carefully comb between the ovarioles, making sure that both ovaries stay attached to the oviduct for easy transport.
28. We prefer to use freshly fixed tissues for immunostaining. However, in our experience, good immunostaining results can be obtained from fixed tissues stored for months at 4 °C.
29. It is good practice to centrifuge the 10× antibody stocks before making the primary or secondary antibody mix (e.g., full speed for 2 min on a benchtop centrifuge). This will dramatically reduce background staining, especially when the antibody solution is not very clear.
30. In the case of a primary antibody directly labeled with a fluorophore, a DNA dye (Hoechst 33342 or DAPI) may be added directly to the mix.
31. We prefer to keep the samples in primary antibody at room temperature (not at 4 °C) for at least one night. This may be extended to several days if there is sufficient time. The same is true for the incubations in secondary antibody.
32. The duration of the washing stage is flexible.
33. We mount samples in secondary antibody mix.
34. We often skip the washing stage. We do not wash off secondary antibodies and do not recommend using a special mounting medium.
35. In our experience, background issues were of low importance, as we used low concentrations of secondary antibodies and confocal microscopy.
36. In our experience, a special mounting medium can dampen the staining signal.
37. Make sure the coverslip is sealed well with nail polish. If there are air bubbles under the coverslip, this can be resolved by adding another layer of nail polish.
38. Prepare the samples fresh before confocal microscopy. Once a slide is made, try to observe it under confocal microscopy within 2 h.
39. If there are too many samples to observe in 1 day, it is better to keep them in a secondary antibody mix in eppendorf tubes rather than mounting them on slides.
40. We prefer to prepare fewer than four slides for a 2 h confocal session, so that we can spend about 30 min of confocal time on each slide. For those slides that require a more extended observation, our aim is to revisit them within 3 days.

41. If using a laser-scanning confocal microscope, make sure the settings of the laser beams and photomultiplier tubes correspond to the excitation and emission spectra of the antibody-labeling fluorophores.

Acknowledgments

The authors wish to thank the *Drosophila* community for generously sharing reagents and antibodies. The research in the Liu Laboratory was supported by the UK Medical Research Council.

References

1. Spradling AC (1993) Developmental genetics of oogenesis. In: Bate M, Arias AM (eds) The development of *Drosophila melanogaster*. Cold Spring Harbor Laboratory Press, Plainview, NY, pp 1–70
2. Shimada Y, Burn KM, Niwa R et al (2011) Reversible response of protein localization and microtubule organization to nutrient stress during *Drosophila* early oogenesis. Dev Biol 355:250–262
3. Buckingham M, Liu JL (2011) U bodies respond to nutrient stress in *Drosophila*. Exp Cell Res 317:2835–2844
4. Bastock R, St Johnston D (2008) *Drosophila* oogenesis. Curr Biol 18:R1082–R1087
5. Giepmans BN, Adams SR, Ellisman MH et al (2006) The fluorescent toolbox for assessing protein location and function. Science 312: 217–224
6. Tsien RY (1998) The green fluorescent protein. Annu Rev Biochem 67:509–544
7. Liu JL (2010) Intracellular compartmentation of CTP synthase in *Drosophila*. J Genet Genomics 37:281–296
8. Lee L, Davies SE, Liu JL (2009) The spinal muscular atrophy protein SMN affects *Drosophila* germline nuclear organization through the U body-P body pathway. Dev Biol 332:142–155
9. Buszczak M, Paterno S, Lighthouse D et al (2007) The carnegie protein trap library: a versatile tool for *Drosophila* developmental studies. Genetics 175:1505–1531
10. Quinones-Coello AT, Petrella LN, Ayers K et al (2007) Exploring strategies for protein trapping in *Drosophila*. Genetics 175:1089–1104
11. Lowe N, Rees JS, Roote J et al (2014) Analysis of the expression patterns, subcellular localisations and interaction partners of *Drosophila* proteins using a pigP protein trap library. Development 141:3994–4005
12. Liu JL, Murphy C, Buszczak M et al (2006) The *Drosophila melanogaster* Cajal body. J Cell Biol 172:875–884
13. Liu JL, Gall JG (2007) U bodies are cytoplasmic structures that contain uridine-rich small nuclear ribonucleoproteins and associate with P bodies. Proc Natl Acad Sci U S A 104:11655–11659
14. Liu JL (2011) The enigmatic cytoophidium: compartmentation of CTP synthase via filament formation. Bioessays 33:159–164
15. Ingerson-Mahar M et al (2010) The metabolic enzyme CTP synthase forms cytoskeletal filaments. Nat Cell Biol 12:739–746
16. Noree C et al (2010) Identification of novel filament-forming proteins in *Saccharomyces cerevisiae* and *Drosophila melanogaster*. J Cell Biol 190:541–551
17. FlyBase Genome (2011) Analysis and update of genes grouped into 34 co-expression clusters by the modENCODE Consortium. Science 330:1787–1797
18. Azzam G, Liu JL (2013) Only One Isoform of *Drosophila melanogaster* CTP Synthase Forms the Cytoophidium. PLoS Genet 9, e1003256
19. Chen K et al (2011) Glutamine analogs promote cytoophidium assembly in human and *Drosophila* cells. J Genet Genomics 38:391–402
20. Gou KM et al (2014) CTP synthase forms cytoophidia in the cytoplasm and nucleus. Exp Cell Res 323:242–253
21. Aughey GN et al (2014) Nucleotide synthesis is regulated by cytoophidium formation during neurodevelopment and adaptive metabolism. Biol Open 3:1045–1056
22. Grace TD (1962) Establishment of four strains of cells from insect tissues grown in vitro. Nature 195:788–789

Chapter 14

Detection of Cell Death and Phagocytosis in the *Drosophila* Ovary

Tracy L. Meehan, Alla Yalonetskaya, Tony F. Joudi, and Kimberly McCall

Abstract

Billions of cells die and are cleared throughout the development and homeostasis of an organism. Either improper death or clearance can lead to serious illnesses. In the adult *Drosophila* ovary, germline cells can die by programmed cell death (PCD) at three distinct stages; here we focus on cell death that occurs in mid- and late oogenesis. In mid-oogenesis, the germline of egg chambers can undergo apoptosis in response to nutrient deprivation. In late oogenesis, the nurse cells are eliminated through a developmentally regulated, non-apoptotic cell death. In this chapter, we describe several methods to detect cell death and phagocytosis in the *Drosophila* ovary. DAPI stains the chromatin of all cells and can be used to detect morphological changes in cells that die by different mechanisms. TUNEL labels fragmented DNA, which can occur in both apoptotic and non-apoptotic death. LysoTracker, an acidophilic dye, marks acidic vesicles and some dying cells; therefore, it can be used to study both death and phagocytosis. We also describe several antibodies that can be used to investigate cell death and/or phagocytosis: active caspase Dcp-1, membrane markers, and lamins. Many of these antibodies can be used in combination with GFP fusion transgenes for further analysis; we show Rab5-GFP and Rab7-GFP, which can be used to study phagocytosis in further detail.

Key words *Drosophila*, Ovary, Cell death, Apoptosis, Phagocytosis, DAPI, TUNEL, LysoTracker

1 Introduction

Throughout the development and homeostasis of an organism, billions of cells are programmed to die. The three main types of programmed cell death (PCD) are apoptosis, autophagic cell death, and necrosis. Many of these dying cells are engulfed by either professional or non-professional phagocytes. In humans, disruption of either the cell death program or clearance of these dead cells has been shown to promote several different disease states, such as cancer, Alzheimer's disease, Parkinson's disease, and lupus [1–5].

The *Drosophila* ovary serves as a physiologically relevant system to study both apoptotic and non-apoptotic death and clearance [6–10]. Each adult female fruit fly has two ovaries that consist of 15–20 strings of progressively developing egg chambers called

Diana P. Bratu and Gerard P. McNeil (eds.), *Drosophila Oogenesis: Methods and Protocols*, Methods in Molecular Biology, vol. 1328, DOI 10.1007/978-1-4939-2851-4_14,

ovarioles [11, 12]. Analysis of cell death is simplified in this system because there are three distinct cell types in each egg chamber: the germline-derived oocyte and large polyploid nurse cells, and the somatically derived follicle cells, which surround and support the germline. Cell death predominantly occurs at three points in oogenesis: early oogenesis (in the germarium), mid-oogenesis, and late oogenesis. Cell death in oogenesis may be stress-induced or developmentally controlled, and the ovary provides an opportunity to study how non-professional phagocytes clear cells that die by different mechanisms.

Programmed cell death in the germarium occurs at the end of region 2a and is dependent on the nutrients available [13–16]; but other causes of cell death are possible. For example, infection by the intracellular bacteria *Wolbachia* was found to decrease PCD by one-half in germaria of *Drosophila mauritiana* [17]. Another potential cause for cell death at this stage could be the result of a meiotic checkpoint, as observed in other organisms [8]. Further work is required to gain a more complete understanding of cell death in the germarium.

In mid-oogenesis, cell death can be induced by several different stressors [8], but the easiest and most reproducible method is starvation. When flies are deprived of nutrients, the nurse cells in stages 7–9 of oogenesis frequently undergo apoptosis and are engulfed by the neighboring follicle cells [13, 16, 18–22]. The dying nurse cells become positive for TUNEL [16] and active caspases [20, 23] (Fig. 2), and require apoptosis and autophagy to die properly [13, 16, 20, 22–24]. Simultaneously, the engulfing follicle cells increase levels of the engulfment receptor Draper and activate transcription of the downstream targets of the JNK pathway [19]. Recent work shows that Draper and JNK work in a positive feedback loop in the follicle cells to clear the dying nurse cells [19]. More recently, additional engulfment markers and corpse processing tools have been developed that enable a more in-depth analysis of the mechanism by which the follicle cells synchronously enlarge and engulf the nurse cells.

In late oogenesis, all 15 nurse cells in each egg chamber undergo developmental PCD to complete the production of the oocyte. Unlike PCD in mid-oogenesis, apoptosis and autophagy do not play a major role in the death of the nurse cells in late oogenesis [20, 25]. However, the nurse cells become TUNEL- and LysoTracker-positive (Fig. 1), indicating that the nurse cells die by a non-canonical method. The surrounding stretch follicle cells also show enrichment of the same engulfment receptors as those seen in mid-oogenesis, suggesting that phagocytosis may play a role in nurse cell removal [6] and may in fact be actively killing the nurse cells.

This chapter focuses on methods for detecting cell death and phagocytosis in mid- and late oogenesis. We describe methods for detecting both apoptotic and non-apoptotic cell death using DAPI,

TUNEL, LysoTracker, and anti-Lamin antibody staining. We also describe recently developed methods for monitoring phagocytosis of apoptotic cells in mid-oogenesis using antibodies against active Dcp-1, Draper, and membrane proteins, as well as Rab-GFP fusion proteins. Several other reporters have been used in other tissues in *Drosophila*, but do not express well in the germline because lines were made with the UASt promoter [26, 27]. There have also been numerous papers, methods chapters, and videos investigating different aspects of cell death [28–31] and engulfment [32–34], but we will focus on the tools that have proved the most successful in our hands.

2 Materials

2.1 General Supplies and Reagents

1. General fly supplies: fly food, vials, CO_2 pads, 25 °C incubator.
2. Yeast paste: combine granular yeast and dH_2O and mix until it is a smooth consistency.
3. Apple juice agar vials for starvation: Add 90 g of agar to 3 l of dH_2O and autoclave for 50 min, then cool to 60 °C using a water bath. Mix 1 l of apple juice with 100 g of sucrose and add to the autoclaved agar; mix well by stirring with a magnetic stir bar. Add 60 ml of 10 % *p*-hydroxy benzoic acid methyl ester (aka Tegosept) dissolved in ethanol. Store in 250 ml capped bottles at 4 °C. To prepare fly vials, melt agar solution in microwave and pour into empty vials. Plug vials with cotton balls after agar has solidified. Store at 4 °C.
4. Fine forceps (Dumont #5), tungsten needles, and glass spot plates or slides for dissection.
5. Glass Pasteur pipettes and bulbs.
6. Plastic fine-tipped transfer pipettes.
7. 0.5 ml and 1.5 ml microcentrifuge tubes.
8. Grace's insect medium.
9. 1× phosphate-buffered saline (1× PBS): 137 mM NaCl, 2.7 mM KCl, 10 mM Na_2HPO_4, 2 mM KH_2PO_4, pH 7.4. Make up as a 10× solution and store at room temperature.
10. 16 % paraformaldehyde (PFA) (EM grade), opened within 1 week.
11. Heptane.
12. 1× PBT: 1× PBS, 0.1 % Triton™ X-100.
13. PBANG: 1× PBT, 0.5 % bovine serum albumin, 5 % normal goat serum.
14. PBTB: PBT, 0.5 % BSA.

15. Rotator (such as Labquake) for use during incubation in microcentrifuge tubes.
16. Glass slides and coverslips (22 × 50 mm, 0.16–0.19 mm thickness).
17. Nail polish.
18. Fluorescence or confocal microscope equipped with rhodamine, fluorescein (FITC), cyanine-5 (Cy5), and ultraviolet (UV) filters, bright field/differential interference-contrast (DIC).
19. Platform shaker.

2.2 TUNEL

1. Reagents from the DeadEnd Fluorometric TUNEL System (Promega):
   (a) Equilibration buffer.
   (b) Nucleotide mix.
   (c) Terminal deoxynucleotidyl transferase, recombinant (rTdT).
   (d) rTdT incubation buffer: 45 µl equilibration buffer, 5 µl nucleotide mix, 1 µl rTdT enzyme.
   (e) 20× saline–sodium citrate (SSC).
   (f) Permeabilization solution: 1× PBS, 0.2 % Triton™ X-100.

2.3 Indicators

1. VectaShield Mounting Medium with DAPI.
2. LysoTracker Red DND-99.

2.4 Antibody Staining

1. Recommended primary antibodies (Table 1):
   (a) Rabbit anti-cleaved *Drosophila* Dcp-1 (Asp216) Antibody (Cell Signaling, #9578S). Use a dilution of 1:100.
   (b) Mouse anti-Discs large (Dlg) antibody (Developmental Studies Hybridoma Bank (DSHB), 4F3 [35]). Use a dilution of 1:100.
   (c) Rat anti-DCAD2 antibody (DSHB, DCAD2 [36]). Use a dilution of 1:50.
   (d) Mouse anti-Draper antibody (DSHB, 5D14, developed by Mary Logan [19]). Use a dilution of 1:50.
   (e) Mouse anti-lamin Dm_0 antibody (DSHB, ADL67.10 [37] or ADL84.12 [38]). Use a dilution of 1:1 or 1:2.
2. Appropriate secondary antibodies, such as:
   (a) Goat anti-rabbit Cy3, goat anti-mouse Cy3, or goat anti-rat Dylight 649 (Jackson ImmunoResearch). Use a dilution of 1:100 or 1:200.
   (b) Goat anti-rabbit Alexa Fluor 488 (Invitrogen). Use a dilution of 1:200.

Table 1
Antibodies recommended for cell death and phagocytosis

Antibody	Source	Recognizes	Notes
Dcp-1*	Cell Signaling	Cleaved Dcp-1	Labels dying germline and vesicles
4F3, Dlg*	DSHB [35]	Membrane	Labels FC and GL membrane
DCAD2	DSHB [36]	Membrane	Labels FC and GL membrane
5D14, Draper	DSHB, Mary Logan [19]	Engulfment Receptor	Labels engulfing FCs
ADL84.12*	DSHB [38]	Lamin Dm_0	Smooth, persists in late oogenesis
ADL67.10	DSHB [37]	Lamin Dm_0	Smooth, persists in late oogenesis
LC28.26	DSHB [37]	Lamin C	Discrete spots
ADL101	DSHB	Lamins Dm_0 and C	Discrete spots, fades in late oogenesis

*Antibodies shown in this chapter

2.5 Fly Strains

Many different fly strains can be obtained from the Bloomington *Drosophila* Stock Center at Indiana University (http://flystocks.bio.indiana.edu/), including several GFP, RFP, or YFP-tagged Rab transgenes (Table 2). The Rab-GFP fusions we have used are marked with asterisks (**—works well; *—studied but no noticeable expression), and images with Rab5- and Rab7-GFP are shown here. A wide array of GFP lines can also be obtained from FlyTrap (http://flytrap.med.yale.edu/). *See* [39] for a list of useful lines for studying oogenesis. The lines shown in this chapter are listed below:

1. Control (w^{1118}). This is a common background strain for many transgenic lines.
2. Follicle cell GAL4 lines [39]:
   (a) *GR1-GAL4* [40].
   (b) *GR1-GAL4, G00089/TM6B* [19]. G00089 (Flytrap) is a GFP protein trap inserted in the *trailer hitch* (*tral*) gene that can be used to specifically mark germline cytoplasm.
3. *w[*]; P{w[+mC]=UAS-GFP-Rab5}3.*
4. *w[*]; P{w[+mC]=UAS-Rab7.GFP}3.*

3 Methods

3.1 Ovary Dissection

At the time of dissection, flies should be ideally 3–10 days old; flies that are too young or too old will not have well-developed ovaries. Prior to dissection, flies should be placed in a new food vial with plenty of yeast paste, in uncrowded conditions, with roughly equal

Table 2
Publicly available *UASt-Rab* fusion transgenic lines

Gene name	Bloomington stock number	Genotype
Rab1	24104	*y[1]w[*]; P{w[+mC]=UAST-YFP.Rab1}Mes2[01]*
Rab2	23246	*y[1] w[*]; P{w[+mC]=UAST-YFP.Rab2}l(3)neo38[02]/ TM3, Sb[1]*
*Rab4**	8505	*w[*]; P{w[+mC]=UAS-Rab4-mRFP}2*
*Rab5***	43336	*w[*]; P{w[+mC]=UAS-GFP-Rab5}3*
Rab6	23251	*y[1] w[*]; P{w[+mC]=UAST-YFP.Rab6}CG10082[01]/CyO*
*Rab7***	42705	*w[*]; P{w[+mC]=UAS-Rab7.GFP}2*
	42706	*w[*]; P{w[+mC]=UAS-Rab7.GFP}3*
*Rab11***	8506	*w[*]; P{w[+mC]=UAS-Rab11-GFP}2*
Rab18	9796	*y[1] w[*]; P{w[+mC]=UAST-YFP.Rab18}CG9775[01]*
*Rab21***	23242	*y[1] w[*]; P{w[+mC]=UAST-YFP.Rab21}pog[04]*

*Lines tested in the *Drosophila* ovary
**Lines tested with notable expression in the *Drosophila* ovary

numbers of male and female flies. To study late oogenesis, transfer the flies to new vials with fresh yeast paste 1–2×/day, for at least 2 days. To study cell death in mid-oogenesis, keep the flies in the same vial with yeast paste for approximately 1.5 days, before starving on apple juice agar vials for 16–20 h.

1. Anesthetize flies on a CO_2 pad (*see* **Note 1**).
2. Using forceps, grab a female by the wings.
3. Submerge female in a glass well (in a spot plate) filled with Grace's Medium unless otherwise noted.
4. Pin down female with the other forceps between the abdomen and thorax.
5. With the first set of forceps, make a hole at the tip of the abdomen and gently remove the ovaries and other organs (*see* **Note 2**).
6. Separate the other organs from the ovaries and place ovaries in a clean well containing Grace's Medium. To ensure that tissue does not degrade, proceed to the first step of desired procedure within 20 min of the dissection.
7. Once approximately 7–10 females have been dissected, use a glass Pasteur pipette to transfer tissue to a 1.5 ml microcentrifuge tube and quickly move to the first step of the procedure desired (*see* **Note 3**).

3.2 DAPI Staining

3.2.1 Applications: Cell Death

DAPI (4′,6-diamidino-2-phenylindole) labels the chromatin of all healthy and dying cells. DAPI is an especially useful tool in the *Drosophila* egg chamber when studying the death of the large polyploid nurse cells. Using DAPI alone, morphological changes that are characteristic of apoptotic cell death can be visualized (Fig. 1 and 2). In [19], DAPI was sufficient to distinguish between egg chambers at different steps of apoptosis.

1. After transferring recently dissected ovaries to a microcentrifuge tube, remove all but 300 µl of Grace's Medium, and add 200 µl of Heptane and 100 µl of 16 % PFA to fix and permeabilize the tissue [41]. Rotate for 20 min at room temperature.
2. Remove and dispose of the fix solution in a hazardous waste container. Immediately rinse tissues 2× with 1× PBT. For each rinse, invert the microcentrifuge tube several times and allow the tissue to settle before removing the solution.
3. Wash 3×10 min with 1× PBT at room temperature, while rotating (*see* **Note 4**).
4. Rinse with 1× PBS and remove as much fluid as possible.
5. Add ~2 drops of VECTASHIELD with DAPI and store at 4 °C in the dark for at least 16 h (*see* **Note 5**).
6. Transfer the tissue to a microscope slide using a glass Pasteur pipette (*see* **Note 6**).
7. Tease apart ovarioles using tungsten needles, add a coverslip, and seal edges with nail polish (*see* **Note 7**).
8. View on a fluorescence or confocal microscope using the UV filter. Nuclei of cells dying by apoptosis in mid-oogenesis will appear brighter and more condensed or fragmented (Fig. 2b″–d″), whereas cells dying by a non-apoptotic mechanism in late oogenesis will have variable appearances with some nuclei appearing brightly and partially condensed and other nuclei showing dimmer, more diffuse staining (Fig. 1b, d, f).

3.3 TUNEL Staining

3.3.1 Applications: Cell Death

TUNEL, or Terminal deoxynucleotidyl transferase-mediated dUTP Nick-End Labeling, allows for the visualization of 3′-OH sites revealed during DNA fragmentation. Traditionally, TUNEL has been used to label apoptotic cells. We find that it also labels nurse cell nuclei during late-stage developmental cell death, which can occur independent of caspase activity [20, 23, 25, 42]. We employ the DeadEnd Fluorometric TUNEL System from Promega since the protocol is quicker than other kits. Additionally, this kit works in the *Drosophila* ovary without the use of Proteinase K, which often damages *Drosophila* ovary tissue.

1. After transferring recently dissected ovaries to a microcentrifuge tube, remove as much Grace's Medium as possible.
2. Fix tissue by adding 375 µl of 1× PBS and 125 µl of 16 % PFA. Rotate for 15 min.

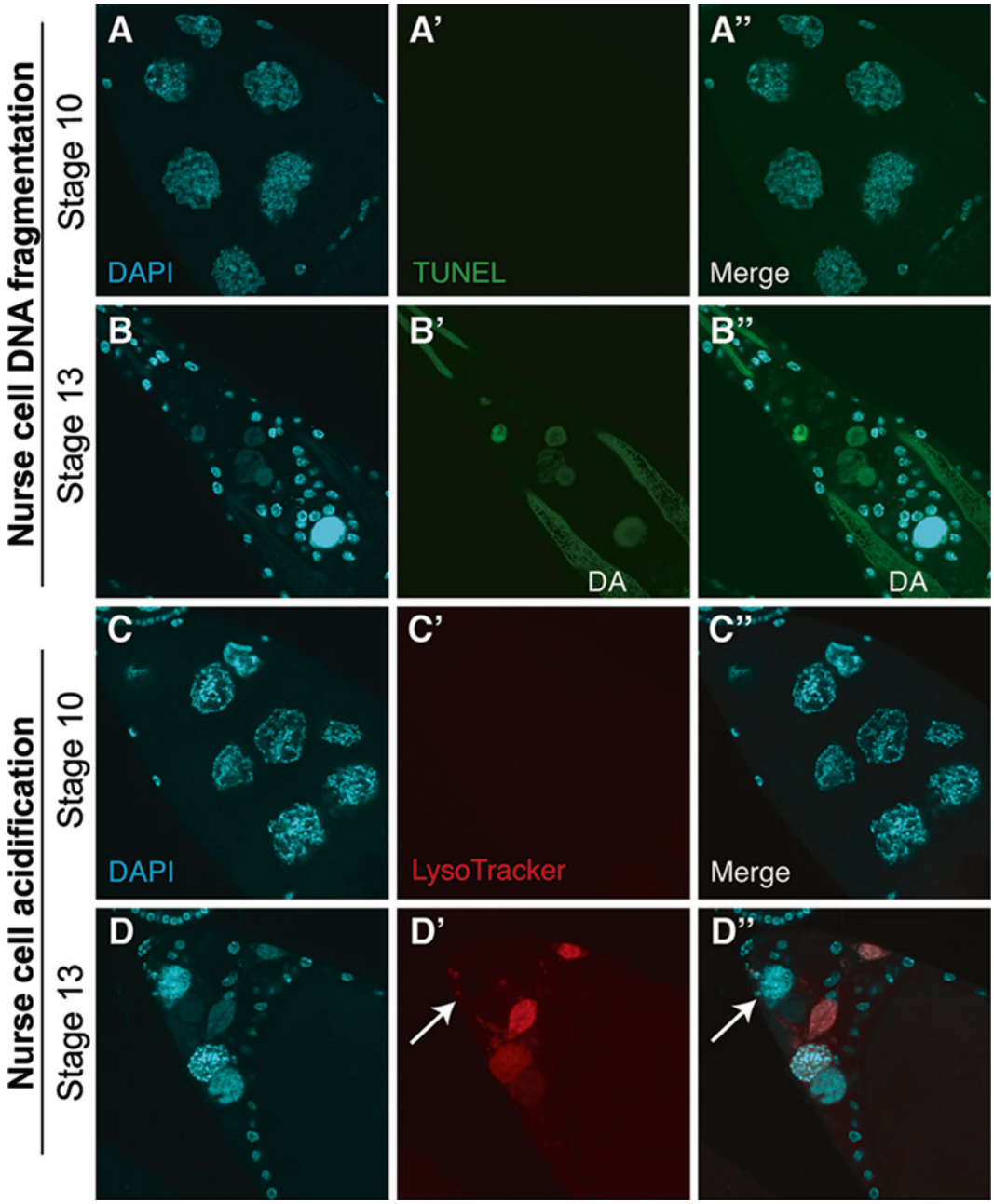

Fig. 1 Cell death in late oogenesis. Ovaries from *w*^{1118} flies were extracted and stained with TUNEL (**a**–**b**″), LysoTracker (**c**–**d**″), or ADL84.12 against Lamin Dm_0 (1:1 concentration; **e**–**f**″) and DAPI. As nurse cells die during late oogenesis, their nuclei begin to label with TUNEL (**b**′) and LysoTracker (**d**′), indicating DNA fragmentation and acidification, respectively. Note that not all nurse cell nuclei label with LysoTracker (**d**′ *arrow*) and TUNEL (not shown) synchronously. LysoTracker staining in follicle cells can range from puncta (**d**′) to more diffuse labeling (not shown). Healthy egg chambers at earlier stages do not label with either TUNEL or LysoTracker (**a**′, **c**′). Staining with Lamin antibodies ADL84.12 or ADL67.10 (not shown) reveals round, expanded nuclei in healthy cells (**e**′). However, as nurse cells die during the final stages of oogenesis, the nuclear lamina forms deep involutions and remains at least partially intact with the condensing nucleus (**f**′ *arrowhead*). *DA* dorsal appendage

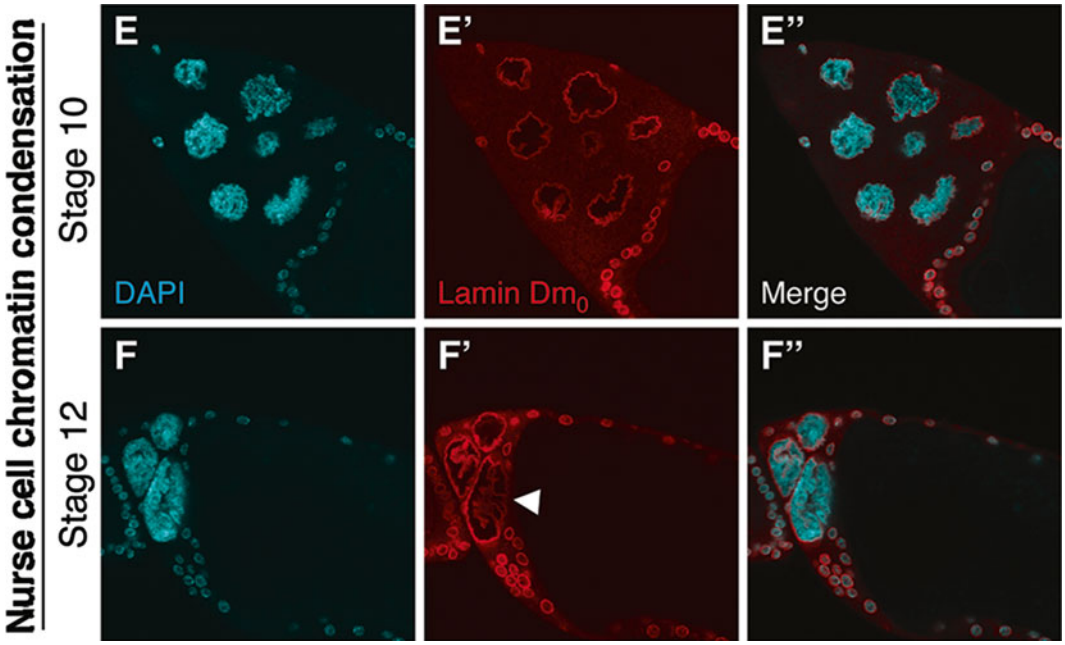

Fig. 1 (continued)

3. Remove the fixation solution and rinse twice with 1x PBT.
4. Wash 3×10 min with 1× PBT (*see* **Note 3**).
5. Permeabilize the tissue in 1 ml of permeabilization solution for 15 min (*see* **Note 8**).
6. Remove the permeabilization solution and wash 2×5 min with 1× PBT.
7. Transfer the tissue to a 0.5 ml microcentrifuge tube on the last wash to allow for minimal equilibration buffer use.
8. Equilibrate by washing tissue for 10 min in 20 μl of equilibration buffer from the kit, or as much needed to cover ovary tissue (*see* **Note 9**). Gently tap on the bottom of the tube to mix and place on a platform shaker (*see* **Notes 10** and **11**).
9. Remove equilibration buffer and add rTdT incubation buffer. From this point forward, keep samples protected from light (*see* **Notes 12** and **13**).
10. Incubate the samples for 3 h in a 37 °C water bath.
11. Stop the reaction by adding 300 μl of 2× SSC solution and rotating the tube for 1 min. Remove the solution and replace it with another 300 μl of 2× SSC, rotating for 15 min (*see* **Note 14**).
12. Remove the SSC solution and wash 3×10 min with 1× PBT while rotating.
13. Remove the PBT and add ~2 drops of VECTASHIELD with DAPI. Store at 4 °C in the dark, for at least 16 h (*see* **Note 5**).

14. Transfer the tissue to a microscope slide using a glass Pasteur pipette (*see* **Note 6**).
15. Tease apart the ovarioles using tungsten needles, add a coverslip, and seal with nail polish (*see* **Note 7**).
16. Observe the tissue on a fluorescence or confocal microscope using the Fluorescein (FITC) filter. Appearance of TUNEL-labeled nuclei will vary (Fig. 1b′): some nuclei have dull, diffuse green staining, which is difficult to discern by eye through a fluorescence microscope, while other nuclei are distinct and label very brightly. We find that observing ovary tissue on the computer, whether connected to a confocal or fluorescence microscope, greatly aids our ability to detect TUNEL-positive nuclei. Representative images are shown in Fig. 1. We find that approximately half of stage 12–13 egg chambers contain TUNEL positive nurse cell nuclei. Whether this is a technical problem or has a biological basis remains to be determined.

3.4 LysoTracker Staining

3.4.1 Applications: Cell Death and Phagocytosis

LysoTracker is an acidophilic probe which is useful for labeling acidic organelles, such as lysosomes and autolysosomes [43], as well as general acidification which may occur to cells dying by necrosis [8, 44]. It may be used for both live-imaging and fixed tissue applications [16, 30, 45], however, we will focus on the latter.

1. After transferring recently dissected ovaries to a microcentrifuge tube, remove as much Grace's Medium as possible and add LysoTracker 1:50 in 1× PBS (*see* **Notes 15** and **16**).
2. Incubate for 3 min at room temperature, flicking tubes gently several times throughout. Tubes may be kept on a shaker in between flicking (*see* **Note 17**).
3. Remove the LysoTracker and 1× PBS solution and wash 3× for a total of 30 min with 1× PBS. The first wash is quick (~2 min), while the other two are longer.
4. Fix for 20 min in 375 μl of Grace's Medium and 125 μl of 16 % PFA.
5. Wash 3× with 1× PBT for a total wash time of 20 min.
6. Remove the PBT and add ~2 drops of VECTASHIELD with DAPI. Store at 4 °C, in the dark, for at least 16 h (*see* **Note 5**).
7. Transfer the tissue to a microscope slide using a glass Pasteur pipette (*see* **Note 6**).
8. Tease apart the ovarioles using tungsten needles, add a coverslip, and seal with nail polish (*see* **Note 7**).
9. View on a fluorescence or confocal microscope using the Rhodamine (TRITC) filter. LysoTracker labeling will appear red throughout the nucleus of acidified dying nurse cells (Fig. 1d′). However, not all nurse cell nuclei within an egg chamber will label simultaneously with LysoTracker, as late

stage nurse cell death is not a synchronous process. Thus, we find egg chambers with varying appearances of nurse cell nuclei (Fig. 1d′). Furthermore, follicle cells surrounding dying nurse cell nuclei may also label with LysoTracker, revealing acidified compartments within these follicle cells (Fig. 1d′). Representative LysoTracker images are shown in Fig. 1.

3.5 Antibody Staining

3.5.1 Applications: Cell Death and Phagocytosis

There are several different antibodies that can be used to study cell death and phagocytosis, and these can be used on fly strains expressing GFP fusion transgenes. To observe vesicle formation and corpse processing, germline-specific GFP traps [19] can be used; however, we have found that the antibody against active caspase Dcp-1 is more sensitive and degrades more slowly (Fig. 2). Active Dcp-1 specifically marks the germline of dying egg chambers [28], but also clearly marks engulfed vesicles (Fig. 2b′–d′). The Dcp-1 antibody can be used on flies expressing Rab-GFP transgenes, which allows for more detailed observations regarding the extent of phagocytosis and corpse processing (Fig. 2c, d). Membrane markers, such as antibodies against Discs large (Dlg), DCAD2, or Draper, can be used to detect membrane enlargement in the engulfing follicle cells.

Antibodies against nuclear lamins can be used to identify subtle changes in the nuclear morphology of dying nurse cells. During apoptosis (as in mid-oogenesis), lamins are cleaved by caspases and they are no longer detectable with antibody staining. However, during non-apoptotic death in late oogenesis, lamins remain visible throughout cell death (Fig. 1f′). Four lamin antibodies are available from DSHB: ADL84.12 and ADL67.10 recognize Dm_0, LC28.26 recognizes lamin C, and ADL101 recognizes both Dm_0 and lamin C (according to DSHB; [37, 38]). These antibodies stain nurse cells differently: ADL101 and LC28.26 appear as discrete spots around nuclei, whereas ADL84.12 and ADL67.10 have a smooth, continuous appearance (Fig. 1e′, f′). ADL101 has also been shown to fade during late oogenesis [46], in contrast to ADL84.12 or ADL67.10. Thus, ADL84.12 and ADL67.10 are preferred for observing nurse cell nuclear architecture, especially during the final stages of oogenesis when the nurse cells die by non-apoptotic means.

1. Fix the tissue as described in the DAPI Staining procedure (Subheading 3.2, **steps 1** and **2**).
2. Wash 3× with 1× PBT, rotating for 20 min each time (*see* **Note 4**).
3. Remove the PBT and add PBANG for blocking. Rotate for 1 h (*see* **Note 4**).
4. Incubate in primary antibody diluted in PBANG (*see* Subheading 2.4, **item 1** for proper dilutions), rotating overnight at 4 °C (*see* **Note 18**).
5. Remove the antibody (*see* **Note 19**) and rinse 2× with 1× PBT.

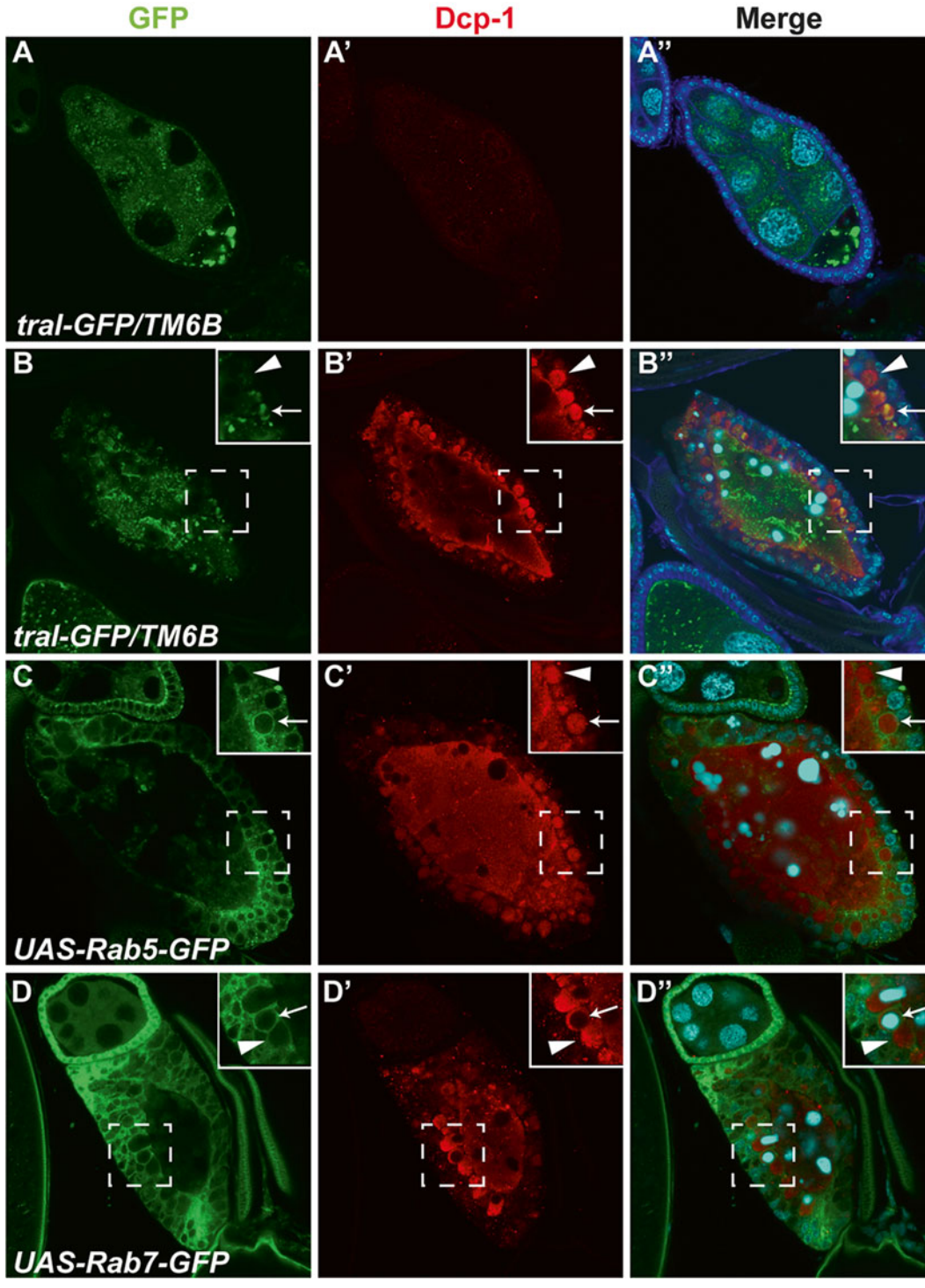

Fig. 2 Cell death and clearance in mid-oogenesis. Flies expressing different GFP fusion transgenes were stained with DAPI (*cyan*), active caspase Dcp-1 (*red*), and Discs large (*blue*, **a** and **b** only). (**a**–**a**″) Healthy egg chambers expressing *tral-GFP* show germline GFP (**a**) but no Dcp-1 expression (**a**′). (**b**–**b**″) Dying egg chambers expressing *tral-GFP* show germline GFP (**b**) and Dcp-1 (**b**′) engulfment. The vesicles that stain positively for both GFP and Dcp-1 are marked with an *arrow*, while vesicles that stain positively for only Dcp-1 are marked with an *arrowhead*. Dying egg chambers expressing either Rab5-GFP (**c**–**c**″) or Rab7-GFP (**d**–**d**″) in the follicle cells show some Dcp-1-positive vesicles that are positive for Rab5 or Rab7 (*arrows*), but some that are not (*arrowheads*)

6. Wash 4× with 1× PBTB, rotating for 30 min each time (*see* **Note 4**).
7. Incubate in secondary antibody diluted in PBANG (*see* **Note 20** and Subheading 2.4, **item 2** for proper dilutions), rotating for 1 h, in the dark.
8. Remove secondary antibody and rinse 2× with 1× PBT.
9. Wash 4× with 1× PBTB, rotating for 30 min each time, in the dark.
10. Rinse 1× with 1× PBS.
11. Add ~2 drops of VECTASHIELD with DAPI and store at 4 °C, in the dark, overnight (*see* **Note 5**).
12. Transfer the tissue to a microscope slide using a glass Pasteur pipette (*see* **Note 6**).
13. Tease apart the ovarioles using tungsten needles, add a coverslip, and seal with nail polish (*see* **Note 7**).
14. View on a fluorescence or confocal microscope using filters appropriate for the secondary antibodies. Representative images for lamin staining in late oogenesis are shown in Fig. 1, while representative images for active Dcp-1 and Dlg in mid-oogenesis are shown in Fig. 2.

4 Notes

1. If CO_2 pads are not available, flies can be anesthetized using ice. Take a thin platform, place it in the ice, transfer your flies to a vial without food, and place it on ice. Remove the platform from the ice and knock your flies onto it to visualize them with a dissecting microscope. This alternative method should be used with caution, as the flies do not stay asleep for very long.
2. If the ovaries are difficult to pull out, one can alternatively press down on the top of the abdomen with forceps and push the ovaries out.
3. For live dyes or antibodies that do not permeate the tissue well, tease apart the ovaries before transferring them to a microcentrifuge tube.
4. All washes in the DAPI or antibody staining protocols can be extended, when needed. If you need to perform washes overnight, place the tissue at 4 °C.
5. If there is a rush to observe your tissue, leave the tissue at room temperature in the dark for 2–4 h and the DAPI will permeate most of the tissue.
6. Be sure to keep the tissue and the VECTASHIELD with DAPI medium in the narrow part of the glass Pasteur pipette to prevent tissue loss due to tissue sticking to the walls of the pipette.

7. If there is excess DAPI/mounting medium, gently press down on the coverslip with a Kimwipe before sealing the slide with nail polish.
8. Shorter permeabilization times have been described in the literature [16] and different times can be used for optimization if necessary.
9. The equilibration buffer is a limiting reagent in the DeadEnd TUNEL kit from Promega if used in excess. We find that 20 μl is sufficient to cover ovaries dissected from 7 to 10 flies. More equilibration buffer may be used if needed to cover more tissue, but not enough is provided to liberally bathe the tissue.
10. Turn on hot water bath at this point so that it can reach 37 °C by the time it is needed.
11. Do not rotate at this step or most tissue will likely get stuck along the walls of the tube.
12. The solutions may be added one at a time to each sample or premixed immediately prior to use.
13. Keep the rTdT enzyme on ice at all times.
14. Be sure to shake the SSC solution to ensure the salts have dissolved.
15. A wide range of LysoTracker dilutions (1:50–1:600) can be used to label the ovarian tissue. Different concentrations can be tested to maximize the signal and reduce the background.
16. Do not wash the tissue in PBT prior to fixing as this will adversely affect the LysoTracker labeling.
17. Microcentrifuge tubes are not protected from light at this point since the incubation time is quick and it is important to flick the microcentrifuge tubes during this time and visually ensure that all tissue stays in the liquid and is not accidentally flicked onto the wall of the microcentrifuge tube.
18. For certain antibodies (including Dcp-1, Dlg, and DCAD2), a 2 h incubation at room temperature is sufficient.
19. Most antibodies (including Dcp-1, Dlg, DCAD2, and Draper) can be reused a few times before they lose their effectiveness.
20. Mix up the secondary antibody immediately before use.

Acknowledgements

We obtained antibodies from the Developmental Studies Hybridoma Bank developed under the auspices of the NIHCD and maintained by the University of Iowa, Department of Biology, Iowa City, IA 52242. We would also like to thank the Bloomington

Stock Center, FlyTrap, and Trudi Schöpbach for flies, and NIH RO1 grants GM060574 and GM094452 for funding. Lastly, we would like to thank members of the McCall lab for edits and discussions.

References

1. Hanayama R, Tanaka M, Miyasaka K et al (2004) Autoimmune disease and impaired uptake of apoptotic cells in MFG-E8-deficient mice. Science 304:1147–1150
2. Kawane K, Fukuyama H, Kondoh G et al (2001) Requirement of DNase II for definitive erythropoiesis in the mouse fetal liver. Science 292:1546–1549
3. Kawane K, Ohtani M, Miwa K et al (2006) Chronic polyarthritis caused by mammalian DNA that escapes from degradation in macrophages. Nature 443:998–1002
4. Gorman AM (2008) Neuronal cell death in neurodegenerative diseases: recurring themes around protein handling. J Cell Mol Med 12: 2263–2280
5. Calissano P, Matrone C, Amadoro G (2009) Apoptosis and in vitro Alzheimer disease neuronal models. Commun Integr Biol 2:163–169
6. Jenkins VK, Timmons AK, McCall K (2013) Diversity of cell death pathways: insight from the fly ovary. Trends Cell Biol 23:567–574
7. McCall K (2004) Eggs over easy: cell death in the *Drosophila* ovary. Dev Biol 274:3–14
8. Pritchett TL, Tanner EA, McCall K (2009) Cracking open cell death in the *Drosophila* ovary. Apoptosis 14:969–979
9. Thomson TC, Fitzpatrick KE, Johnson J (2010) Intrinsic and extrinsic mechanisms of oocyte loss. Mol Hum Reprod 16:916–927
10. Di Bartolomeo S, Nazio F, Cecconi F (2010) The role of autophagy during development in higher eukaryotes. Traffic 11:1280–1289
11. King RC (1970) Ovarian development in *Drosophila melanogaster*. Academic, New York
12. Spradling AC (1993) Developmental genetics of oogenesis. Cold Spring Harbor Laboratory Press, Cold Spring Harbor
13. Drummond-Barbosa D, Spradling AC (2001) Stem cells and their progeny respond to nutritional changes during *Drosophila* oogenesis. Dev Biol 231:265–278
14. Smith JE III, Cummings CA, Cronmiller C (2002) *Daughterless* coordinates somatic cell proliferation, differentiation and germline cyst survival during follicle formation in *Drosophila*. Development 129:3255–3267
15. Panagopoulos DJ, Chavdoula ED, Nezis IP et al (2007) Cell death induced by GSM 900-MHz and DCS 1800-MHz mobile telephony radiation. Mutat Res 626:69–78
16. Hou CY-C, Chittaranjan S, Barbosa SG et al (2008) Effector caspase Dcp-1 and IAP protein Bruce regulate starvation-induced autophagy during *Drosophila melanogaster* oogenesis. J Cell Biol 182:1127–1139
17. Fast EM, Toomey ME, Panaram K et al (2011) *Wolbachia* enhance *Drosophila* stem cell proliferation and target the germline stem cell niche. Science 18:990–992
18. Giorgi F, Deri P (1976) Cell death in ovarian chambers of *Drosophila melanogaster*. J Embryol Exp Morphol 35:521–533
19. Etchegaray JI, Timmons AK, Klein AP et al (2012) Draper acts through the JNK pathway to control synchronous engulfment of dying germline cells by follicular epithelial cells. Development 139:4029–4039
20. Mazzalupo S, Cooley L (2006) Illuminating the role of caspases during *Drosophila* oogenesis. Cell Death Differ 13:1950–1959
21. Tanner EA, Blute TA, Brachmann CB et al (2011) Bcl-2 proteins and autophagy regulate mitochondrial dynamics during programmed cell death in the *Drosophila* ovary. Development 138:327–338
22. Nezis IP, Stravopodis DJ, Papassideri I et al (2000) Stage-specific apoptotic patterns during *Drosophila* oogenesis. Eur J Cell Biol 79: 610–620
23. Peterson JS, Barkett M, McCall K (2003) Stage-specific regulation of caspase activity in *Drosophila* oogenesis. Dev Biol 260:113–123
24. Laundrie B, Peterson JS, Baum JS et al (2003) Germline cell death is inhibited by P-element insertions disrupting the *dcp-1/pita* nested gene pair in *Drosophila*. Genetics 165:1881–1888
25. Peterson JS, McCall K (2013) Combined inhibition of autophagy and casapase fails to prevent developmental nurse cell death in the *Drosophila melanogaster* ovary. PLoS One 8
26. Florentin A, Arama E (2012) Caspase levels and execution efficiencies determine the apoptotic potential of the cell. J Cell Biol 196:513–527

27. Williams DW, Kondo S, Kryzanowska A et al (2006) Local caspase activity directs engulfment of dendrites during pruning. Nat Neurosci 9:1234–1236
28. Sarkissian T, Timmons A, Arya R et al (2014) Detecting apoptosis in *Drosophila* tissues and cells. Methods 68:89–96
29. Fogarty C, Bergmann A (2014) Detecting caspase activity in *Drosophila* larval imaginal discs. Methods Mol Biol 1133:109–117
30. Timmons AK, Meehan TL, Gartmond TD et al (2013) Use of necrotic markers in the *Drosophila* ovary. Methods Mol Biol 1004:215–228
31. Fishilevich E, Fitzpatrick JAJ, Minden JS (2010) pHMA, a pH-sensitive GFP reporter for cell engulfment, in *Drosophila* embryos, tissues, and cells. Dev Dyn 239:559–573
32. Shklyar B, Shklover J, Kurant E (2013) Live imaging of apoptotic cell clearance during *Drosophila* embryogenesis. J Vis Exp. 18
33. Silva EA, Burden J, Franc NC (2008) Chapter 3 In vivo and in vitro methods for studying apoptotic cell engulfment in *Drosophila*. Methods Enzymol 446:39–59
34. White K, Lisi S, Kurada P et al (2001) Methods for studying apoptosis and phagocytosis of apoptotic cells in *Drosophila* tissues and cell lines. Methods Cell Biol 66:321–338
35. Parnas D, Haghighi AP, Fetter RD et al (2001) Regulation of postsynaptic structure and protein localization by the Rho-type guanine nucleotide exchange factor dPix. Neuron 32: 415–424
36. Oda H, Uemura T, Harada Y et al (1994) A *Drosophila* homolog of cadherin associated with armadillo and essential for embryonic cell-cell adhesion. Dev Biol 165:716–726
37. Riemer D, Stuurman N, Berrios M et al (1995) Expression of *Drosophila* lamin C is developmentally regulated: analogies with vertebrate A-type lamins. J Cell Sci 108:3189–3198
38. Stuurman N, Maus N, Fisher PA (1995) Interphase phosphorylation of the *Drosophila* nuclear lamin: site-mapping using a monoclonal antibody. J Cell Sci 108:3137–3144
39. Hudson AM, Cooley L (2014) Methods for studying oogenesis. Methods 68:207–217
40. Goentoro LA, Yakoby N, Goodhouse J et al (2006) Quantitative analysis of the GAL4/UAS system in *Drosophila* oogenesis. Genesis 44:66–74
41. Frydman HM, Spradling AC (2001) The receptor-like tyrosine phosphatase Lar is required for epithelial planar polarity and for axis determination within *Drosophila* ovarian follicles. Development 128:3209–3220
42. Baum JS, Arama E, Steller H et al (2007) The *Drosophila* caspases Strica and Dronc function redundantly in programmed cell death during oogenesis. Cell Death Differ 14:1508–1517
43. Klionsky DJ, Abdalla FC, Abeliovich H et al (2012) Guidelines for the use and interpretation of assays for monitoring autophagy. Autophagy 8:445–544
44. Golstein P, Kroemer G (2006) Cell death by necrosis: towards a molecular definition. Trends Biochem Sci 32:37–43
45. Barth J, Szabad J, Hafen E et al (2011) Autophagy in *Drosophila* ovaries is induced by starvation and is required for oogenesis. Cell Death Differ 18:915–924
46. McCall K (1998) Requirement for DCP-1 caspase during *Drosophila* oogenesis. Science 279:230–234

Chapter 15

Analysis of Cell Cycle Switches in *Drosophila* Oogenesis

Dongyu Jia, Yi-Chun Huang, and Wu-Min Deng

Abstract

The study of *Drosophila* oogenesis provides invaluable information about signaling pathway regulation and cell cycle programming. During *Drosophila* oogenesis, a string of egg chambers in each ovariole progressively develops toward maturity. Egg chamber development consists of 14 stages. From stage 1 to stage 6 (mitotic cycle), main-body follicle cells undergo mitotic divisions. From stage 7 to stage 10a (endocycle), follicle cells cease mitosis but continue three rounds of endoreduplication. From stage 10b to stage 13 (gene amplification), instead of whole genome duplication, follicle cells selectively amplify specific genomic regions, mostly for chorion production. So far, *Drosophila* oogenesis is one of the most well studied model systems used to understand cell cycle switches, which furthers our knowledge about cell cycle control machinery and sheds new light on potential cancer treatments. Here, we give a brief summary of cell cycle switches, the associated signaling pathways and factors, and the detailed experimental procedures used to study the cell cycle switches.

Key words Endocycle, Mitotic cycle, Gene amplification, *Drosophila* oogenesis, Follicle cell

1 Introduction

In *Drosophila*, the female has two ovaries, each of which is composed of 16–20 ovarioles. The ovariole is a string of progressively developing egg chambers. Each egg chamber, the developmental unit of oogenesis, consists of 16 germ-line cells, one oocyte and 15 nurse cells, covered by a single layer of somatic follicle cells [1]. Egg chamber development is divided into 14 stages. Based on the cell cycle programs of the main-body follicle cells, egg chamber stages are further grouped into three different categories: the mitotic cycle (stages 1–6), the endocycle (stages 7–10a), and gene amplification (stages 10b–13). A stage-14 egg chamber is the mature egg, ready to be laid. During the mitotic cycle, the main-body follicle cells undergo mitotic divisions for a total of 8–9 rounds with complete cell cycles (G1, S, G2, M phases), increasing the follicle cell number to approximately 650 [2, 3]. During the endocycle, follicle cells continue an additional three rounds of endoreduplication without dividing, skipping the G2 and M phases.

Diana P. Bratu and Gerard P. McNeil (eds.), *Drosophila Oogenesis: Methods and Protocols*, Methods in Molecular Biology, vol. 1328, DOI 10.1007/978-1-4939-2851-4_15,

During gene amplification, the follicle cells cease whole genome duplication, and instead selectively amplify specific genomic regions, mostly related to chorion (egg shell) production [4–7].

For more than a decade, researchers have intensively studied oogenesis to understand how *Drosophila* precisely control mitotic cycle/endocycle (M/E) and endocycle/gene amplification (E/A) switches during oogenesis. Many publications, including ours, have provided evidence that the Notch pathway is a key player in regulating the switches of the cell cycle programs in egg chamber development, which signals between the germ line and follicle cells to coordinate their development [8, 9]. Notch signaling activation at stages 6/7 transitions the mitotic cycle into the endocycle and its inactivation at stages 10a/10b switches the endocycle into gene amplification [4, 10–12]. In addition to Notch signaling, other pathways also have been found involved in cell cycle regulation. The Hippo pathway promotes Notch signaling during the M/E switch [13]. Shaggy and Disheveled, downstream factors of the Wingless pathway, independently potentiate Notch signaling for the M/E switch [14, 15]. Ecdysone signaling activity at stage 10b is required in main-body follicle cells for proper entry into gene amplification [12].

Here, we discuss the methods used to analyze cell cycle switches using available markers and reporters. Follicle cells undergo rounds of complete cell cycles (G1, S, G2, M phases) in mitotic cycle, but skip G2 and M phases during the endocycle and gene amplification. Antibodies against mitotic cell cycle markers, including Cyclin A (CycA) for labeling G2 and M phases, Cyclin B (CycB) and Phospho-Histone-3 (PH3) for M phase, can be applied in follicle cells to specifically mark the mitotic cycle. Otherwise, absence of these mitotic markers suggests follicle cells have ceased mitosis. For S phase detection, the presence of Cyclin E (CycE), MPM2 (Anti-phospho-Ser/Thr-Pro), dE2F1, Origin recognition complex (ORC) and incorporation of Bromodeoxyuridine (5-bromo-2′-deoxyuridine, BrdU) is crucial. CycE together with Cyclin-dependent kinase 2 (cdk2) is required for the G1/S transition. The MPM2 antibody has been developed to recognize the CycE/Cdk2-dependent phosphoepitope at the histone locus body [16]. The ORC is required for gene replication during S phase, and dE2F1 restricts the ORC2 to amplification foci [12, 17]. BrdU is an analog of thymidine, which has been applied to the detection of newly synthesized DNA. CycE, dE2F1, MPM2-staining, ORC2 and BrdU-incorporation oscillate during the mitotic cycle and the endocycle, which changes to uniform expression during gene amplification as main-body follicle cells synchronously allow specific genomic regions to be replicated. Antibodies against CycE and dE2F1 present donut-like staining at stage 10b, while MPM2,

ORC2, and BrdU staining show a unique foci-like pattern [5, 12, 17]. Failure to detect a uniform CycE, dE2F1, MPM2, ORC2, and BrdU pattern at stage 10b would be indicative of a defective E/A switch. Newly developed FLY-FUCCI lines (available from the Bloomington *Drosophila* stock center) have worked successfully in imaginal discs and some other tissues to distinguish G1, S, G2 phases [18]. Unfortunately, ubi-mRFP-CycB, a key component of the FLY-FUCCI system, is not detectable in the egg chamber system (our lab unpublished data). However, FLY-FUCCI UAS lines still represent a possible way to identify the cell cycle phase of each follicle cell. Besides cell cycle markers, some cell fate markers may also be used to indicate cell cycles. In early oogenesis, main-body follicle cells are not fully differentiated and can be labeled with Fasciclin III (FasIII) and Eye absent (Eya), which are considered immature cell fate markers. Later, in endocycling ("mature") main-body follicle cells, FasIII is no longer detectable and Eya expression is severely reduced between stages 7 and 8 before becoming completely absent after stage 8 [5, 6, 19]. Thus, main-body follicle cells labeled by FasIII and Eya maintain an immature cell fate, suggesting they are in the mitotic cycle program. Moreover, some signaling pathway reporters and transcription factors can identify the cell cycle program in follicle cells as well, such as the Notch signaling reporters *E(spl)mβ-CD2* [20], *E(spl)m7-lacZ* [21], *Gbe+Su(H)m8-lacZ* [22], and *NRE-EGFP* [23] and its downstream factors Cut, Hindsight (Hnt), and Broad (Br) [5, 6, 19]. Hnt, Br, and Notch signaling reporters are upregulated by Notch signaling during the M/E switch, while Cut, a Notch negative target during oogenesis, is suppressed. Br has been confirmed to be directly regulated by Notch signaling via the *brE* enhancer [19]. Defective Notch activity has been shown to disrupt the M/E and E/A switches, and corresponding cell cycle programs as well. There is also a Zinc-finger protein, Tramtrack (Ttk), which must be dramatically upregulated at stage 10b for proper gene amplification entry [12]. All markers and reporters mentioned above are summarized in Fig. 1. Additionally, ploidy of DAPI-stained follicle cell nuclei can be estimated based on nuclear volume, and applying fluorescence-activated cell sorting (FACS) analysis can select specific groups of cells to further determine DNA copy number and thus decipher their endocycle progression. Mitotic cycling follicle cells are diploid, showing a 2C peak by FACS analysis. Endocycling follicle cells undergo three rounds of endoreduplication, demonstrating distinctive 4C, 8C, and 16C peaks. Follicle cells that undergo an extra cell cycle can be determined by the appearance of a 32C peak (*see* [12]). Follicle cells with defective endocycle progression show a reduced 16C peak. Detailed experimental procedures are illustrated below.

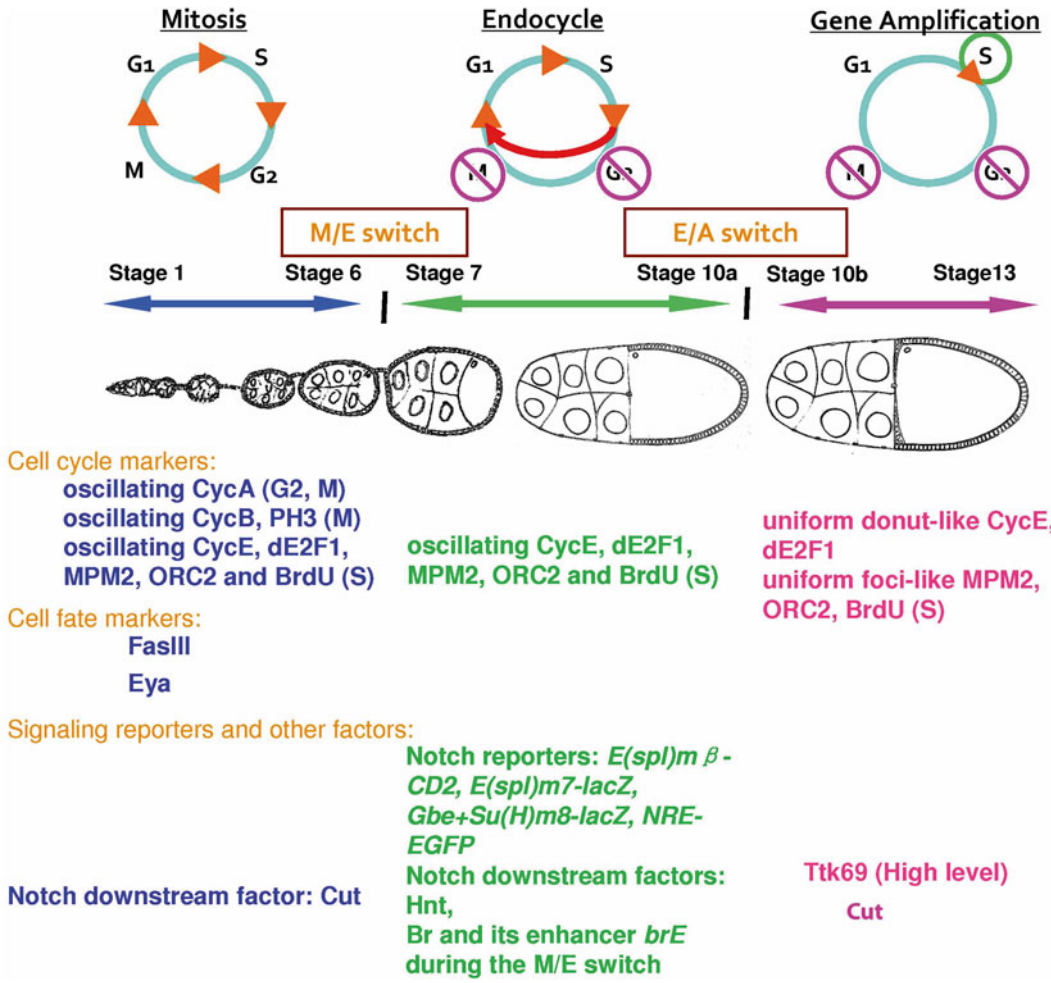

Fig. 1 The cell cycle switches during *Drosophila* oogenesis. Follicle cells undergo a mitotic cycle (stages 1–6, complete G1, S, G2, M phases), an endocycle (stages 7–10a, G1, S phases), and gene amplification (stages 10b–13, DNA synthesis at specific genomic loci). Specific cell cycle markers (CycA, CycB, PH3, CycE, dE2F1, MPM2, ORC2, BrdU), cell fate markers (FasIII, Eya), and signaling reporters and factors (*E(spl)mβ-CD2*, *E(spl)m7-lacZ*, *Gbe+Su(H)m8-lacZ*, *NRE-EGFP*, Hnt, Br, *brE*, Cut, Ttk) can be applied to determine the follicle cell cycle programs

2 Materials

2.1 Fly Stocks

Notch activity reporters: *E(spl)mβ-CD2* [20], *E(spl)m7-lacZ* [21], *Gbe+Su(H)m8-lacZ* [22], *NRE-EGFP* (#30727, #30728; Bloomington *Drosophila* Stock Center) [23], *brE-GFP* and *brE-lacZ* [19, 24].

2.2 Antibodies

1. Primary antibodies :Rabbit anti-CycA 1:500 (provided by C. Lehner, University of Zurich, Zurich, Switzerland), mouse

anti-CycB 1:5 (F2F4; Developmental Studies Hybridoma Bank, DSHB), guinea pig anti-CycE 1:500 (provided by T. Orr-Weaver, Whitehead Institute, Cambridge, MA), rabbit anti-PH3 1:200 (Ser10, Millipore), mouse anti-BrdU 1:50 (BD Biosciences), mouse anti-FasIII 1:15 (7G10; DSHB), mouse anti-Eya 1:10 (10H6; DSHB), mouse anti-CD2 1:50 (AbD Serotec), rabbit anti-β-galactosidase 1:2000 (MP Biomedicals), mouse anti-β-galactosidase 1:500 (Promega), rabbit anti-Cut 1:500 (provided by Y.N. Jan, University of California, San Francisco, CA), mouse anti-Cut 1:15 (2B10; DSHB), anti-Hnt 1:15 (1G9; DSHB), mouse anti-Br-core 1:30 (25E9; DSHB), rabbit anti-Ttk69 and rat anti-Ttk69 1:200 (provided by P. Badenhorst, University of Birmingham, Edgbaston, Birmingham, UK), guinea pig anti-dE2F1 1:500 (provided by T. Orr-Weaver, Whitehead Institute, Cambridge, MA), rabbit anti-ORC2 1:3000 (provided by S.P. Bell, Whitehead Institute, Cambridge, MA), mouse anti-Ser/Thr-ProMPM-2 1:1000 (Millipore).

2. Secondary antibodies: According to primary antibodies, select corresponding Alexa Fluor 488, 546, or 633 secondary antibodies at a dilution of 1:400.

2.3 Reagents

1. 1× PBS: 137 mM NaCl, 2.7 mM KCl, 10 mM Na_2HPO_4, 1.8 mM KH_2PO_4.
2. 1× PBT: 1× PBS supplemented with 0.2 % Triton™ X-100.
3. 1× PBT (0.4 % T): 1× PBS supplemented with 0.4 % Triton™ X-100.
4. Grace's insect medium.
5. Fix solution: 4 % formaldehyde (EM Grade) in 1× PBS.
6. PBTG: 0.2 % bovine serum albumin, 5 % normal goat serum in 1× PBT.
7. Mounting solution: 1 g *n*-propyl gallate, 5 ml of 10× PBS, 40 ml of glycerol and 5 ml of dH_2O.
8. Buffer B: 100 mM KH_2PO_4/K_2HPO_4, pH 6.8, 450 mM KCl, 150 mM NaCl, 20 mM $MgCl_2$.
9. DNase I.
10. DNase I reaction buffer: 3.3 ml of 1 M Tris-HCl, pH 7.5, 0.125 ml of 2 M $MgCl_2$, 0.004 ml of 2-mercaptoethanol (98 %) and 46.575 ml of dH_2O.
11. 10 % fetal calf serum.
12. BrdU.
13. DAPI (10 μg/ml) for DNA/nuclei staining.
14. 0.25 % trypsin (diluted in 1× PBS).

2.4 Equipment

1. Dissecting forceps.
2. Embryo dish.
3. CO_2 tank and pad.
4. Centrifuge for eppendorf tubes.
5. Nutator.
6. Stereoscopic (dissecting) microscope.
7. Confocal microscope.
8. Flow cytometer.

3 Methods

3.1 Classic Immunostaining of Ovaries [25]

1. Feed the flies with yeast for 2–3 consecutive days before dissection (*see* **Note 1**).
2. Fill the embryo dish with 3 ml of 1× PBS.
3. Anesthetize the flies on a CO_2 pad.
4. Select a female fly, then use a pair of dissecting forceps to gently grab the lower thorax and submerge it into a 1× PBS solution in the embryo dish.
5. Pinch the lower abdomen with another pair of forceps, then pull gently to expose the internal organs.
6. Find the pair of ovaries and detach them from the fly body.
7. At the posterior end of the ovaries, break the muscular sheath and tease apart the ovarioles (*see* **Note 2**).
8. Transfer the ovaries into 500 μl of 1× PBS into a 1.5 ml eppendorf tube, while placing the tube on ice until enough ovaries are collected.
9. Remove the 1× PBS and add 0.5 ml of fix solution.
10. Place the tube to rock on a nutator for 10 min.
11. Remove the fix solution and discard in an appropriate waste container.
12. Wash the ovaries 3 × 15 min in 1 ml of 1× PBT.
13. Remove last PBT wash and add 1 ml of PBTG to block nonspecific binding. Rock on a nutator for 1 h at room temperature or overnight at 4 °C.
14. Remove the PBTG, add 150 μl of primary antibody (select desired markers to test for cell cycle switches). Incubate overnight at 4 °C with rocking (*see* **Notes 3–5**).
15. Remove the primary antibody (return to a 1.5 ml eppendorf tube for reuse) and wash 3 × 15 min with 1 ml of 1× PBT.
16. Add 150 μl of secondary antibody, incubate for 2 h at room temperature or overnight at 4 °C with rocking.

17. Remove the secondary antibody (return to a 1.5 ml eppendorf tube for reuse) and wash 2 × 15 min with 1 ml of 1× PBT.
18. Add 150 µl of DAPI (10 µg/ml) for 10–15 min.
19. Remove the DAPI and wash 1 × 10 min with 1 ml of 1× PBT.
20. Discard the PBT and wash 2 × 10 min with 1 ml of 1× PBS.
21. Remove the PBS leaving about 300 µl in the tube with the ovaries.
22. Using a 200 µl pipette tip, pipet the ovaries up and down several times to free the egg chambers.
23. Spin down slightly and remove as much 1× PBS as possible.
24. Add 120 µl of mounting solution (*see* **Note 6**).
25. Cut approximately 0.3 mm off the tip of a 200 µl pipette tip, then use it to transfer the mounting solution with the egg chambers to a microscope glass slide.
26. Cover the solution with a coverslip glass and seal the edges with nail polish (*see* **Notes 7** and **8**).

3.2 BrdU Incorporation Assay

1. For dissection the ovaries follow the **steps 1–8** in Subheading 3.1, except replace the 1× PBS solution with Grace's insect medium.
2. Remove the ovaries from Grace's insect medium into 1 ml of a BrdU solution (0.5 mg/ml BrdU in Grace's insect medium). Incubate for 1 h at room temperature.
3. Remove the BrdU solution and discard in an appropriate waste container. Wash 2 × 3 min with 1 ml of 1× PBS.
4. Remove and discard the 1× PBS. Fix the ovaries for 15 min in 500 µl of fix solution (32 % EM grade formaldehyde, Buffer B, and H_2O at 1:1:4).
5. Remove the fix solution and discard in an appropriate waste container. Wash 2 × 15 min with 1 ml of 1× PBT.
6. Remove and discard the PBT. Wash the ovaries 2 × 15 min with 1 ml of DNase I reaction buffer.
7. Remove the DNase I reaction buffer and discard in sink. Add DNase I (0.1 U/µl) in 1 ml of DNase I reaction buffer. Incubate for at least 45 min at 37 °C. Remove and discard the DNase I and the buffer.
8. Wash 3 × 1 min with 1 ml of 1× PBT.
9. Wash 2 × 15 min with 1 ml of 1× PBT.
10. For anti-BrdU antibody labeling, DAPI staining, and preparing the ovaries for mounting, follow the **steps 13–26** as described in Subheading 3.1.

3.3 Fluorescence-Activated Cell Sorting (FACS) Analysis [12, 26]

1. Follow the steps in Subheading 3.1 **step 1–8**, except replace the 1× PBS solution with Grace's insect medium, supplemented with 10 % fetal calf serum and 1× antibiotic–antimycotic. Approximately 80–150 females per experiment are needed for dissection.
2. Wash the ovaries 3 × 2 min in 1 ml of 1× PBS.
3. Incubate the ovaries for 15 min in 0.7 ml of 0.25 % trypsin (diluted in 1× PBS) with intermittent vortexing at room temperature.
4. To isolate the follicle cells, remove the supernatant and pass it through a 40-μm nylon filter into 1 ml of Grace's insect medium.
5. Centrifuge at 1700 × *g* (4000 rpm) for 7 min.
6. Repeat the trypsinization and filtration steps 2–3× or until the supernatant becomes clear.
7. Resuspend the follicle cells in 0.5 ml of Grace's insect medium containing 1 μl of 5 mM Vybrant DyeCycle DNA-specific stain, and incubate for 30 min at room temperature.
8. Rinse 1× with 1 ml of 1× PBS and store on ice.
9. Use a flow cytometer to determine the follicle cell ploidy by FACS analysis of Vybrant DyeCycle-stained cell preparations with excitation at 407 nm for Vybrant DyeCycle stain and at 488 nm for GFP (*see* **Notes 9** and **10**).

4 Notes

1. It is important to feed flies with yeast for 2–3 consecutive days before dissection in order to fatten the ovaries prior to harvesting.
2. It is necessary to break the muscular sheath and tease apart the ovarioles, in order to obtain better antibody staining results.
3. For antibody staining, as long as the primary antibodies are not from the same species, they can be mixed and co-stained with corresponding secondary antibodies using in different fluorescence channels. However, in our experience, when BrdU incorporation is done it cannot co-stain with other antibodies. Although an EdU incorporation assay allows for co-staining, its quality is not as good as BrdU incorporation in follicle cells.
4. Some primary antibodies are very expensive or difficult to obtain. In this case, we suggest to reuse the antibodies. Exactly how many times they can be reused depends on the quality of the antibodies.
5. Sometimes, the quality of antibodies varies between lots/batches, including commercially available ones.

6. Since the mounting solution is very sticky, it is hard to transfer exactly 120 μl into a tube. As an easy alternative, use a 1000 μl pipette tip to transfer three drops of mounting solution into the tube.
7. The thickness of the cover glass depends on the confocal imaging system.
8. Sealing the edges of the cover glass is necessary to avoid the egg chambers from flowing inside of the mounting solution when taken for confocal imaging. The nail polish mentioned in **step 26**, Subheading 3.1 should be transparent.
9. From the FACS analysis, we can determine the 2C, 4C, 8C, 16C, and 32C peaks. Based on the results, follicle cells that undergo extra or fewer cell cycles can be determined.
10. Most importantly, keep in mind which cell cycle program is being tested and apply the corresponding primary antibodies to study the cell cycle switches.

Acknowledgements

We would like to thank Gabriel Calvin, Gengqiang Xie, Allison Jevitt, and Sarayu Row for critical reading of and comments on the manuscript. Special thanks to Jianjun Sun and other former and current members of the Deng lab for developing protocols on this topic; W.-M.D. is supported by NIH grant R01GM072562.

References

1. Spradling A (1993) Developmental genetics of oogenesis. The development of *Drosophila melanogaster*. Cold Spring Harbor Lab Press, New York
2. Nystul T, Spradling A (2010) Regulation of epithelial stem cell replacement and follicle formation in the *Drosophila* ovary. Genetics 184:503–515
3. Skora AD, Spradling AC (2010) Epigenetic stability increases extensively during *Drosophila* follicle stem cell differentiation. Proc Natl Acad Sci U S A 107:7389–7394
4. Calvi BR, Lilly MA, Spradling AC (1998) Cell cycle control of chorion gene amplification. Genes Dev 12:734–744
5. Sun J, Deng WM (2005) Notch-dependent downregulation of the homeodomain gene cut is required for the mitotic cycle/endocycle switch and cell differentiation in *Drosophila* follicle cells. Development 132:4299–4308
6. Sun J, Deng WM (2007) Hindsight mediates the role of notch in suppressing hedgehog signaling and cell proliferation. Dev Cell 12:431–442
7. Shyu LF, Sun J, Chung HM et al (2009) Notch signaling and developmental cell-cycle arrest in *Drosophila* polar follicle cells. Mol Biol Cell 20:5064–5073
8. Ruohola H, Bremer KA, Baker D et al (1991) Role of neurogenic genes in establishment of follicle cell fate and oocyte polarity during oogenesis in *Drosophila*. Cell 66:433–449
9. Xu T, Caron LA, Fehon RG et al (1992) The involvement of the Notch locus in *Drosophila* oogenesis. Development 115:913–922
10. Deng WM, Althauser C, Ruohola-Baker H (2001) Notch-Delta signaling induces a transition from mitotic cell cycle to endocycle in *Drosophila* follicle cells. Development 128: 4737–4746
11. Lopez-Schier H, St Johnston D (2001) Delta signaling from the germ line controls the proliferation and differentiation of the somatic follicle cells during *Drosophila* oogenesis. Genes Dev 15:1393–1405
12. Sun J, Smith L, Armento A et al (2008) Regulation of the endocycle/gene amplification

switch by Notch and ecdysone signaling. J Cell Biol 182:885–896

13. Yu J, Poulton J, Huang YC et al (2008) The hippo pathway promotes Notch signaling in regulation of cell differentiation, proliferation, and oocyte polarity. PLoS One 3:e1761
14. Axelrod JD, Matsuno K, Artavanis-Tsakonas S et al (1996) Interaction between Wingless and Notch signaling pathways mediated by dishevelled. Science 271:1826–1832
15. Jordan KC, Schaeffer V, Fischer KA et al (2006) Notch signaling through tramtrack bypasses the mitosis promoting activity of the JNK pathway in the mitotic-to-endocycle transition of *Drosophila* follicle cells. BMC Dev Biol 6:16
16. White AE, Leslie ME, Calvi BR et al (2007) Developmental and cell cycle regulation of the *Drosophila* histone locus body. Mol Biol Cell 18:2491–2502
17. Royzman I, Austin RJ, Bosco G et al (1999) ORC localization in *Drosophila* follicle cells and the effects of mutations in dE2F and dDP. Genes Dev 13:827–840
18. Zielke N, Korzelius J, van Straaten M et al (2014) Fly-FUCCI: A versatile tool for studying cell proliferation in complex tissues. Cell Rep 7:588–598
19. Jia D, Tamori Y, Pyrowolakis G et al (2014) Regulation of broad by the Notch pathway affects timing of follicle cell development. Dev Biol 392:52–61
20. de Celis JF, Tyler DM, de Celis J et al (1998) Notch signalling mediates segmentation of the *Drosophila* leg. Development 125:4617–4626
21. Assa-Kunik E, Torres IL, Schejter ED et al (2007) *Drosophila* follicle cells are patterned by multiple levels of Notch signaling and antagonism between the Notch and JAK/STAT pathways. Development 134:1161–1169
22. Furriols M, Bray S (2001) A model Notch response element detects Suppressor of Hairless-dependent molecular switch. Curr Biol 11:60–64
23. Saj A, Arziman Z, Stempfle D et al (2010) A combined ex vivo and in vivo RNAi screen for notch regulators in *Drosophila* reveals an extensive notch interaction network. Dev Cell 18:862–876
24. Fuchs A, Cheung LS, Charbonnier E et al (2012) Transcriptional interpretation of the EGF receptor signaling gradient. Proc Natl Acad Sci U S A 109:1572–1577
25. Wong LC, Schedl P (2006) Dissection of *Drosophila* ovaries. J Vis Exp 52
26. Bryant Z, Subrahmanyan L, Tworoger M et al (1999) Characterization of differentially expressed genes in purified *Drosophila* follicle cells: toward a general strategy for cell type-specific developmental analysis. Proc Natl Acad Sci U S A 96:5559–5564

Chapter 16

Global Run-On Sequencing (GRO-seq) Library Preparation from *Drosophila* Ovaries

Nikolay V. Rozhkov

Abstract

In the past decade, deep-sequencing approaches have greatly improved our knowledge of the genome's potential and have become a crucial milestone for new discoveries in genomics. Transcription is the first step of gene expression; therefore, the detection and measurement of transcription rates is of great interest. Here, a detailed protocol for global run-on sequencing (GRO-seq) library preparation from *Drosophila* ovaries is described. The method relies on rapid isolation of nuclei with halted transcription, then restarting transcription in physiological conditions in the presence of a labeled nucleotide. The newly transcribed nascent RNA is then isolated and cloned using a small RNA cloning protocol. Although it is time-consuming, the global run-on method allows the user to profile the position, orientation and amount of transcriptionally engaged RNA polymerases across the genome, therefore providing a snapshot of genome-wide transcription.

Key words *Drosophila*, Germline, GRO-seq, Nuclear Run-On, Nascent RNA, Transcriptome

1 Introduction

Next-generation sequencing of nucleic acids is a very powerful method to study various aspects of DNA, RNA and protein turnover in a cell [1, 2]. Recent years have witnessed numerous fundamental discoveries that led to phenomenal progress in RNA biology. For example, various RNA sequencing (RNA-seq) approaches have allowed researchers to sequence and identify millions of RNAs, termed noncoding RNAs, which are now recognized as important players in gene regulation and genome protection [3–5].

The steady-state level of a given RNA transcript represents a balance between the transcription rate and the stability of the RNA. Therefore, either transcriptional or post-transcriptional changes in gene expression will affect the RNA output as revealed by RNA-seq. Over the past 5 years, a battery of methods have been developed that can measure qualitative and quantitative outputs of

Diana P. Bratu and Gerard P. McNeil (eds.), *Drosophila Oogenesis: Methods and Protocols*, Methods in Molecular Biology, vol. 1328, DOI 10.1007/978-1-4939-2851-4_16,

RNA from the moment of its synthesis by RNA polymerase, as well as detecting post-transcriptional modifications and determining whether the RNA is translated [6–9]. Assessing nascent RNA synthesis is of particular interest, because it defines the dynamic state of transcription events and can detect transcripts that are prone to degradation and therefore may be difficult to detect by traditional RNA-seq.

There are a handful of genome-wide methods to measure nascent RNA transcription: global run-on sequencing (GRO-seq) and precision nuclear run-on sequencing (PRO-seq) [6, 10], native elongating transcript sequencing (NET-seq) [11], Nascent-seq [12], bromouridine sequencing (Bru-seq) and its derivation bromouridine-chase sequencing (BruChase-seq) [13]. The methods have various advantages and limitations; some approaches are suitable for use both in vivo and in vitro, whereas some are mainly used in in vitro systems. Here, a detailed protocol is described for GRO-seq library preparation from *Drosophila* ovaries that we used together with chromatin immunoprecipitation in our recent study to dissect the role of Piwi in transcriptional silencing of transposable elements in *Drosophila* [14].

This GRO-seq method allows the user to profile the position, orientation and amount of transcriptionally engaged RNA polymerases throughout the genome, therefore providing a snapshot of genome-wide transcription. It is based on rapid isolation of nuclei, subsequent run-on with a ribonucleotide analog (BrUTP) and immunoaffinity isolation of nuclear run-on RNA (NRO-RNA). The NRO-RNA is further cloned using a small RNA cloning protocol and repeatedly immunopurified with anti-BrUTP [6, 15] (Fig. 1). Although the method is time-consuming and requires triple immunoprecipitations of NRO-RNA, it is being widely used by the scientific community and has become a gold standard for studies of transcription, along with traditional RNA-seq and chromatin immunoprecipitation of RNA-polymerase II (PolII ChIP) [16–18].

2 Materials

All solutions for the protocol must be freshly prepared and RNase-free. In order to reduce the risk of RNase activity, it is necessary to use nuclease-free water or DEPC-treated water for the preparation of all solutions, as well as the addition of RNase inhibitors to all RNA reactions. To avoid RNA and DNA loss throughout the protocol, it is recommended to use siliconized tubes with a low binding surface.

2.1 Sample Preparation

1. *Drosophila* ovaries (50–100 pairs) (*see* **Note 1**).
2. Eppendorf DNA LoBind tubes, 1.5 ml, PCR clean.

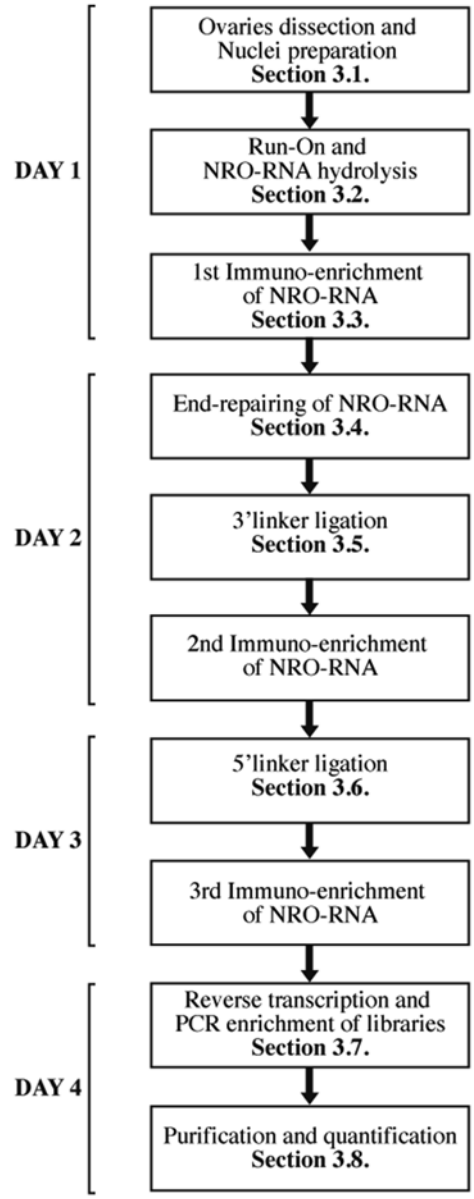

Fig. 1 Schematic overview of the major step in the GRO-seq protocol with potential stopping points

3. Phosphate-buffered saline (1× PBS): 137 mM NaCl, 2.7 mM KCl, 10 mM Na_2HPO_4, 2 mM KH_2PO_4, pH 7.4.
4. 1 ml tissue grinder, Dounce with "tight" pestle.
5. 1 M Dithiothreitol (DTT): Dissolve 1.5 g of DTT in 8 ml of H_2O. Adjust the total volume to 10 ml, make aliquots, and store them in the dark at −20 °C.

6. Complete Protease Inhibitor tablets (Roche).
7. Igepal CA-630 (Sigma).
8. SUPERase-In RNase Inhibitor (Life Technologies).
9. Nuclease-free H_2O (not DEPC-treated) or UltraPure DEPC-treated H_2O.
10. 0.35 M sucrose homogenization buffer (0.35 M-Sucrose HB): 0.35 M Sucrose, 10 mM Tris–HCl, pH 7.5, 10 mM KCl, 2.5 mM $MgCl_2$, 0.1 mM EDTA, 0.5 mM EGTA, 0.05 % NP-40 (Igepal CA-630), 1 mM DTT, 1 cOmplete Protease Inhibitor tablet, and 2 U/ml SUPERase-In. Add the DTT, the cOmplete Protease Inhibitor tablet, and the SUPERase-In to the buffer immediately before using.
11. 0.8 M sucrose homogenization buffer (0.8 M-Sucrose HB): 0.8 M sucrose, 10 mM Tris–HCl, pH 7.5, 10 mM KCl, 2.5 mM $MgCl_2$, 0.1 mM EDTA, 0.5 mM EGTA, 0.05 % NP-40 (Igepal CA-630), 1 mM DTT, 1 cOmplete Protease Inhibitor tablet, and 2 U/ml SUPERase-In. Add the DTT, the cOmplete Protease Inhibitor tablet, and the SUPERase-In to the buffer immediately before using.
12. Freezing buffer: 50 mM Tris–HCl, pH 8.3, 40 % glycerol, 5 mM $MgCl_2$, 0.1 mM EDTA, 1 mM DTT, and 2 U/ml SUPERase-In. Add the DTT and the SUPERase-In to the buffer immediately before using.
13. Liquid nitrogen.

2.2 Nuclear Run-On Reaction and NRO-RNA Hydrolysis

1. 2× Reaction buffer: 10 mM Tris–HCl, pH 8.0, 5 mM $MgCl_2$, 1 mM DTT, 300 mM KCl, 20 U of SUPERase-In, 1 % Sarkosyl, 500 μM ATP, GTP, and Br-UTP, 2.33 μM CTP.
2. TE buffer: 10 mM Tris–HCl, pH 8.0 and 1 mM EDTA.
3. 10 mM BrUTP (5-bromouridine 5′-triphosphate) in TE buffer.
4. Ribonucleoside triphosphate set: 100 mM of ATP, CTP, GTP, and UTP.
5. *N*-lauroylsarcosine sodium salt solution.
6. Cut-off 200 μl pipette tips (*see* **Note 2**).
7. TRIzol-LS (Life Technologies).
8. Acid phenol–chloroform, pH 4.5 (with isoamyl alcohol—IAA, 125:24:1).
9. Micro Bio-Spin™ P-30 Gel Columns, Tris-HCl Buffer (RNase-free) (Bio-Rad).
10. 1 M (1 N) NaOH, store aliquots at –20 °C.
11. 96 % ethanol.
12. GlycoBlue Coprecipitant (15 mg/ml).
13. Block heater.

2.3 Immunoprecipitation of NRO-RNA

1. Agarose conjugated BrdU antibody (IIB5).
2. UltraPure BSA (50 mg/ml).
3. Blocking buffer: 0.25× SSPE, 1 mM EDTA, 0.05 % Tween-20, 0.1 % PVP, and 1 mg/ml UltraPure BSA, 2 U/ml SUPERase-In.
4. Binding buffer: 0.2× SSPE, 37.5 mM NaCl, 1 mM EDTA, 0.05 % Tween 20, 2 U/ml SUPERase-In.
5. Low-salt buffer: 0.25× SSPE, 1 mM EDTA, 0.05 % Tween, 2 U/ml SUPERase-In.
6. High-salt buffer: 0.25× SSPE, 137.5 mM NaCl, 1 mM EDTA, 0.05 % Tween 20, 2 U/ml SUPERase-In.
7. TET buffer: 10 mM Tris–HCl, pH 7.5, 1 mM EDTA, 0.05 % Tween 20, 2 U/ml SUPERase-In.
8. Elution buffer: 5 mM Tris–HCl, pH 7.5, 300 mM NaCl, 1 mM EDTA, 20 mM DTT, and 0.1 % SDS, 2 U/ml SUPERase-In (*see* **Note 3**).

2.4 End-Repairing of NRO-RNA

1. T4 polynucleotide kinase (PNK), 10 U/μl.
2. Tobacco acid pyrophosphatase (TAP), 10 U/μl.
3. Adenosine 5′-triphosphate (ATP), 10 mM.

2.5 3′-Adapter Ligation

1. 3′-adapter (RA3), 100 μM: /5rApp/TGGAATTCTCG GGTGCCAAGG/3ddC/ (Illumina) (*see* **Note 4**).
2. T4 RNA ligase 2, truncated, 200 U/μl.
3. ATP-free buffer for T4 RNA ligase 2, truncated: 500 mM Tris–HCl, pH 7.5, 100 mM $MgCl_2$, 100 mM DTT, 600 μg/ml BSA. Aliquots should be stored at −20 °C (*see* **Note 5**).
4. 50 % PEG 8000.

2.6 5′-Adapter Ligation

1. 5′-adapter (RA5), 100 μM: rGrUrUrCrArGrArGrUrUrCr UrArCrArGrUrCrCrGrArCrGrArUrC.
2. T4 RNA Ligase 1, 10 U/μl with commercially supplied buffer.

2.7 Reverse Transcription and PCR Amplification

1. SuperScript® III Reverse Transcriptase (Life Technologies).
2. PCR Nucleotide Mix: 10 mM of dATP, dCTP, dGTP, and dTTP.
3. RT primer (RTP), 100 μM: GCCTTGGCACCCGAGAATTCC.
4. Ribonuclease H (RNase H), 2 U/μl.
5. Phusion® High-Fidelity PCR Master Mix with HF Buffer (NEB).
6. TruSeq primers:

Forward PCR primer (RP1), 50 μM: AATGATACGGCG ACCACCGAGATCTACACGTTCAGAGTTCTA CAGTCCGA.

Reverse PCR primer with Index (RPI), 50 μM: CAAGCAGAAGACGGCATACGAGAT **NNNNNN** GTGACTGGAGTTC CTTGGCACCCGAGAATTCCA, where **NNNNNN** is a six letters index (*see* Illumina Truseq sequences list for further details at http://truseq.illumina.com/truseq.html).

2.8 Purification and Quantification of GRO-seq Libraries

1. Phenol–chloroform–isoamyl alcohol (25:24:1) saturated with 10 mM Tris-HCl, pH 8.0, 1 mM EDTA.
2. Novex® TBE Gels, 6 %, 10 well (Life Technologies) or custom prepared gels.
3. Low Molecular Weight DNA Ladder.
4. Gel loading dye, 6× Orange.
5. Agilent DNA 1000 Kit (Agilent Technologies).
6. SYBR Gold.
7. Clean razor blade.
8. Spin X filtration tube.

3 Methods

3.1 Sample Preparation and Nuclei Isolation

1. Dissect 100 pairs of ovaries in 200 μl of 1× PBS on ice. Remove the PBS, add 300 μl of 0.35 M sucrose buffer, and transfer the ovaries to a prechilled 1 ml tissue grinder.
2. Homogenize the ovaries using a "tight" pestle; perform 20 strokes on ice.
3. Overlay the resulting homogenate onto a sucrose cushion containing 800 μl of 0.8 M sucrose buffer (bottom phase) and 300 μl of 0.35 M sucrose buffer (upper phase) in a 1.5 ml Eppendorf tube. Centrifuge for 10 min at 10,000×*g* (*see* **Note 6**).
4. Discard the supernatant and resuspend the nuclei pellet in 500 μl of freezing buffer. Centrifuge for 3 min at 10,000×*g*.
5. Discard the supernatant and resuspend the nuclei pellet in freezing buffer to make the final volume 100 μl.
6. Snap-freeze the nuclei in liquid nitrogen and store the samples at −80 °C indefinitely, or proceed to the next step immediately.

3.2 Run-On Reaction and NRO-RNA Hydrolysis

1. Mix 100 μl of nuclei with 100 μl of pre-warmed (30 °C) 2× reaction buffer; carefully pipet up and down with a cut-off 200 μl pipet tip 15–20 times, then place the tube in a pre-heated thermo block and allow the reaction to proceed for 2.5 min at 30 °C (*see* **Note 7**).

2. Pipet again while keeping the tubes in a thermo block, and continue the reaction for an additional 2.5 min, for a total reaction time of 5 min at 30 °C.
3. Stop the reaction by adding 3 volumes (600 μl) of TRIzol-LS and vortex for 30 s (*see* **Note 8**).
4. Add 1/5 volume (160 μl) of chloroform, vortex for 30 s, and then centrifuge for 10 min at 12,000 × *g* at 4 °C.
5. Transfer the upper phase to a new tube, and add an equal volume of acid phenol–chloroform. Vortex for 30 s and then centrifuge for 10 min at 12,000 × *g* at 4 °C.
6. Transfer the upper phase to a new tube and add an equal volume of chloroform. Vortex for 30 s and then centrifuge for 10 min at 12,000 × *g* at 4 °C.
7. Transfer the upper phase to a new tube containing 2 μl of GlycoBlue.
8. Precipitate the NRO-RNA by adding 0.7 volumes of 100 % isopropanol to the supernatant.
9. Incubate at −20 °C for 2 h or overnight.
10. Centrifuge at maximum speed for 30 min in a refrigerated centrifuge, wash the pelleted NRO-RNA with 75 % ethanol and dry the pellet for 2 min.
11. Dissolve the NRO-RNA pellet in 20 μl of nuclease-free H_2O. If needed, incubate at 50 °C for 5 min, vortex for 5 s, spin down and place on ice.
12. Add 5 μl of 1 M NaOH, mix by pipetting, and incubate on ice for 20 min.
13. Neutralize the reaction by adding 25 μl of 1 M Tris–HCl (pH 6.8). Vortex briefly.
14. Exchange the buffer by running the reaction through a Micro Bio-Spin P-30 Gel Column according to the manufacturer's protocol.
15. Bring the volume of the eluate to 100 μl with nuclease-free H_2O.

3.3 Immunoenrichment of NRO-RNA

All buffers should be supplemented with SUPERase-In and kept on ice. After each washing step, the agarose beads can be centrifuged in a cold centrifuge at 1000 × *g* for 30 s.

1. For each IP, pipet 60 μl of bead slurry into a 1.5 ml tube, and wash the beads twice by inverting and flicking the tube with 500 μl of blocking buffer. Centrifuge the beads for 30 s at 1000 × *g* between washes.
2. Add 500 μl of blocking buffer to the washed beads and incubate for 1 h on a rotating platform in the cold room.

3. Centrifuge the beads for 30 s at 1000 × *g*, discard the supernatant, and resuspend the beads in 400 µl of binding buffer.
4. Denature the NRO-RNA (from **step 15** of Subheading 3.2) at 70 °C for 5 min and then place on ice for 2 min.
5. Add the NRO-RNA to the 400 µl of beads from **step 3** and incubate on a rotating wheel for 1 h in the cold room.
6. Spin down the beads and discard the supernatant.
7. Add 500 µl of ice-cold low-salt buffer and incubate on a rotating platform for 5 min. Starting from this step, the washes can be performed at room temperature with ice-cold washing buffers.
8. Spin down the beads and discard the supernatant.
9. Wash 2 × 5 min with 500 µl of ice-cold high-salt buffer, while incubating on a rotating platform.
10. Spin down the beads and discard the supernatant.
11. Wash 2 × 5 min with 500 µl of ice-cold TET buffer, while incubating on a rotating platform.
12. Spin down the beads and discard the supernatant.
13. Elute the NRO-RNA by adding 150 µl of elution buffer and incubating on a rotating platform for 5 min.
14. Spin down the beads and transfer the eluate containing the NRO-RNA to a new tube.
15. Repeat the elution twice more, each time adding another 150 µl of elution buffer to the beads, incubating on a rotating platform for 5 min, spinning down the beads, and transferring the eluate to the new tube. After a total of three elutions, there should be approximately 450–500 µl of total eluate.
16. Add equal volume (500 µl) of acid phenol–chloroform to the elute, vortex for 30 s, and centrifuge at maximum speed for 5 min in a refrigerated centrifuge.
17. Transfer the upper phase to a new tube and add an equal volume of chloroform. Vortex for 30 s and centrifuge at maximum speed for 5 min in a refrigerated centrifuge.
18. Transfer the upper phase to a new tube, add 2 µl of GlycoBlue and precipitate the NRO-RNA with 2.5–3 volumes of ice-cold 96 % ethanol at –20 °C for 2 h or overnight.
19. Centrifuge at maximum speed for 30 min at 4 °C and wash the pelleted NRO-RNA once with 75 % ethanol.
20. Dry the pellet for 3 min.
21. Dissolve the pellet in 20 µl nuclease-free H_2O. Proceed to the next step or store the NRO-RNA at –20 °C.

3.4 End-Repair of NRO-RNA

1. Denature the NRO-RNA at 70 °C for 3 min, and place on ice for 2 min.
2. Set up the following reaction in a 1.5 ml tube: 4.5 µl nuclease-free H_2O, 3 µl TAP buffer, 1 µl SUPERase-In, and 1.5 µl TAP enzyme. Mix by pipetting and incubate the reaction for 1.5 h at 37 °C.
3. Add 1 µl of 300 mM $MgCl_2$ and 1 µl of PNK, mix by pipetting and incubate for 30 min at 37 °C.
4. Add 125 µl nuclease-free H_2O, 20 µl 10× PNK buffer, 20 µl 10 mM ATP, 1 µl SUPERase-In, and 2 µl PNK enzyme. Mix by pipetting and incubate the reaction for 30 min at 37 °C.
5. Stop the reaction by adding 40 µl of nuclease-free dH_2O and 10 µl of 0.5 M EDTA, such that the final concentration of EDTA in the reaction is 20 mM and the final volume is 250 µl.
6. Add one volume of acid phenol–chloroform, vortex for 30 s, and centrifuge at maximum speed for 5 min at 4 °C.
7. Transfer the upper phase to a fresh tube, add one volume of chloroform, vortex for 30 s, and centrifuge at maximum speed for 5 min at 4 °C.
8. Transfer the upper phase to a new tube, add 2 µl of GlycoBlue and 15 µl of 5 M NaCl such that the final concentration of NaCl is 300 mM. Precipitate the end-repaired NRO-RNA by adding 2.5–3 volumes of 96 % ethanol at –20 °C for 2 h or overnight.
9. Centrifuge at maximum speed for 30 min.
10. Wash the pellet once in 75 % ethanol.
11. Dry the pellet for 3 min.
12. Dissolve the pellet in 10 µl of nuclease-free dH_2O and store the NRO-RNA at –20 °C or proceed to the next step.

3.5 3′-Adapter Ligation

1. Ligation reaction: 10 µl NRO-RNA, 1 µl 3′-adapter (100 µM), 4 µl PEG 8000 (50 %). Mix by pipetting and incubate for 3 min at 70 °C and then place on ice for 2 min.
2. Spin down briefly and add: 2 µl 10× T4 RNA ligase 2 buffer (ATP free), 1 µl SUPERase-In, 2 µl T4 RNA ligase 2, truncated. Mix by pipetting up and down and then incubate at room temperature for 4 h.
3. Bring the volume up to 100 µl by adding 80 µl of nuclease-free dH_2O.
4. Immunoprecipitate the 3′-ligated NRO-RNA using anti-BrUTP-agarose beads as described in Subheading 3.3.
5. Precipitate and dissolve the pellet in 10 µl of nuclease-free dH_2O.

3.6 5′-Adapter Ligation

1. Ligation reaction: 10 μl NRO-RNA, 1 μl 5′-adapter (100uM), 4 μl PEG 8000 (50 %). Mix by pipetting and incubate for 3 min at 70 °C and then place on ice for 2 min.
2. Spin down briefly and add: 2 μl 10× T4 RNA ligase 1 buffer, 1 μl SUPERase-In, 2 μl T4 RNA ligase 1. Mix by pipetting up and down and then incubate at room temperature for 4 h.
3. Bring the volume to 100 μl by adding 80 μl of nuclease-free dH_2O.
4. Immunoprecipitate the 5′-ligated NRO-RNA using anti-BrUTP-agarose beads as described in Subheading 3.3.
5. Precipitate and dissolve the pellet in 11 μl of dH_2O.
6. Transfer the NRO-RNA to a PCR tube.

3.7 Reverse Transcription and PCR Amplification of the GRO-seq Library

1. Reverse transcription (RT) reaction (prepared in a PCR tube): 11 μl NRO-RNA, 1 μl 10 mM dNTPs, 1 μl 100 μM RTP. Mix by pipetting up and down, incubate for 5 min at 65 °C, and then place the tube on ice for 2 min.
2. Spin down briefly and add: 4 μl 5× First-Strand buffer, 1 μl DTT, 1 μl SUPERase-In, 1 μl SSIII. Mix by pipetting up and down, place the tube in a pre-warmed thermocycler and run the following program: 50 °C—1 h, 70 °C—15 min.
3. Add 1 μl of RNaseH and incubate an additional 20 min at 37 °C.
4. Store the cDNA at –20 °C or proceed to the next step.
5. PCR reaction (prepared on ice in a PCR tube): 7 μl cDNA, 25 μl 2× Phusion HF MM, 1 μl RP1 (50 μM), 1 μl RPI1-12 (50 μM), 16 μl of nuclease-free dH_2O. Mix and spin down briefly.
6. Place the tube in a pre-warmed thermocycler and run the following program: 98 °C—30 s, 4× {98 °C—10 s, 54 °C—30 s, 72 °C—15 s}, 14× {98 °C—10 s, 60 °C—30 s, 72 °C—15 s}, 4 °C—forever.
7. Run 3 μl of the PCR reaction on a 2 % agarose gel containing 0.5 μg/ml of ethidium bromide at a constant 100 V for 30–45 min. Use a low molecular weight DNA ladder as a size control.
8. Visualize the DNA fragments under a UV transilluminator. If there are DNA smears around 150–500 bp, proceed to the next step.

3.8 GRO-seq Library Purification and Quantification

1. Add 250 μl of nuclease-free dH_2O to the remaining 47 μl of the PCR reaction to make the final volume ~300 μl, then add an equal volume of phenol–chloroform, pH 8.0, vortex for 30 s, and centrifuge at maximum speed for 5 min at room temperature (*see* **Note 9**).

2. Transfer the upper phase to a new tube; add an equal volume of chloroform, vortex for 30 s, and centrifuge at max speed for 5 min at room temperature.
3. Transfer the upper phase to a new tube, add 2 μl of GlycoBlue, 14 μl of 5 M NaCl and precipitate the DNA with 2.5–3 volumes of 96 % ethanol at −80 °C for 30 min.
4. Centrifuge for 15 min at maximum speed at 4 °C.
5. Air-dry the pelleted DNA on the bench top for 2 min.
6. Dissolve the pellet in 20 μl of nuclease-free H_2O.
7. Add 4 μl of 6× Orange gel loading dye. Load the GRO-seq library on a 10 cm × 10 cm × 1 mm pre-cast 6 % PAGE gel and run at a constant 200 V in 1× TBE until the dye exits the gel.
8. Open up the gel, while keeping on the plastic case of the pre-cast gel place it in a container with 1× TBE containing 1× SYBR Gold and shake on a rocking platform for 5 min.
9. Under UV light, excise the DNA region from 140 to 400 bp using a clean razor (Fig. 2).

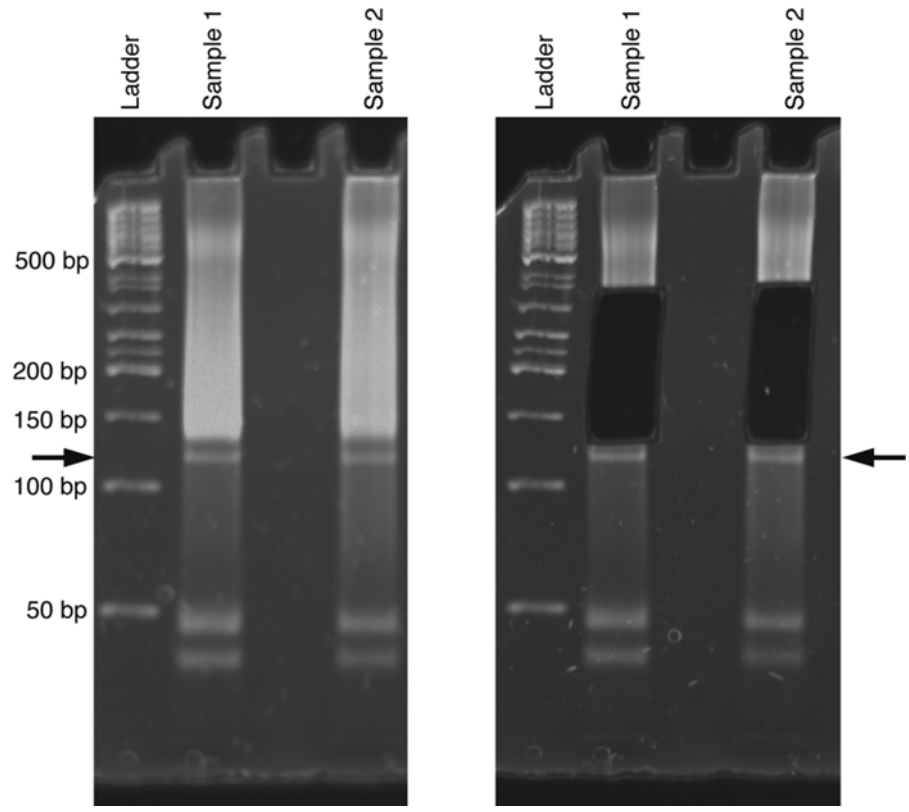

Fig. 2 Size selection of GRO-seq libraries on a 6 % native polyacrylamide gel. The gel was stained with ethidium bromide for 15 min and libraries were excised between 140 bp (just above adapter-dimer band) and 400 bp. *Arrows* indicate the adapter-dimer band. The 50 bp DNA Ladder is shown on the *left*

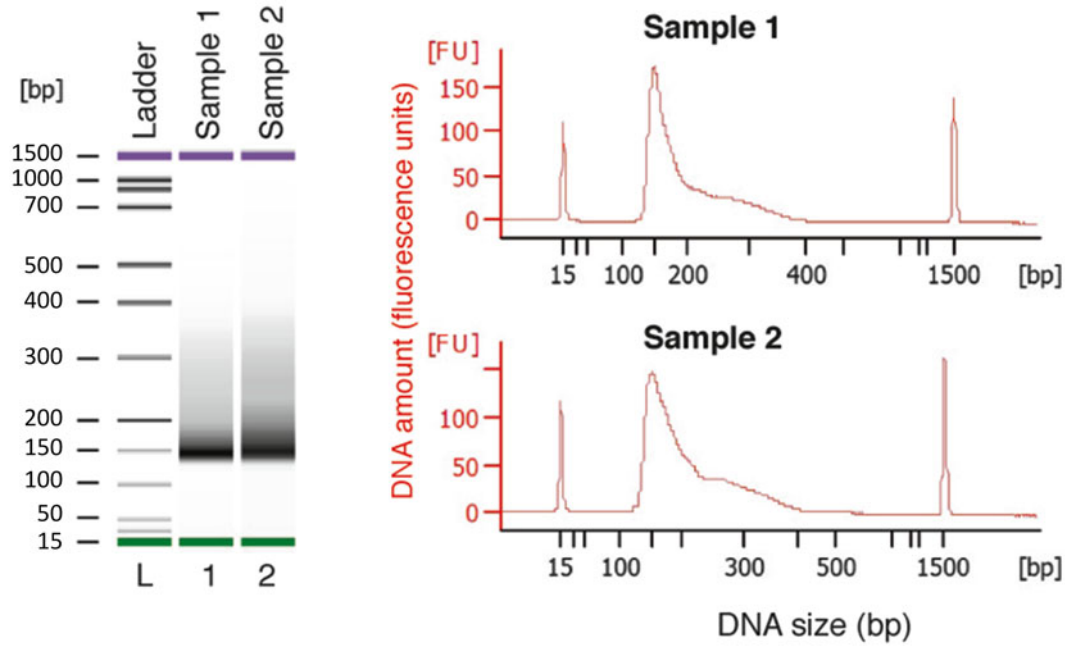

Fig. 3 Bioanalyzer electropherograms of GRO-seq libraries. Sample 1 and 2 purified from a 6 % PAGE. The profile has a peak at 150 bp and the overall size range corresponds to excised fragments shown in Fig. 2

10. Place the gel slice in a new tube, add 450 μl of 400 mM NaCl and elute overnight on a shaking platform at room temperature.
11. Transfer the eluate together with any remaining gel fragments to a Spin-X filtration tube and spin at 12,000 × *g* for 5 min at room temperature.
12. Add 2 μl of GlycoBlue to the eluate and precipitate the DNA with 2.5–3 volumes of 96 % ethanol at −80 °C for 30 min.
13. Centrifuge at maximum speed for 30 min in a refrigerated centrifuge, discard the supernatant and wash the pellet with 80 % ethanol.
14. Air dry the pelleted DNA for 2 min.
15. Dissolve the pellet in 20 μl of nuclease-free H_2O.
16. Run 1 μl of the GRO-seq library on a Bioanalyzer using a Agilent DNA 1000 or Agilent High Sensitivity DNA chip (Fig. 3).
17. Perform quantification of the GRO-seq library using qPCR and sequence on a suitable platform.

4 Notes

1. The number of ovaries required for a single run-on reaction will depend on the ovary size. Use about 50–70 pairs of wild-type ovaries; however, greater numbers of ovaries are needed if using mutants or knockdowns that affect ovary size. To improve the yield of ovaries, it is recommended to keep the flies on fly food or grape agar plates supplemented with yeast for at least 2 days prior to harvesting the ovaries.
2. Cut 2–3 mm from the end of 200 μl or 1 ml pipette tip with scissors or a sterile blade.
3. Add SUPERase-IN RNase inhibitor to all buffers immediately before using. While all buffers should be used ice-cold, the elution buffer should be kept at room temperature to prevent SDS precipitation.
4. The present protocol utilizes Illumina TruSeq small RNA cloning adapters and barcoded primers. However, any small RNA-compatible system can be used [19, 20].
5. In our experience, using the homemade buffer instead of commercial for T4 RNA ligase 2, truncated, along with PEG 8000, as well as an excess of the 3′-adapter, greatly improves 3′-ligation efficiency.
6. Here I Use a slightly modified version of previously described nuclei isolation protocols [21, 22]. The run-on reaction does not require pure nuclei; therefore, filtering through Miracloth can be omitted.
7. During run-on, Sarcosyl releases genomic DNA from nuclei and makes the solution very viscous. Therefore, it is necessary to use cut-off tips in order to reduce the loss of material during pipetting. Due to this reason, and for convenience, it is recommended to perform this step with no more than two run-on reactions at the same time.
8. If TRIzol reagent is used instead of TRIzol-LS, add 1 ml of TRIzol to 200 μl of run-on reaction, vortex for 30 s, split the mixture into two equal volumes (600 μl) and add 500 μl of TRIzol to each, so the final ratio of sample to TRIzol is 1:10.
9. Samples can also be concentrated using commercial spin columns, e.g., “DNA clean and concentrator-5” (Zymo) or “MinElute PCR Purification Kit” (Qiagen). Elute DNA twice with 8 μl of nuclease-free dH_2O or elution buffer, making the final volume 16 μl.

Acknowledgments

I thank J. Lis and A. Kalmykova laboratories for their efforts on improving GRO-seq and run-on protocols, respectively, which influenced the present work. I am grateful to Leah Sabin for critical reading of the manuscript, language editing, and helpful suggestions.

References

1. Zentner GE, Henikoff S (2014) High-resolution digital profiling of the epigenome. Nat Rev Genet 15:814–827
2. Wang Z, Gerstein M, Snyder M (2009) RNA-Seq: a revolutionary tool for transcriptomics. Nat Rev Genet 10:57–63
3. Cech TR, Steitz JA (2014) The noncoding RNA revolution-trashing old rules to forge new ones. Cell 157:77–94
4. Rinn JL, Chang HY (2012) Genome regulation by long noncoding RNAs. Annu Rev Biochem 81:145–166
5. Sabin LR, Delas MJ, Hannon GJ (2013) Dogma derailed: the many influences of RNA on the genome. Mol Cell 49:783–794
6. Core LJ, Waterfall JJ, Lis JT (2008) Nascent RNA sequencing reveals widespread pausing and divergent initiation at human promoters. Science 322:1845–1848
7. Ingolia NT, Ghaemmaghami S, Newman JR et al (2009) Genome-wide analysis in vivo of translation with nucleotide resolution using ribosome profiling. Science 324:218–223
8. Batut P, Dobin A, Plessy C et al (2013) High-fidelity promoter profiling reveals widespread alternative promoter usage and transposon-driven developmental gene expression. Genome Res 23:169–180
9. Chang H, Lim J, Ha M et al (2014) TAIL-seq: genome-wide determination of poly(A) tail length and 3′ end modifications. Mol Cell 53:1044–1052
10. Kwak H, Fuda NJ, Core LJ et al (2013) Precise maps of RNA polymerase reveal how promoters direct initiation and pausing. Science 339:950–953
11. Churchman LS, Weissman JS (2012) Native elongating transcript sequencing (NET-seq). Curr Protoc Mol Biol Chapter 4;Unit 4, 14, 11–17
12. Khodor YL, Rodriguez J, Abruzzi KC et al (2011) Nascent-seq indicates widespread cotranscriptional pre-mRNA splicing in *Drosophila*. Genes Dev 25:2502–2512
13. Paulsen MT, Veloso A, Prasad J et al (2014) Use of Bru-Seq and BruChase-Seq for genome-wide assessment of the synthesis and stability of RNA. Methods 67:45–54
14. Rozhkov NV, Hammell M, Hannon GJ (2013) Multiple roles for Piwi in silencing *Drosophila* transposons. Genes Dev 27:400–412
15. Core LJ, Waterfall JJ, Gilchrist DA et al (2012) Defining the status of RNA polymerase at promoters. Cell Rep 2:1025–1035
16. Chopra VS, Hendrix DA, Core LJ et al (2011) The polycomb group mutant esc leads to augmented levels of paused Pol II in the *Drosophila* embryo. Mol Cell 42:837–844
17. Larschan E, Bishop EP, Kharchenko PV et al (2011) X chromosome dosage compensation via enhanced transcriptional elongation in *Drosophila*. Nature 471:115–118
18. Mohn F, Sienski G, Handler D et al (2014) The rhino-deadlock-cutoff complex licenses noncanonical transcription of dual-strand piRNA clusters in *Drosophila*. Cell 157: 1364–1379
19. Hafner M, Renwick N, Farazi TA et al (2012) Barcoded cDNA library preparation for small RNA profiling by next-generation sequencing. Methods 58:164–170
20. McGinn J, Czech B (2014) Small RNA library construction for high-throughput sequencing. Methods Mol Biol 1093:195–208
21. Shpiz S, Olovnikov I, Sergeeva A et al (2011) Mechanism of the piRNA-mediated silencing of *Drosophila* telomeric retrotransposons. Nucleic Acids Res 39:8703–8711
22. Sigova A, Vagin V, Zamore PD (2006) Measuring the rates of transcriptional elongation in the female *Drosophila melanogaster* germ line by nuclear run-on. Cold Spring Harb Symp Quant Biol 71:335–341

Chapter 17

Bioinformatics Analysis to Identify RNA–Protein Interactions in Oogenesis

Ravinder Singh

Abstract

Hundreds of RNA-binding proteins are known, but the biological functions are known for only a few of them. They regulate various aspects of RNA processing or biogenesis such as splicing, polyadenylation, and translation. Here I describe a bioinformatics approach that we developed to identify potential new mRNA target(s) of the *Drosophila* master sex-switch protein Sex-lethal (SXL) by combining computational analysis with genetic and biochemical investigation. This approach could be used to identify new RNA–protein interactions during oogenesis in the female germline and should be applicable to numerous other posttranscriptional regulatory events.

Key words Sex determination, RNA-binding proteins, Germline, Oogenesis, Polyadenylation, Translation

1 Introduction

A combination of genetic, biochemical, and computational approaches has identified numerous RNA-binding proteins that are likely to function in a multitude of biological processes and regulate many genes posttranscriptionally. The cellular functions and RNA binding sites have been identified for only a small number of these proteins. The majority of functional studies on RNA–protein interactions have focused on a single or a few genes at a time. More recently, genomes of various model organisms have been sequenced, thereby allowing genome-wide investigations using computational analysis. Furthermore, several approaches have been developed to study RNA–protein interactions: for example, CLIP [1]; PAR-CliP (Photoactivatable-Ribonucleoside-Enhanced Cross-Linking and Immunoprecipitation) [2]; RIP-Seq (or RIP-ChIP); yeast-three-hybrid assay [3]; Fast-FIND (*Fast-F*ully *I*ndexed *N*ucleotide *D*atabase) [4]; RNA-Seq [5], and phylogenetic sequence analysis. Given that each approach has inherent limitations, such as background problems, antibody cross-reactivity,

Diana P. Bratu and Gerard P. McNeil (eds.), *Drosophila Oogenesis: Methods and Protocols*, Methods in Molecular Biology, vol. 1328, DOI 10.1007/978-1-4939-2851-4_17,

lack of functional relevance, spurious or pseudo sites, identification of functionally relevant RNA–protein interactions has been a challenge. Regulatory RNA-binding proteins bind to sequences that are typically short and degenerate (Table 1). Consequently, binding sequences for RNA-binding proteins occur frequently in the genome. This situation makes identification of biologically relevant downstream targets challenging and simultaneously interesting. Thus, in the future it will become necessary to combine these approaches or their variations to obtain overlapping sets of targets to narrow down the list of potential candidates (Fig. 1) and to provide genome-wide perspectives of functionally relevant RNA–protein interactions.

Oogenesis in *Drosophila* is an excellent model system allowing the combination of both biochemical and genetic tools to study sexual differentiation. The master sex-switch protein Sex-lethal (SXL) of *Drosophila* is an example of an RNA-binding protein that is important in this process. SXL is present only in females and binds to uridine-rich sequences or pyrimidine-tracts adjacent to particular splice sites in specific pre-mRNAs (Fig. 2). While SXL function and regulation has been extensively studied in somatic cells, it also controls sexual differentiation in the female germline, which is more complex and poorly understood [6–9]. SXL likely regulates additional targets in the female germline [6, 10–16]. Thus, SXL function in the female germline provides an excellent model to identify new RNA–protein interactions that regulate gene expression during oogenesis.

The bioinformatics approach, described below, combines computational analysis with the power of *Drosophila* genetics to identify new RNA–protein interactions relevant for regulation in the

Table 1
Most RNA-binding proteins recognize short, degenerate sequences that occur frequently in transcripts; for additional sequences, *see* [28]

hnRNP or SR Protein	Preferred sequence or consensus binding site
hnRNP A1	UAGGG(A/U)
hnRNP C	UUUUUU
hnRNP I PTB)	UCUUC/CUCUCU rich
Sxl	U8-U17 (with Gs)
ASF/SF2	RGAAGAAC/AGGACRRAGC/SRSASGA
SC35	AGSAGAGUA/UGUUCSAGWU/AGGAGAU/GRYYMCYR
SRp54	C rich
Tra2beta	GAA repeat

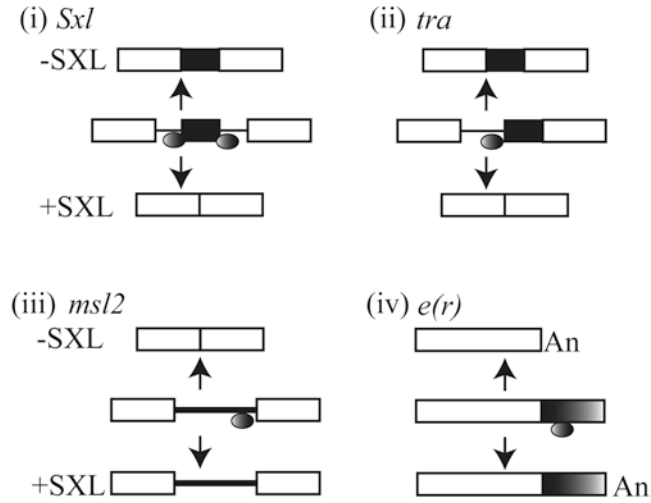

Fig. 1 Alternative mRNA isoforms of SXL targets. Primary transcripts are shown in the *middle* and alternative mRNA isoforms are shown *above* or *below*, indicated by *arrows* (+/−SXL). *Open boxes* are constitutive exons, *black boxes* are alternative exons (or 3′ splice sites), *lines* are introns, *filled ovals* are SXL proteins, *shaded boxes* are alternative 3′ UTRs, and An is poly(A) tail. SXL binding site(s) are present in the 3′ UTR of *nanos* that affect translation [16], which cannot be identified in transcriptome profiling studies

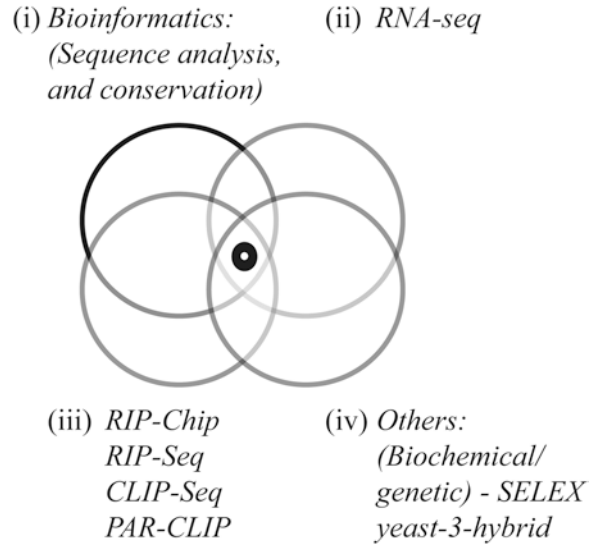

Fig. 2 Multiple high-throughput approaches. *Overlapping circles* represent various datasets from RNA–protein interactions studies or from transcriptome profiling using various approaches (*i–iv*) that can be used to narrow down the list of potential candidates

female germline, *see* refs. 17, 18. Our approach involves identification of a suitable sequence or sequence feature for a genomic search, validation of candidates from the search using Northern analysis for mRNA isoforms, use of transgenic flies for regulation in vivo, and characterization of RNA–protein interactions using gel mobility shift and cross-linking assays in vitro.

2 Materials

2.1 Fly Stocks

1. Appropriate fly stocks are available from various laboratories or from the Bloomington Stock Center (http://flystocks.bio.indiana.edu/).
2. Flies are raised at 25 °C on standard corn meal food.

2.2 cDNA Clones/ ESTs

1. cDNA clones/ESTs are available from commercial vendors, from various laboratories, or can be easily amplified by polymerase chain reaction (PCR).
2. Gene-specific fragments can be obtained using PCR.

2.3 Northern Blot Analysis

1. TRI Reagent.
2. PolyA Tract mRNA isolation system.
3. Duralose-UV membrane (Stratagene).
4. Phosphorimager.
5. SSC (10×): 87.6 g NaCl, 44.1 g sodium citrate, pH 7.0.
6. Nick translation mix (total 50 µl): 8 µl of Milli-Q H_2O, 10 µl of 5× labeling buffer, 2 µl of dNTP mix (A,G,T), 2 µl of 10× BSA, 6 µl of α ^{32}P-dCTP (10 mCi/ml), 2 µl of DNA Pol-I, 20 µl of denatured DNA.
7. Hybridization solution: 50 ml of deionized formamide, 20 ml of 50 % dextran sulfate, 10 ml of 10 % SDS, 20 ml of 5 M NaCl.
8. 5× Formaldehyde gel running buffer: 0.1 M 3-(*N-morpholino*) propanesulfonic acid (MOPS), pH 7.0, 40 mM sodium acetate, 5 mM EDTA, pH 8.0.
9. 10× MOPS (1 l): 41.9 g of 3-(*N*-morpholino) propanesulfonic acid, 8.2 g of sodium acetate·3H_2O, 3.72 g EDTA.
10. 37 % formaldehyde.

2.4 Gel Mobility Shift Assay or RNA Binding

1. Buffer D: 20 mM HEPES, pH 8.0, 1 mM dithiothreitol, 0.2 mM EDTA, 0.05 % NP-40, 20 % glycerol.
2. RNA Binding reaction: 10 mM Tris–HCl, pH 7.5, 50 mM KCl, 1 mM dithiothreitol, 0.09 µg/µl acetylated bovine serum albumin (BSA), 0.5 U/µl RNasin, 0.15 µg/µl tRNA, 1 mM EDTA, 6 µl of the appropriate protein dilution.

3. 5× TBE (per liter): 54 g of Tris base, 27.5 g of boric acid, 20 ml of 0.5 M EDTA, pH 8.0.
4. Native 5 % non-denaturing polyacrylamide gel (60:1 acrylamide–bis-acrylamide) in 0.5× TBE.

2.5 RNA–Protein UV Cross-Linking Assay

1. RNase A.
2. A germicidal G15T8 UV lamp.
3. 12.5 % SDS-polyacrylamide gel.

2.6 Whole-Mount Fluorescence and Immunostaining

1. 1× PBS (per liter): 8 g of NaCl, 0.2 g of KCl, 1.44 g of Na_2HPO_4, 0.24 g of KH_2PO_4, pH 7.4.
2. PBST: 1× PBS, 0.1 % Triton™ X-100.
3. 4 % Formaldehyde.
4. DAPI.
5. Anti-GFP antibodies.

3 Methods

3.1 Sequence Search

1. Download the *Drosophila* genome [19] to perform a sequence search (http://www.fruitfly.org/).
2. Identify the binding site for the RNA-binding protein of interest. For example, the SXL-binding site consensus [20–23] used for the genomic search, based on a selection-amplification (SELEX) experiment, is a G/U-rich sequence (UUUUGUU (G/U)U(G/U)UUU(G/U)UU) [20].
3. Use one of the following approaches to search for occurrences of all such sites in the genome:
   (a) If the sequence is unique, which is rare for a typical RNA-binding protein (Table 1), perform the genomic search using standard string matching.
   (b) If the binding site is like the SXL-binding site, which is an example of a degenerate G/U-rich sequence, generate all possible combinations of the degenerate sequence and then perform standard string matching for each possible pattern as above.
   (c) Alternatively, search the genome using a weight matrix corresponding to the SXL-binding site (*see* **Note 1**).
4. For each overlapping string, where the length depends on the length of the binding site, in the *Drosophila* genome, calculate the total score using the weight matrix by summing up the highest log-score number for each position, as highlighted in boxes (Table 2) (*see* **Note 2**).

Table 2
Scores for two nucleotides (G and U) at each of the 16 positions (Pos) in the SXL site. *Boxed numbers* represent the relative weights of preferred nucleotides at these positions

Pos	G	U
1	-1.5	0.6
	-0.2	0.5
	-0.5	0.5
	0.5	-0.1
	-0.8	0.6
	0.0	0.4
	-0.1	0.4
	-1.5	0.5
	0.5	-0.3
	-0.5	0.5
	-1.5	0.6
	-1.5	0.6
	0.4	-0.1
	-1.5	0.6
	-0.2	0.5
16	0.2	0.1

$$\log \frac{\left(n_{i,j} + p_i\right) / \left(N + 1\right)}{p_i}$$

N = number of sequences, pi = a priori probability of nucleotide i, and ni,j = number of times nucleotide i appears at position j [24].

5. When the total score for a string/sequence is above a user-defined threshold save the genomic location of the binding site (*see* **Note 2**).
6. Retrieve the sequence adjacent to the binding site referenced above.
7. Narrow down the number of potential candidates to a number that can be experimentally analyzed by applying several biological filters, depending on the protein or regulation of interest. For example, the choice of appropriate biological filters can include:
   (a) That the binding site is in the coding region of the genome, by comparing with ESTs and based on genome annotation;
   (b) That the binding site is on the sense strand, based on genome annotation;

(c) That the binding site is near a splice site, a polyadenylation site (based on genome annotation), or adjacent to any other known feature relevant for gene regulation from prior studies, depending on the protein of interest (*see* **Note 3**); and/or

(d) That the sequence is conserved (depending on if sequence information from other species is available) (*see* **Note 4**).

3.2 Northern Blot Analysis

1. To experimentally validate the candidate genes for expression and/or mRNA isoforms in fruit flies, isolate total RNA by grinding adult flies or isolated ovaries in TRI Reagent (*see* **Note 5**).
2. Obtain poly(A)$^+$ RNA by passing the total RNA through an oligo(dT) column.
3. Prepare a denaturing agarose gel (typically 1 %) containing formaldehyde by dissolving 1.6 g of agarose in 135.2 ml of milli Q water by boiling. When it cools down to 45 °C, add 16 ml of 10× MOPS and 8.8 ml of 37 % formaldehyde, mix thoroughly and pour into a gel tray with combs in a Fume hood (to avoid Formaldehyde fumes).
4. Prepare an RNA sample (40 μl) containing standard 2 μl of 10× MOPS, 6.6 μl of 37 % formaldehyde, 20 μl of formamide dye (bromophenol blue and Xylene cyanol), and 11.4 μl (1.0 μg) of poly(A)$^+$ RNA. Mix and keep in a heating block at 55 °C for 15 min.
5. Load the poly(A)$^+$ RNA, along with a separate lane for RNA markers, and subject to electrophoresis in a denaturing agarose gel (80 V for 3 h at room temperature) using appropriately diluted formaldehyde gel running buffer.
6. Transfer the separated RNA on to a Duralose-UV membrane using standard gel transfer.
7. Using a standard nick translation reaction (incubation time—1.0 h), synthesize gene-specific probes using gene-specific cDNA fragments and a radioactive nucleotide and passing through G25 Sephadex column (to remove unincorporated radioactivity).
8. Pre-hybridize the membrane in an appropriate volume of the hybridization solution with 100 μg/ml of sonicated, single-stranded salmon sperm DNA at 42 °C for 2–5 h. Hybridize the membrane with fresh hybridization solution containing the radioactive probe, ~5×10^5 to 5×10^6 cpm/ml (denatured at 80 °C for 5 min), by incubating (constant shaking/rotating) it at 42 °C overnight.
9. Wash the membrane on a shaker thoroughly in 2× SSC + 0.1 % SDS for 15 min at room temperature, 0.2× SSC + 0.1 % SDS

for 15 min at room temperature, and in 0.2× SSC +0.1 % SDS for 15 min at 42 °C. Do not let the membrane dry.

10. Detect the RNA size and expression levels by autoradiography on X-ray films or imaged using a Phosphorimager.
11. Detect RNA size markers, on the marker lane cut from the rest of the gel, by staining with 0.1 % methylene blue for 2 min and rinsing with milli Q H_2O.

3.3 Generation of Transgenic Lines

1. To determine whether the binding site identified using the genomic search is important for the mRNA regulation and whether such regulation is functionally important, clone an appropriate gene fragment in a plasmid, use mutagenic oligonucleotides to introduce mutations in the potential binding site of the cloned fragment, and confirm by sequencing.
2. Introduce these plasmids containing wild-type or mutant transgenes into the *Drosophila* genome using *P* element-mediated transformation [25].
3. Obtain transgenic animals using standard genetic procedures (*see* **Note 6**).
4. Analyze reporter or mini-gene expression, from the native gene promoter or from a regulated promoter for desired expression, for RNA levels or RNA isoforms using Northern blot analysis or RNase protection, as described above. It may be necessary to use a probe(s) unique to the transgene to distinguish the transgene transcript from the endogenous transcript.

3.4 Gel Mobility Shift Assay

1. For an RNA-binding assay, estimate the protein concentration by comparing with Coomassie blue staining of a BSA standard on an SDS polyacrylamide gel or by a spectrophotometer.
2. Store and dilute recombinant protein in Buffer D.
3. Prepare a 20 μl RNA binding reaction.
4. Prepare a native 5 % (non-denaturing) polyacrylamide gel. Prerun it for 15 min at 250 V in a cold room at 4 °C.
5. Incubate the binding reaction for 30 min at 25 °C or on ice [20, 26].
6. Load the entire binding reaction on to the native gel described above.
7. Separate the RNA–protein complexes by electrophoresis at 50 V for 15 min, followed by 250 V for 1–3 h in a cold room, depending on the size of the RNA–protein complex.
8. Transfer the gel onto 3MM Whatman paper, cover with saran wrap, dry using a vacuum-dryer, and detect using autoradiography or a Phosphorimager.

3.5 RNA–Protein UV Cross-Linking Assay

1. For UV cross-linking, cross-link the binding reaction on ice using UV light for 10 min with a germicidal G15T8 UV lamp (held close to the top of an eppendorf tube with lid open) or with the lamp available in standard tissue-culture hoods.
2. Treat the sample with ribonuclease A for 10–20 min.
3. Load onto a standard 12.5 % SDS-polyacrylamide gel and separate by electrophoresis.
4. Visualize the radioactive signal using a Phosphorimager or by autoradiography.

3.6 Whole-Mount Fluorescence and Immunological Detection of Reporter Translation

1. Clone different 3′ UTRs (wild type and mutants) downstream of a GFP reporter or 5′ UTRs upstream of the reporter.
2. Introduce the plasmid containing the reporter transgene into flies to obtain transgenic animals, as described above.
3. After eclosion, feed yeast paste to female flies for 2–4 days.
4. Dissect the ovaries in PBST.
5. Fix ovaries for 15 min in PBST with 4 % formaldehyde.
6. Stain the ovaries with DAPI or immunostain using anti-GFP antibodies.
7. Examine under a Zeiss 2.2.1 microscope to detect EGFP signal by fluorescence microscopy or immunostaining using appropriate antibodies (*see* **Note 7**).

4 Notes

1. An inherent limitation is that the consensus-binding site does not capture quantitative differences that are apparent at various positions in a typical binding site. Although this approach is computationally fast, there are concerns that certain binding sites are likely to be missed. In contrast to string matching, the weight matrix approach allows quantitative (versus qualitative) description of the binding site because for each sequence position we are able to assign relative weights to various nucleotides, thus generating a weight matrix of log-likelihood scores from the alignment matrix, as described [24]. Another alternative is to search for base composition, which we developed subsequently [4], but was not an option at the time of this search.
2. A 16-nucleotide string is an example for the SXL site in Table 2. Because the SXL site is a G/U-rich sequence, accordingly, the values for C and A residues are not particularly important and thus are not shown for clarity in Table 2. When the score is above a user-defined threshold, the genomic location of the binding site is saved. A maximum score of 7.88 is possible for

the SXL binding sites and we use 5.1 as cutoff to obtain high-affinity binding sites. This cutoff allows identification of natural high affinity SXL binding sites similar to those present in known mRNAs targets such as *tra*, *Sxl*, and *msl2*, while ignoring short pyrimidine-tracts typically present near 3′ splice sites in introns.

3. There were over 14,000 hits for the SXL site in the *Drosophila* genome (~13,600 predicted *Drosophila* genes [19]). Therefore, we used criteria to successively eliminate hits, for example, that are outside of 3 kb of known ESTs (expressed sequence tags), that are more than 100 bases away from annotated splice sites, that are on the antisense strand, and that show no evidence of alternative splicing based on ESTs. Eventually, the last step also involves manual inspection and results in experimentally manageable potential candidates (including three known SXL targets—*Sxl*, *tra*, and *msl2*).
4. Sequences for the 12 *Drosophila* species and other insects are available online.
5. For all RNA work, wear gloves all the time, do not touch any equipment with bare hands, keep the gel apparatus for RNA-only, and make solutions in DEPC-treated and autoclaved water.
6. We did all of the transgenic work in house, although several services for transgenic flies have recently become available, for example, http://www.geneticservices.com/injection/drosophila-injections/ or http://www.thebestgene.com/ or http://www.rainbowgene.com/.
7. Additional technical details are available at ref. [27].

Acknowledgements

I thank Andrew Rahn and Mark Robida for their notes consulted for materials and methods and the American Cancer Society and the Butcher Foundation for grants to RS that supported this work.

References

1. Ule J, Jensen K, Mele A et al (2005) CLIP: a method for identifying protein-RNA interaction sites in living cells. Methods 37(4):376–386
2. Hafner M, Landthaler M, Burger L et al (2010) PAR-CliP--a method to identify transcriptome-wide the binding sites of RNA binding proteins. J Vis Exp (41) http://www.jove.com/details.php?id=2034, doi:10.3791/2034
3. Zhang B, Kraemer B, SenGupta D et al (1999) Yeast three-hybrid system to detect and analyze interactions between RNA and protein. Methods Enzymol 306:93–113
4. Hamady M, Peden E, Knight R et al (2006) Fast-Find: a novel computational approach to analyzing combinatorial motifs. BMC Bioinformatics 7:1
5. Heimiller J, Sridharan V, Huntley J et al (2014) *Drosophila* polypyrimidine tract-binding protein (DmPTB) regulates dorso-ventral patterning genes in embryos. PLoS One 9(7):e98585

6. Schutt C, Nothiger R (2000) Structure, function and evolution of sex-determining systems in Dipteran insects. Development 127(4):667–677
7. Mahowald AP, Wei G (1994) Sex determination of germ cells in *Drosophila*. Ciba Found Symp 182:193–202
8. Steinmann-Zwicky M (1992) How do germ cells choose their sex? *Drosophila* as a paradigm. Bioessays 14(8):513–518
9. Salz HK (2013) Sex, stem cells and tumors in the *Drosophila* ovary. Fly 7(1):3–7
10. Samuels ME, Bopp D, Colvin RA et al (1994) RNA binding by Sxl proteins in vitro and in vivo. Mol Cell Biol 14(7):4975–4990
11. Fujii S, Amrein H (2002) Genes expressed in the *Drosophila* head reveal a role for fat cells in sex-specific physiology. EMBO J 21(20):5353–5363
12. Kelley RL, Solovyeva I, Lyman LM et al (1995) Expression of msl-2 causes assembly of dosage compensation regulators on the X chromosomes and female lethality in *Drosophila*. Cell 81(6):867–877
13. Hager J, Cline T (1997) Induction of female Sex-lethal RNA splicing in male germ cells: implications for *Drosophila* germline sex determination. Development 124(24):5033–5048
14. Vied C, Halachmi N, Salzberg A et al (2003) Antizyme is a target of Sex-lethal in the *Drosophila* germline and appears to act downstream of Hedgehog to regulate Sex-lethal and Cyclin B. Dev Biol 253(2):214–229
15. Chau J, Kulnane LS, Salz HK (2009) Sex-lethal facilitates the transition from germline stem cell to committed daughter cell in the *Drosophila* ovary. Genetics 182(1):121–132
16. Chau J, Kulnane LS, Salz HK (2012) Sex-lethal enables germline stem cell differentiation by down-regulating Nanos protein levels during *Drosophila* oogenesis. Proc Natl Acad Sci U S A 109(24):9465–9470
17. Gawande B, Robida MD, Rahn A et al (2006) *Drosophila* Sex-lethal protein mediates polyadenylation switching in the female germline. EMBO J 25(6):1263–1272
18. Robida MD, Rahn A, Singh R (2007) Genome-wide identification of alternatively spliced mRNA targets of specific RNA-binding proteins. PLoS One 2(6):e520
19. Adams MD, Celniker SE, Holt RA et al (2000) The genome sequence of *Drosophila melanogaster*. Science 287(5461):2185–2195
20. Singh R, Valcarcel J, Green MR (1995) Distinct binding specificities and functions of higher eukaryotic polypyrimidine tract-binding proteins. Science 268(5214):1173–1176
21. Singh R, Banerjee H, Green MR (2000) Differential recognition of the polypyrimidine-tract by the general splicing factor U2AF65 and the splicing repressor sex-lethal. RNA 6(6):901–911
22. Sakashita E, Sakamoto H (1994) Characterization of RNA binding specificity of the *Drosophila* sex-lethal protein by in vitro ligand selection. Nucleic Acids Res 22(20):4082–4086
23. Kanaar R, Lee AL, Rudner DZ et al (1995) Interaction of the sex-lethal RNA binding domains with RNA. EMBO J 14(18): 4530–4539
24. Hertz GZ, Hartzell GWD, Stormo GD (1990) Identification of consensus patterns in unaligned DNA sequences known to be functionally related. Comput Appl Biosci 6(2):81–92
25. Serano TL, Cheung HK, Frank LH et al (1994) P element transformation vectors for studying *Drosophila melanogaster* oogenesis and early embryogenesis. Gene 138(1–2):181–186
26. Valcarcel J, Singh R, Zamore PD et al (1993) The protein Sex-lethal antagonizes the splicing factor U2AF to regulate alternative splicing of transformer pre-mRNA. Nature 362(6416):171–175
27. Mohr SE, Dillon ST, Boswell RE (2001) The RNA-binding protein Tsunagi interacts with Mago Nashi to establish polarity and localize oskar mRNA during *Drosophila* oogenesis. Genes Dev 15(21):2886–2899
28. Singh R, Valcarcel J (2005) Building specificity with nonspecific RNA-binding proteins. Nat Struct Mol Biol 12(8):645–653

Index

Diana P. Bratu and Gerard P. McNeil (eds.), *Drosophila Oogenesis: Methods and Protocols*, Methods in Molecular Biology, vol. 1328, DOI 10.1007/978-1-4939-2851-4, © Springer Science+Business Media New York 2015

G

I

M

O

P

R

S

T